



GAS TURBINE LUBRICANT EVALUATION

by

MATTHEW RICHARD SPENCER

A thesis submitted to
The University of Birmingham
for the degree of
DOCTOR OF ENGINEERING

School of Chemical Engineering,
The University of Birmingham,
Edgbaston,
Birmingham,
B15 2TT,
UK

July 2014

UNIVERSITY OF
BIRMINGHAM

University of Birmingham Research Archive

e-theses repository

This unpublished thesis/dissertation is copyright of the author and/or third parties. The intellectual property rights of the author or third parties in respect of this work are as defined by The Copyright Designs and Patents Act 1988 or as modified by any successor legislation.

Any use made of information contained in this thesis/dissertation must be in accordance with that legislation and must be properly acknowledged. Further distribution or reproduction in any format is prohibited without the permission of the copyright holder.

ABSTRACT

This thesis is a study of the chemical and physical changes which can occur to gas turbine lubricants as a result of exposure to operational conditions. The continual evolution toward more efficient gas turbines is accompanied by increasing thermal and mechanical loading which the lubricant must be able to withstand.

In engine operation, some level of degradation of the lubricant will occur, it is vital to the gas turbine manufacturers to be able to assess accurately the extent to which lubricant performance will change during operation as a result. In this thesis two major degradation issues are studied; thermal oxidative degradation and lubricant deposition.

In the area of thermal oxidative degradation, efforts are made to better understand the key parameters which determine the lubricant breakdown mechanism. Through control of these parameters and comparison to service derived gas turbine oil samples, a new laboratory methodology is proposed for the assessment of lubricant oxidative degradation. Critically, this method is shown to be more engine representative than other, similar methods, meaning the mechanism and rate of fluid degradation can be correlated to the service operation of gas turbines.

The study of lubricant deposition in this thesis is concentrated on the regions of highest risk, the bearing chamber feed (single phase) and vent (two phase) oil pipes. Development of the Feed Pipe Simulator and Vent Pipe Simulator deposition test equipment was conducted to increase how representative of gas turbine conditions the methods are and, in the case of the FPS, to allow automated testing. Testing showed oil brand differentiation akin to service experience and allowed an assessment of deposit accumulation. Conditions following engine

shutdown were found to be at higher risk for feed pipe deposition than the conditions during engine running. The process of draining oil pipes at shutdown resulted in greater deposition than if they remain fully filled with oil.

Pipe surface modifications were evaluated for their ability to reduce deposition formation rates under single phase and two phase conditions. Initial work demonstrated that some coatings reduced deposition although difficulties in coating complex geometries meant surface modification technologies were favoured. Electropolishing and acid pickling of pipes exhibited positive results with deposit reduction of up to 50 %, depending on specific conditions.

Additional scoping testing was also conducted in the area of oil tribology to understand the influence of formulation chemistry on abrasive wear. Increasing tricresyl phosphate concentration was found, in the case of one lubricant, to give a small reduction in abrasive wear but this was not the case for the other two lubricants tested. Additionally an apparent synergistic effect was noted between TCP and 1,4-dihydroxyanthraquinone resulting in significant wear reduction.

ACKNOWLEDGEMENTS

I would firstly like to thank Professor Mark Simmons, Dr Richard Greenwood and Tim Shepherd for their supervision throughout the project and for their dedication in seeing the project through to completion.

During my time based at Rolls-Royce, I have learnt much and received assistance and guidance from many individuals. Of particular use, were the many full and often very 'to the point' conversations with those in the Fluids Team; Dr David Ferreday, Dr John Askins, Alastair Hobday, Chris Lewis, Ray Munn and Andy Smith.

I would also like to thank those from the wider gas turbine lubricant industry, particularly the members of the 'SAE E34 Propulsion Lubricants Committee' for allowing me to present and discuss my work on numerous occasions and to draw on their collective experience.

Financial assistance was gratefully received from the EPSRC and Rolls-Royce plc.

Finally, I want to thank my friends, family and girlfriend Ally, for their support throughout my EngD. Perhaps one day I might be able to explain to them what all this oil stuff is about!

This thesis is dedicated to my grandfather, James Perry, the man who first inspired in me an interest in science, engineering and the way things work.

CONTENTS

Abstract.....	II
Acknowledgements	IV
Contents.....	VI
List Of Figures	X
List Of Tables	XVII
Nomenclature.....	XVIII
CHAPTER 1: Introduction	- 1 -
1.1. Background	- 1 -
1.1.1. The Gas Turbine.....	- 1 -
1.1.2. Thermal Oxidative Degradation.....	- 2 -
1.1.3. Lubricant Deposition	- 5 -
1.1.4. Lubricant Tribological Properties.....	- 8 -
1.2. Aims and Objectives	- 10 -
1.3. Thesis Structure.....	- 11 -
1.4. Achievements and Publications.....	- 12 -
CHAPTER 2: Literature Review	- 13 -
2.1. The Development of Aviation Lubricants	- 13 -
2.2. Formulation Chemistry.....	- 14 -
2.2.1. Base Stocks	- 15 -
2.2.2. Additive Chemistry	- 17 -
2.3. Oil Specifications	- 19 -
2.4. Gas Turbine Oil System.....	- 22 -
2.4.1. Oil System Layout	- 22 -
2.4.2. Oil System Conditions and Demands.....	- 28 -
2.5. Bulk Thermal Oxidation Degradation	- 29 -
2.5.1. Thermal Oxidative Mechanisms	- 29 -
2.5.2. Laboratory Test Methods	- 38 -

2.6.	Lubricant Deposition	- 39 -
2.6.1.	Deposition Reactions	- 39 -
2.6.2.	Transport and Fouling.....	- 42 -
2.6.3.	Lubricant Deposition Types and Conditions	- 46 -
2.6.4.	Laboratory Test Methods	- 47 -
2.7.	Deposition Reduction Techniques	- 47 -
2.7.1.	Surface Coating.....	- 49 -
2.7.2.	Surface Modification	- 50 -
2.8.	Lubricant Tribology.....	- 52 -
2.8.1.	Lubrication Regimes	- 52 -
2.8.2.	Aviation Test Methods	- 52 -
2.8.3.	Influence of Thermal Oxidation on Tribological Performance	- 53 -
2.8.4.	Tricresyl Phosphate Influence.....	- 53 -
2.9.	Summary	- 54 -
CHAPTER 3: Methods and Materials		- 55 -
3.1.	Methods	- 55 -
3.1.1.	Thermal Oxidative Stability Methods	- 55 -
3.1.2.	Deposition Methods	- 60 -
3.1.3.	Surface Coating and Treatment Methods.....	- 69 -
3.1.4.	Tribology.....	- 70 -
3.1.5.	Analysis Methods	- 71 -
3.2.	Materials	- 73 -
3.2.1.	Lubricants	- 73 -
CHAPTER 4: Thermal Oxidative Stability		- 75 -
4.1.	Introduction and Business Case.....	- 75 -
4.2.	Critical Review of Current Methodology	- 76 -
4.2.1.	Life Prediction.....	- 81 -
4.3.	Testing using current industry techniques	- 82 -
4.3.1.	Ministry of Defence, Defence Standard 05-50 (Part 61) Method 9	- 83 -
4.3.2.	ASTM D4636	- 89 -
4.3.3.	Comparison between Def. Stan. Method 9 and ASTM D4636	- 90 -
4.4.	Degradation Parameter Sensitivity	- 92 -
4.4.1.	Effect of Air Flow Rate	- 93 -

4.4.2.	Effect of Oil Replenishment	- 98 -
4.4.3.	Effect of Evaporation	- 102 -
4.4.4.	Effect of Metal Test Specimens	- 105 -
4.4.5.	Gel Permeation Chromatography.....	- 108 -
4.5.	Test Method Modifications	- 112 -
4.6.	Modified Method Data.....	- 115 -
4.7.	Closing Remarks	- 123 -
CHAPTER 5:	Deposition.....	- 125 -
5.1.	Introduction and Business Case.....	- 125 -
5.2.	Current Laboratory Deposition Methods	- 127 -
5.2.1.	Hot Liquid Process Simulator (HLPS).....	- 128 -
5.2.2.	ERDCO Bearing Rig.....	- 130 -
5.2.3.	Vapor Phase Coking Test	- 131 -
5.2.4.	Summary of Laboratory Deposition Tests.....	- 132 -
5.3.	Vent Pipe Simulator (VPS)	- 133 -
5.3.1.	Flow conditions	- 134 -
5.3.2.	Temperature Study.....	- 135 -
5.3.3.	Oil Brand Differentiation	- 139 -
5.3.4.	Deposition Accumulation Study	- 145 -
5.3.5.	Oil Chemistry	- 149 -
5.4.	Feed Pipe Simulator	- 152 -
5.4.1.	Development Work	- 156 -
5.4.2.	Feed Pipe Simulator Improvements	- 161 -
5.4.3.	Oil Chemistry	- 163 -
5.5.	Closing Remarks	- 166 -
CHAPTER 6:	Surface Technology.....	- 168 -
6.1.	Introduction and Business Case.....	- 168 -
6.2.	Deposition Testing Methodology	- 170 -
6.3.	Surface Metallurgy	- 171 -
6.3.1.	Single Phase.....	- 171 -
6.3.2.	Two Phase Flow	- 176 -
6.4.	Surface Modification	- 179 -
6.4.1.	Modified Surface Characterisation	- 180 -

6.4.2.	Single Phase.....	- 182 -
6.4.3.	Two Phase Flow.....	- 189 -
6.5.	Closing Remarks	- 191 -
CHAPTER 7: Tribology		- 194 -
7.1.	Introduction and Business Case.....	- 194 -
7.2.	Aviation Lubricant Tribology Evaluator (ALTE)	- 195 -
7.3.	Oil Brand Evaluation	- 196 -
7.4.	Tricresyl Phosphate Concentration	- 200 -
7.5.	Additive Contribution Testing.....	- 202 -
7.6.	Closing Remarks	- 206 -
CHAPTER 8: Conclusions and Further Work		- 207 -
8.1.	Conclusions	- 207 -
8.2.	Impact on the Business	- 209 -
8.3.	Further Work.....	- 210 -
CHAPTER 9: References.....		- 212 -
Appendix 1		- 223 -
Appendix 2		- 232 -

LIST OF FIGURES

Figure 1.1 Schematic showing bearing chamber conditions	- 3 -
Figure 1.2 Schematic of a bearing chamber showing oil and air pipes	- 6 -
Figure 1.3 Examples of lubricant deposition found in gas turbine oil pipes	- 7 -
Figure 2.1 Synthesis of diester base stocks	- 15 -
Figure 2.2 β -hydrogen abstraction degradation mechanism	- 15 -
Figure 2.3 Synthesis of polyol ester base stocks	- 16 -
Figure 2.4 N-phenyl-1-naphthylamine (PANA) and (b) 4,4'-diocetyldiphenylamine (DODPA) antioxidant compounds (c) Oligomeric antioxidant	- 18 -
Figure 2.5 Tricresyl Phosphate (TCP), mixture of isomers, anti-wear additive	- 19 -
Figure 2.6 Oil system schematic	- 23 -
Figure 2.7 Neopentyl hexanoate model ester	- 30 -
Figure 2.8 Free radical degradation initiation steps	- 31 -
Figure 2.9 Interchain free radical reaction mechanisms	- 31 -
Figure 2.10 Antioxidant radical scavenging example mechanism	- 33 -
Figure 2.11 Aldol condensation mechanism	- 40 -
Figure 2.12 Knoevenagel condensation mechanism	- 40 -
Figure 2.13 Polymerisation by esterification and transesterification	- 40 -
Figure 2.14 General fouling reaction	- 42 -
Figure 2.15 Diagram of the proposed lubricant deposition fouling reactions	- 42 -
Figure 2.16 Diagram of potential fouling cases	- 43 -
Figure 3.1 Schematic of Defence Standard, Method 9 equipment	- 56 -
Figure 3.2 Schematic of ASTM 4636 standard test equipment	- 57 -
Figure 3.3 FPS control unit screenshot showing the 'Test Schedule' tab	- 69 -

Figure 4.1 Equipment set up for: (a) Fed. Stan. 3411 (b) Turbomeca Thermal Ageing Method (c) ASTM D4636 (d) Def. Stan. Method 9	- 79 -
Figure 4.2 Method 9, change in Total Acid Number as a function of temperature (192 hour tests)	- 84 -
Figure 4.3 Method 9, percentage viscosity increase as a function of temperature (192 hour tests)	- 84 -
Figure 4.4 Method 9, percentage volatilisation loss as a function of temperature (192 hour tests)	- 85 -
Figure 4.5 Method 9, change in Total Acid Number as a function of time (215 °C test)	- 86 -
Figure 4.6 Method 9, Viscosity increase as a function of time (215 °C test)	- 87 -
Figure 4.7 Method 9, Volatilisation loss as a function of time (215 °C test)	- 87 -
Figure 4.8 Arrhenius plot for four lubricants	- 88 -
Figure 4.9 ASTM D4636 Oil oxidation data. Total Acid Number, viscosity and volatilisation increase as a function of temperature (72 hour tests)	- 90 -
Figure 4.10 Comparison of viscosity and Total Acid Number of laboratory and engine derived samples	- 92 -
Figure 4.11 A schematic of the ASTM D4636 equipment used for the parameter sensitivity testing	- 93 -
Figure 4.12 Graph showing the influence of air flow rate on Total Acid Number and change in viscosity, volatilisation (195 °C, 72 hour tests)	- 95 -
Figure 4.13 Total Acid Number and viscosity increase for two service engines operating typical flight cycles	- 97 -
Figure 4.14 Viscosity increase as a function of time, for SPC and HPC oils at three oil replenishment rates	- 99 -

Figure 4.15 Total Acid Number change as a function of time for SPC and HPC at three oil replenishment rates	- 100 -
Figure 4.16 Density increase for SPC and HPC oils at three oil replenishment rates	- 101 -
Figure 4.17 Percentage composition of volatilised carboxylic acid species constituents collected throughout the process of oil degradation	- 103 -
Figure 4.18 Mass loss of test metals in two lubricants at three test temperatures (72 hour tests)	- 105 -
Figure 4.19 Steel test specimens pre-test (left) and post-test (right). Showing carbon deposits within the machining grooves (post-test)	- 106 -
Figure 4.20 The influence of test metal specimens on change in viscosity and Total Acid Number	- 107 -
Figure 4.21 Gel Permeation Chromatogram showing a range of laboratory degraded oil samples, an engine derived sample and a reference sample of oil as new	- 110 -
Figure 4.22 Gel Permeation Chromatography of oil replenishment test samples (0.63 % per hour)	- 112 -
Figure 4.23 A schematic of the modified oil oxidation method	- 113 -
Figure 4.24 Increase in lubricant Total Acid Number as a function of time using the modified method (175 and 185 °C)	- 117 -
Figure 4.25 Increase in lubricant Total Acid Number as a function of time using the modified method (195, 204 and 218 °C)	- 117 -
Figure 4.26 Increase in lubricant viscosity as a function of time using the modified method (175 and 185 °C).....	- 119 -
Figure 4.27 Increase in lubricant viscosity as a function of time using the modified method (195, 204 and 218 °C).....	- 119 -

Figure 4.28 Increase in lubricant density as a function of time using the modified method (175 and 185 °C).....	- 121 -
Figure 4.29 Increase in lubricant density as a function of time using the modified method (195, 204 and 218 °C).....	- 121 -
Figure 4.30 Comparison of ASTM D4636 to the modified method (72 hour duration)	- 122 -
Figure 4.31 Comparison of oil Viscosity and Total Acid Number including modified method data	- 123 -
Figure 5.1 Hot Liquid Process Simulator (HLPS), taken from: SAE ARP5996 (2013)	- 129 -
Figure 5.2 Vapor Phase Coking Test, SAE ARP5921 (2014).....	- 132 -
Figure 5.3 Vent Pipe Simulator Schematic	- 134 -
Figure 5.4 (a) Vent Pipe Simulator predicted flow conditions. (b) image of Vent Pipe Simulator flow through a transparent tube, by experiment.....	- 135 -
Figure 5.5 Increase in gas outlet temperature as a function of time.....	- 136 -
Figure 5.6 Length of turbulent flow following a range of flow disturbance heights. Calculated by $0.05 \text{ Re} \cdot \text{Pr} \cdot \text{Deposit Height}$	- 137 -
Figure 5.7 Outlet gas temperature at the end of test for a range of test durations and artificial deposits.....	- 138 -
Figure 5.8 Vent Pipe Simulator data, at five temperatures after an 18 hour test - all oils ..	- 139 -
Figure 5.9 SPC 1 lubricant deposit mass as a function of temperature (18 hour test)	- 141 -
Figure 5.10 Vent Pipe Simulator data at four temperatures (18 hour test) - HPC oils.....	- 143 -
Figure 5.11 Vent Pipe Simulator data expressed as a line graph (break-point).....	- 144 -
Figure 5.12 Deposit formed as a function of time (SPC 1 oil, 300 °C wall temperature)	- 145 -
Figure 5.13 Image showed the heated region, measured wall temperatures and the areas of deposit formation (75 hour test, 300 °C outer wall temperature)	- 146 -

Figure 5.14 Images showing deposit building up at a range of durations, (a) 3 hours, (b) 18 hours, (c), 60 hours, (d) 100 hours	- 147 -
Figure 5.15 An example of gas turbine vent pipe deposits	- 148 -
Figure 5.16 Scanning Electron Microscope images of VPS deposit	- 149 -
Figure 5.17 Gas Chromatograms of fresh oil (top), oil mist (middle) and liquid oil samples (bottom).....	- 151 -
Figure 5.18 Gel permeation chromatograph of Vent Pipe Simulator samples	- 152 -
Figure 5.19 The Feed Pipe Simulator	- 153 -
Figure 5.20 Feed Pipe Simulator schematic	- 155 -
Figure 5.21 Oil brand comparison under constant oil flowing conditions, (375 °C wall temperature, 18 hour cycle)	- 157 -
Figure 5.22 Graph showing the influence of shutdown conditions on deposition mass (375 °C wall temperature, 18 hour cycle)	- 158 -
Figure 5.23 Feed Pipe Simulator deposit images under a range of shutdown conditions (a) continuous oil flowing (b) drained shutdown (c) flooded shutdown	- 159 -
Figure 5.24 Shortened test cycle conditions	- 160 -
Figure 5.25 Shortened cycles, brand differentiation using drained shutdown conditions (375 °C wall temperature)	- 161 -
Figure 5.26 Feed Pipe Simulator control unit	- 162 -
Figure 5.27 Gel permeation chromatogram of FPS oil samples at a range of durations	- 164 -
Figure 5.28 Relationship between antioxidant consumption and Total Acid Number	- 165 -
Figure 6.1 Deposit mass formed with a range of test specimen metallurgies using the HLPs (375°C, 20 hours)	- 172 -
Figure 6.2 SEM Images of test piece surfaces. (a) Nickel (b) Chromium (c) Stainless Steel .	- 174 -

Figure 6.3 Deposit mass formed with gold and silicon test specimens at a range of temperatures using the HLPS.....	- 176 -
Figure 6.4 Vent Pipe Simulator results for stainless steel, titanium and Inconel following an 18 hour test duration	- 178 -
Figure 6.5 Deposit mass accumulation as a function of time at 300 °C for stainless steel and Inconel test specimens (VPS)	- 179 -
Figure 6.6 SEM images. a) Standard untreated tube b) Electropolished c) Acid Pickled	- 182 -
Figure 6.7 Graph showing the deposit mass produced by three lubricants with electropolished and standard tubes at 375°C test temperature.....	- 183 -
Figure 6.8 HLPS Tubes after a testing using SPC 2 at 350°C, Electropolished (Top) and Standard (Bottom).....	- 184 -
Figure 6.9 Graph showing the deposit mass produced at three temperatures for the SPC oils ...	- 185 -
Figure 6.10 Image showing deposit on SPC 1 electropolished test specimens at 375 °C (Top), 350 °C (Middle), and 325 °C (Bottom)	- 186 -
Figure 6.11 Percentage elemental composition of stainless steel and electropolished test specimens before and after test	- 187 -
Figure 6.12 FPS Data, deposit mass formed with SPC lubricant with a standard, electropolished and acid pickled test specimens.....	- 189 -
Figure 6.13 VPS results at a range of durations for standard, electropolished and acid pickled test pieces. SPC 1 lubricant with a wall temperature of 300°C	- 190 -
Figure 6.14 An enlargement of Figure 6.13, showing the low duration VPS results for testing at a range of durations for standard, electropolished and acid pickled test pieces. SPC 1 lubricant with a wall temperature of 300°C	- 191 -

Figure 7.1 Oil brand evaluation at 100 °C. The TCP concentration of each oil is shown in brackets..... - 197 -

Figure 7.2 Image showing the wear scar generated on the ball bearing at the contact..... - 198 -

Figure 7.3 Oil brand evaluation at 150 °C. The TCP concentration of each oil is shown in brackets..... - 199 -

Figure 7.4 Oil brand evaluation, comparison of 100 °C and 150 °C - 200 -

Figure 7.5 Graph showing the influence of tricresyl phosphate concentration (proportional to concentration of phosphorus) on wear scar diameter at 150 °C with a 4 kg load..... - 202 -

Figure 7.6 Abrasive wear results showing the contribution of different additives..... - 203 -

Figure 9.1 Surface finish measured areas..... - 232 -

LIST OF TABLES

Table 2.1 Overview of the properties specified by SAE AS5780 (2013) and MIL-PRF-23699 (US Department of Defense, 1997)	- 20 -
Table 2.2 Summary of physical and chemical property changes as a lubricant degrades	- 35 -
Table 2.3 Major factors that influence the deposition formation rate.....	- 45 -
Table 3.1 Metal specimen specification	- 58 -
Table 3.2 Modified test method parameters	- 60 -
Table 3.3 Aviation Lubricant Tribology Evaluator test conditions	- 70 -
Table 3.4 Bespoke oil blend compositions	- 71 -
Table 4.1 Comparison of the thermal degradation test methods	- 78 -
Table 4.2 Arrhenius plot equations and R squared values	- 89 -
Table 5.1 Example Feed Pipe Simulator test cycles.....	- 163 -
Table 6.1 Summary of surface finish measurements	- 181 -
Table 6.2 Feed Pipe Simulator test cycle conditions	- 188 -

NOMENCLATURE

ALTE	Aviation Lubricant Tribology Evaluator
CI	Corrosion Inhibiting
cSt	Centistokes
CVD	Chemical Vapour Deposition
DODPA	4 4-dioctyldiphenylamine
EP	Extreme Pressure
FOHE	Fuel Oil Heat Exchanger
FPS	Feed Pipe Simulator
HLPS	Hot Liquid Process Simulator
HPC	High Performance Capability
HTS	High Thermal Stability
IFSD	In Flight Shutdown
MCD	Magnetic Chip Detector
MOD	Ministry of Defence
OPANA	N-(4-octylphenyl)-1-naphthylamine
PANA	N-phenyl-1-naphthylamine
PVD	Physical Vapour Deposition
SPC	Standard Performance Capability
STD	Standard Thermal Stability
TAN	Total Acid Number
TCP	Tricresyl Phosphate
VPS	Vent Pipe Simulator

CHAPTER 1: INTRODUCTION

1.1. Background

1.1.1. The Gas Turbine

Gas turbines or jet engines provide power for aircraft, marine vessels and energy generation across the world. Since the idea was first patented by Sir Frank Whittle in 1930 (Whittle, 1930), gas turbines have continually evolved as engineers strive to push the limits of power and efficiency. Each evolutionary gas turbine design is made possible by the parallel advancement in materials technology.

The first aviation gas turbines, turbojets, employed Newton's third law of motion to propel aircraft through the air. After ingesting large quantities of air, compressing it to high pressure, combusting with fuel and turning a turbine, air leaves the engine as a high velocity jet, thus providing thrust. The turbojet configuration of gas turbine is still used today where high speeds are required and as such, is commonly applied in military applications. However turbojets are relatively noisy and inefficient and therefore, for applications where high speed is not required, turbofans were developed. Turbofans differ from turbojets through the inclusion of a bypass duct which allows some of the air, after passing the first compressor stage (the fan), to pass around the core of the engine and be expelled. This gives rise to quieter, more efficient yet low velocity propulsion, therefore turbofan configurations are common place in the civil aviation market.

In recent years, efforts to further improve the efficiency of gas turbines have involved more incremental improvements. Using the theory described by the Brayton Cycle, manufacturers continually strive for higher compression ratios in order to increase the efficiency of the

system (Rajadurai, 2003). Increased compression ratio for combustion gives a higher power output but also leads to higher gas temperatures. This has led to turbine entry temperatures in excess of 1500°C providing a considerable challenge to engineers to produce materials capable of withstanding these extreme conditions (Rolls-Royce, 2005).

An increase in gas and metal temperatures throughout the system, in addition to increased rotation speed, leads to more severe conditions within the gas turbine oil system. Whilst lubricant technology has also advanced, since the advent of polyol ester based lubricants in the 1940s, developments have been incremental (Rudnick, 2013). The oil system provides a number of functions critical to gas turbine operation; reduction of friction, heat management, debris removal and corrosion protection. It is therefore of increasing importance for manufacturers to be able to evaluate lubricants across a range of properties to determine their ability to provide these functions both when new and as they begin to degrade through use.

1.1.2. Thermal Oxidative Degradation

Perhaps the most severe conditions in the oil system are found in mainline bearing chambers where oil is exposed to elevated temperature and pressure in an oxidative and catalytic environment (Figure 1.1). Heat transmitted from the gas path, in addition to that generated by shearing of the fluid itself, can give bulk oil temperatures up to 250 °C upon exit from the bearing chamber via the scavenge pipe (Bakunin and Parenago, 1992). In addition to the harsh physical conditions, when air sealing is used, the air will cause the oil to be heavily aerated; the presence of air promotes breakdown of the oil as oxygen can react with the lubricant.

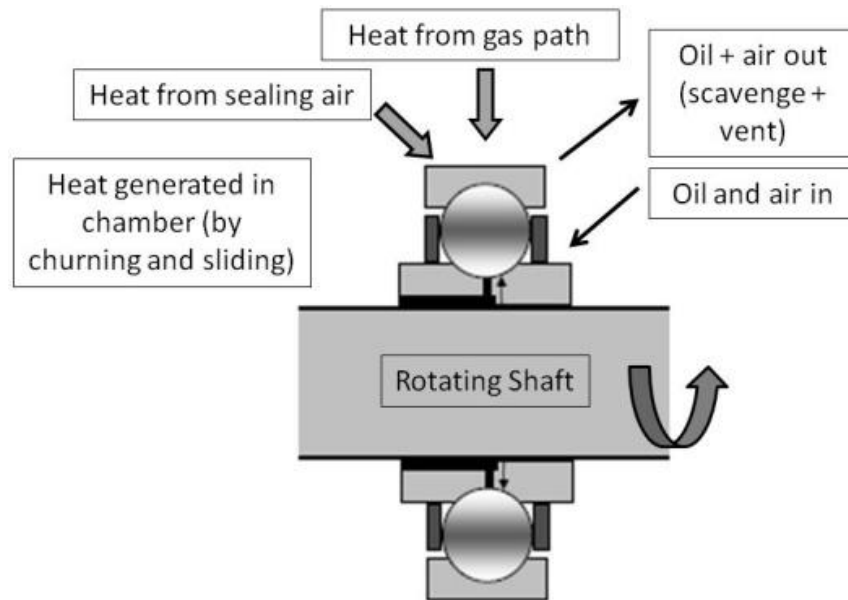


Figure 1.1 Schematic showing bearing chamber conditions

Thermal degradation of the lubricant can result in an increase in viscosity, acidity, density, flammability and the formation of precipitates. A change in transport properties of the lubricant can result in additional strain on mechanical components, particularly under lower temperature start up conditions. This can result in the premature failure of pumps and drive shafts leading to a failed engine start or In Flight Shutdown (IFSD). Extreme increases in the lubricant acidity brought about by heavy degradation of the lubricant can reduce the life of elastomeric seals used commonly within the oil system which can lead to oil leakage. Therefore the result of oil degradation derived issues can range from service disruption to aircraft safety issues.

Oil changes on civil gas turbines require costly maintenance and are therefore undesirable. Instead the oil will commonly remain in the engine for the entire duration that the engine is 'on-wing' with oil changes only being undertaken at workshop maintenance intervals, often after many thousands of hours of operation. However oil will be added in order to replenish

losses from the oil system. It is this process of loss and replenishment which allows a suitably thermally stable lubricant to achieve 'infinite' life. It is therefore important to Rolls-Royce to be able to predict how a lubricant will perform in service under the range of transient conditions to which it will be exposed.

Whilst the engine development programme which new engines undergo prior to entry into service gives some information on how a lubricant will perform, the conditions employed are often far more extreme than service conditions. Given that engine testing is an expensive and time consuming process, it is not possible to evaluate candidate lubricants for the required duration to generate robust data to define oil life in service. Therefore a laboratory based test method is required which allows the thermal oxidative degradation reactions to be accurately replicated on a shortened timescale and at greatly reduced cost, (when compared to engine testing). This method would allow the generation of data to determine the rate at which the oil degrades and how the physical properties of the oil are impacted when exposed to thermal oxidative conditions.

Once accurate test data has been generated under laboratory conditions, pseudo-kinetic equations for these changes in physical properties can be devised so that the physical properties of service oils undergoing transient conditions can be predicted. This capability would enable Rolls-Royce to accurately predict the impact of particular service conditions on a lubricant to allow the selection of the most appropriate lubricant brand or where required, to predict oil change requirements before any impact to engine operation.

Development of simplistic laboratory techniques which can accurately replicate the complicated and varied lubricant breakdown reactions which occur in gas turbines is a significant challenge. The mechanism and rate of lubricant degradation is extremely

dependant on the conditions it is exposed to (Koh and Butt, 1995). It is necessary, for reasons of practicality, to accelerate and simplify these methods compared normal engine operation. However, the challenge is to not greatly deviate from the mechanisms and degradation rates seen in service. The current industry laboratory techniques for this purpose were all developed a number of years ago. Therefore, since the development of the vast majority of these methods, advancements in lubricant chemistry, engine technology, laboratory methodology and analytical techniques have occurred. If accurate lubricant degradation data is to be generated this methodology must be constantly reviewed to ensure that, as far as practically possible, the method matches engine oil degradation mechanisms.

1.1.3. Lubricant Deposition

A typical gas turbine bearing chamber is serviced by three oil pipes as shown in Figure 1.2, the first of these is the feed pipe (green) which provides the oil input to the chamber. The second two pipes are used to remove oil from the chamber, the scavenge pipe (red) is designed to remove oil from the chamber whereas the vent pipe (yellow) allows the removal of sealing air which has entered the chamber. In reality, both the vent and scavenge pipe will carry a mixture of oil and air. These oil pipes must transition through the gas path of the engine in order to reach the bearing chamber and as such their pipe walls can reach 400 °C. It is these high temperatures, transient flow conditions and in the case of the vent and scavenge, the availability of oxygen, which make them particularly at risk to the formation of fouling deposits caused by degradation of the lubricant.

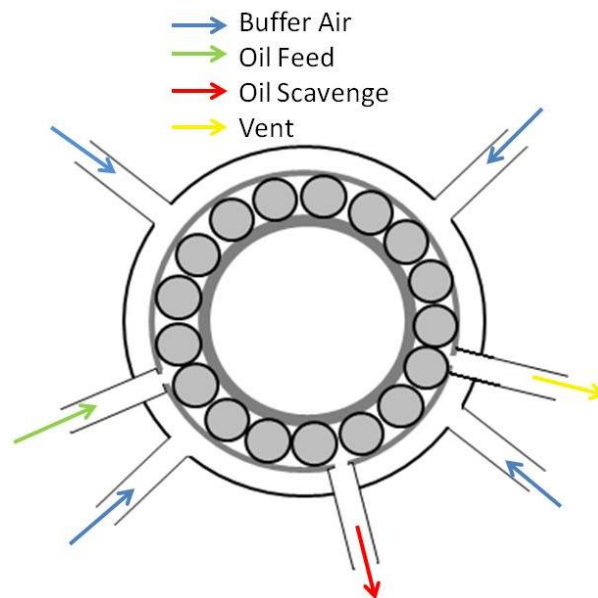


Figure 1.2 Schematic of a bearing chamber showing oil and air pipes

Whilst thermal oxidative degradation can be considered to affect the bulk properties of the lubricant, lubricant deposition, in contrast, is an inherently localised phenomenon. Lubricant deposition occurs when a lubricant is pushed beyond its thermal capabilities in a localised area resulting in polymerisation of lubricant species to form high molecular weight compounds. As these high molecular weight species possess zero or limited solubility in oil, they accumulate at the surfaces of the metal pipe walls.

The accumulation of deposits on the walls of oil pipes can become a significant issue if the deposits build up to the point where they restrict or entirely block the flow of oil. The potential consequences of blocking or restricting oil flow depend upon which oil pipe is affected. Blockage of the oil feed pipe will result in insufficient oil to lubricate bearings and gears, resulting in overheating and possible damage. Blockage of the scavenge oil pipe will result in the oil being inadequately removed resulting in bearing chamber flooding and oil loss through the air blown seals. Both of these consequences can have significant impact to engine

operation and result in an In Flight Shutdown (IFSD). Two examples of lubricant deposit within oil pipes are shown in Figure 1.3.

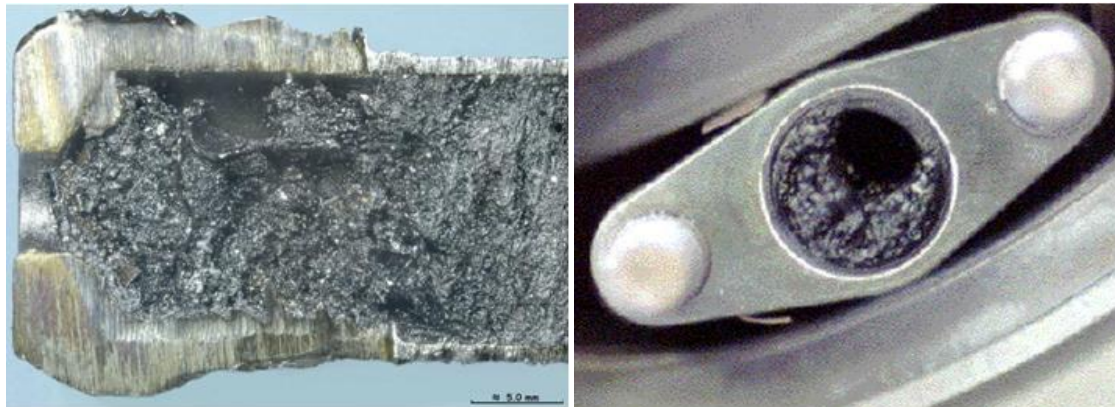


Figure 1.3 Examples of lubricant deposition found in gas turbine oil pipes

In service, oil deposition is managed by carrying out visual inspections and performing remedial actions as required. The inspection of internal oil system components requires pipe connections to be opened to gain access. This entails a level of risk that the connections will be damaged, or fail to seal on reassembly. This risk combined with the cost and inconvenience to the engine operators means that such maintenance is only performed when necessary. In order to accurately predict when this maintenance will be required, knowledge of the rate at which particular oil brands will form deposits when exposed to certain conditions in service, is required.

The rate at which oil deposits form will depend on a number of factors including temperature, oil flow rate, air/oil ratio, oil formulation and the surface at which deposition occurs. A number of these key factors will vary depending on the particular oil system location; the feed, vent and scavenge pipe of each bearing chamber having different conditions to suit the requirements of that bearing. To further complicate this, the conditions found in each location will be dependent upon transient engine conditions; take off, climb, cruise and descent all

require different levels of power and therefore give different temperatures and oil flows. Indeed, one of the most high risk engine conditions in terms of deposition formation is following shutdown, where the heat within the engine remains, lubricant flow stops, leaving oil in high temperature locations.

As lubricant deposition can take thousands of hours of engine running to occur, evaluation of all candidate lubricants through engine testing is both expensive and impractical. Therefore there is a need for laboratory or rig scale test equipment to allow the evaluation of lubricants on an accelerated time scale and at greatly reduced cost. Current industry techniques focus on evaluating the relative performance of lubricants and are therefore not focused on specific engine conditions and demands. In contrast the Rolls-Royce strategy is to develop methodology which directly mimics specific oil system locations and conditions, albeit on a scaled system, allowing direct comparisons to service conditions to be drawn.

Testing of this type allows the selection of the most suitable lubricant for particular gas turbine models and applications to reduce the risk and consequences of oil deposition. Where maintenance is required, laboratory testing allows more effective scheduling to reduce service disruption to a minimum. This capability also provides a research and development tool in order to evaluate potential methods by which lubricant deposition could be reduced by modifications to engine hardware.

1.1.4. Lubricant Tribological Properties

Creation of the high compression ratios required for efficiency as described in § 1.1.1, requires multistage compressors rotating at high speeds. This creates high loads which the transmission components such as bearings, gears and shafts must be able to endure. As a result of friction

between moving elements a wide variety of wear mechanisms can occur which act to shorten the life of these components.

Failure of major transmission components is likely to result in an IFSD event where the engine is powered down during flight. As such an event is a serious issue, transmission components are classified as critical components and subject to component life assessment to define the maximum component lifetimes. Unfortunately these components are some of the more expensive and difficult to replace in the gas turbine, therefore manufacturers seek to achieve the maximum possible component life.

One of the key functions of a lubricant is to provide a separating oil film, reducing friction and therefore minimising the wear of metallic components. Prior to the formation of an elastohydrodynamic / hydrodynamic film, at start-up or during other transient conditions, boundary lubrication regimes will occur (Hutchings, 1992). Under these conditions, anti-wear additives in the formulation will be critical (Chung, 1992). The extent to which a lubricant is able to inhibit wear mechanisms is described in broad terms, as its tribological properties.

In order to generate the maximum possible life for expensive transmission components the tribological performance of a lubricant is a critical property in the selection of a lubricant brand for use in a gas turbine. As with thermal properties, laboratory testing is required to gain an understanding of how different lubricant formulations and constituent additives can provide a reduction in component wear. This allows the gas turbine manufacturer to select the optimum lubricant to prevent issues occurring in service.

1.2. Aims and Objectives

The main aims of the work described in this thesis are as follows:

- 1) Develop an improved laboratory thermal oxidative test method which has the ability to replicate the degradation mechanisms which lubricants undergo in service. This will allow the following to be achieved:
 - a. A better understanding of the chemistry of lubricant degradation and how this is influenced by the conditions the oil is exposed to.
 - b. Generation pseudo-reaction kinetics for thermal degradation processes in order to define the life of lubricants at elevated temperature.
- 2) Enhance the capability of laboratory scale deposition simulators to better replicate engine conditions in the following areas:
 - a. Bearing chamber feed pipe (single phase oil flow). Developing the ability to evaluate lubricant deposition through the replication of complete engine cycle conditions.
 - b. Bearing chamber vent pipe (two phase – air/oil mist). Gaining an understanding of how lubricant vent pipe deposits accumulate over time for a range of oil brands and conditions.
- 3) Evaluate a range of metal surface treatments and coatings for their ability to reduce the rate at which lubricant deposit occurs.
- 4) Investigate the influence of oil formulation and additives on the ability of a lubricant to inhibit metallic wear mechanisms.

1.3. Thesis Structure

This thesis is structured in the following way. Chapter 2 contains a literature review which includes details of typical gas turbine lubricant formulation constituents and their role in the gas turbine oil system. The remainder of Chapter 2 is then focused on a literature review of the four major element of this thesis; thermal oxidative degradation, deposition formation, deposition reduction and tribology.

Chapter 3 contains details of the methodology and materials used in the results chapters 4-7.

A review of current thermal oxidative stability test methods and the results of the influence of a range of parameters on thermal oxidative degradation are described in Chapter 4. Chapter 4 also contains suggested improvements to create a new, more engine representative, test methodology and the data generated by this improved method.

Chapter 5 contains the results of studies into the assessment of lubricant solid deposition formation. Current industry methodology is discussed and critiqued before results of single and two phase deposition testing are presented. The efforts to evaluate pipe surface techniques intended to reduce solid lubricant deposition are described in Chapter 6. The techniques explored include changes made to pipe metallurgy and to the surface finish.

The final results chapter (Chapter 7) contains initial work to explore the influence of lubricant formulation on the inhibition of wear in sliding contacts. This Chapter concentrates on defining the influence which different additives (anti-wear, antioxidants and metal deactivators) have on wear.

Chapter 8 includes conclusions drawn from the work and also contains suggestions made for future work in this research area.

1.4. Achievements and Publications

Journal Papers:

Spencer, M., Shepherd, T., Greenwood, R., and Simmons, M., (2013) "An Assessment of the Influence of Gas Turbine Lubricant Thermal Oxidation Test Method Parameters Towards the Development of a New Engine Representative Laboratory Test Method", *SAE Int. J. Aerosp.* 6(2): 819-827 doi:10.4271/2013-01-9004. (Appendix 1)

Laboratory Methods:

Sponsoring author for: SAE International, (2013) "Aviation Lubricant Tribology Evaluator (ALTE) Method to determine the lubricating quality of gas turbine lubricants" Aerospace Recommended Practice, ARP6255

Patents:

Spencer, M. R., Askins, J. S., Shepherd, T. A., "Cyclic Feed Pipe Simulator" Patent currently awaiting filing.

Oral Presentations:

Spencer, M., "Thermal Oxidative Stability Assessment", SAE E34 Propulsion Lubricants Symposium, October 3, 2013, Prague, Czech Republic.

Spencer, M., "Thermal Oxidative Stability of Aviation Lubricants", SAE E34 Propulsion Lubricants Committee, October 15-18, 2012, Portland OR.

Spencer, M., "Thermal Oxidative Stability of Aviation Lubricants", SAE E34 Propulsion Lubricants Committee, October 3-6, 2011, Austin TX.

CHAPTER 2: LITERATURE REVIEW

This literature review commences with an introduction to aviation gas turbine lubricants, § 2.1 gives a brief history of their development and § 2.2 discusses the chemistry of the formulations used. The industry oil specifications used are introduced in § 2.3 and defines the specific oil types on which this thesis will concentrate. § 2.4 provides an overview of the gas turbine oil system and role of the lubricant within it. This section also highlights regions of the engine which give particular demands on the lubricant.

The remaining four sections of this literature review provide an overview of the available literature surrounding each of the results chapters. § 2.5 describes bulk thermal oxidation degradation, § 2.6 lubricant deposition and § 2.7 discusses methods for reducing deposit formation by modification to oil pipe hardware. The final section, § 2.8, discusses literature of relevance to the final results chapter, reviewing lubricant tribology and the influence of oil chemistry. The chapter is then summarised in § 2.9.

2.1. The Development of Aviation Lubricants

Early gas turbine lubricants were highly refined mineral oils which were derived from the lubricants already in use in piston engine aircraft. The rapid development of the gas turbines, leading to higher temperature operating conditions, left mineral derived products unable to withstand the thermal demands.

Research in the 1930s and 1940s led by Professor Zorn at IG Farben (later to become BASF) (Jantzen, 1996) was into diester and polyol ester lubricant base stocks. When compared to mineral oils, esters had much improved resistance to degradation in the higher temperature lubricant systems of the day. In the 1950s, both the UK and US militaries adopted diester

lubricant technology. However, the two countries had different requirements. The UK Ministry of Defence (MOD) concentrated on the demands of its turboprop powered fleet; the highly loaded reduction gearboxes in this type of gas turbine meant that high viscosity oil was needed. Conversely, the US military developed lower viscosity lubricants for their turbojet fleet; which did not have such high load requirements but required a lower temperature starting capability. The different requirements led to the UK MOD developing a 7.5 centistoke (cSt) (at 100°C) specification, DERD2487 (superseded by Defence Standard 91-98) and the US military a 3 cSt (at 100°C) specification, MIL-L-7808 (superseded by MIL-PRF-7808).

The continued increase in oil system temperatures meant these diester lubricants soon lacked the thermal capability to meet the temperature requirements. Instead, 5 cSt polyol ester lubricants were favoured, leading to the development of MIL-PRF-23699 (US Department of Defense, 1997) which was first issued in 1963 (Fowler *et al.*, 1996). The move from diester to polyol ester lubricants represents the last significant revolutionary development in aviation oil technology. Although the gas turbine oils used today are still primarily polyol ester base stock lubricants, evolutionary improvements in base stock quality and additive technology have led to incremental improvements in oil properties.

2.2. Formulation Chemistry

Synthetic lubricants are a formulated product of which the base stock, *e.g.* diester or polyol ester, comprises approximately 95 % of the total. It is the base stock that defines the majority of the lubricant's properties, nevertheless, a range of additives are also commonly employed to enhance oil properties to meet specific requirements. These additives include antioxidants, anti-wear, metal deactivator and anti-foaming additives. It is the synergistic effect of the complete formulation which gives the lubricant its final properties.

2.2.1. Base Stocks

Diesters

Diester oils are formed from the reaction of a di-basic carboxylic acid such as azelaic acid (nonanedioic acid) with an alcohol such as octanol as shown in Figure 2.1. The chain length and amount of chain branching of both the acid and alcohol constituents can be used to determine the viscosity of the ester and therefore the lubricant.

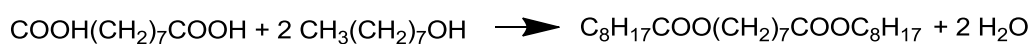


Figure 2.1 Synthesis of diester base stocks

Diester lubricants are susceptible to β -hydrogen abstraction due to the stable intermediate which forms as a result of hydrogen bonding. This hydrogen bonding occurs between the β -hydrogen and carbonyl group, promoting elimination of the β -hydrogen (Mortier *et al.*, 2010). β -hydrogen abstraction leads to the formation of an alkene and a carboxylic acid as shown in Figure 2.2. As further reaction of these alkene species is known to form solid particulates, this degradation reaction is particularly undesirable.

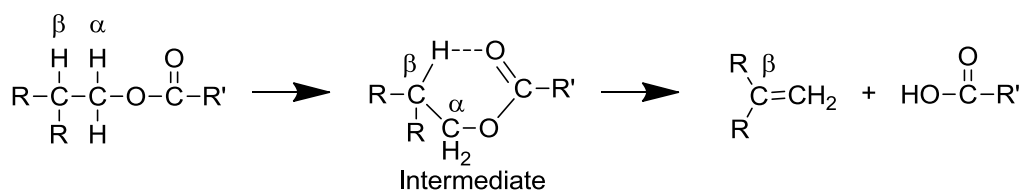


Figure 2.2 β -hydrogen abstraction degradation mechanism

The β -hydrogen degradation reaction limits the thermal capability of the lubricant, improvements in thermal stability are only possible if this reaction is prevented.

Polyol Esters

Polyol ester base stocks are often called hindered esters as their structure provides steric hindrance to reaction of the ester group. Polyol esters are formed from the reaction of polyhydric alcohol such as pentaerythritol or neopentyl glycol, with a monocarboxylic acid resulting in a tri or tetra ester as shown in Figure 2.3.

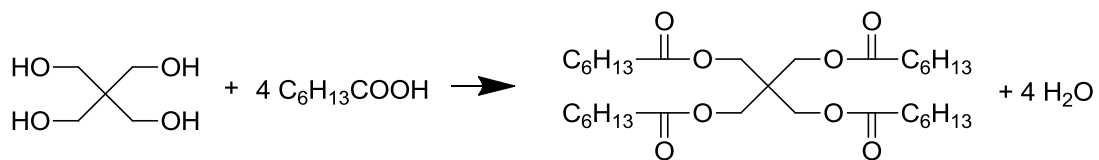


Figure 2.3 Synthesis of polyol ester base stocks

As polyol esters do not contain a β -hydrogen as with diesters, they are not susceptible to β -hydrogen abstraction and the resulting degradation mechanism. This simple structural development means that polyol ester lubricants are inherently more thermally stable than their diester equivalents.

By selecting the chain length and level of chain branching of the base stock, the oil viscosity along with other transport properties can be defined. Short chain (5-7 carbon units) length polyol ester base stocks have low enough viscosity at cold temperatures to allow low temperature engine starts. However, they are often not sufficiently viscous at higher temperatures to provide the oil film thickness required for efficient lubrication. Longer chain base stocks (8-12 carbon units) suffer the reverse; they provide good oil films at high temperatures, but, are too viscous at low temperatures. The length of the carbon chain will also influence the hydrolytic and thermal stability of the lubricant. Shorter chain lengths are generally more stable than longer chain esters, this is discussed in more detail in § 2.5.1. Therefore to produce the required properties a blend of different chain length compounds

must be used. This allows the correct variation of viscosity with temperature, or viscosity index (VI), and the required thermal and hydrolytic stability to be achieved (Fowler *et al.*, 1996).

2.2.2. Additive Chemistry

Whilst the base stock of the lubricant formulation is responsible for determining the majority of the oil's properties, additives are used to enhance a number of critical lubricant properties. These properties and some example additive compounds are discussed in this section.

Antioxidants

The major degradation reactions which affect polyol ester lubricants are initiated by free radical species. Therefore removal of free radical degradation precursors allows the rate of degradation to be reduced thereby prolonging the life of the lubricant. Antioxidants preferentially react with free radicals, prior to reaction with the base stock, thus protecting the base stock from free radical attack (Dexter, 1992). As a result of reaction with free radical species the antioxidants themselves become oligomerised and subsequently polymerised. For this reason they are often considered to be consumed as the lubricant ages. Whilst it is true that the antioxidant may not be present in its original form, oligomers of antioxidants can still perform their required function. If however, the antioxidant grows too large, solubility within the oil can be an issue. Indeed some manufacturers utilise oligomerised antioxidants in the starting lubricant formulation (Braid and Law, 1971). Addition of these preformed antioxidant additives have been found to give improved oxidative resistance, over certain monomeric antioxidant formulations (Frapin *et al.*, 2010).

The antioxidants used in gas turbine lubricants are hindered amines such as the monomeric species N-phenyl-1-naphthylamine (PANA) and 4,4-dioctyldiphenylamine (DODPA), or oligomerised hindered amines, as shown in Figure 2.4. Commonly, antioxidant packages

containing two or more different antioxidants are used as their combined effects have been found to be more effective than a single compound alone (Hunter *et al.*, 1993). It is this complicated additive package which can differentiate lubricants with similar base stocks from one another with regards to their thermal stability and is therefore treated as closely protected proprietary information by the lubricant manufacturer.

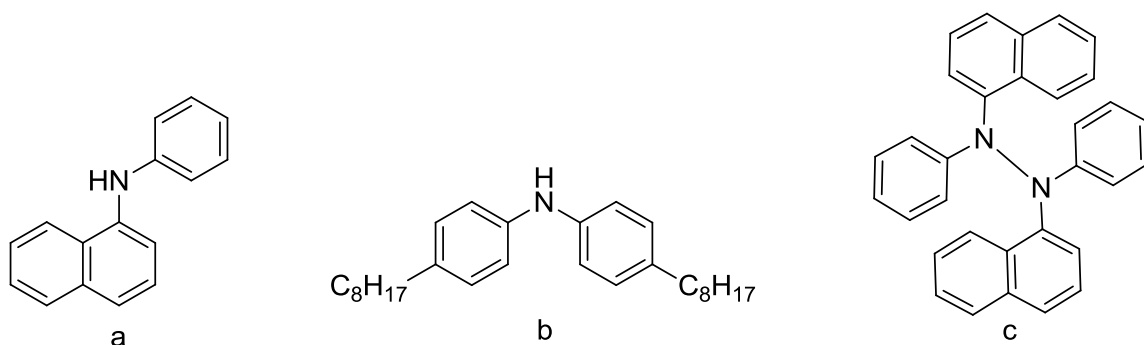


Figure 2.4 N-phenyl-1-naphthylamine (PANA) and (b) 4,4'-diocetyl-diphenylamine (DODPA) antioxidant compounds (c) Oligomeric antioxidant

Anti-wear

Tricresyl phosphate (TCP), shown in Figure 2.5, comprises between 1-3 % of the formulation of the vast majority of polyol ester lubricants. It is in the formulation due to its ability to prevent excessive wear of metallic components which may occur otherwise. TCP acts by chemical adsorbance at the metal surface therefore creating a barrier layer at the metal surface (Godfrey, 1965). During the boundary lubrication regime, as asperities come into contact, TCP is preferentially removed from the surface without metallic wear occurring. TCP can therefore reduce both abrasive and adhesive wear mechanisms which would otherwise occur when elastohydrodynamic films no longer provide full component separation (Bieber *et al.*, 1968).

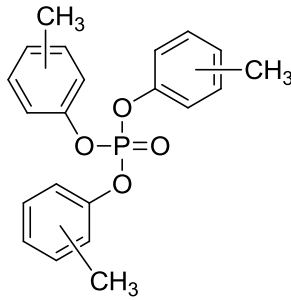


Figure 2.5 Tricresyl Phosphate (TCP), mixture of isomers, anti-wear additive

Metal Deactivation

Metal deactivator additives, like TCP, act by binding to the surface of metal components unlike TCP their purpose is to inhibit surface initiated reactions. These reactions can be problematic for two main reasons: they can cause corrosion to the metal surface or the metal can catalyse the degradation of the oil. Carboxylic acids such as nonanedioic acid and decanedioic acid are often used as well as 1,4-dihydroxyanthraquinone. As these additives are surface active they will compete with other additives, such as TCP, to occupy available metal surfaces.

Anti-foaming

The formation of oil foam following the introduction of air can cause oil pressure fluctuations due to inefficient pumping and lubrication film breakdown. In order to reduce the ability of the polyol ester oil to form stable foam, a high viscosity silicone based anti-foaming additive is commonly used. This additive in low concentrations (2-3 ppm) reduces foaming of the oil in heavily aerated conditions (Mortier, 2010).

2.3. Oil Specifications

From this point forward, only the 5 cSt (at 100 °C) polyol ester lubricants specified to the most recent SAE AS5780 (SAE, 2013) and MIL-PRF-23699 (US Department of Defense, 1997) specifications will be considered. These lubricants represent the vast majority of lubricants

used in the aviation gas turbine markets including most Rolls-Royce aviation gas turbines. They are therefore of the greatest interest.

These two specifications provide minimum requirements for number of physical and chemical properties as listed in Table 2.1. They each have two levels for which an oil brand can be qualified to, with the higher class demanding higher minimum specification requirements to be met. These levels are termed High Performance Capability (HPC) or Standard Performance Capability (SPC) in SAE AS5780 (2013) and High Thermal Stability (HTS) or Standard (STD) in MIL-PRF-23699 (US Department of Defense, 1997). In this thesis the SAE AS5780 (2013) definitions of the performance capability will be used and both HPC and SPC lubricants considered.

Table 2.1 Overview of the properties specified by SAE AS5780 (2013) and MIL-PRF-23699 (US Department of Defense, 1997)

Property	Definition
Total Acid Number (TAN)	A measure of lubricant acidity determined by the mass of potassium hydroxide required to neutralise one gram of oil (SAE AIR6056, 2014).
Kinematic Viscosity	A measure of the resistance of a fluid to deformation by shear stress or tensile stress.
Viscosity Stability	A measure of a lubricant ability to resist changes in viscosity over a period of time.
Density	The mass per unit volume at a specific temperature.
Pour Point	The lowest temperature at which the lubricant demonstrates flow under specific conditions.
Flash Point	The lowest temperature at which the lubricant can form an ignitable mixture in air.
Evaporation	A measure of volatility, the tendency of a fluid pass from the liquid to gaseous state.

Property	Definition
Foaming Tendency	The propensity of oil to form foam when aerated or mechanically agitated in air.
Sediment	The amount of solid particulate present in the lubricant.
Trace Metals	The determination of the concentration of metals within the lubricant.
Shear Stability	The change in lubricant viscosity as a result of shear stress.
Lubricant Compatibility	An assessment of the test lubricants compatibility with a range of other lubricant types.
Elastomer Compatibility	The assessment of a lubricants chemical compatibility with elastomeric materials.
Thermal and Oxidative Stability	The ability of a lubricant to resist degradation as a result of exposure to elevated temperature and oxygen (air).
Deposition Formation	The ability of a lubricant to resist the formation of solid deposits.
Hydrolytic Stability	The ability of a lubricant to resist degradation as a result of exposure to moisture (water).
Load Carrying Properties	An assessment of the lubricants ability to reduce mechanical wear under loaded conditions.
Pressure-Viscosity Coefficient	An assessment of the influence of pressure on lubricant viscosity
Thermal Conductivity	The ability of the lubricant to conduct heat
Electrical Conductivity	The ability of the lubricant to conduct an electric current
Heat Capacity	The amount of heat energy required to raise the one unit mass of lubricant by one unit of temperature.

2.4. Gas Turbine Oil System

2.4.1. Oil System Layout

The primary function of the oil system is to provide cooling and lubrication to the moving components within the gas turbine. Without oil present the heat generated in mainline bearing locations would lead to overheating and failure of the bearing within seconds. Additionally it serves to inhibit corrosion of metallic components and to transport any debris generated, allowing its removal from the system.

The oil system lubricates the mainline bearings which allow the rotation of the shafts supporting the large number of rotating aerofoils. In addition, oil is provided to the splines which allow shaft to shaft coupling and to gears in a number of locations. Squeeze films are also used to separate metallic components and thereby provide vibration damping where required.

The design of the oil systems varies with each engine; the schematic shown in Figure 2.6 represents a simplified general arrangement.

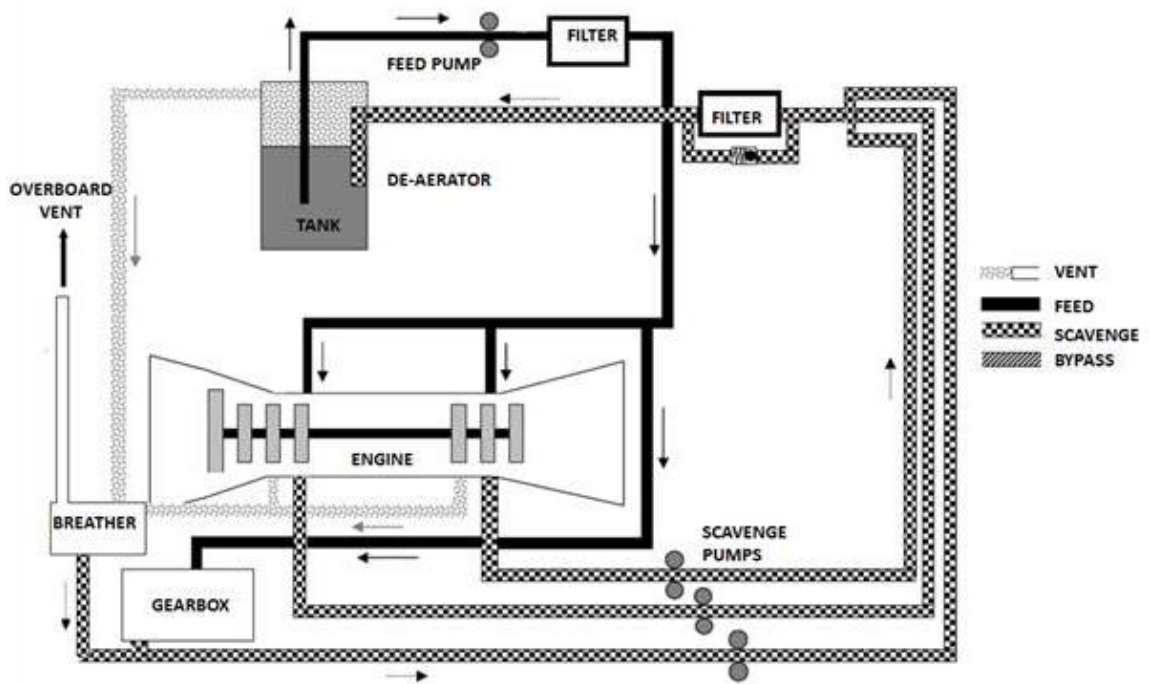


Figure 2.6 Oil system schematic

Oil Supply (Feed System)

Oil is drawn from the tank using a pump driven by the external gearbox through a network of pipes to the locations where it is required. To ensure that each location receives the flow which it requires, different sized oil jets, distributors and restrictors are used. Therefore, the ratio of oil provided to each bearing and gearbox location can be matched to its requirements simply by defining the restriction of a particular path. Oil jets are narrow orifices which provide a high velocity spray of oil onto the bearing or gear surface. Bearings can also be under shaft fed. In this instance the oil distributor relies on the centrifugal forces imparted by the rotating shaft to draw the oil to the bearing surface from a sump underneath the bearing raceway. The pump must be sized to ensure that the required oil flow can be delivered at all engine conditions. Therefore at conditions where the pump flow provided is too great, some of the oil is returned directly to the tank using the 'spill' system.

For the Rolls-Royce Trent® series of engines the total oil system volume is around 40 Litres with a maximum oil flow rate in excess of 100 Litres per minute. (Hart, 2008) This means that it will take only 25 seconds to complete one loop of the oil system.

Oil Scavenge System

After the oil has entered the bearing or gearbox it must be quickly and efficiently removed to prevent overheating. Centrifugal forces cause the oil to be flung outwards to the component walls where it rapidly decelerates. A scavenge outlet is positioned at the low point of the bearing chamber or gearbox with a specifically designed sump geometry to ensure recirculation within the chamber is minimised. Oil is recovered from each chamber by an individual scavenge pump element so that flow from each chamber can be guaranteed. After passing the scavenge pump, the individual scavenge flows are connected to create a combined scavenge flow which is returned to the tank. The temperature of the combined scavenge flow is monitored to provide an indication of the temperature within bearings and gearboxes.

The scavenge oil is heavily aerated with air which is entrained under agitation in the bearing chamber and gearbox, therefore the capacity of each scavenge pump must be much greater than the oil feed. This air is removed from the scavenged oil by the tank de-aerator before recirculation.

In order to detect the presence of magnetic debris in the scavenge system, Magnetic Chip Detectors (MCD) are positioned in the oil flow at a number of locations. These detectors capture metallic debris, consequently the quantity and type of material found on the MCD can be used as an early warning of bearing, gear or pump failures.

Sealing

Effective oil sealing is necessary to ensure losses from the oil system are minimised: leakage into high temperature gas path locations can result in fire or in an oil odour in the cabin bleed air. Sealing of dynamic components is a particular challenge which can be overcome in a number of ways including carbon seals, brush seals and labyrinth seals. Labyrinth seals are most commonly used to seal high temperature mainline bearings due to their mechanical and thermal resilience. Labyrinth seals are non-contacting, instead a series of seal fins on one component are arranged with a very tight clearance against another component. Although the tortuous leak path past the fins acts to reduce leakage, a positive air pressure must also be applied ensuring that the flow through the fins is air inwards not oil outwards. Air sealing methods will therefore result in air being introduced into the oil system, this results in oil becoming aerated, which must then be vented from the oil system.

Oil Vent System

In order for air sealing to be effective, the pressure outside the chamber must be higher than the pressure inside; therefore a vent system is incorporated. The capacity of the vent system is important: too low and sealing will not be achieved, too high and the efficiency of the engine will be reduced. Vent pipes, whilst intended to carry only air, will inevitably transport an air and oil mist/vapour. For this reason the vent system is commonly connected to centrifugal oil breather. The breather is a rotating housing containing metallic foam which allows oil to be centrifuged from the air. The oil is then returned to the oil system and the air, containing only vaporised oil components, is vented to the atmosphere. As previously mentioned, as the scavenge system also carries some air it is also necessary to vent the oil tank. As oil system venting preferentially favours the removal of the more volatile species present within the oil,

its use will have an influence on the composition of the remaining lubricant in the oil system. The extent of this influence will depend on the efficiency of the oil breather.

Oil Filtration

Inevitably, as the gas turbine begins to age, wear debris will form due to material removal from rotating components. If allowed to remain in the oil system this debris could result in indentation damage or 3-body abrasive wear of other components, it is therefore filtered from the oil system. Most gas turbines have oil filters on both feed and scavenge systems, the scavenge filter is usually the finer filter (~15-30 μm) and the feed a coarser filter (~125 μm). The scavenge filter is often fitted with a bypass which is activated in the event of a filter blockage, the feed filter is not, thereby insuring bearings are not exposed to large particles of debris.

In addition to the metallic and non-metallic debris generated from engine components, oil filters can also be exposed to particles generated by breakdown of the lubricant. If degradation products of the oil become larger than filter pores and are insoluble, they will be filtered out of the oil.

Heat Management

Heat generated in, or transferred to, bearing chambers and gearboxes must be removed in order to maintain the life and integrity of metallic components. Oil is used to transfer this heat away from critical areas but in doing so is subjected to substantial heating. This oil heating can occur from a number of sources. Heat can be transferred directly from gas path, the extent of which is dependent on the gas path temperature in the region which the oil operates. The sealing air used will also usually be of higher temperature than the lubricant and as such will result in heating. Heat generated in the chambers will be from shearing of the oil and frictional

heating from sliding surfaces. These combined heat sources mean that the total heat transferred to the oil in a large civil gas turbine can be in excess of 250 kW with peak scavenge temperatures up to 250°C (Hart, 2008).

This heat must then be removed from the oil; this is ideally achieved by transferring the heat energy to the fuel. Heat is transferred to fuel using a Fuel Oil Heat Exchanger (FOHE); this is preferable to air cooling as it retains the energy within the gas turbine thereby improving efficiency. Only where fuel cooling is not sufficient to reduce oil feed temperature to less than 100°C will additional air cooling be used.

Servicing

Oil changes in-service can be time consuming, expensive and introduce a level of risk so will only be undertaken when required, thus the lubricant will be required to perform, without oil change, for many thousands of hours. In order to reduce the risk of unexpected oil deterioration, operators will often undertake periodic oil sampling to assess oil quality.

Oil consumption will occur during engine use through seal leakage and through vent losses therefore oil will have to be regularly replenished to ensure it remains above a minimum level. Oil consumption and subsequent replenishment has the additional benefit of replacing a proportion of used oil with fresh lubricant thereby reducing the duration of time each molecule of lubricant is required to perform its function. If the life of a lubricant is longer than the time an oil molecule is likely to remain in the engine then the lubricant can be considered of “infinite life” (Edge and Squires, 1969).

2.4.2. Oil System Conditions and Demands

Operation of gas turbines, particularly in aviation applications, can be described as 'cyclic'. This term is used to describe the repetition of a defined series of operations, for example an engine could be started and idled for a short period before taxiing to the runway. It would then use high power at take-off and throughout climb. When at cruising altitude engine power will be reduced until the aircraft descends when the power will reduce further. Following landing, the aircraft will apply thrust reversers with high power before once again idling and shutting down.

Each of these specific engine conditions will impose different demands on the fluid, for example under high power take-off conditions temperatures, loads, pressures and rotation speeds will be very high as will be the oil flow rate. However, at 'max continuous' power - the maximum permissible sustained duration power, these conditions will be less severe and the oil flow will also be less.

When the engine is shutdown and the flow of oil ceases, the heat stored within large metal components, such as turbine disks, remains. This heat will flow into the previously oil cooled components. This phenomenon known as 'soak-back', means that some of the hottest conditions the oil is exposed to can actually be after the engine is shutdown. Some engines are designed such that the oil will flow out of the hot regions back to the tank on shutdown. However, thin films of oil still remain on components and in pipes which have the potential to form oil deposits. Oil systems can also be designed to ensure that oil pipes and chambers remain oil filled; this means that less air is present and that thin films are not available but the volume of oil which is exposed to temperature is higher.

In addition to the conditions mentioned previously, the oil will also come into contact with sealing air; the oxygen in the air will react with the lubricant at high temperature thus promoting its degradation. This process can also be catalysed by the presence of the metals found within the oil system, expatiating oil degradation (Naidu *et al.*, 1984). The combined effect of all of these oil system conditions means that the lubricant is exposed to particularly severe conditions which can result in its degradation.

2.5. Bulk Thermal Oxidation Degradation

This section describes the thermal oxidative degradation processes which occur in the fluid bulk. Bulk degradation refers to chemical and physical changes to the oil in the system as a single homogenous fluid. This process can therefore be differentiated from degradation mechanisms which occur in localised regions, for example deposition. This process requires the presence of oxygen at an elevated temperature (Koh and Butt, 1995).

Significant degradation of the lubricant can result in physical property changes, such as an increase in viscosity which can significantly influence fluid transport (Karis *et al.* 1999). This can cause damage to pumps and a reduction of oil delivery to some regions of the oil system, this issue can ultimately result in significant damage and an IFSD of the engine.

2.5.1. Thermal Oxidative Mechanisms

The primary process by which polyol ester lubricants degrade is oxidation (Naidu *et al.*, 1986) because thermal degradation in the absence of oxygen is considerably slower (Fuchs and Zeman, 1993). Gas turbine oil systems, as discussed previously, contain large amounts of air, resulting in oxidative mechanisms being the most relevant.

In order to understand how oxidation reaction mechanisms propagate it is important to first understand the relative reactivity of the groups within the polyol ester chain. Sniegowski (1977) showed the relative reactivity of the CH₂ groups of a model ester, neopentyl hexanoate as shown in Figure 2.7.

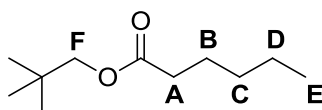


Figure 2.7 Neopentyl hexanoate model ester

If the rate of reaction of the alkyl end group 'E', the least reactive group, is deemed to be unity, then the relative reactivity of the other groups can be described as follows. The methylene group 'A' is 2, the internal methyl groups 'B'-'D' would be 15 and the alcohol CH₂ fragment ('F'), 4. This shows that the internal methyl groups on the alkyl chain are the most susceptible to degradation reactions.

However, this model compound contains minimal steric hindrance around the alcohol component of the ester. It has been shown that the use of a pentaerythritol alcohol substituent leads to an increase in oxidative stability of >10 times (Bakunin and Parenago, 1992).

Oxidative reaction of the alkyl chain occurs via a free radical mechanism initiated by the formation of a carbon radical as shown in Figure 2.8 A (Karis *et al.* 1999).

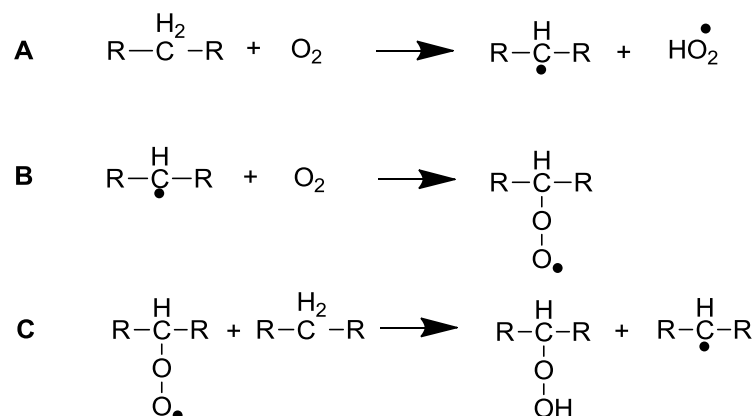


Figure 2.8 Free radical degradation initiation steps

The carbon radical can then subsequently react with a further oxygen molecule to produce a peroxy radical (Figure 2.8 B) which can then abstract a further proton to form a hydroperoxide (Figure 2.8 C). This proton can be abstracted from the same chain as the previous reaction (intrachain) or another chain (interchain).

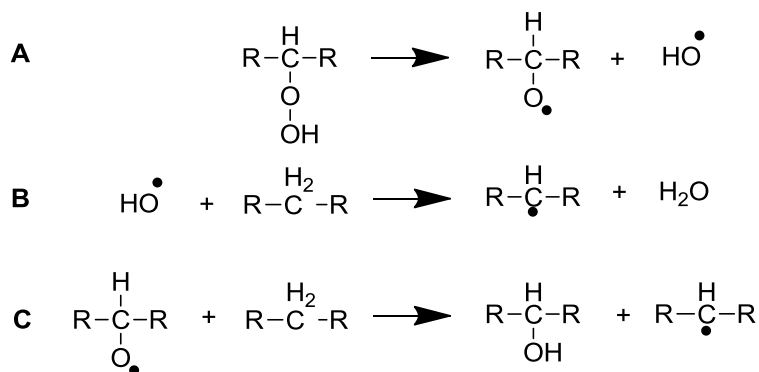


Figure 2.9 Interchain free radical reaction mechanisms

The interchain reaction sequence, as shown in Figure 2.9, requires first that the hydroperoxide radical decomposes to an alkoxy radical and a hydroxyl radical (Figure 2.9 A). The hydroxyl radical can react with a further alkyl radical to give water and a carbon radical (Figure 2.9 B). The alkoxy radical, following an interchain reaction, results in the formation of a hydroxyl group on the chain and a third carbon radical (Figure 2.9 C). It should be noted that one

carbon radical formed through oxidation has created three further carbon radicals, hence this mechanism is self-propagating. Termination of the free radical reaction will only occur when two radical species combine to produce a neutral species. The substitution of a hydroxyl group into a carbon chain can have a significant influence on its physical properties; due to an increase in hydrogen bonding between chains. Karis *et al.* (1999) reported that this increase was greatly in excess of the increase expected by an increase in chain size alone, thus emphasising the marked influence which oxidation can have on lubricant properties.

Intrachain reactions are possible by mechanisms similar to those seen which proceed via an interchain mechanism. (α,γ)-Abstraction can lead to the formation of a β -hydroxy ketone which will also increase lubricant viscosity through increased hydrogen bonding. (α,δ)-Abstraction however, can lead to chain cleavage resulting in the formation of ketone and carboxylic acid products (Jensen *et al.*, 1981).

As intrachain reactions require a minimum of a three carbon section of alkyl chain, reactivity depends on the chain length. The order of reactivity is therefore as follows: octanoate > heptanoate > hexanoate > pentanoate. As pentanoate esters only have two internal CH_2 groups, they have a limited number of reaction mechanisms possible and therefore their reactivity will be significantly lower as shown by Nakanishi *et al.* (1997).

The Role of Antioxidants

As discussed previously, the primary mechanisms associated with polyol ester breakdown are via free radical mechanisms. Therefore, if the free radical initiators which would otherwise propagate degradation reactions are removed then the rate of degradation will decrease. Antioxidants are included in the lubricant formulation to act as radical scavengers by

preferentially reacting with radical initiators thereby increasing the thermal stability of the lubricant (Mousavi *et al.*, 2006).

The secondary aromatic amines such as DODPA and PANA which are commonly included in polyol ester aviation lubricants have been shown to perform well in reducing the degradation of these lubricants (Hunter *et al.*, 1993).

Figure 2.10 shows an antioxidant mechanism by which radical scavenging can occur. It can be seen that the antioxidant reacts with the radical by the donation of a proton to form a stable product and an antioxidant radical. Subsequent reaction of the antioxidant radical with a further radical initiator gives a neutral species.

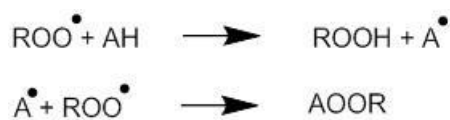


Figure 2.10 Antioxidant radical scavenging example mechanism

Sniegowski (1982) reported the depletion of the original PANA and DODPA antioxidants in oil samples taken during a 180 hour gas turbine test. The two antioxidants were found to follow an approximate first order reaction profile. PANA however was found to deplete most readily with only 35 % remaining after 180 hours, DODPA however, remained at 80 %. It should be noted that these findings are complicated somewhat by addition of lubricant during the test which was required in order to replenish losses.

A detailed study of the fate of PANA, N-(4-octylphenyl)-1-naphthylamine (OPANA) and DODPA, antioxidants was conducted by Zeman *et al.* (1986 & 1987). They showed that these antioxidants, as a result of undergoing free radical scavenging reactions, formed dimers and trimers with other antioxidant molecules. This process of oligomerisation and subsequent

polymerisation of the antioxidant species does not necessarily inhibit the ability of the antioxidant to reduce oil degradation. Oligomerisation, however, does somewhat complicate the discussion of antioxidant depletion. Whilst antioxidants in their original form are depleted, the products which they become are often still active antioxidants in their own right. Nevertheless if polymerisation of antioxidants progresses the molecule can become too large to remain soluble within the oil and therefore result in particulate or deposit formation (Zeman *et al.* 1986 & 1987). As shown by Zeman *et al.* (1986 & 1987), the number of possible antioxidant reaction products is very large and therefore discussion of antioxidant depletion in terms of the removal of the original species still provides a useful, if simplified, description of oil ageing.

Physical and Chemical Property Changes as a Result of Degradation

As the number of possible reactions which polyol ester base stocks and their additives can undergo when thermal degradation occurs is extensive, it is very difficult to fully describe chemically the degradation of a formulated lubricant product. However, it is more practical to determine major degradation products and to understand the influence which these key reactions have upon the physical properties of the lubricant. Table 2.2 provides a summary of some of the most significant physical and chemical property changes, the influence they have on lubricant performance and a description of chemical reactions which cause them.

Table 2.2 Summary of physical and chemical property changes as a lubricant degrades

Physical/ Chemical Change	Chemical Species Responsible	Effect on Lubricant Performance	Discussion
Kinematic Viscosity (Increase)	Formation of higher molecular weight species and the addition of hydroxyl groups to the chain.	Transport of the lubricant, particularly at low temperature becomes more difficult. This can cause strain or damage to pumps and inefficient lubrication.	As part of the degradation process high molecule weight species can begin to accumulate within the lubricant, these high molecular weight species are intrinsically of high viscosity. However, one of the most significant drivers of viscosity increased is an increase in intramolecular hydrogen bonding. Hydrogen bonding is increased by the addition of hydroxyl groups to carbon chains as a result of oxidative degradation. (Ali <i>et al.</i> , 1978)
Density (Increase)	Formation of higher molecular weight species and the evaporation of lower molecular weight species.	Similar to the effect of kinematic viscosity increase.	Density increases are primarily due to accumulation of high molecular weight species and the loss, by evaporation, of those of lower molecular weight. This gives rise to a lubricant which is denser than when new.
Volatilisation (Increase)	Loss of more volatile species present in the original oil formulation and those formed by degradation.	Leads to an increase in viscosity and density. Volatilisation also leaves the remaining lubricant inherently less thermally stable.	The most volatile compounds present within the lubricant will be preferentially evaporated and therefore can leave the oil as a vapour. The most volatile species tend to be those of lowest molecular weight. Therefore evaporation will leave an oil with a higher molecular weight, viscosity and density (Wang <i>et al.</i> , 2004). The less volatile species which remain are also likely to be less thermally stable.

Physical/ Chemical Change	Chemical Species Responsible	Effect on Performance	Lubricant	Discussion
Total Acid Number (TAN) (Increase)	Oxidation products - carboxylic acids, aldehydes and other mildly acidic organic species (Kohler and Heeb, 2001).	Mild increases in oil acidity do not affect oil performance. A heavily acidic lubricant however can result in chemical attack of elastomer seals and also act to promote metallic corrosion.		These products form as a result of the free radical degradation of the base stock initiated by oxygen. Once formed, the presence of these species within the oil will increase its acidity. As acidic species are often more volatile than the majority of the lubricant, acidity is dependent on their evaporation rate
Flash Point (Decrease)	Volatile oil breakdown products	Increase likelihood of oil fire.		Ignition of the lubricant will occur from the vapour phase, therefore can occur following the evaporation of new oil. As oil degrades, ignition of volatile degradation species can also occur. An increased concentration of volatile species can lead to a lower flash point, and therefore more flammable oil. (Wirtz and Zeman, 1987)
Colour (Darkens)	Oxidation products - Carbonyl groups and other unsaturated hydrocarbon groups.	No significant influence on performance. In fact some lubricants are dark in colour when new if certain unsaturated additives are used.		These unsaturated groups absorb certain light wavelengths and thereby create the colour. The progress of degradation results in an increase in these products, and therefore a darkening of the lubricant. A dark colour may or may not be indicative of degradation.(Mousavi <i>et al.</i> , 2006)

Physical/ Chemical Change	Chemical Species Responsible	Effect on Performance	Lubricant	Discussion
Insoluble content/ particulate (Increase)	Insoluble high molecular weight compounds	Blockage or restriction of filters, oil jets and other small orifices. This can result in an inability to deliver lubricant to required areas.		As a result of degradation high molecular weight compounds can form from both base stock and additives. If these species become sufficiently large, they will no longer be soluble within the oil and therefore form particulate species.

2.5.2. Laboratory Test Methods

Laboratory test methods are small scale methods which allow the operator to generate degradation chemical and physical property data much more quickly, simply and inexpensively than rig or engine scale testing. Laboratory methods should allow key test parameters to be controlled more tightly than large scale testing and therefore allow improved repeatability as well as reproducibility. Finding a compromise between practicality and accurate replication of engine degradation processes is a difficult challenge. It is for these reasons that a number of these methods for thermal or thermal oxidative stability form part of the SAE AS5780 (2013) lubricant specification. These methods are as follows:

- ASTM D4636 (ASTM International, 2009), Corrosiveness and Oxidation Stability of Light Oils (Metal Squares) (Incorporating - Federal Standard 791, Method 5308 (US Defense Logistics Agency, 2007));
- Defence Standard 05-50 (Part 61), Method 9, Resistance to Oxidation and Thermal Decomposition (UK Ministry of Defence, 2003);
- Federal Standard 791, Method 3411, Thermal Stability and Corrosivity of Aircraft Turbine Engine Lubricants (US Defense Logistics Agency, 2007);
- Turbomeca Thermal Ageing Method (No published method, SAE AS5780, Appendix Item, 2013).

Since the initial development of these methods, advancements in lubricant chemistry, engine technology, laboratory methodology and analytical techniques have occurred. Therefore, full critical reviews of these test methods and their applicability today can be found in § 4.2.

2.6. Lubricant Deposition

Lubricant deposition describes the breakdown of lubricants to produce oil insoluble solids on the surfaces with which it comes into contact. Lubricant deposits, if allowed to accumulate, have been known to cause restriction or blockage to lubricant flow. As the restriction of oil flow to many engine locations has the potential to result in an In Flight Shutdown (IFSD), it is critical for engine manufacturers to be able to evaluate and select lubricant brands based on their ability withstand thermal stresses without the formation of deposits.

2.6.1. Deposition Reactions

As discussed previously, lubricants can degrade through exposure to temperature in the presence of oxygen, resulting in a change in the bulk lubricant properties. Generally, the presence of antioxidants inhibits the reaction sufficiently that the lubricant remains fluid. Deposition, however, is a localised phenomenon whereby the lubricant reacts further to form solid, oil insoluble products which commonly adhere to metal surfaces such as pipe walls. Naidu *et al.* (1986) describe lubricant deposition as being a result of hot spots in the oil system resulting in the temperature exceeding the thermal capability of the lubricant and antioxidant system.

Oil deposits derive from further reaction of the ketone, aldehyde, alcohol and carboxylic acid species formed as a result of free radical degradation (Karis *et al.*, 1999). The mechanism by which high molecular weight deposits form is debated in the literature, however, Naidu *et al.* (1984) propose an aldol condensation reaction, shown in Figure 2.11, to form polymeric unsaturated ketone groups from aldehyde or ketone precursors.

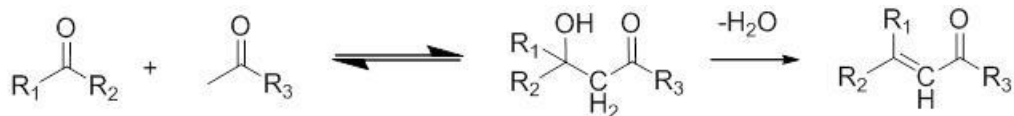


Figure 2.11 Aldol condensation mechanism

Conversely, aldol reactions normally require strong acid or base conditions in order to be initiated, which are not found in the oil. Bakunin and Parenago (1992) postulated that high temperatures could initiate the reaction without the need for acid or base conditions.

Bakunin and Parenago (1992) also suggested the Knoevenagel-type condensation reaction which can easily occur when methylene groups are activated by the presence of two electron withdrawing groups such as ketones, esters and aldehydes. If a chain has already undergone oxidation and is therefore activated, condensation of ketone or aldehyde groups can occur. This mechanism is shown in Figure 2.12.

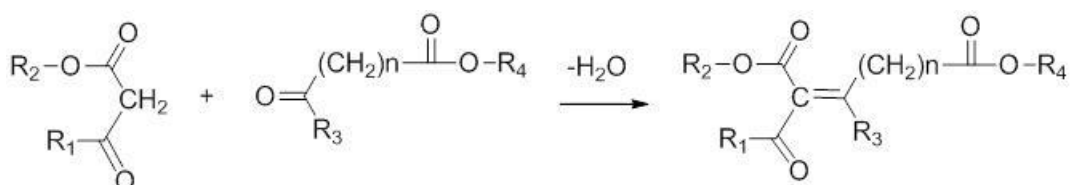


Figure 2.12 Knoevenagel condensation mechanism

A third possible polymerisation route, suggested by Bakunin and Parenago (1992), is the esterification of polyfunctional oxidised degradation products to create a wide range of possible polymer products. This mechanism is shown in Figure 2.13.

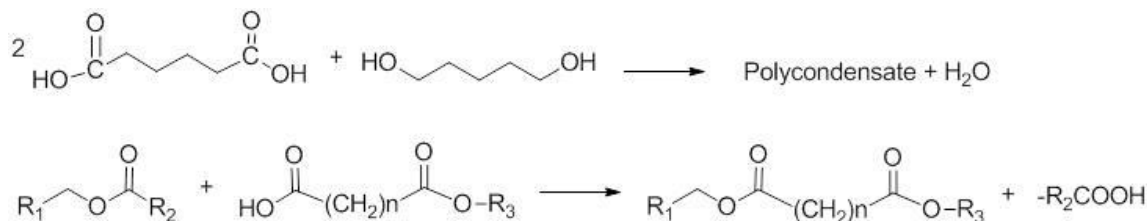


Figure 2.13 Polymerisation by esterification and transesterification

It should be noted that a number of these polymerisation reactions which occur as a result of advanced degradation or deposition, result in the formation of water as a by-product. Due to its relatively high volatility when compared to the lubricant, water would be lost through the gas turbine vent system. Therefore, in laboratory methods, venting of degradation by-products, including water, should be considered.

The exact mechanism or mechanisms, by which polymerisation occurs to form deposits is not known, with many in the literature simply referring to polymerisation processes leading to deposition (Zeman *et al.* 1986 & 1987; Maier, 1986; Bartl *et al.*, 2008). The work of Maier *et al.* (1989) showed that service derived oil deposits are rich in oxygen, strengthening the hypothesis that they form by further reaction of oxidation products. It is likely, that due to the wide variety of oxidation products formed by initial free radical degradation processes, a number of different polymerisation reactions occur. This reinforces the need, in laboratory testing, to degrade the oil in a manner representative of lubricant degradation in the engine, therefore creating a similar range of products from which solid deposits can form.

In addition to the breakdown of the oil base stock, polymerisation of lubricant additives can also occur to form large oil insoluble products which will also give rise to solid deposits (Zeman *et al.*, 1993). The formation of large insoluble products derived from antioxidant species was reported by Zeman *et al.* (1986 & 1987). However, the proportion of antioxidant species which reach the required size to become insoluble, is likely to be small.

As deposit formation rate depends primarily on the breakdown of the base stock it is influenced by the specific composition of the oil formulation. D’Orazio *et al.* (1976) stated that a lubricant comprised of esters formed from longer chain carboxylic acids had a greater propensity to form deposits than shorter chain esters. This can be explained, as discussed

previously, by the increased reactivity of methyl groups further from carbonyl groups, longer chains being more susceptible to initial and subsequent reactions than short chains. They also noted that where more hindered alcohol components were used, the stability of the lubricant increased. This is presumably due to an increase in steric hindrance around the reactive sites.

2.6.2. Transport and Fouling

In addition to the chemical mechanisms associated with deposition, it is also important to consider where these reactions take place – in the bulk, at the boundary or the surface.

The formation of most fouling deposits which have formed as a result of a chemical reaction, can be described by the general reaction shown in Figure 2.14, this accepted general reaction can be found widely in the literature including Watkinson and Wilson (1997).

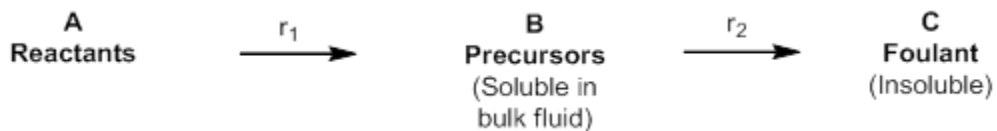


Figure 2.14 General fouling reaction

If we apply this general reaction to the deposition reaction discussed previously we can modify the chemical equation as shown in Figure 2.15.

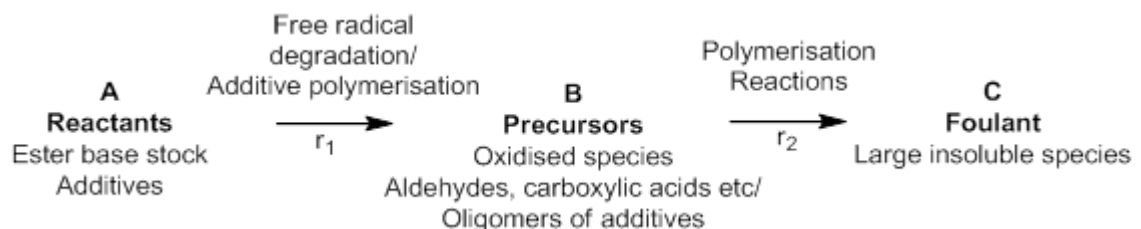


Figure 2.15 Diagram of the proposed lubricant deposition fouling reactions

Panchal and Watkinson (1994) propose three potential cases by which deposition can occur, differing in the reaction zones in which reactions r_1 and r_2 occur. These zones are the fluid bulk, thermal boundary and the wall. The cases are as follows:

- Case 1: Precursor (r_1) is formed in the bulk
- Case 2: Precursor (r_1) is formed at the boundary layer
- Case 3: Precursor (r_1) is formed at the wall

Case 1 and 2 can be further sub divided depending the location which reaction r_2 occurs.

- Case 1a: Insoluble foulant (r_2) formed at the wall
- Case 1b: Insoluble foulant (r_2) formed in the bulk
- Case 2a: Insoluble foulant (r_2) formed at the wall
- Case 2b: Insoluble foulant (r_2) formed at the boundary layer

This is shown diagrammatically in Figure 2.16.

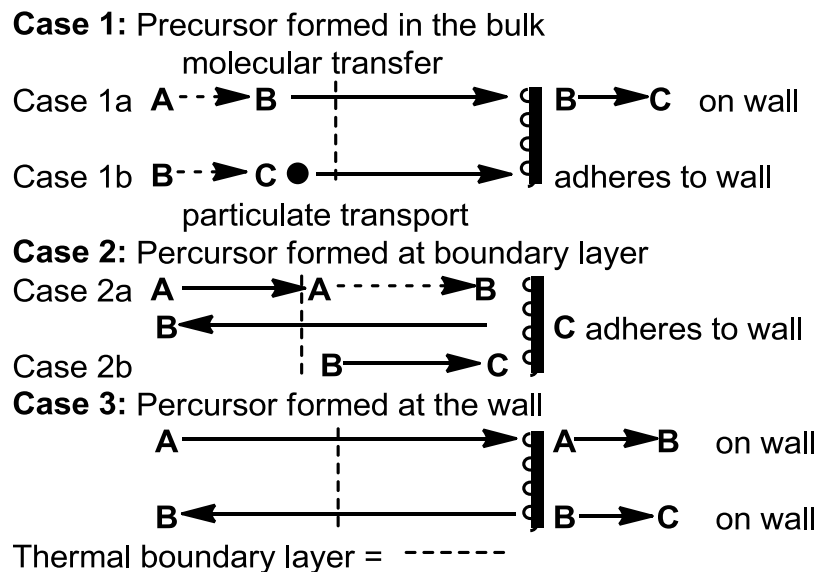


Figure 2.16 Diagram of potential fouling cases

The presence of deposit precursors in the bulk fluid is widely reported in the literature (Bakunin and Parenago; 1992, Karis *et al.*, 1999; Kunina *et al.*, 1991; Naidu *et al.*, 1984) therefore cases 2a, 2b and 3 are less likely mechanisms. Insoluble products are commonly found in the bulk fluid at much lower levels than the amount found in wall deposits and as such, case 1b is less likely to be the major deposition mechanism (Edge and Squires, 1969). This leaves case 1a as the most likely fouling mechanism in the case of polyol ester lubricant deposition. Precursors are formed in the bulk, and then transferred to the wall where the polymerisation reactions and adhesion occurs. Whilst it is possible that fouling occurs by a combination of a number of mechanisms, it is postulated that case 1a is the major mechanism.

The rate at which deposition occurs will depend on a number of factors; these factors are discussed in Table 2.3.

Table 2.3 Major factors that influence the deposition formation rate

Factor	Influence on deposit formation rate
Temperature	Temperature has a direct effect on the rate at which both free radical oxidative degradation and polymerisation reactions occur. Temperature will also influence the type of reactions which occur, depending on whether the activation energy of the specific reaction can be achieved (Naidu <i>et al.</i> , 1986).
Residence Time	The time which the oil spends at temperature in the reaction zone (e.g. the wall) will affect the amount of deposit formation. If the oil or degradation products are transported out of the reaction zone prior to the formation of a solid at the wall, then deposition will not occur. Therefore if residence time is minimised then deposit will also be minimised (Moses, 2002)
Shear Stress	Shear stress at the surface can influence the rate at which deposits form. High shear stress will facilitate the removal of deposits and deposit precursors and therefore reduce fouling (Young <i>et al.</i> , 2011).
Oxygen Presence	As the deposition process is preceded by the formation of bulk oxidation products, the availability of oxygen as a reagent will therefore affect the rate at which deposits can form (Karis <i>et al.</i> , 1999).
Film Thickness/ Surface Area	The lubricant film thickness or the surface to volume ratio will have an influence on a number of factors linked to deposition. A large surface to volume ratio renders a greater proportion at the interface with both oxygen (in the air) and metal walls (Diaby <i>et al.</i> , 2009). This can therefore be expected to give greater deposit formation than a smaller area. However, a large surface area also allows more volatilisation of the oil or its constituents to occur which conversely, could reduce deposit formation.
Catalytic Surface	The presence of a catalytic metal surface has the potential to increase the rate at which deposition reactions occur. Therefore the type of metal surface used will affect the rate of deposition formation (Zeman <i>et al.</i> , 1984).

2.6.3. Lubricant Deposition Types and Conditions

The following deposition conditions are a selection of the key and most relevant deposition conditions as defined by the now discontinued, European Deposition Group (Maier, 1989)

Mist and reclassified mist

Fine droplets of oil can be suspended in air to form a mist or aerosol. Mists, following impact with a metal surface can coalesce to form a layer of oil at the surface; this oil can therefore form a deposit on the hot surface. Oil mist is most commonly found within the bearing chamber vent pipe as a result of oil mixing with sealing air under high shearing conditions.

Thin Films

A thin layer of oil which forms on a heated surface will have a high surface to volume ratio. This can lead to a thin layer of deposit being formed; this deposit can then build up on a cyclic basis. Deposits of this type are most commonly formed under shutdown condition where oil flow ceases and drains back to the tank, this leaves oil wetted surfaces in areas such as hot pipe walls.

Thick Films

Thick films are regions where oil is present with a low surface to volume ratio. Volatilisation under these conditions is less than that of thinner films and therefore if held in a high temperature region for a long enough period of time, large deposit areas can form. Thick, stationary films are not usually formed by design but can occur in regions where puddles of oil are allowed to form.

Vapour Phase

Deposits can form from evaporated oil or oil fractions, these vapour fractions react with oxygen to create degraded species. The degraded species will then accumulate on hot metal surfaces at which point they can form solid deposits. These conditions are most commonly associated with bearing chamber vent pipes.

The presence of transient conditions within the gas turbine oil system, due to the power setting of the engine at a particular point in time, mean that a particular location in the oil system may experience transient deposit forming conditions. Therefore deposition formation can be complicated by more than one of the above deposit types forming in a given region.

2.6.4. Laboratory Test Methods

Laboratory test methods vary in the particular deposition conditions which they attempt to simulate but can be most simplistically be spilt into two categories: single phase and two phase (oil and air mixtures). As there are many conditions under which lubricant deposits can form, a number of deposition test methods are used by the aviation lubricant industry. Each of these methods has positive and negative aspects as a result of attempting to find a compromise between practicality and replication of engine conditions. A review of these available techniques is given in § 5.2.

2.7. Deposition Reduction Techniques

Modification of the environment in which the oil is used to make it more resistant to lubricant deposition is a topic which has been studied for a number of years. The most obvious solution, decreasing the temperature, is greatly undesirable due to the impact on gas turbine efficiency (Rajadurai, 2003). Another possibility, deoxygenation, has been studied widely for reducing

deposits formed by jet fuel (kerosene), however, due to the current widespread use of air sealing in oil systems, this would require major advances in seal design (Taylor, 1974; Hazlett, 1991; Ervin and Williams, 1996; Spadaccini and Huang, 2003).

Another, potentially more practical method to reduce deposition, is to modify the surface at which the deposits form. Ali *et al.* (1979), showed the presence of metal catalysts under thermal oxidative degradation conditions led to a faster rate of degradation and a larger proportion of higher molecular weight species. Ali *et al.* also showed that degradation depended on the type of metal used, reporting that low carbon steel was the most active followed by stainless steel and copper. This result was in direct disagreement with Diamond *et al.* (1952), who found that copper was more active than iron. However the work of Diamond *et al.* (1952), Brook *et al.* (1953) and Chakraverty (1963) showed that these metals can act as homogeneous catalysts and therefore their catalytic activity will depend on their activity with the oil once dissolved. Klaus *et al.* (1973) showed that copper is more readily dissolved within ester lubricants and therefore would be in higher concentration for catalysis.

Zeman *et al.* (1984) used Differential Scanning Calorimetry (DSC) to study the degradation of polyol ester based lubricants in the presence of a range of metals. They reported that the catalytic activity of metals was influenced by both temperature and the antioxidants present in the oil formulation.

For oil containing DODPA and phenothiazine at 260 °C, metal activity was as follows:

Fe >> Cr/Ni steel >> Zn > Ta > Ni >> Ti > Al > Mo

For the same oil with DODPA and OPANA antioxidants at 260 °C, metal activity was as follows:

Fe >> Zn > Cr/Ni steel, Ni > Ta > Al, Ti > Mo

2.7.1. Surface Coating

Steel, which is used routinely within the gas turbine oil system, has a significant catalytic activity in oil degradation and subsequent deposit formation. Yet steel also has a number of benefits which prohibit its complete substitution from the oil system: it has good mechanical and thermal properties and is relatively low cost. Therefore coating the surface of steel could provide deposit resistant pipes and other components, without compromising on component integrity.

Coating of metal surfaces can be achieved by a number of different techniques including Physical Vapour Deposition (PVD) and Chemical Vapour Deposition (CVD)

Physical Vapour Deposition (PVD)

Physical vapour deposition is a general term for any vapour deposition technique where the vapour source is a solid or liquid surface. PVD techniques create a vapour flux of the required film material which is condensed on the surface of the substrate. There are a number of different PVD techniques which can be differentiated by the method of vapour formation (Mattox, 2003).

All PVD techniques are generally undertaken in a vacuum, the use of a vacuum environment is to decrease gas particle density, limit gaseous contamination, establish partial pressures and control gas flow. The quality of a vacuum is usually defined by pressure, mean free path and the arrival rate ratio. Arrival rate ratio is the ratio of film vapour to that of residual gas atoms and can be improved by either reducing the pressure or increasing deposition rate (Mattox, 2010).

Physical deposition techniques are line of sight techniques, meaning that they are only able to deposit on surfaces which are within a direct straight line path of the source. This limitation means that the coating of irregular surfaces and pipe interiors is very difficult and PVD techniques are most suitable for use on accessible surfaces (Mattox, 2010).

Chemical Vapour Deposition

Chemical Vapour Deposition (CVD) techniques are based on homogenous or heterogeneous chemical reactions. They employ gaseous, liquid and solid chemicals as sources of the elements from which the film is made. Therefore the range of possible coatings is dependent of the available reaction products. CVD techniques, unlike PVD can allow complex geometries without a line of sight to be coated (Glocker and Shah, 1995).

2.7.2. Surface Modification

As part of a previous Rolls-Royce and University of Birmingham EngD project, it was found that surface finish and surface chemistry have an influence on lubricant deposit formation. (Askins, 2010). Askins (2010) found that if the internal surface of a pipe was altered, for example through the introduction of a weld bead, an increase in deposit mass formed could be seen. Askins showed that some of the metals within stainless steel alloy were more catalytically active than others. Iron was found to be more active than stainless steel in promoting deposition, whereas heat treatment to increase the chromium oxide layer was found to decrease deposition rate. Therefore surface modification of the existing steel surface, both in terms of finish and chemistry, without the need for coating, could potentially reduce the deposit formation rate.

Nitriding

Nitriding is a heat treating process which alloys nitrogen into the surface of the metal to create a passive case hardened surface. This technique is predominantly used for steels, however, it is possible to also to apply the technique to titanium and aluminium surfaces.

Selective Oxidation

Various selective oxidation techniques can allow the selective oxidation of a particular metal present within an alloy to be oxidised. For example, chromium can be preferentially oxidised over iron to produce a passive layer. This technique can be applied to a number of metal and metal alloy surfaces.

Anodising

Anodising is an electrolytic passivation process which increases the natural oxide layer present on the surface of metals and metal alloys. Applying an electrical charge with the surface which is being treated acting as the anode, produces a passive and hardwearing oxide surface. Anodising is commonly used for aluminium but can also be used on titanium and zinc amongst other metals.

Acid Pickling

Immersion in an acid solution removes surface impurities producing a fresh layer which is then allowed to form a natural oxide layer. This oxide will passivate the surface and potentially reduce its catalytic role in oil deposit formation.

Electropolishing

Electropolishing is an electrochemical process where the component is immersed in an electrolyte and connected in a circuit with the component itself acting as the anode. The

surface of the component is dissolved into the electrolyte and transferred to the cathode. Material removal from the component surface results in an improvement in surface finish.

2.8. Lubricant Tribology

2.8.1. Lubrication Regimes

Aviation lubricants most commonly lubricate ball bearings, roller bearing and gears; they therefore operate under the elastohydrodynamic regime. Elastohydrodynamic lubrication is defined by a small contact area resulting in high contact pressures (1-3 GPa), this results in elastic deformation of the surface and an increase in lubricant viscosity (Hamrock *et al.*, 2004).

During engine start up, prior to the formation of an elastohydrodynamic film, boundary lubrication will occur resulting in asperity contact between the metal surfaces. It is during this regime where anti-wear additives such as TCP are required to provide sacrificial protection (Godfrey, 1965, Bieber *et al.*, 1968).

2.8.2. Aviation Test Methods

Currently the aviation industry evaluates oil via a number of methods each aimed at replicating particular tribological conditions. The SAE AS5780 (2013) specification includes three tribology methods listed below:

- Aviation Lubricant Tribology Evaluator (ALTE) SAE ARP6255, (SAE International, 2013).
This method assesses abrasive and adhesive wear in pure sliding contact.
- Ryder Gear Method, Method 6508 (US Defense Logistics Agency, 2007). This method assesses gear scuffing interactions.

- WAM High Speed Load Capacity Test Method, SAE ARP6156 (SAE International, In draft, 2010). The test consists of a rolling/sliding contact between a ball and disc test specimens. The test characterises the oil for wear, scuffing and traction (friction) coefficient.

It should be noted that all testing for the purpose of lubricant specification approval is conducted on fully formulated un-aged lubricant. Therefore limited data is available on how individual additives contribute and on how tribological performance varies as the lubricant ages.

2.8.3. Influence of Thermal Oxidation on Tribological Performance

As discussed earlier in this chapter, when oil is degraded by thermal oxidation it undergoes chemical and physical changes. Viscosity and density of the oil both increase, addition of oxygen containing functional groups also occurs (Karis, 1999). Wu *et al.* (2013) studied the effect of oxidative degradation of a simple di-2-ethylhexyl sebacate lubricant in terms of its ability to reduce wear. They found that under mild degradation, wear of the steel specimens increased. As oil oxidation progressed further, wear performance improved from that of the fresh lubricant. Wu *et al.* attributed this to the incorporation of polar oxygen containing groups within the chain increasing the lubricating performance.

2.8.4. Tricresyl Phosphate Influence

Han and Masuko (1998) determined the tribological performance of a range of ester based lubricants using a four-ball-tribometer. To each of these lubricants a range of anti-wear additives, including TCP, were added in a variety of concentrations. They reported that whilst low concentrations of TCP caused wear to reduce, higher concentrations had the opposite

effect. This increase in wear was attributed to the excess adsorption of phosphates to the surface when TCP was in high concentration resulting in corrosion-like wear mechanisms.

2.9. Summary

In recent years performance improvements in gas turbine lubricants have been small, while developments in gas turbine technology have meant that the thermal and mechanical stresses which the lubricant is exposed to, are increasing. Therefore there is a greater requirement to be able to assess lubricant performance, particularly in the areas of thermal stability and tribological performance, to ensure the capability of the lubricant is not exceeded.

Whilst methodology does exist to assess both thermal oxidative and deposition formation, there is scope for development of methodology which is more representative of the oil system conditions which they mimic. Such methodology would also allow testing and validation of surface modifications, like those discussed in this section, to determine their ability to reduce lubricant deposition.

Additionally, the area of lubricant tribology is one where understanding of the influence of lubricant formulation is less than other areas of lubricant performance. Therefore, research is required to determine the individual and combined effects which lubricant additives have on mechanical wear.

CHAPTER 3: METHODS AND MATERIALS

3.1. Methods

3.1.1. Thermal Oxidative Stability Methods

Ministry of Defence, Defence Standard 05-50 (Part 61) Method 9

The methodology used in § 4.3.1 was as described in Ministry of Defence, Defence Standard 05-50 (Part 61), Method 9 (2003). A schematic of the test equipment used is shown in Figure 3.1 and can be summarised as follows. For the purpose of this thesis, the method title is abbreviated to Method 9. The equipment consists of a borosilicate glass boiling tube containing the oil sample (50 mL), which is heated externally using an aluminium heater block. At the start of test, the oil sample is placed into a weighed sample tube and heated at the required temperature. During the test, air is introduced through a central glass tube (at 250 mL min⁻¹), which flows through the oil and is allowed to exit via two outlet ports at the top of the vessel. Following the required test duration, (a range of durations are explored in § 4.3.1) the sample tube is removed from the heater block and allowed to cool. The sample tube is then reweighed, weight loss determined, before fresh lubricant is added to restore the sample to its pre-test mass. The sample is then analysed for viscosity, Total Acid Number and assessed for solid formation (§ 3.1.5).

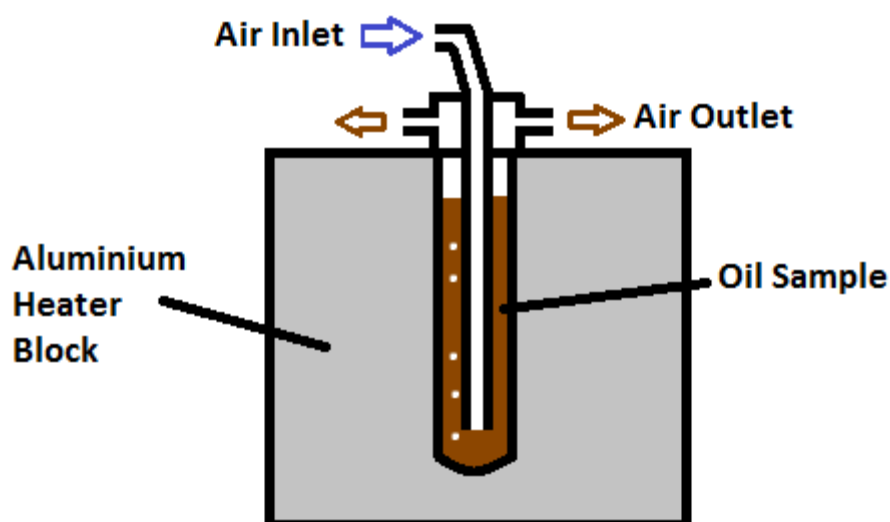


Figure 3.1 Schematic of Defence Standard, Method 9 equipment

For the work conducted in this thesis, the only deviation from the published method was to post-test oil top up. The method states that, post-test, the mass of oil lost by volatilisation should be replenished with fresh lubricant. Therefore as more oil is lost through volatilisation, then more fresh oil is added at the end. This of course will affect the results determined for viscosity and TAN and for this reason, post-test oil top up was not used for the testing in this thesis.

ASTM D4636

For the testing conducted in § 4.3.2 the method used was as described in ASTM D4636-09 (2009), Alternative Procedure 2. The test equipment set up is shown in Figure 3.2. The equipment consists of a glass tube containing the oil sample (100 ± 1 mL) which is heated externally by an aluminium heater block, controlled by a Eurotherm 2132 temperature controller. Air flow is controlled using a Bronkhorst F-201CV-500 mass flow controller at 83 mL min^{-1} ($\pm 0.5\%$) and is introduced via a central glass tube. The temperature of the test lubricant is monitored using an internal k-type thermocouple ($\pm 0.6^\circ\text{C}$). A water condenser, held at 18°C

($\pm 3^{\circ}\text{C}$) by using a recirculating water cooler, is used to condense volatile species so the volatile component evaporated is returned to the liquid phase. Following the standard test duration (72 hours) the sample is cooled to ambient temperature, and then analysed for viscosity, Total Acid Number and the weight loss (percentage volatilisation) determined (§ 3.1.5).

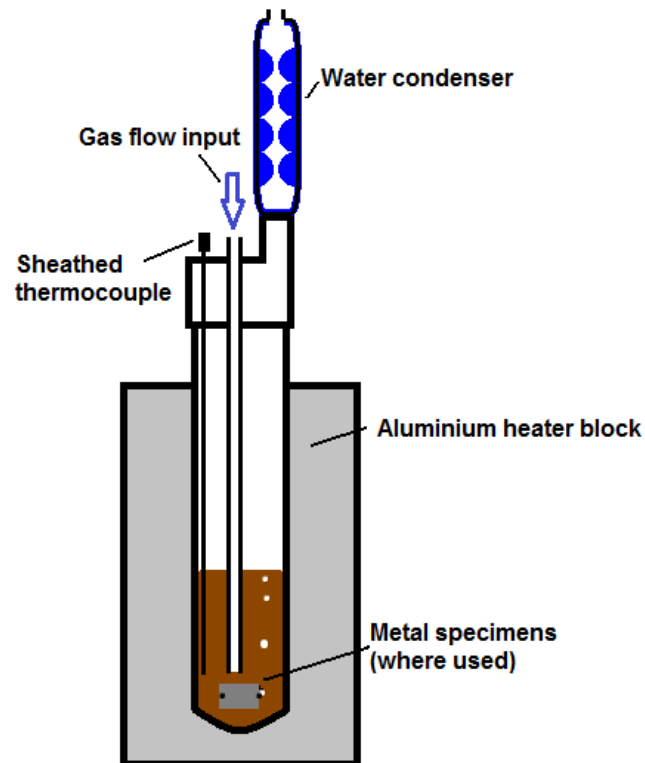


Figure 3.2 Schematic of ASTM 4636 standard test equipment

In § 4.3.2 and § 4.4.4 metal test specimens were submerged in the test lubricant, at the base of the glass tube. These specimens were 0.81 x 25.4 x 25.4 mm square metal specimens of the metallurgies given in Table 3.1. The specimens were tied together as described in ASTM D4636 (2009), using a Nichrome wire to ensure the metal surfaces of the specimens were exposed to the test lubricant.

Table 3.1 Metal specimen specification

Metal Type	Specification
Aluminium Alloy 2024, T-3	QQ-A-250/4
Copper, Electrolytic Tough Pitch (ETP) CA-110	QQ-C-576
Magnesium Alloy, AZ31B H-24	QQ-M-44
Silver, 99.9 % Pure	MIL-S-13282
Steel, Low-Carbon Steel 1010	QQ-S-698
Titanium Alloy (8% Manganese)	AMS4908 / MIL-T-9046

ASTM Degradation Parameter Modifications

The testing in § 4.4 required changes to be made to the standard ASTM D4636 method in order to explore the influence of different parameters on oil degradation, these changes were as follows.

§ 4.4.1 Effect of Air Flow Rate: This testing was conducted to the standard method, using the SPC 1 lubricant at 195 °C for the 72 hour duration. However, without the metal test specimens and with the following range of air flow rates: 0, 25, 50, 150, 200, 300, 400 and 500 mL min⁻¹.

§ 4.4.2 Effect of Oil Replenishment: This testing was conducted to the standard method equipment, using the SPC 1 lubricant at 195 °C with the following modifications. A larger 300 mL oil volume and a 150 mL min⁻¹ air flow rate were used, however metal specimens were not used. Oil samples were taken during the test using a vacuum pump to draw the oil sample through the air flow tube into a sample bottle (Figure 4.23). Three tests were conducted with three different sampling volumes being taken each at approximately 72 hour intervals, these volumes were: 40, 100, 150 mL. After the sample was removed the same volume of fresh

lubricant was added into the vessel. The replenishment rate was calculated as a percentage of the total oil volume.

§ 4.4.3 Effect of Evaporation: For the assessment of volatilisation products, the equipment was modified using 'quickfit' glassware such that the condenser was held below horizontal, with a round bottomed flask attached in order to collect the condensate. The round bottomed flask was immersed in an ice bath to ensure subsequent evaporation of the most volatile species did not occur. A 100 mL sample of SPC 1 lubricant was heated at 190 °C whilst passing 83 mL min⁻¹ of air through it, at intervals throughout the test the round bottomed flask was removed and the sample collected into hexane solvent for analysis by Gas Chromatography Mass Spectrometry (§ 3.1.5).

§ 4.4.4 Effect of Metal Test Specimens: This testing was conducted to the standard method, using an SPC and a HPC lubricant (oil 1 and 2 respectively) at 175, 195, 204 and 218 °C for the 72 hour duration. For each of the tests a pre-weighed test specimen of different metallurgy (aluminium, copper, magnesium, silver, steel or titanium) was placed in the oil sample. The specimens used were as shown in Table 3.1. Following the test duration the oil was analysed for viscosity and Total Acid Number and dissolved metal content by ICP-OES. The metal specimen mass change was determined gravimetrically, and the surface assessed using optical microscopy (§ 3.1.5).

Modified Method

Improvement modifications to ASTM D4636 were made as part of this EngD project and are discussed in detail in § 4.5. However the conditions used and post-test analysis are summarised in Table 3.2 and the equipment arrangement shown in Figure 4.23.

Table 3.2 Modified test method parameters

Temperatures (°C)	175, 185, 195, 204, 218	
Test Volume (mL)	300	
Oil Sample Volume (mL)	50	
Air Flow Rate (mL min ⁻¹)	150	
Water Condenser Temperature (°C)	18	
Metal Specimens	Aluminium	12.7 mm OD Tube, 0.88 mm wall thickness, 10 mm length, ASTM B210-12
	Copper	12.7 mm OD Tube, 1.24 mm wall thickness, 10 mm length, ASTM B75-11
	Inconel	12.7 mm OD Tube, 0.88 mm wall thickness, 10 mm length, ASTM B163-11e1
	Stainless Steel	12.7 mm OD Tube, 0.88 mm wall thickness, 10 mm length, ASTM A269-13, Grade 316
	Titanium	12.7 mm OD Tube, 0.88 mm wall thickness, 10 mm length, ASTM B338-13a
Post-test Analysis	Oil Kinematic Viscosity (mm ² s ⁻¹)	
	Oil Total Acid Number (TAN) (mg KOH g ⁻¹)	
	Oil Density (kg m ⁻³)	
	Metal weight change (mg)	

3.1.2. Deposition Methods

Hot Liquid Process Simulator (HLPS)

All testing performed in this thesis (§ 6.3.1 and § 6.4.2) was conducted using the methodology defined in SAE ARP5996, Revision B (2013). The only deviations from this method were the use of additional test temperatures (300, 325, 350 and the standard 375 °C) and the use of the

coated or modified test specimens. The coating and modification of the test specimens is described in § 3.1.3.

Vent Pipe Simulator (VPS)



The method described in this section is the method used for the Vent Pipe Simulator testing conducted in § 5.3, § 6.3.2 and § 6.4.3.


Test Section Preparation

1. Cut a 30 cm length piece of 316 stainless steel tube ($\frac{1}{2}$ " / 12.7 mm outer diameter, 0.035" / 0.89 mm wall thickness). Deburr the ends of the test section to remove sharp edges
2. Clean the test section with acetone, taking care to wash both the interior and exterior of the tube and to remove any printed writing on the tube exterior
3. Take a measuring cylinder or container, large enough to hold the test section, and fill it with petroleum spirit (boiling point 100-120 °C). Place the test section in the measuring cylinder and agitate using an ultrasonic bath for at least 10 minutes. Discard the petroleum spirit
4. Place the test section and measuring cylinder or container in a drying oven at 100 °C for 1 hour or until dry
5. Allow cooling to ambient temperature and weigh the test section to the nearest 0.0001 g

Test Start Procedure

1. Lower the heater block housing from the 45° position so that it rests at its lowest position

2. Place a nut and 2 o-rings (fluorocarbon type) at each end of the test section such the o-rings provide an air/oil seal
3. Attach one end of the test section to the exit T-piece. Attach the other end of the test section to the mist inlet to the heated block housing
4. Raise the heater block housing to the 45° position and secure with the locking pins. Close and fasten heated block housing
5. Place oil pump feed inlet pipe in the oil reservoir and ensure the pre heated chamber exit pipe and pre heated chamber bypass exit pipe are located above the oil reservoir. Fill the oil reservoir to 500 mL with the test lubricant
6. Turn on the pump. Turn the oil flow valve to the left such that the oil flow bypasses the pre heated chamber. Adjust the pump speed to gain the required oil flow rate (30 mL min⁻¹)
7. Turn the oil flow valve to the right, to direct the oil flow to the preheated chamber and ensure oil returns via the preheated chamber return pipe
8. Adjust the band heater on the preheated chamber to the required temperature (150 °C metal wall temperature) using the eurotherm controller on the right hand side (RHS) of the control unit
9. Programme the heated block eurotherm on the LHS:
 - a. Press and hold the  button (located on the left hand side).
 - b. Change to "level 2" using the up arrow.
 - c. Change "CODE" to "2".
10. Press the  button repeatedly to cycle through until TSP1 (Target set point 1) is displayed, adjust to the required pipe wall temperature using the up and down arrows

11. Use the  button to cycle through until TSP2 (Target set point 2) is displayed; adjust to the same temperature as TSP1
12. Wait 5 seconds until the control panel returns to the main screen
13. When the band heater reaches the required test temperature, simultaneously press the up and down arrow on the LHS eurotherm, this will begin the main heater cycle
14. Adjust the air mass flow meter to the required flow rate (4.5 mL min^{-1}) and observe the mist outlet to ensure mist flows without any obstructions
15. When the heated block has reached the test temperature record the volume of oil in the reservoir and record the time
16. Following the 18 hour test duration, the heater will automatically switch off. After the test record the oil level remaining in the oil reservoir and the time. Calculate oil consumption rate
17. Switch off the band heater and once the brass block in the heated chamber is below $250 \text{ }^{\circ}\text{C}$, open the heated block housing taking care not to touch the brass block, the test section or any connected pipe work; they may still be hot
18. Once the brass block heater has returned to ambient temperature, turn off the air and oil flow
19. Remove the test section by loosening the nuts at the top and bottom. Close the heater block housing
20. Rinse the test section with petroleum spirit and discard the petroleum spirit
21. Fill a measuring cylinder containing the test section with petroleum spirit and leave to soak for 20 minutes, then discard petroleum spirit
22. Place the test section and measuring cylinder in an oven at $100 \text{ }^{\circ}\text{C}$ for approximately 1 hour or until dry

23. Remove the test section from the oven and allow to cool to ambient temperature
24. Weigh the test section to the nearest 0.0001 g and calculate the mass of deposit

Cleaning Procedure

1. Empty and clean oil reservoir manually using acetone or a suitable dishwasher
2. Position an empty beaker under the pump inlet, and fill the beaker (~200 mL) with petroleum spirit
3. Place an empty beaker at the preheating chamber outlet
4. Pump the petroleum spirit through the preheating chamber and into the beaker at its exit. Discard the petroleum spirit. Repeat this process
5. Fill the inlet beaker with new test oil (~200 mL)
6. Pump the oil through the preheating chamber and into the beaker at its exit. Discard the oil. Turn off the pump

Reporting

Test (pipe wall) temperature (°C) should also be reported along with the mass of deposit which should be reported to the nearest 0.0001 g. Oil consumption (mL) should be recorded.




Feed Pipe Simulator (FPS) (Development testing § 5.4.1)

The method described in this section is the method which was used for the Feed Pipe Simulator testing conducted in § 5.4.1.

Test Section Preparation

Test sections used are identical to those used for the Vent Pipe Simulator and therefore were prepared as described in § 3.1.2.

Test Start Procedure

1. Place a nut and 2 o-rings at each end of the test section to produce an air/oil seal
2. Attach one end of the test section to the oil inlet T-piece union. Attach the other end of the test section to the oil outlet T-piece union
3. Ensure T-piece unions are located correctly and test piece sits in the groove in the brass block. Close and fasten heated block housing
4. Fill the oil reservoir with the test lubricant (1 L)
5. Open valve 1 and close valve 2
6. Switch on gear pump at required flow rate (25 mL min^{-1})
7. Turn the air control valve to direct the flow to the test section outlet, start air flow at required flow rate (1.5 L min^{-1})
8. Ensure oil is returning to the oil reservoir via the cooling coil
9. Adjust the oil preheater ($225 \text{ }^\circ\text{C}$, wall temperature) to the required temperature using the eurotherm controller on the right hand side (RHS) of the control unit
10. Programme the heated block eurotherm on the LHS:
 - a. Press and hold the  button (located on the left hand side)
 - b. Change to "level 2" using the up arrow
 - c. Change "CODE" to "2"
11. Press the  button repeatedly to cycle through until TSP1 (Target set point 1) is displayed, adjust to the required wall temperature ($375 \text{ }^\circ\text{C}$) using the up and down arrows
12. Use the  button to cycle through until TSP2 (Target set point 2) is displayed; adjust to the same temperature as TSP1

13. Wait 5 seconds until the control panel returns to the main screen
14. When the band heater reaches the required test temperature, simultaneously press the up and down arrow on the LHS eurotherm
15. When the heated block has reached the test temperature record the volume of oil in the reservoir and the time

Drain Down Flow Cycles

1. Whilst oil is flowing: open valve 2, allow oil to drain for 1 minute, turn off the oil pump
2. Reduce air flow to 0.1 L min^{-1} , turn air control valve so that air is introduced into inlet of test piece
3. Leave oil in drained scenario for 1 hour (or as required)
4. To restart flow: Turn on pump and close valve 2, return air flow to test piece exit and increase flow to 1.5 L min^{-1}

Flooded Pipe Cycles

1. Close valve 1 and valve 2, turn off pump and air flow
2. Leave oil in flooded pipe scenario for 1 hour (or as required)
3. To restart flow: Open valve 1, turn on pump, return air flow to test piece exit and increase flow to 1.5 L min^{-1}

End of Test

1. At the end of the test period (18 hours), the main block heater will switch off
2. Take note of the oil level remaining in the oil reservoir and record the time. Turn off the oil preheater

3. Once the brass block in the heated chamber is below 250 °C, open the heated block housing taking care not to touch the brass block, the test section or any connected pipe work as they may still be hot
4. Once the brass heater has returned to ambient temperature, open valve 2, turn off the air and oil flow
5. Remove the test section by loosening the nuts at each end of the test section. Close the heater block housing
6. Rinse the test section with petroleum spirit and discard the petroleum spirit
7. Fill a measuring cylinder containing the test section with petroleum spirit and leave to soak for 20 minutes, then discard petroleum spirit
8. Place the test section and measuring cylinder in an oven at 100 °C for approximately 1 hour or until dry
9. Remove the test section from the oven and allow to cool to ambient temperature
10. Weigh the test section to the nearest 0.0001 g and calculate the mass of deposit

Rig Cleaning Procedure

1. Empty waste oil into solvent waste disposal and clean oil reservoir using petroleum spirit
2. Open valve 1, close valve 2
3. Position an empty beaker below the cooling coil exit. Ensure the air is switched off and that the entire rig has cooled and drained of oil
4. Fill reservoir with petroleum spirit (approximately 500 mL)
5. Pump the petroleum spirit through the system until no oil colouration can be seen in the petroleum spirit leaving the cooling coil. Open valve 2 to drain

6. Close valve 2 and fill reservoir with oil
7. Pump the petroleum spirit through the system until no oil colouration can be seen in the petroleum spirit leaving the cooling coil. Open valve 2 to drain

Feed Pipe Simulator (FPS) (§ 6.4.2)

The testing conducted in § 6.4.2, following FPS modifications was conducted using the method described above however, the new control unit allowed the following test automation.

A test schedule can be defined by using the 'Test Schedule' tab (Figure 3.3). This tab allows the prior input of a number of a test parameters as well as the number of test cycles required. The test can then be started removing the need for the manual 'drain' and 'flooded' elements of the cycle described above. Test setup and cleaning procedures remain as described above.

Additionally temperature data, from thermocouples around the system will be recorded throughout the test, such that test to test variation can be detected.

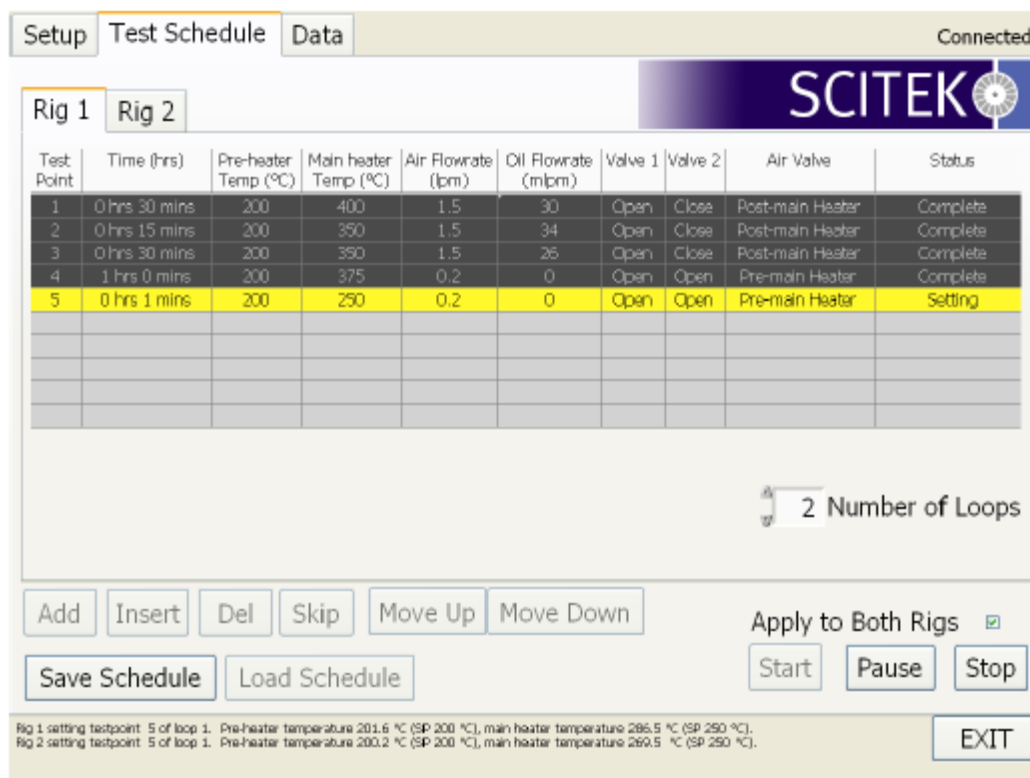


Figure 3.3 FPS control unit screenshot showing the 'Test Schedule' tab

3.1.3. Surface Coating and Treatment Methods

Physical Vapour Deposition Coating

The standard HLPS test specimens, as described in SAE ARP5996 (2013) were coated using PVD. Coating was conducted by the Department of Materials Science & Metallurgy at Cranfield University, using a proprietary coating methodology. The following coating metallurgies were produced: stainless steel, nickel, chrome, tungsten, silicon and gold.

Electropolishing

Electropolishing of test specimens was conducted by Stainless Restoration Ltd. Test specimens were submerged in an electrolyte bath (of a mixture of phosphoric and sulphuric acids) and

arranged in a circuit such that the test specimen is the anode. When a DC current (6-18 V, up to 1000 A) is applied, electropolishing occurs at the test specimen.

Acid Pickling

Acid Pickling of test specimens was conducted by Stainless Restoration Ltd. Specimens were pickled by submersion in a bath of hydrofluoric acid using the Stainless Restoration Ltd process.

3.1.4. Tribology

Aviation Lubricant Tribology Evaluator (ALTE)

Testing using the ALTE was conducted to the SAE ARP6255 (2013) method using the 'Mild Wear' regime. The test conditions are shown in Table 3.3. Bespoke lubricant blends were used for this testing as described in § 3.2.1 and Table 3.4.

Table 3.3 Aviation Lubricant Tribology Evaluator test conditions

Parameter	
Oil Temperatures (°C)	150 and 170
Ball Load (kg)	§ 7.3: 4-16 kg § 7.4: 4 kg § 7.5: 28 kg
Test Duration (minutes)	30
Rotation Speed (rpm)	220
Test Lubricant Volume (mL)	40

Table 3.4 Bespoke oil blend compositions

Oil Number	Blend	Base stock	Anti-wear (TCP)	Antioxidant	Metal Deactivator (1,4-dihydroxy anthraquinone)
1		✓	-	-	-
2		✓	2.4 %	-	-
3		✓	0.6 %	Monomeric	-
4		✓	2.4 %	Monomeric	-
5		✓	2.4 %	Polymeric	-
6		✓	-	-	0.06 %
7		✓	2.4 %	-	0.06 %
8		✓	2.4 %	Polymeric	0.06 %

3.1.5. Analysis Methods

Oil Volatilisation Loss

As it is assumed that all losses from the oil oxidation test method equipment (Defence Standard Method 9 and ASTM D4636) must occur due to volatilisation losses, the mass of oil lost can be determined gravimetrically. The mass of the test equipment is obtained prior to the test both with and without the test lubricant (to the nearest 0.01 g). After the test, the test equipment is re-weighed allowing the calculation of the mass of sample which has been lost by volatilisation. Volatilisation loss is reported as a percentage of the original oil mass.

Kinematic Viscosity

The kinematic viscosity of lubricants was measured at 100 °C using ASTM D445 (2012) 'Kinematic Viscosity of Transparent and Opaque Liquids (and calculation of Dynamic Viscosity)'. This method allows kinematic viscosity to be determined using the time which a fixed volume of lubricant requires to flow, under gravity through the capillary of a viscometer, at a known temperature. The temperature selected was 100 °C, the aviation industry standard for elevated temperature viscosity measurement. Kinematic viscosity is reported in the industry standard, centistokes (cSt) equivalent to $\text{mm}^2 \text{s}^{-1}$.

Total Acid Number (TAN)

Total Acid Number (TAN) is the aviation industry standard method for determining acidity due to mildly acidic constituents. These constituents could be those included in the original formulation or form as a result of oil degradation. TAN was determined using the method described in SAE ARP5088 (2006). This method is a potentiometric titration method which uses a cell voltage corresponding to pH 11 buffer as an end point. TAN is reported as the mass of potassium hydroxide (KOH) required to neutralise 1 gram of lubricant (mg KOH g^{-1}).

Density

Lubricant density was determined using a digital density meter using the method defined in ASTM D4052 (2011). Density is determined at 15 °C and reported as kg m^{-3} (g L^{-1}).

Inductively Coupled Plasma Optical Emission Spectrometer (ICP-OES)

ICP-OES was used to determine the concentration of dissolved metals within oil samples following the methodology defined in ASTM D5185 (2013). A Perkin Elmer 8300 Inductively Coupled Plasma Optical Emission Spectrometer (ICP-OES) was used to determine the concentration of the following metals: aluminium, beryllium, boron, cadmium, calcium,

chromium, copper, iron, lead, magnesium, molybdenum, nickel, phosphorus, silicon, silver, sodium, tin, titanium, vanadium and zinc.

Chemical Analysis Methods

Infra spectroscopy was carried out using a Thermo Nicolet iS10 with a Smart iTR ATR attachment with diamond crystal. Gas Chromatography Mass Spectrometry (GC-MS) was performed, using a PerkinElmer AutoSystem XL Gas Chromatograph with a Turbomass Mass Spectrometer. Gel Permeation Chromatography was carried out using a Viscotek GPC Max with 2 x 30 cm PLgel 50&500A columns, the eluent was tetrahydrofuran at a flow rate of 0.8 mL min⁻¹.

Surface Analysis Methods

The Scanning Electron Microscope used for metal surface imaging and surface composition analysis were a CAMSCAN Series 2 with an EDAX X-Ray Detector and a Philips XL30 ESEM-FEG. Surface finish measurements were obtained using an Alicona Infinite Focus Microscope. These measurements were obtained from a representative area and in most cases, report results are an average of a number of areas of the surface.

3.2. Materials

3.2.1. Lubricants

All of the lubricants used and evaluated in this thesis conform to either (or both) of the following specifications, SAE AS5780 (2013) or MIL-PRF-23699 (1997). These are commercially available blends and their specific formulations are proprietary to the relevant manufacturer. For reasons of confidentiality and simplicity, a coding system is applied whereby the oils have been designated a number within a performance capability. These performance capabilities

refer to their designation within SAE AS5780 (2013) as Standard Performance Capability (SPC) or High Performance Capability (HPC).

Where formulation constituent specific testing was conducted, bespoke blends were used. These were kindly provided by an oil manufacturer and are tabulated in Table 3.4 shown previously.

CHAPTER 4: THERMAL OXIDATIVE STABILITY

4.1. Introduction and Business Case

There is an increasing trend towards higher oil system temperatures; these higher temperatures have a detrimental effect on the condition of the oil. Excessive increases in oil viscosity and density can result in lubricant transport issues. This can cause increased strain on the oil pump (potentially leading to oil pump failure) and a reduction in flow to some or all of the lubricated regions. Transmission system component failure is likely to result in an In Flight Shutdown (IFSD) event. IFSD events will often result in the aircraft making an unscheduled landing and therefore are a significant and undesirable event.

To ensure that component failure due to excessive oil deterioration does not occur, knowledge of oil life in service is required. This allows suitably thermally stable lubricants to be selected for each required application. If oil life is longer than the average residence time within the engine, then oil loss and replenishment will allow 'infinite life' to be achieved. Where this is not possible, oil life prediction could allow scheduling of preventative maintenance such as full or partial oil changes. Accurate scheduling of maintenance gives a significant cost saving as it minimises of the time during which the aircraft is unavailable for service.

Oil life prediction can only be achieved if a fundamental understanding of the rate of degradation is known, therefore laboratory based testing is required to generate data to enable the relationship between the oil degradation and the time, its time-temperature history, to be obtained. In order for this data to be relevant and accurate, it is important that the laboratory method from which it is generated has the ability to mimic the degradation

mechanisms seen in the gas turbine. Many of the laboratory methods currently used by Rolls-Royce and the wider gas turbine lubricant industry were developed a number of decades ago and were designed to suit the requirements of older technology lubricants and gas turbines than those used today. There is a need to re-evaluate how closely these methods meet modern requirements and where necessary, improve upon them. Accurate laboratory methods will allow the most precise oil life data to be generated.

In addition to a method for determining lubricant life, this method could also be used as a research and development technique to evaluate candidate lubricant formulations. Formulation research is commonly undertaken by lubricant companies, however there are significant benefits to Rolls-Royce in providing the best possible methodology to develop the most suitable lubricants for Rolls-Royce products.

This chapter is structured as follows: § 4.2 contains a critical review of current industry laboratory methodologies, including a description of the generation of life relationships from laboratory data. § 4.3 presents results from two of the most widely used laboratory methods and provides comparison between them. § 4.4 describes the work carried out to determine the influence which key parameters have on oil degradation and chemistry. The knowledge obtained from the work presented in § 4.2 to § 4.4 was used to produce the modified test method which is described in § 4.5. The data produced using this method is presented in § 4.6. § 4.7 contains closing remarks on the chapter and provides a link to the following chapter 5.

4.2. Critical Review of Current Methodology

Currently the aviation lubricant industry evaluates lubricant bulk thermal stability, at laboratory scale by four techniques; Federal Test Method Standard No 791C Method 3411 (US Defense Logistics Agency, 2007), Turbomeca Thermal Ageing Test (unpublished), ASTM

Method D4636 (ASTM, 2009) and Defence Standard 05-50 (Part 61) Method 9 (UK MOD, 2003). These methods are requirements for either (or both) MIL-PRF-23699 (US Department of Defense, 1997) and/or SAE AS5780 (2013) lubricant specifications. These methods all differ in the equipment, degradation parameters and analysis used, some of which are summarised in Table 4.1. All of these methods are constrained by the need to be low cost and reproducible. However, they do share the similarity that they are fundamentally laboratory glassware based methods - Figure 4.1 gives an example of the equipment used. These differences give rise to advantages and disadvantages for each technique in order to find a compromise between a wide range of factors but as the SAE AS5780 (2013) specification currently requires all of these methods, there is duplicated effort.

Table 4.1 Comparison of the thermal degradation test methods

	Federal Test Method 3411	Turbomeca Ageing Test	ASTM D4636	Defence Standard Method 9	
Oxidative method?	x	✓	✓	✓	
Degradation Parameters	Air flow rate (mL min ⁻¹)	-	83	250	
	Includes condenser?	x	✓	x	
	Includes rate relationship?	x	x	✓	
	Includes metal specimens	x	x	✓	x
	Viscosity	✓	✓	✓	✓
Total Acid Number	✓	✓	✓	✓	
Oil Analysis	Insoluble formation	x	x	✓	✓
	Volatilisation	x	x	✓	✓
	Density	x	✓	x	x
	Flash Point	x	✓	x	x
	Antioxidant Depletion	x	✓	x	x

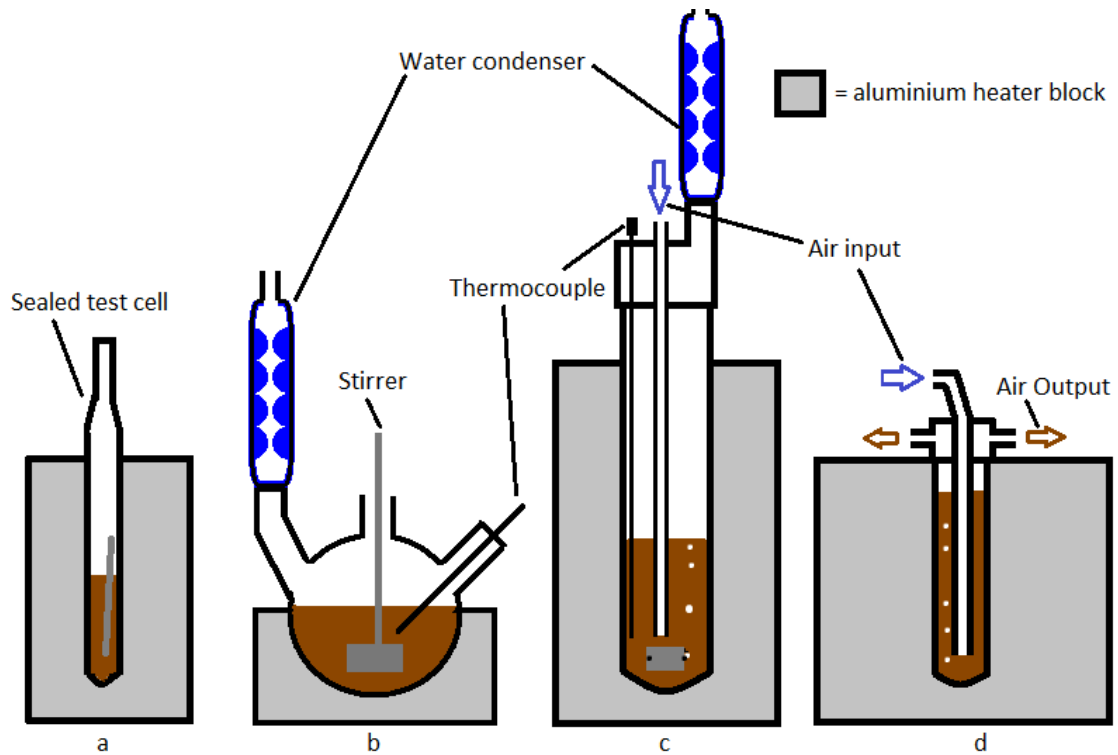


Figure 4.1 Equipment set up for: (a) Fed. Stan. 3411 (b) Turbomeca Thermal Ageing Method (c) ASTM D4636 (d) Def. Stan. Method 9

- Air Flow

Federal Test Method Standard No 791C Method 3411 (Figure 4.1 a) is not an oxidative method as it evaluates the thermal degradation of oil in a sealed system in the absence of air. As discussed in § 2.5, lubricant degradation primarily proceeds by oxidative mechanisms, with degradation in the absence of air being much slower. Therefore as service oil is typically heavily oxygenated, particularly in the regions of highest temperature, it is of limited use in the prediction of service degradation. The Turbomeca Thermal Ageing Test (Figure 4.1 b) is considered as an oxidative test method as it is not a sealed system like Federal Test Method 3411, given that no positive air flow is applied, air flow is dependant purely on convection, control of air flow and therefore test repeatability and reproducibility are compromised. ASTM Method D4636 (Figure 4.1 c) and Defence Standard 05-50 (Part 61) Method 9 (Figure 4.1 d)

are both thermal oxidation methods yet the equipment set up and air flow rate differ (83 and 250 ml min⁻¹ respectively). In all three oxidative methods, the amount of oxygen available for oxidative processes will be different and perhaps more importantly, so will the amount volatilised from the test vessel.

- Water Condenser

The Turbomeca Thermal Ageing Method (Figure 4.1 b) and ASTM Method D4636 (Figure 4.1 c) both use a water cooled condenser to limit the volatilisation rate, Defence Standard 05-50 (Part 61) Method 9 (Figure 4.1 d) does not, rather it has two openings at the top of the vessel. These differences in both input and output will naturally influence the chemical species available to participate in any degradation reaction.

- Metal Specimens

Another difference is the inclusion of metal specimens used to assess the catalytic and corrosive effects, ASTM Method D4636 (Figure 4.1c) is the only oxidative method which also includes metal specimens within the test lubricant and these are believed to influence the rate at which the oil degrades. Defence Standard 05-50 (Part 61) Method 9 (Figure 4.1 d) and the Turbomeca Thermal Ageing Method (Figure 4.1 b) are purely oxidation methods and therefore discount catalytic effects. This has the benefit of increasing test control but potentially discounts an important variable.

- Temperature and duration

The standard test parameters of temperature and duration vary between test methods therefore, some of the methods are more extreme than others in terms of the thermal stress to which the oil is exposed. It is important to Rolls-Royce to encompass the temperature range

which the oil is likely to operate in a gas turbine. Testing at higher temperatures, whilst having the benefit of accelerating testing, is arguably not relevant to engine operation.

Each of the parameters discussed will influence the mechanism and rate of oil degradation, it is therefore important that their effect is understood in order to match the laboratory conditions as closely as possible to engine conditions.

4.2.1. Life Prediction

Laboratory thermal oxidative test methods are used most routinely to allow comparison of relative performance of lubricant formulations, and for quality control and development reasons. However, it is also possible to use the data generated from these test methodologies to develop degradation reaction kinetic models for lubricant life prediction.

An example of a reaction kinetic model is Defence Standard Method 9 (UK Ministry of Defence, 2003) which defines four 'deterioration parameters' assumed to follow an Arrhenius relationship in order to determine the point at which the 'assessment level' for that parameter is reached. At these assessment levels the lubricant is no longer considered to be fit for service and therefore represents the end of lubricant life. The determination of activation energy and effective collision frequency from laboratory generated data allows the prediction of lubricant life at any temperature by using equation 4.1 shown below.

$$D = \frac{1}{m} \cdot \exp\left(\frac{E_a}{R\theta}\right), \quad (4.1)$$

where:

D = effective life (hrs),

θ = absolute temperature (K),

R = molar gas constant = 1.98719 cal mol⁻¹ K⁻¹,

E_a = apparent activation energy (cal mol⁻¹) (given incorrectly as 'cal' in Defence Standard Method 9) and

m = effective collision frequency (hrs⁻¹)

Having established values for activation energy (E_a) and effective collision frequency (m), the time taken for a lubricant to degrade to reach the 'assessment level' can be determined from Arrhenius equation at any temperature. This provides a means for modelling the extent of degradation of oil in a gas turbine. The quality of this model relies heavily on the quality of the laboratory method and its data.

4.3. Testing using current industry techniques

In order to compare the data each test method produces, a range of testing was conducted with Defence Standard 05-50 (Part 61) Method 9 and ASTM D4636. These methods were selected as they are the two most widely used industry oxidative methods and have a proven ability to differentiate oil brands, with respect to their thermal oxidative stability. This testing was intended to identify key variables and to define the level to which they should be controlled in any method improvements. The Turbomeca Thermal Ageing method was not selected for testing as the lack of a positive air flow and an opening at the top of the vessel is known to lead to a number of issues with accuracy and repeatability of the test method. This is due to a lack of control over inputs and outputs from the vessel.

4.3.1. Ministry of Defence, Defence Standard 05-50 (Part 61) Method 9

Testing was undertaken using Ministry of Defence Method 9 on four lubricant brands: one SPC lubricant and three HPC lubricants. These four lubricants are proprietary commercial blends and as such the names of the lubricants are not given, instead they are referred to as SPC, HPC 1, 2, and 3. This testing was carried out as described in the Method 9 (UK Ministry of Defence, 2003) (§ 3.1.1) by first degrading the oil at a range of temperatures for a fixed duration of 192 hours. The precision of this test method is such that repeated result would be expected to be within 3 % of each other. Results displayed in Figures 4.2 - 4.7 represent the average of triplicate tests which were found to be consistent with the 3 % repeatability value. Figure 4.2 shows how Total Acid Number (TAN) varies as the lubricant begins to degrade. It can be seen that for all lubricants the TAN after 192 hours increases gradually with temperature until at a specific temperature there is a large increase in TAN. The temperature at which TAN increases rapidly was found to be approximately 5 °C higher for the HPC lubricants than the SPC.

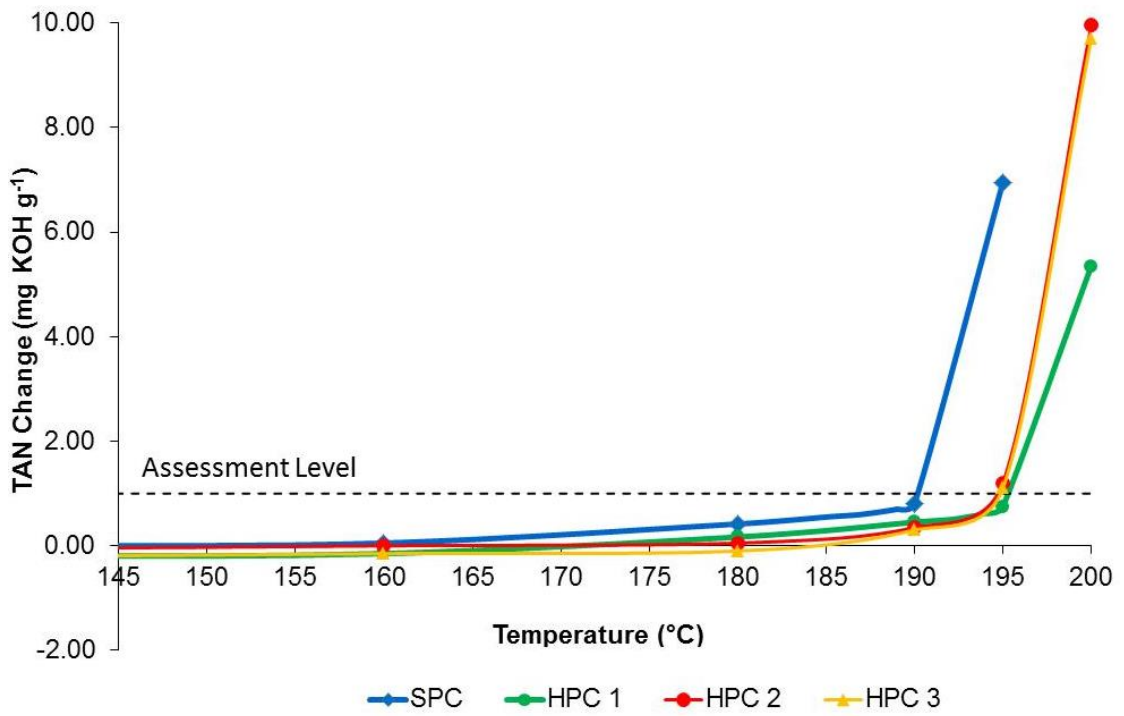


Figure 4.2 Method 9, change in Total Acid Number as a function of temperature (192 hour tests)

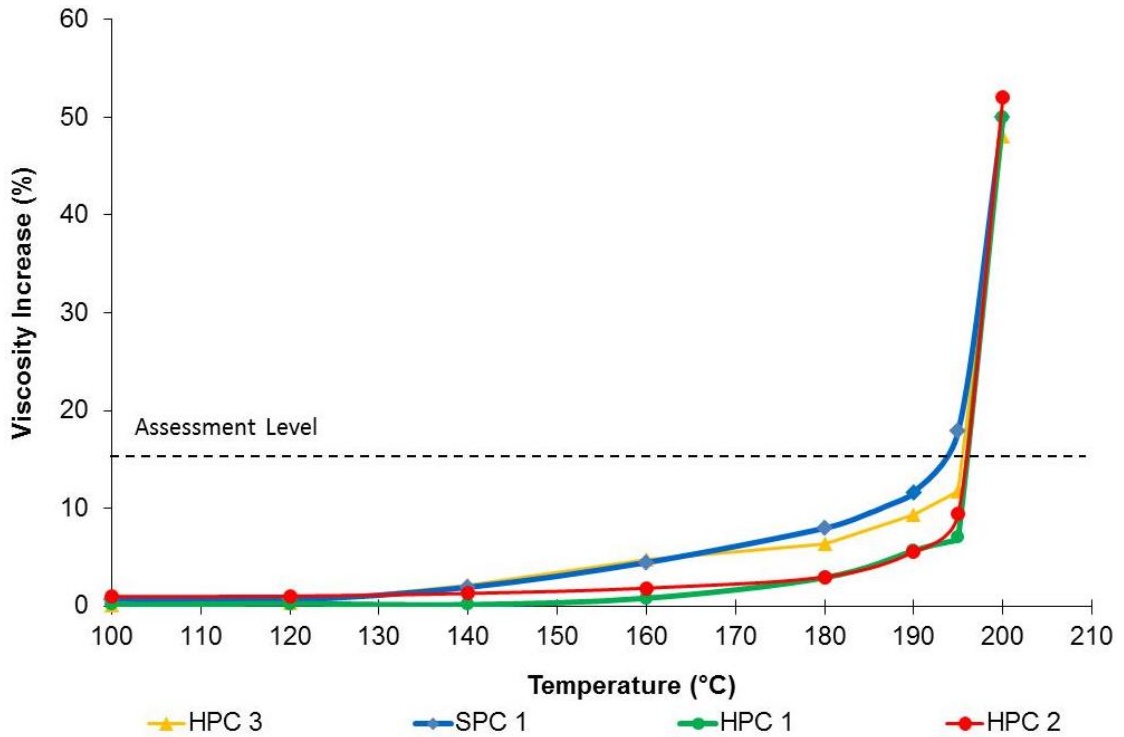


Figure 4.3 Method 9, percentage viscosity increase as a function of temperature (192 hour tests)

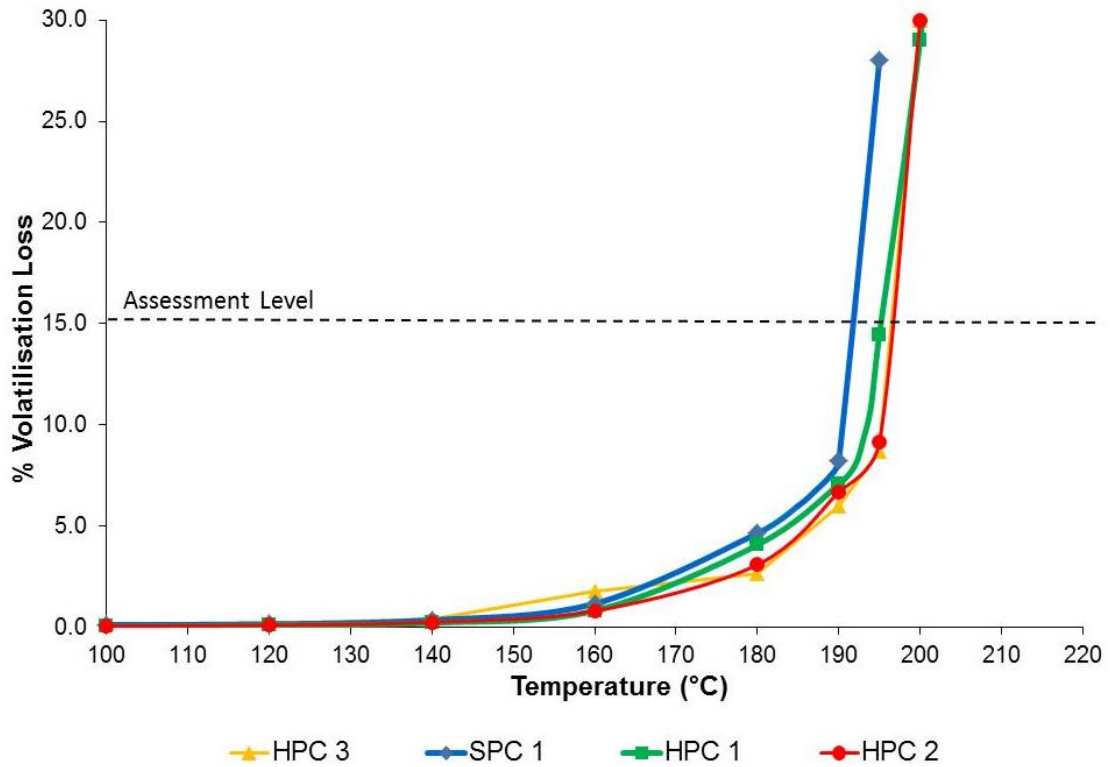


Figure 4.4 Method 9, percentage volatilisation loss as a function of temperature (192 hour tests)

Figure 4.3 and Figure 4.4 respectively show the viscosity increase and volatilisation loss for the four oils. A similar trend and thus strong correlation is seen for all three of the parameters measured (TAN, viscosity and volatilisation).

Additional degradation tests were undertaken where the temperature was kept constant and the duration of each test was varied. This produced similar trends to the fixed duration test, with the TAN rising steeply after a given duration in time. At 215 °C, as shown in Figure 4.5 this duration was found to be almost twice as long for the HPC lubricants compared to the SPC lubricants. Figure 4.6 shows the percentage viscosity increase of the lubricant, which followed similar trends to Total Acid Number with the HPC lubricants increasing steeply after twice the duration. Figure 4.7 shows the loss by volatilisation over time. As evaporative weight loss will occur due to degraded species and compounds present in the original formulation,

volatilisation will occur from the onset of the test. Therefore the increase in volatilisation loss was less steep than Total Acid Number and viscosity, equally, the difference between SPC and HPC oils was less pronounced.

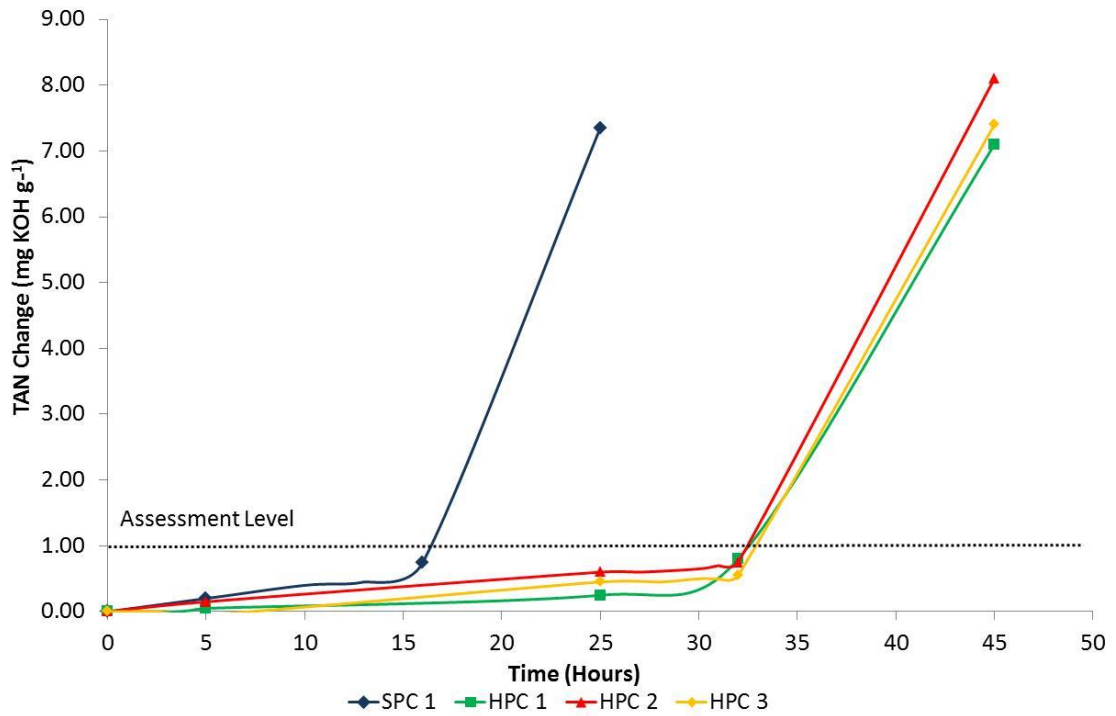


Figure 4.5 Method 9, change in Total Acid Number as a function of time (215 °C test)

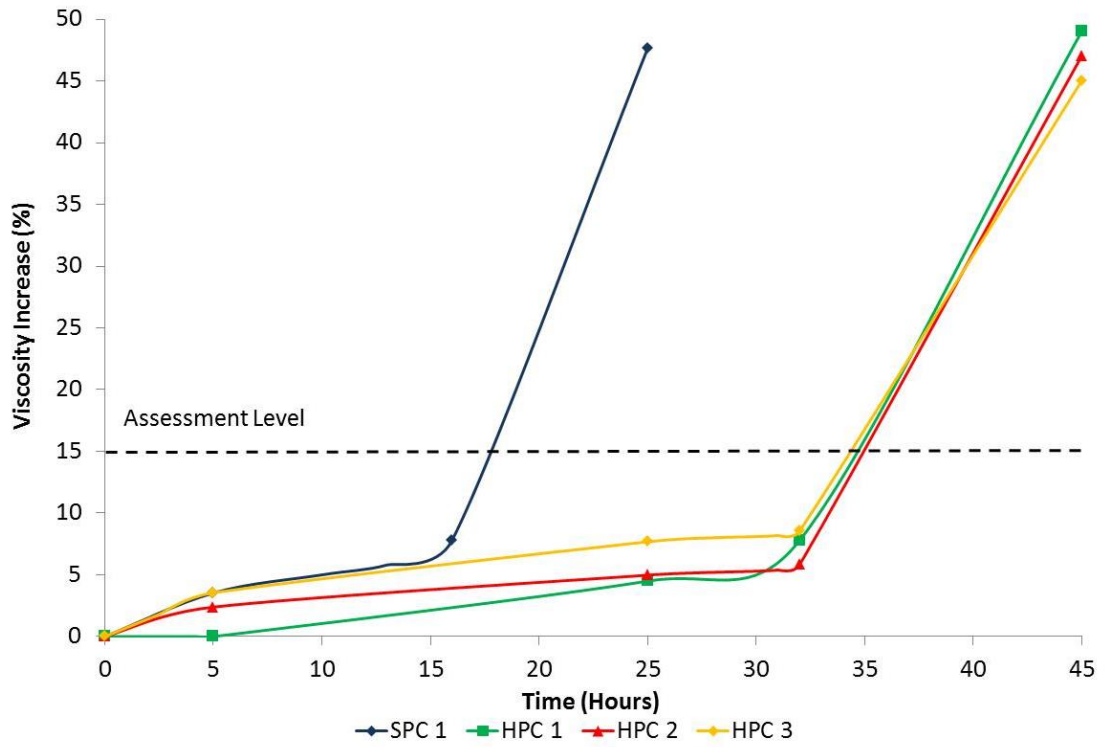


Figure 4.6 Method 9, Viscosity increase as a function of time (215 °C test)

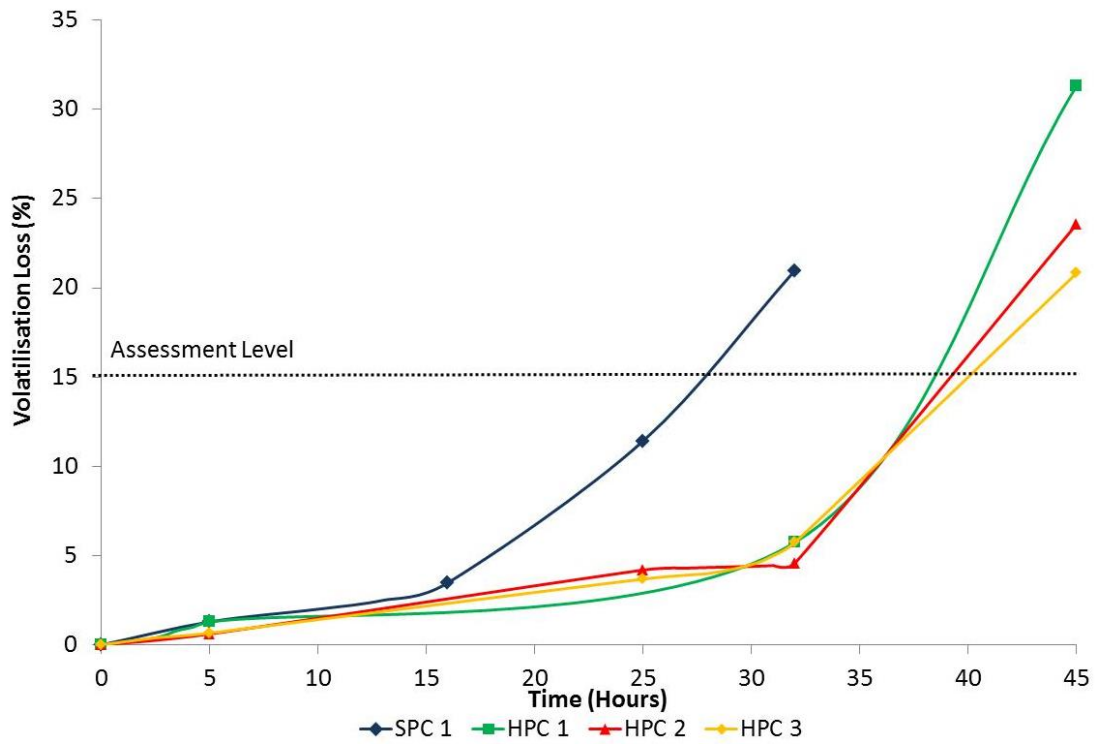


Figure 4.7 Method 9, Volatilisation loss as a function of time (215 °C test)

Defence Standard, Method 9 defines an 'Assessment Level' for each parameter measured; these assessment levels are 1 mg KOH g^{-1} , for TAN and a 15 % change in viscosity and lubricant mass (volatilisation). These assessment levels were determined based on the point at which the given oil property is considered to be no longer fit for purpose. Using both the fixed duration and fixed temperature testing, it is possible to define a range of durations at a given temperature at which the assessment level is reached. By using the Arrhenius relationship which is required by Method 9, described in § 4.2.1 and defined in equation (4.1), it is possible to determine the life of a lubricant by using this relationship.

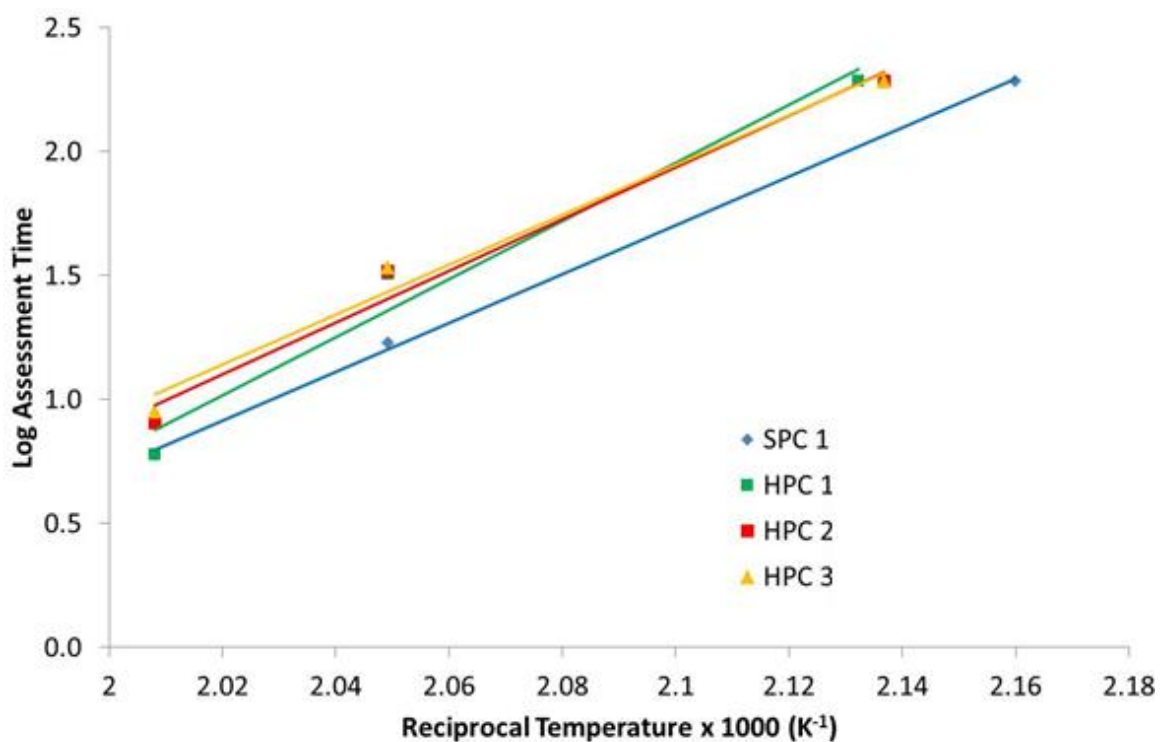


Figure 4.8 Arrhenius plot for four lubricants

The Arrhenius plot, Figure 4.8, shows that as expected, the SPC lubricant has a lower life than the three HPC lubricants at all temperatures. The three HPC lubricants are closely grouped yet HPC 1 has a marginally different gradient, indicating that HPC 1 performs worse at the higher

temperature than the other oils. All four lubricants show a linear relationship on a semi log plot; the line gradients and the R^2 values are given in Table 4.2.

Table 4.2 Arrhenius plot equations and R squared values

Lubricant	Linear Equation	R^2	E_a (cal mol ⁻¹)	m (hrs ⁻¹)
SPC 1	$y = 9.83x - 18.94$	0.999	44783	8.83×10^{18}
HPC 1	$y = 11.72x - 22.66$	0.970	53639	4.63×10^{22}
HPC 2	$y = 10.41x - 19.93$	0.980	47632	8.43×10^{19}
HPC 3	$y = 10.05x - 19.16$	0.983	45990	1.46×10^{19}

4.3.2. ASTM D4636

Oil oxidation was undertaken with two lubricants, one HPC and one SPC at four temperatures. These are the three temperatures 175, 204 and 218 °C as defined by SAE AS5780 (2013), and an additional temperature of 190 °C, added to give further data in the temperature region experienced in gas turbine oil systems. The precision of this test method is such that repeated result would be expected to be within 2 % of each other. Results displayed in Figure 4.9 represent the average of duplicate tests which were found to be consistent with the 2 % repeatability value. This data is plotted in Figure 4.9. Volatilisation from the test vessel was seen to be consistent for both lubricants indicating that losses from the system were consistent. TAN and viscosity rose more rapidly for the SPC lubricant indicating, as expected, that the method can differentiate between the more or less thermally stable oils. It was noted that for a given viscosity, oil degraded via this method appeared to have a higher TAN than via Defence Standard Method 9, this was therefore investigated further in § 4.3.3 below.

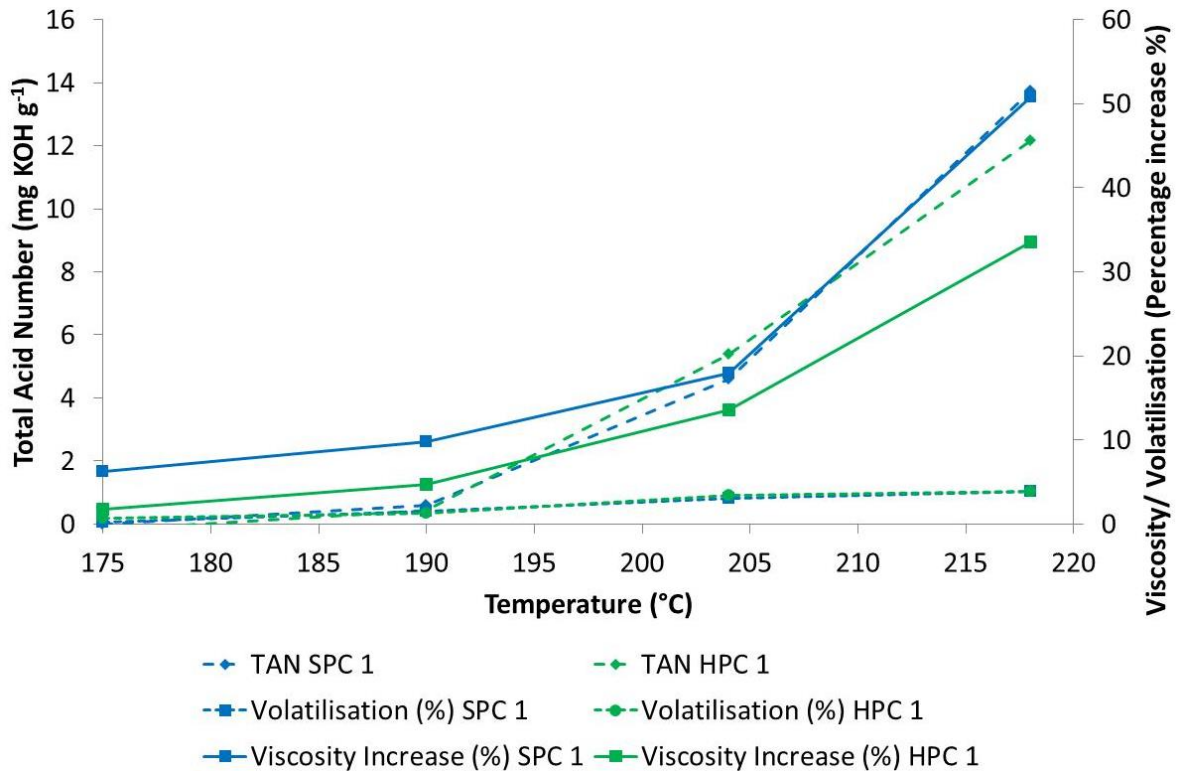


Figure 4.9 ASTM D4636 Oil oxidation data. Total Acid Number, viscosity and volatilisation increase as a function of temperature (72 hour tests)

4.3.3. Comparison between Def. Stan. Method 9 and ASTM D4636

Viscosity is influenced primarily by the level of degradation of a lubricant. TAN is dependent both on the rate of formation of acidic species and the rate of their loss. For a constant degradation rate (a constant acidic species formation rate) an oil sample will have a lower TAN when evaporation from the system is higher. As a result, a comparison of viscosity to TAN is believed to give an expression of how the system losses affect the lubricant properties. The ‘thermal history’ or the duration and magnitude of thermal exposure, is easily determined for laboratory derived samples, however this is very difficult for a service oil sample where the actual operating conditions must be approximated. Therefore, as a validation exercise, direct comparison of laboratory and service samples can be difficult. By plotting viscosity against TAN allows comparison of degraded oil without the need to know its thermal history.

Figure 4.10 shows a viscosity and TAN plot for data generated by Defence Standard, Method 9 and by ASTM D4636 along with engine samples taken from a range of gas turbines. It should be noted that for an engine operating normally, TAN will usually remain below a TAN of 1 mg KOH g⁻¹ and a viscosity of 6 cSt (at 100 °C, this is the industry standard measure of viscosity). Therefore, a large proportion of the data shown represents oil taken beyond its normal operational limit under development engine test conditions. It can be seen that for a given TAN, Defence Standard, Method 9 gives a higher viscosity than both ASTM D4636 and the engine samples. This is believed to be due to the lack of any restriction to volatilisation of the oil from the test vessel and a higher air flow rate through the vessel. ASTM D4636 however, has a condenser fitted which is able to regulate the passage of volatilised components from the vessel. As volatiles are most likely to be low viscosity and higher acidity, evaporation will, as shown for Defence Standard Method 9, lead to high viscosity and lower acidity.

ASTM D4636, like the engine derived oil samples, shows an approximately linear relationship between TAN and viscosity. Similar to Defence Standard, Method 9, ASTM D4636 does not show large increases in viscosity (up to 25 cSt at 100 °C). This is consistent with the engine data which, due to the oil breather system restricting volatilisation, does not result in a skewed TAN to viscosity relationship. The linearity of the ASTM D4636 data suggests a much greater control in evaporation losses than Defence Standard, Method 9. This control is likely to result in better repeatability and reproducibility which is of course, desirable. While both approximately linear, the engine data shows marginally higher viscosity than the ASTM D4636 data. This could be due to marginally higher evaporation for the engine but it could also be an effect of oil replenishment. As high viscosity species are not lost through evaporation they can begin to accumulate, leading to slightly higher viscosity. The effect of oil replenishment is explored in detail in § 4.4.2.

This comparative work demonstrates that, whilst more pronounced for more degraded oils, the losses from the system could potentially affect both the precision and applicability to engine degradation of the method. The effect of air flow rate on volatilisation and the chemistry of the evaporated species were therefore studied as part of the following section (§ 4.4) on parameter sensitivity. This section also contains a study on the effect of metal catalysts which represents another significant difference between Defence Standard, Method 9 and ASTM D4636.

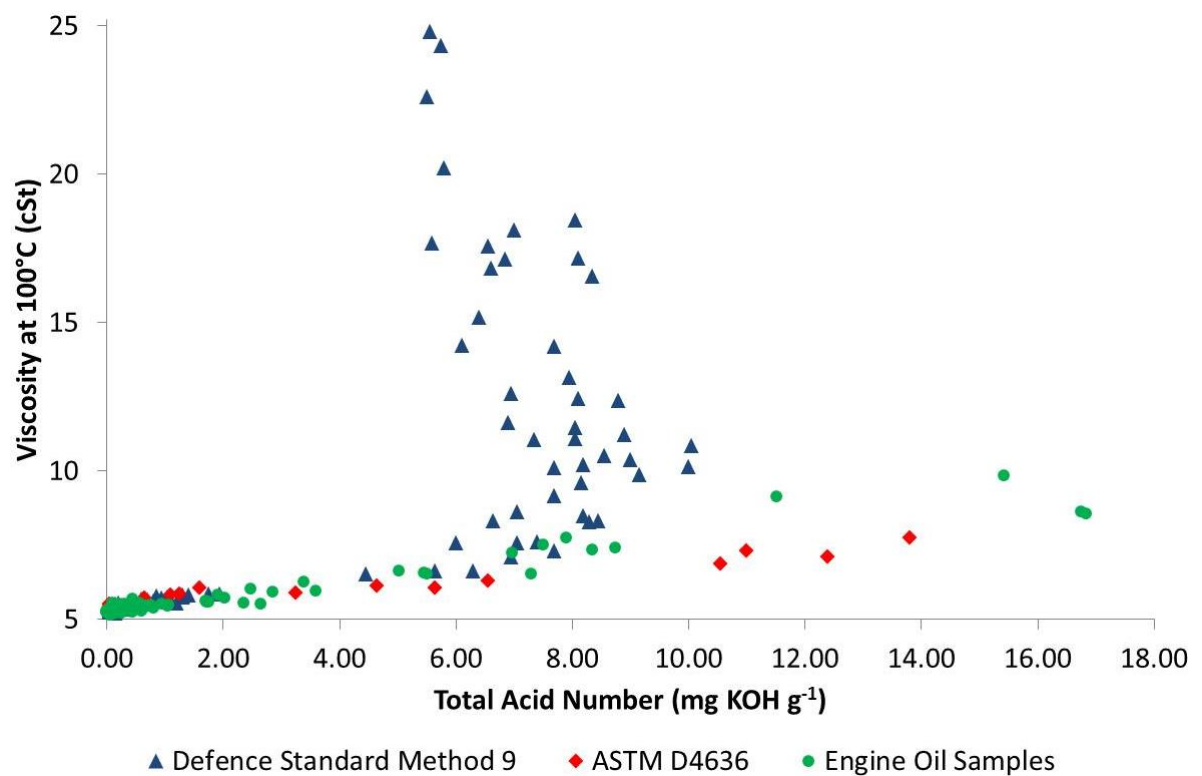


Figure 4.10 Comparison of viscosity and Total Acid Number of laboratory and engine derived samples

4.4. Degradation Parameter Sensitivity

For the purposes of studying the effect of different parameters on the physical and chemical properties of lubricants, ASTM Method D4636 was selected. This method was chosen as it incorporates a water condenser to control volatilisation, allows easy use of metal specimens

and through the use of quick-fit type glassware, can be readily modified. As results generated in this section utilise the ASTM D4636 equipment they are expected to comply with the 2 % repeatability determined in ASTM D4636.

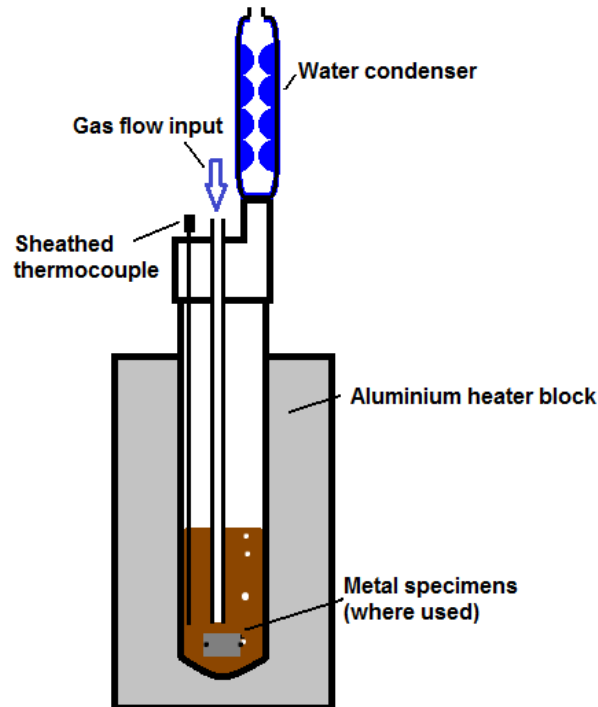


Figure 4.11 A schematic of the ASTM D4636 equipment used for the parameter sensitivity testing

4.4.1. Effect of Air Flow Rate

To determine the influence of air flow rate through the test vessel as well as volatilisation of oil derived species from the system, a series of tests were performed using the test methodology defined in ASTM D4636 but incorporating a range of air flow rates. This differs from the standard 83 mL min^{-1} single fixed rate as defined in ASTM D4636. The lubricant was assessed post test to determine the change in mass, viscosity and Total Acid Number. It is assumed that any changes to the mass of the lubricant were as a result of volatilisation of the oil or oil degradation species; hence the percentage volatilised mass was calculated. In Figure 4.12, oil volatilisation, measured by weight loss, can be seen to positively correlate to air flow,

the increased flow rate allowing more volatile species to be carried past the condenser and exit the test vessel. Volatilisation at the highest flow rate 500 mL min^{-1} can be seen to deviate from the linear relationship showing that the rate of volatilisation has reached the maximum of this equipment setup.

Whilst still only mildly acidic, degradation products can be significantly more acidic than the lubricant itself; therefore milligram quantities of degradation products can give rise to a measureable acidity change. Although lubricant acidity is not an issue in terms of lubricant performance, until it becomes significantly higher than value recorded here, it is a useful indicator of general lubricant degradation. Total Acid Number was shown to have an inverse relationship to air flow rate as acidic degradation species tend to be more volatile and therefore can be volatilised from the test vessel at a rate dependent on the flow through the vessel. For values above 400 mL min^{-1} air flow rate, the Total Acid Number, as with percentage volatilisation, is constant, showing that the volatilisation rate has reached the maximum for the test equipment setup used.

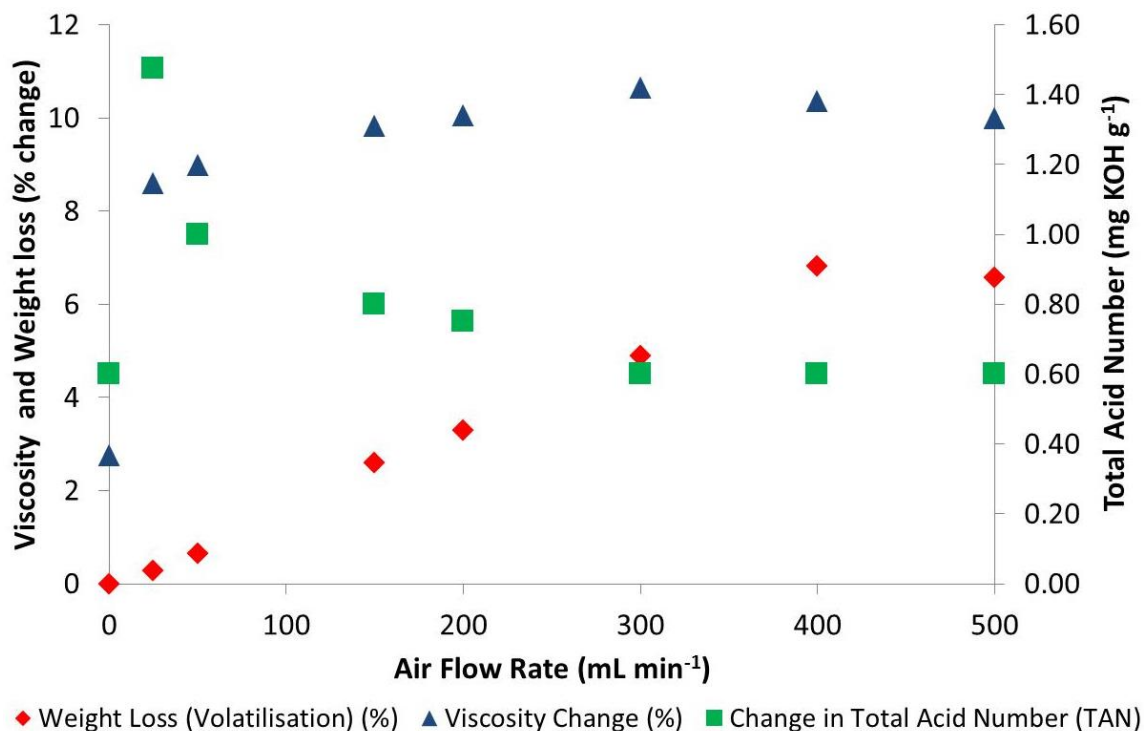


Figure 4.12 Graph showing the influence of air flow rate on Total Acid Number and change in viscosity, volatilisatation (195 °C, 72 hour tests)

The lubricant viscosity change appears much less sensitive to air flow rate, with the exception of the lowest air flow, the increase in viscosity is approximately constant. It could therefore be postulated that samples at 50 mL min⁻¹ air flow and above are not limited by the amount of available oxygen and therefore the reaction rate is constant.

When no air flow is applied, it can be seen that oil degradation still occurs as acidity and viscosity both increase. This is because air/oxygen is still available in the headspace above the oil as well as dissolved within the oil itself. If we assume that only monobasic acids are present and therefore 1 mole of KOH neutralizes 1 mole of carboxylic acid species then a Total Acid Number of 0.6 mg KOH g⁻¹ equates to 1.4 mg of carboxylic acid species present per gram, if the assumed average carbon chain length is 7. Generating this amount of acid would only require an oxygen volume of 0.26 cm³ (1.2 cm³ air) per gram of oil. Therefore the limited amount of air

available within the oil and at the oil surface (approximately 500 cm³) is more than enough to allow this reaction to proceed to this extent. However, this appears to be transport limited as this air is only available at the surface, a small percentage of the oil volume; therefore, viscosity increase is only ~2.5 %.

With an excess of oxygen and good mixing, when air flow is $\leq 50 \text{ mL min}^{-1}$, the reaction can progress to a greater extent and as such, viscosity is seen to increase further to the point where the reaction is limited by the availability of oxygen. At the low flow rates, although an excess of oxygen is provided such that oxidative degradation can occur, physical agitation of the oil is low, as is volatilisation for the test vessel, giving rise to high acidity. This is consistent with the findings of Siouris *et al.* (2013) who reported that where sufficient vapour venting was not present on their oil system simulator rig (LSIS), oil acidity was considerably higher than would be predicted, for a service oil of that viscosity.

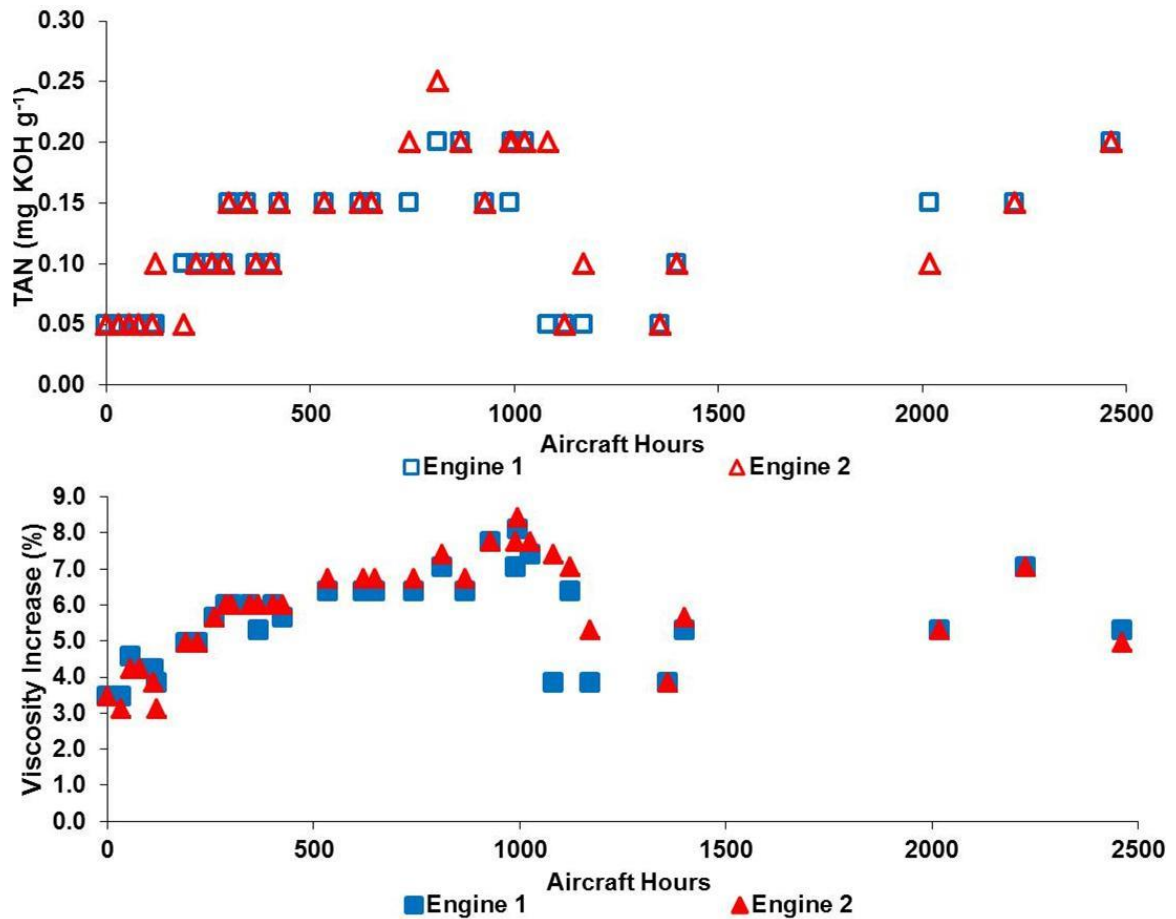


Figure 4.13 Total Acid Number and viscosity increase for two service engines operating typical flight cycles

In service, the oil within healthy engines tends to reach approximately constant values for TAN and viscosity, at which point oil degradation is in equilibrium with oil loss and subsequent replenishment. Oil replenishment on service engines is carried out when required to ensure that the oil tank fill level remains between a defined maximum and minimum. Figure 4.13 shows the Total Acid Number and viscosity over a 2500 hour period for two service engines undertaking typical flight cycles. These samples were taken from tank before any oil replenishment was conducted. It should be noted that any decreases in oil viscosity and TAN, particularly at 1000 hours, can be attributed to top up of the oil system with fresh lubricant. For these two engines the TAN remains consistently between 0 and 0.3 mg KOH g⁻¹ and a viscosity between 4 and 8 % above its new value.

4.4.2. Effect of Oil Replenishment

In order to explore the effect of oil loss and replenishment, which is believed to result in oil condition parameters reaching the steady state seen in service, a laboratory based replication was conducted. Tests were undertaken at 190 °C where regular samples were withdrawn for analysis, unlike the previous testing the volume removed was replaced with fresh lubricant. The samples and replenishments were conducted at approximately 72 hour intervals and the replenishment rates shown represent a per hour average throughout the test. Figure 4.14 shows how viscosity increases for three top up rates and two lubricants (one SPC and one HPC). When the lowest rate, where 0.16 % of the volume is replenished per hour, lubricant viscosity increases rapidly and exponentially. This increase is most severe for the SPC lubricant with the HPC lubricant having a delayed onset to degradation. At a rate of 0.41 % per hour, the viscosity increase is much slower but with the trend still towards increasing lubricant viscosity. Again, the SPC lubricant possesses higher viscosity values than the HPC lubricant. For a rate of 0.63 % per hour the viscosity of the oil samples increases gradually for the first 200 hours: after this duration a constant value is reached for both lubricants. At this point, the amount of oil replenishment is sufficient to keep the viscosity of the oil constant. The constant value for viscosity appears to be marginally higher for the SPC oil than the HPC oil.

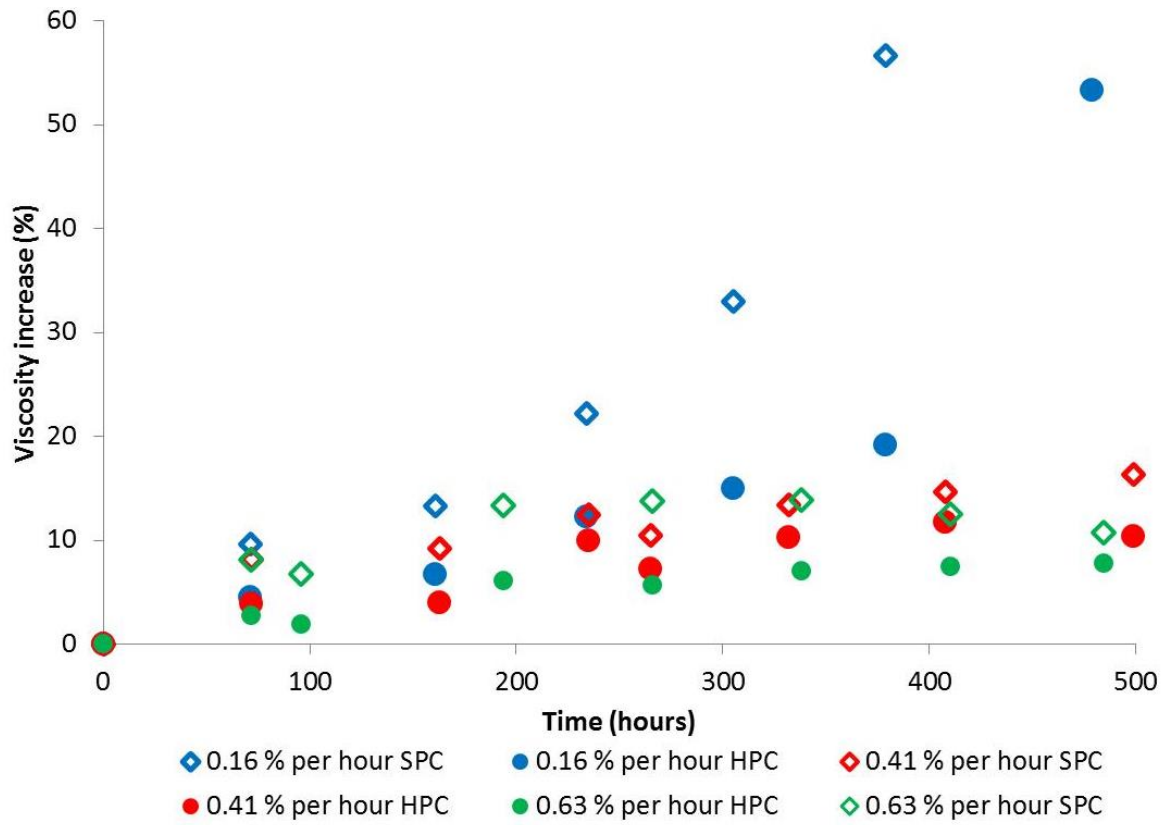


Figure 4.14 Viscosity increase as a function of time, for SPC and HPC oils at three oil replenishment rates

Figure 4.15 shows the change in Total Acid Number for these experiments. The trends are similar to those for viscosity excepting the differences between the 0.41 % and 0.63 % where the replenishment rate is less pronounced; indeed a constant value is reached for both.

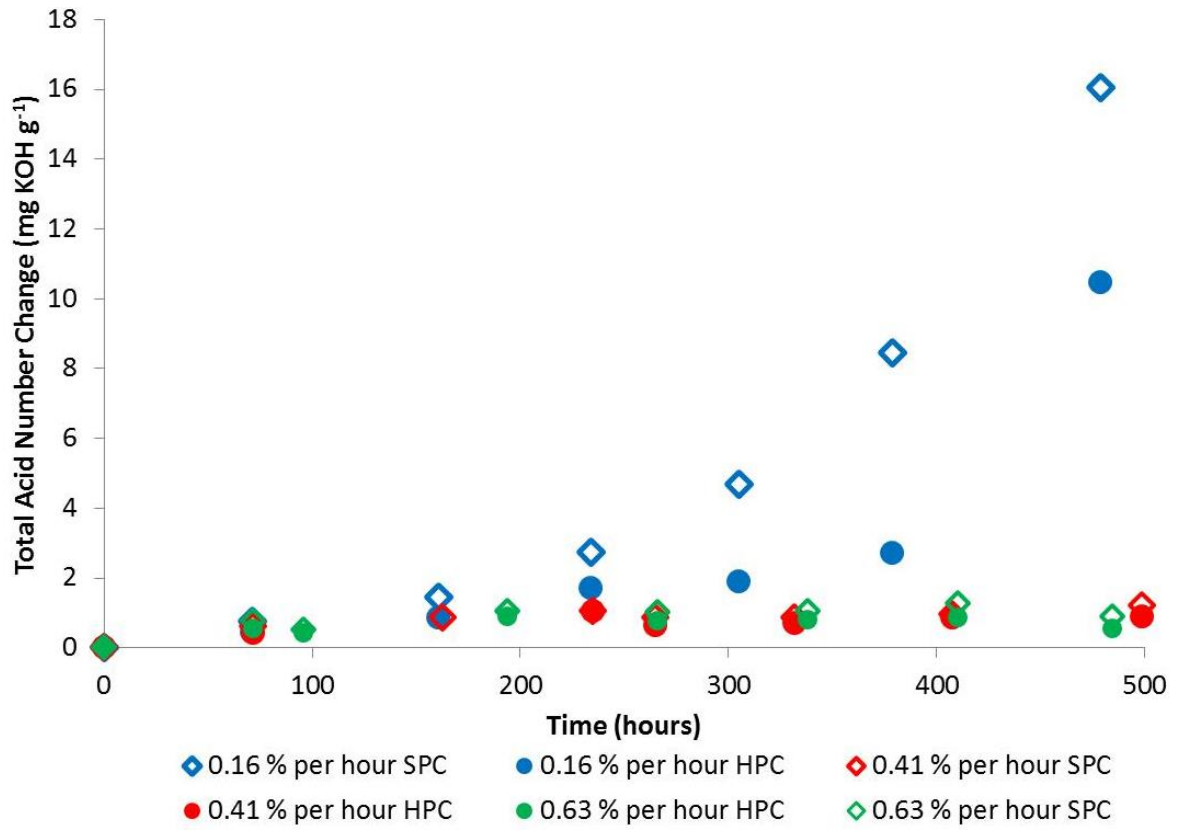


Figure 4.15 Total Acid Number change as a function of time for SPC and HPC at three oil replenishment rates

Figure 4.16 shows the density change for the three replenishment rates; again the trends are similar to viscosity and Total Acid Number. Like viscosity, a small difference can be seen between the 0.41 % and 0.63 % replenishment rates.

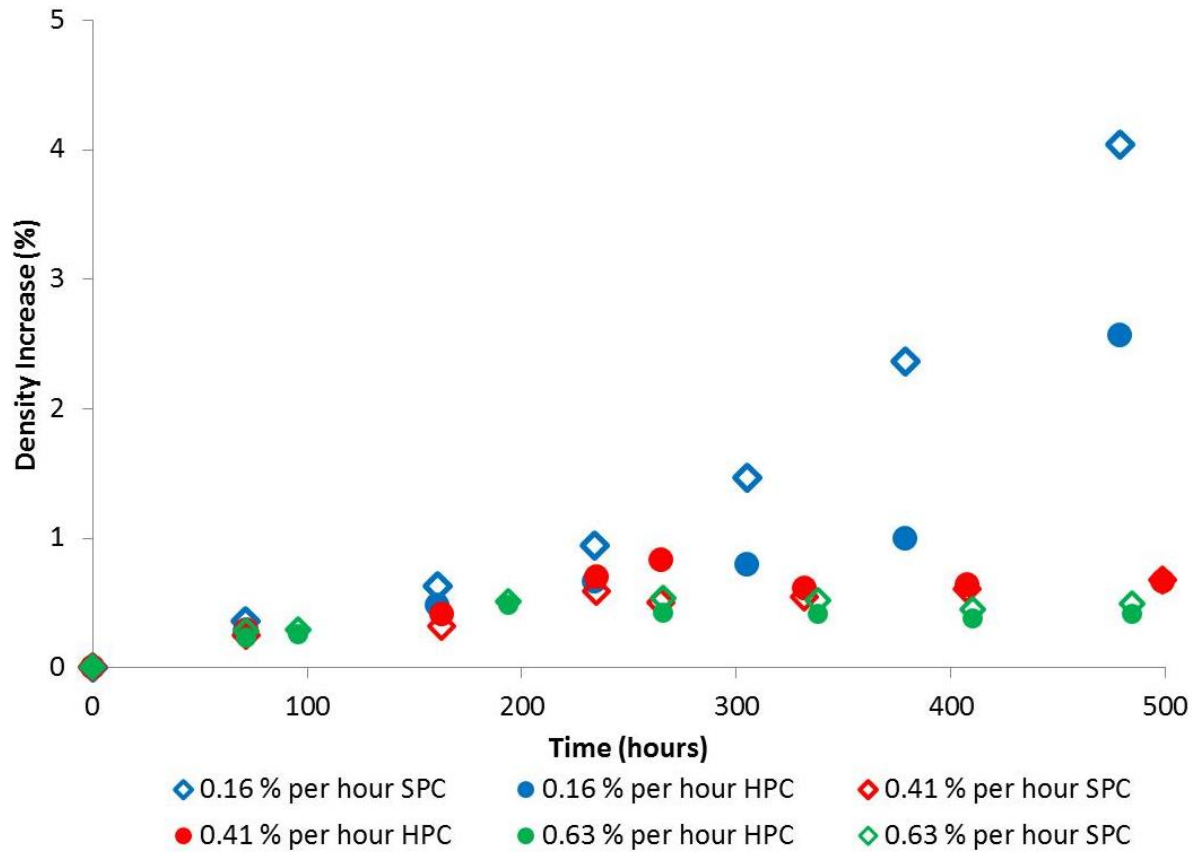


Figure 4.16 Density increase for SPC and HPC oils at three oil replenishment rates

The actual replenishment rate of oil in service is dependent on oil losses and therefore will vary between specific engines. A likely range is expected to be within 0.1 - 0.7 % of the oil system per hour. For an oil to reach the desired 'infinite oil life', the point at which a constant value is achieved, replenishment rate must be at a level which gives an oil condition which is still suitable for use. From the results shown, it is clear that oil replenishment rate would have a significant influence of oil life in service with temperature also being a major factor. For the 190 °C conditions tested, it would appear that the upper end (> 0.63 %) of expected oil consumption values would be required to give 'infinite oil life' for these two lubricants.

4.4.3. Effect of Evaporation

As degradation species, if not volatilised from the system, could potentially participate in further reactions, it is important to understand the chemistry of the volatiles. Therefore a test was carried out where volatiles were condensed, captured and analysed. Samples of vapour were collected at intervals throughout the test period and GC-MS analysis was used to separate and ascertain the chemical species present. Integration of the major peak areas allowed the ratio of compound concentrations to be plotted as test duration and therefore oil degradation progressed.

A similar experiment was undertaken by Zeeman *et al.* (1985), this work however, did not use modern aviation lubricants. Also Zeeman *et al.* (1985) did not take multiple samples in the early stages of degradation (< 72 hours). As this time period represents the extent of the degradation for the majority of service operation, it is therefore of the most interest and requires this study.

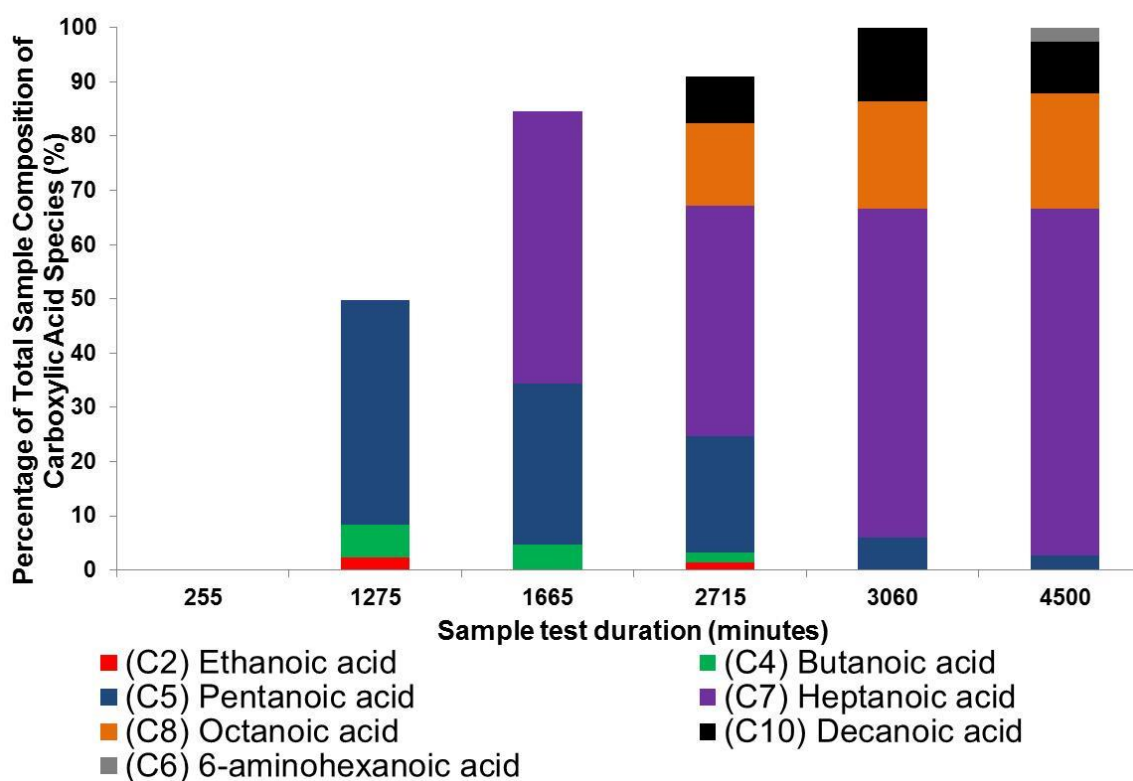


Figure 4.17 Percentage composition of volatilised carboxylic acid species constituents collected throughout the process of oil degradation

Figure 4.17 shows the percentage of each of the carboxylic acid species detected at a range of test durations, the majority of the remaining composition was found to be ester compounds, which for clarity, are not shown. These ester species are believed to have been formed as a result of Baeyer-Villiger oxidation of ketone precursors as described by Zeeman *et al.* (1984) and not as an initial constituent of the ester base stock.

The first sample taken at 255 minutes contained only ester species whilst the second sample (1275 minutes) contained both ester and carboxylic acid degradation products. It is therefore thought that in the early stages of degradation these reactions dominate, however, as degradation progresses carboxylic acids become the major products. As a result of this the ratio of ester degradation products to carboxylic acid products can be seen to change as the ester products which are formed initially, are volatilised or reacted further. Carboxylic acids

continue to form such that after 1665 minutes 85 % of the sample is carboxylic acid with only 15 % ester remaining. After 3060 minutes no ester compounds were detected in the sample vapour comprising wholly of carboxylic acids.

The carboxylic acid species formed at low duration were found to be of short chain length (2-5 carbon units), after longer duration there were an increasingly large percentage of longer chain species (greater than 7 carbon units). The short chain species present could be as a result of degradation of either base stock or additive species, such as metal deactivating additives. As described by Karis *et al.* (1999), the energy required for proton extraction next to the carbonyl group is high, therefore initial degradation reactions are likely to occur at the end of chains preferentially, resulting in the formation of short (C₂-C₅) chain carboxylic acids. Cleavage of the carbon chain near to the carbonyl group to produce long chain acids requires high energy and is therefore unlikely; however, short chain degradation species present within the oil can react further to produce longer chain molecules. The change in the carbon chain length of the volatiles detected as degradation progresses, can therefore be attributed to a reduction in chain cleavage as the ester chains become shortened and thus less reactive. However, further reaction of acid degradation products already present within the oil gives rise to large chain acid volatile products of increased chain length.

As subsequent reaction of lubricant degradation products has been shown to result in the formation of further products, it is important that volatilisation from the test vessel of any degradation products should be controlled. The level of volatilisation from the laboratory test vessel should be as close to the volatilisation losses of the gas turbine oil system as possible, ensuring the species present for further reaction are as near as possible to the service condition (Zeman *et al.*, 1985).

4.4.4. Effect of Metal Test Specimens

The gas turbine oil system contains a range of metals and metal alloys which can interact with the lubricant by catalysing the processes by which esters degrade and therefore affecting their rate of degradation (Zeman *et al.*, 1984). In addition, oil can also corrode or dissolve metals which can potentially cause damage to metal surfaces. In order to understand the influence of different test metal specimens, in the laboratory based method a series of tests were undertaken, again using ASTM Method D4636. As large numbers of different metals and alloys are used across the many different engine types, testing of lubricants with each of the individual metallurgies is impracticable. Therefore, testing was carried out using a range of generalised metals; steel, magnesium, aluminium, copper, titanium and silver, as described in § 3.1.1.

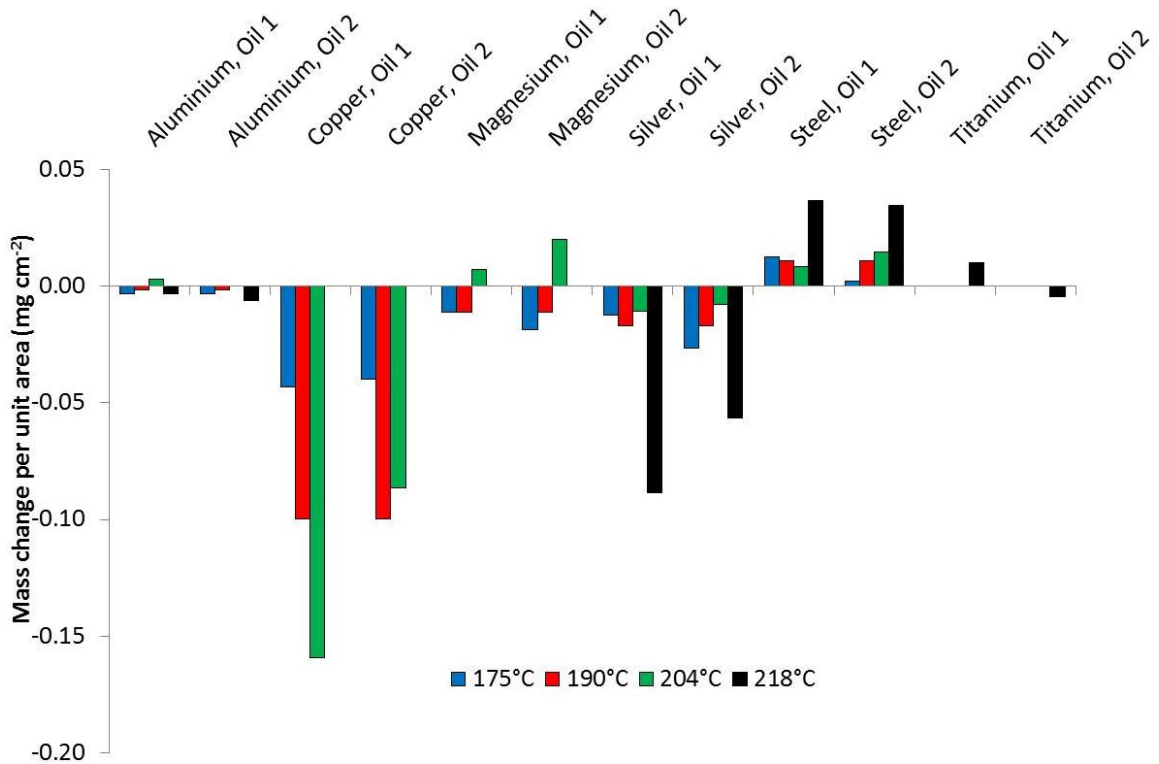


Figure 4.18 Mass loss of test metals in two lubricants at three test temperatures (72 hour tests)

Figure 4.18 shows the change in mass of each test metal when they were heated in the presence of lubricant and air for a 72 hour period. Figure 4.18 shows that some metals gain mass through the addition of material, where as other metals decrease in mass as a result of the removal of some of the material. The steel specimens all increased in mass during the test and microscope inspection showed that the surface of the metal had material present, consistent with carbon deposits, particularly at the highest temperature (Figure 4.19).

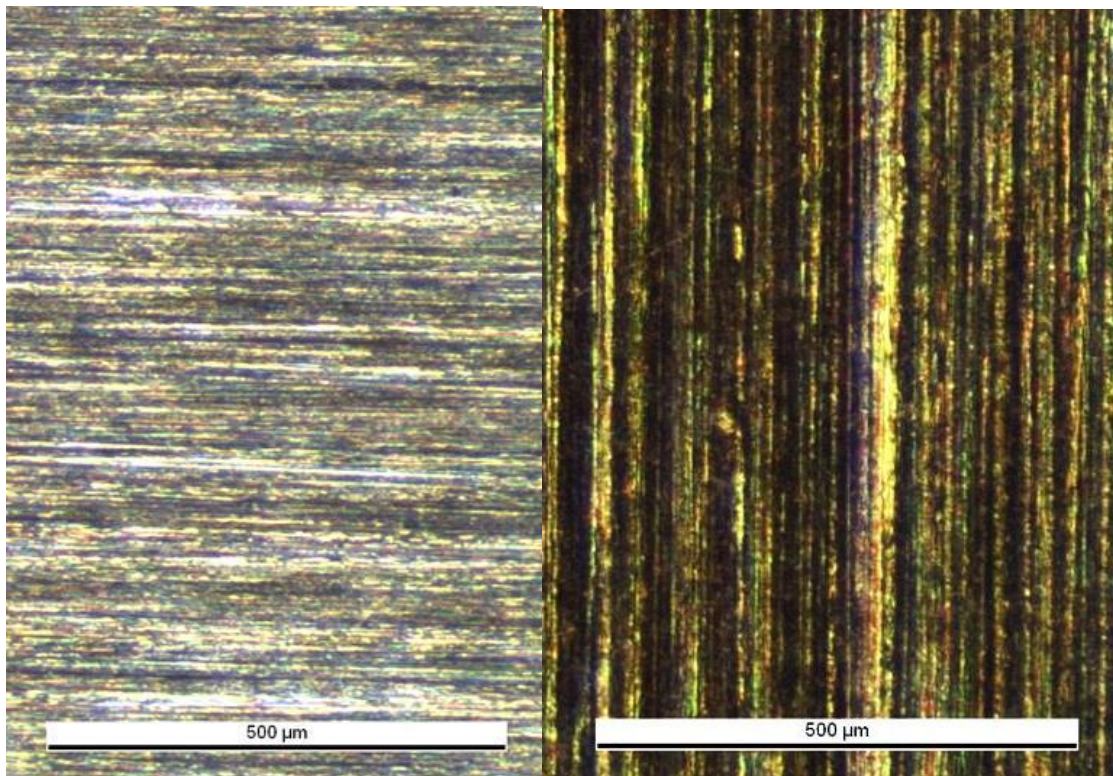


Figure 4.19 Steel test specimens pre-test (left) and post-test (right). Showing carbon deposits within the machining grooves (post-test)

Both silver and copper specimens lost metal mass suggesting that some of the material has reacted or dissolved into the oil. IPC-OES analysis was undertaken on the 190 °C oil samples, which detected 10 and 6 mg kg⁻¹ of copper in oils 1 and 2 respectively. As the total metal area of the specimens used was approximately 13 cm² and the mass of oil was 0.1 kg, these values are approximately consistent with that determined to have been lost from the metal by

gravimetric means (13 and 12 mg kg⁻¹ for oils 1 and 2 respectively). All other metals were below the limit of detection for this technique (1 mg kg⁻¹) and therefore were considered to be negligible; this is again consistent with the gravimetric findings. Increased temperatures again gave rise to a greater mass change, the 218°C test was particularly severe with a greater rise in mass, out of line with that expected by linear extrapolation and this was most pronounced for silver. Aluminium, magnesium and titanium all gave minimal mass change and optical and scanning electron microscopy showed minimal change to the metal surface.

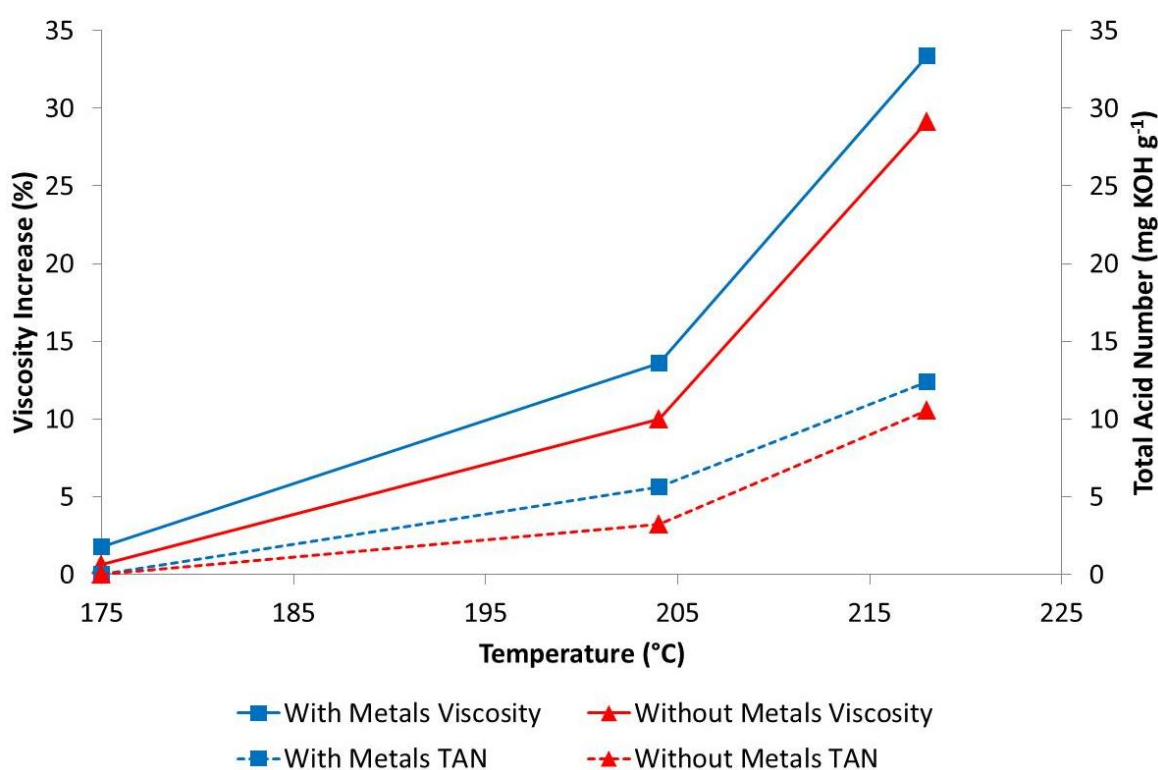


Figure 4.20 The influence of test metal specimens on change in viscosity and Total Acid Number

Figure 4.20 shows the viscosity and Total Acid Number of lubricants tested at three temperatures for a fixed duration of 72 hours. To assess the role metal catalysts have in oil degradation these tests were conducted with all of the following metal specimens present; steel, silver, aluminium, magnesium, copper and titanium and in their absence. The increase in

viscosity is approximately 4 % greater at 204 and 218 °C when metal specimens are present, this trend is the same for TAN for which the influence of metal specimens causes the values to be approximately 2 mg KOH g⁻¹ higher. At the lowest temperature, 175 °C, the viscosity and TAN increase is much smaller as degradation occurs more slowly at lower temperature, however, the catalytic influence of metal is still evident.

Although the influence of metal catalysts can be detected, the differences in degradation rates are quite small, likely due to the presence of metal deactivators such as 1,4-dihydroxyanthraquinone which are present in the formulation. The purpose of metal deactivators is to preferentially bind to the surface of the metal surface in order to inhibit catalytic reactions which may otherwise occur at the metal surface.

4.4.5. Gel Permeation Chromatography

Analysis of both laboratory degraded samples and engine derived samples by Gas Chromatography and Infrared Spectrometry proved ineffective at differentiating chemical changes in the lubricant unless the oil was heavily degraded. Lubricants are usually operated at levels of degradation below that which these two techniques show significant changes in lubricant chemistry. This is due to the fact, as discussed previously, that very subtle changes in the base stock chemistry can have a pronounced influence on the physical properties of the lubricant, therefore GC-MS and Infrared Spectrometry are not useful techniques in assessing changes in base stock chemistry, (Karis *et al.* 1999). It is also known that as lubricants become degraded they contain a larger proportion of high molecular weight species. In order to measure the changes in molecular weight distribution of the lubricant, Gel Permeation Chromatography (GPC) was used, this allowed comparison of the laboratory samples in varying stages of degradation to engine derived samples.

Figure 4.21 shows five overlaid chromatograms; the unused lubricant, an engine derived oil and three laboratory degraded samples at varying stages of degradation. The Total Acid Numbers and viscosities of each of these samples are shown in the legend. The samples are normalised to the molecular weight of largest concentration for each sample allowing changes in molecular weight distribution to be seen. The peak at 2.5 (log Mw) contains two additives of similar mass, an anti-wear additive, tricresyl phosphate (TCP) and an antioxidant, DODPA. TCP acts to form a film at metal surfaces such that the TCP is preferentially removed in favour of the metal on moving contact surfaces such as bearings and gears, protecting the metal surface from excessive wear (Mortier *et al.*, 2010). As TCP is sacrificed in this process, it will be consumed through engine use, this can be seen in Figure 4.21, as the engine derived sample has a depleted peak at a value of 2.45. Laboratory degraded samples, however, where wear processes do not occur, do not have the peak depleted to the same extent. The small reduction in the peak at 2.5 (log Mw) can most likely be explained by the loss of some of the DODPA antioxidant and not TCP.

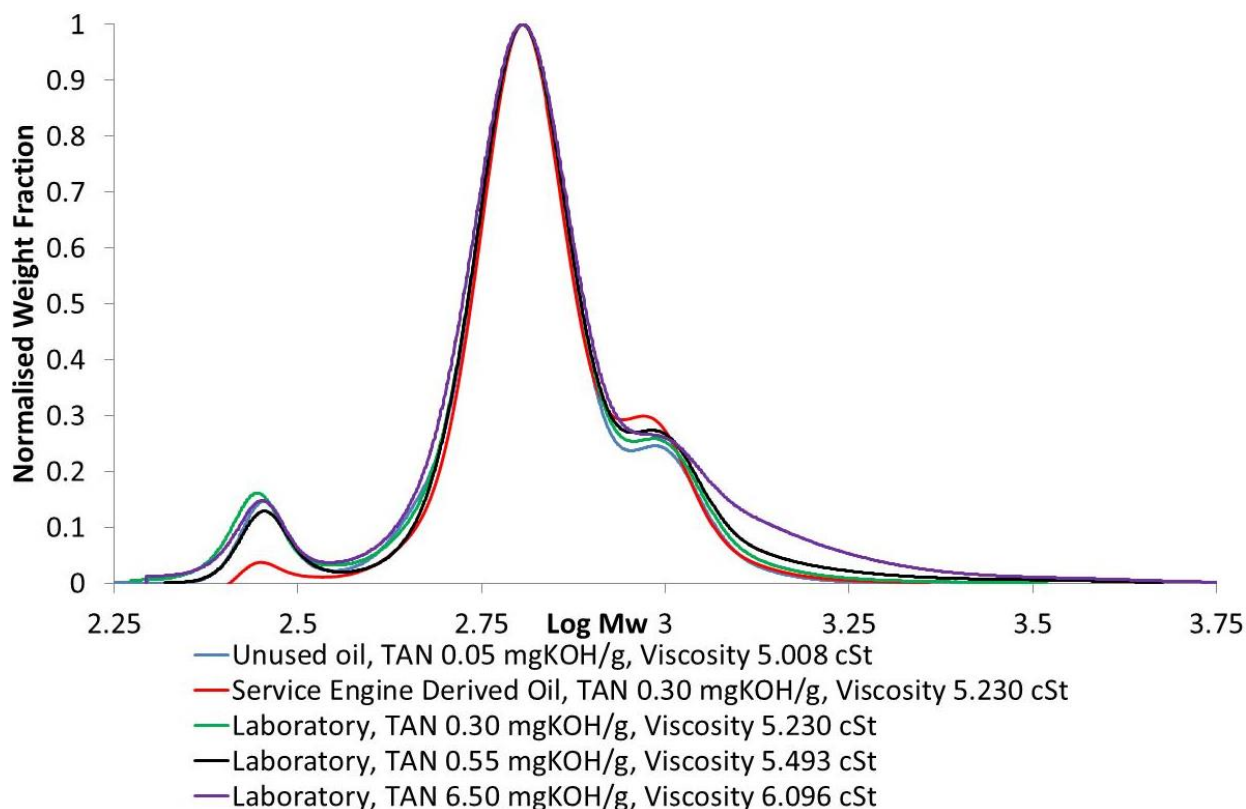


Figure 4.21 Gel Permeation Chromatogram showing a range of laboratory degraded oil samples, an engine derived sample and a reference sample of oil as new

The general trend is that as oil becomes more degraded a greater proportion of the formulation is of higher molecular weight, this can be attributed to the oligomerisation and polymerisation of oil species. This broadening towards higher molecular weight can be seen to increase as the laboratory samples become more degraded, these results are consistent with an increase in viscosity and acidity. The most heavily degraded laboratory sample with a Total Acid Number of $6.5 \text{ mg KOH g}^{-1}$ also gave a slight spread in low molecular weight species which was attributed to the cleavage of base stock species which have not been volatilised from the test vessel.

A broadening across the chromatograph shows that the range of molecular weights present has increased and therefore the number of different individual compounds has increased

through reaction. The chromatogram of the engine sample, when compared to the laboratory sample with the same viscosity and Total Acid Number had a similar shape however, it showed an increase in the high molecular weight species at 3.0 (log Mw). This was believed to be due to the fact that engine oil is regularly topped up with fresh oil in order to replenish losses. As some of these losses can occur through volatilisation, the more volatile species, which tend to be those of low molecular weight, will be preferentially removed; therefore higher molecular weight species will begin to accumulate within the oil system.

In order to understand the influence of oil replenishment on molecular weight distribution, oil samples generated in the testing conducted in § 4.4.2 were analysed by GPC. Figure 4.22 shows the chromatograph enlarged to show the areas of interest: the high molecular weight species in the laboratory samples, fresh unused lubricant and a service engine derived samples. The laboratory samples (at 4 durations) were from the highest oil replenishment rate test (0.63 % per hour), as these were found (§ 4.4.2) to give the closest TAN and viscosity values to service operation. Minimal difference could be seen between the laboratory samples at varying durations with only a very small increase in molecular weight with increasing duration. This would indicate that the loss and replenishment rate was sufficient to keep a constant molecular weight distribution.

It can be seen that the proportion of species at 3.0 (log Mw) was similar to that seen in the service derived sample. As this was not the case for laboratory testing without oil replenishment it is likely that this is due to accumulation of this species as suggested previously. The laboratory samples however also show an increase in species > 3.0 (log Mw) which was not seen in the service sample. This is likely to be an indicator that the laboratory

conditions are marginally more severe than the engine conditions as a result of an increased temperature accelerated test.

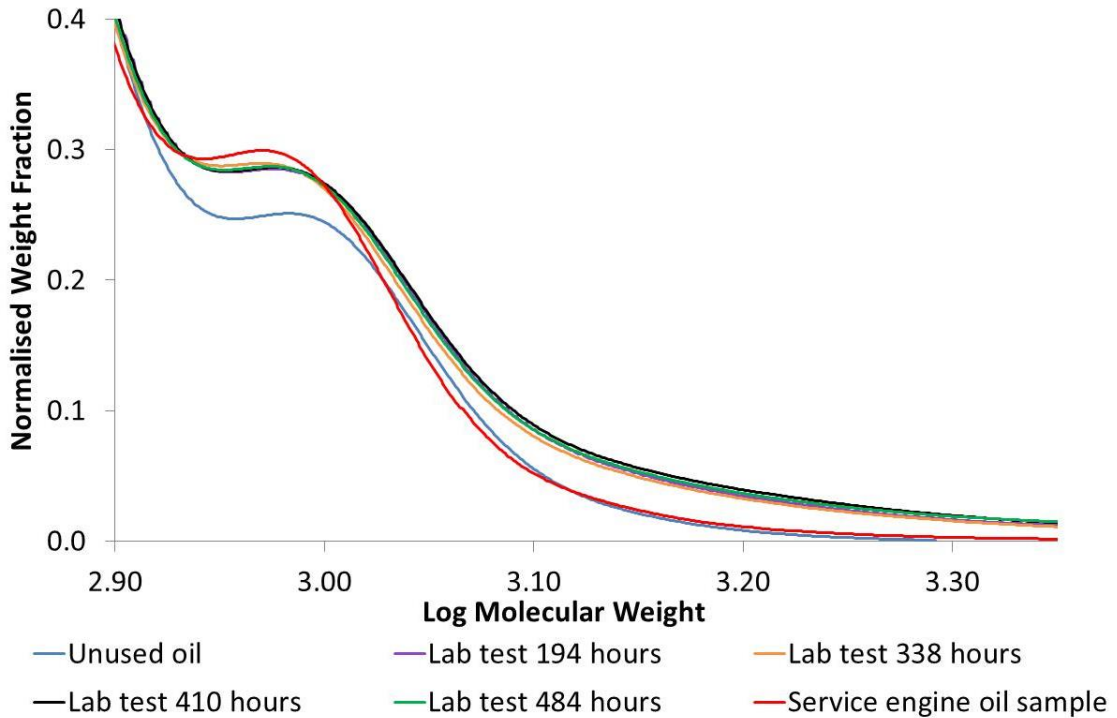


Figure 4.22 Gel Permeation Chromatography of oil replenishment test samples (0.63 % per hour)

4.5. Test Method Modifications

From the work presented in this thesis, in addition to work previously conducted by the E34 Propulsion Lubricants Committee (Lee, 2008), it is clear that there are changes to the current oxidative degradation methods which could be made to improve the quality of data generated. As industry specification methods are used by a number of parties, there is a degree of resistance to change particularly where the change involves financial or time costs. Therefore, it is important that any proposed method can be widely and simply implemented at minimal cost. As such, it was decided that modification to the existing ASTM D4636 equipment and method, could allow improvements to be made with minimal cost and difficulty. This would make the method more likely to be incorporated across the industry. Additionally,

combining the benefits of a number of methods into one could allow the removal of one or more methods from the specification reducing the cost and time involved in future testing.

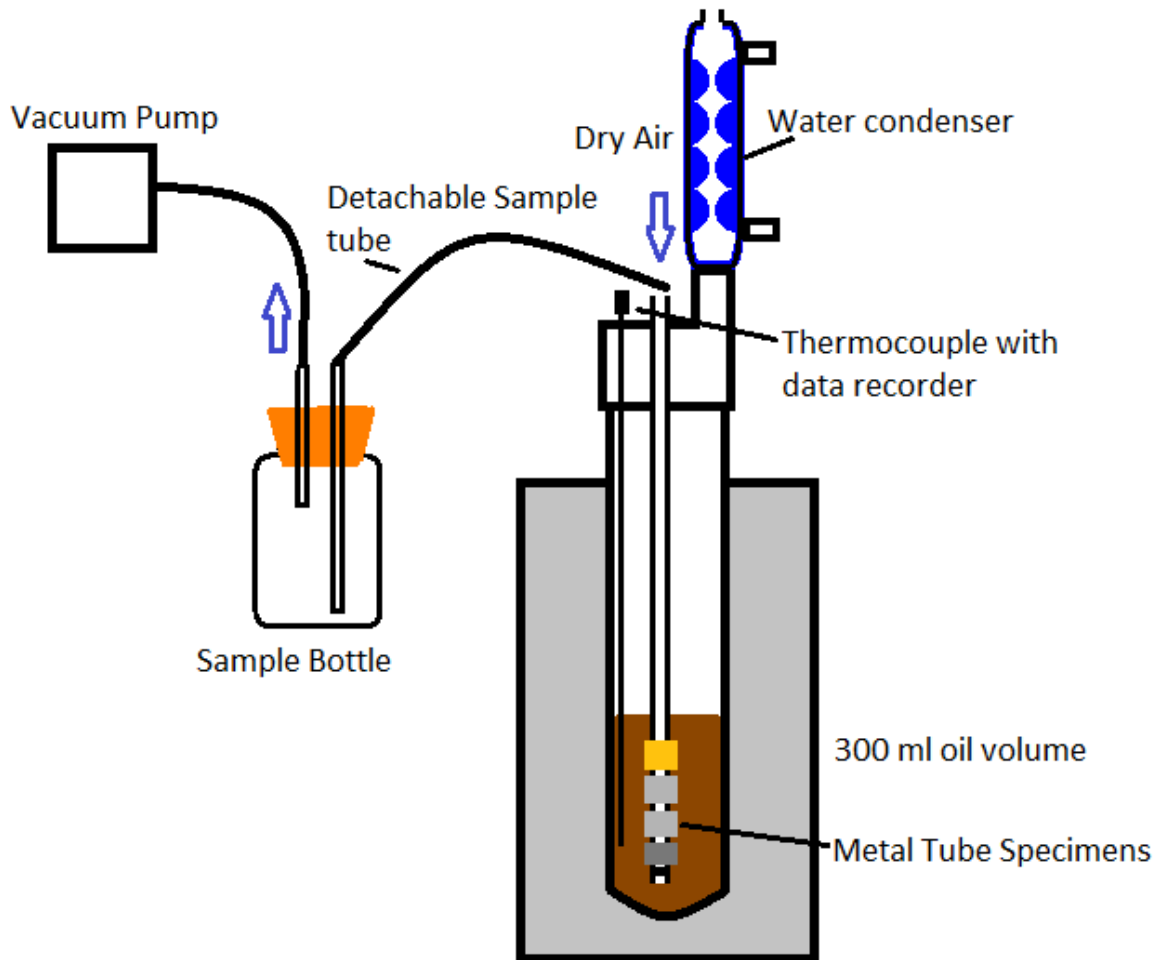


Figure 4.23 A schematic of the modified oil oxidation method

Figure 4.23 shows a schematic of the modified method equipment. The improvements to the method were made for one or more of four key reasons, to increase precision, practicality, volume of data and engine applicability.

- Precision Modifications

The precision modifications made are centred around key variables. Temperature is controlled as with ASTM D4636, however, the addition of a data logger allows the actual temperature of

the oil (rather than metal block) to be monitored throughout the test. This allows any fluctuations in temperature to be detected and the average temperature to be calculated.

As determined previously, air flow can have a marked effect on degradation and volatilisation, therefore control of flow rate is important. Digital flow controllers are now used to allow flow to be regulated to $\pm 0.5\%$ with automatic adjustments made for fluctuations in inlet air flow. The air is also filtered to remove moisture, hydrocarbons and particulate contamination.

The water temperature of the condensers is controlled by a recirculating water cooler with an inline data recorded thermocouple such that any deviation is detected. This ensures a constant volatilisation loss rate is maintained.

- Practicality Modifications

The sampling method is such that a vacuum pump can be used to draw a sample through the air tube and into a sample bottle. This allows a sample to be removed easily and safely whilst the test is in progress without opening the test vessel. Current metal test specimens are expensive and require time consuming preparation. This modified method incorporates specimens which can be easily cut from a length of tube and simply inserted over the current air tube. This allows metal tubing, which is low cost and readily available, to be purchased to a defined specification.

- Volume of Data

Defence Standard, Method 9 allows the generation of a large amount of data to be generated as both temperature and duration are varied. This requires an individual test to be conducted for each test point and therefore is a very laborious process. By incorporating a larger test volume and a sampling procedure, four test points can be achieved from a single test. Each

sample can be analysed for viscosity, Total Acid Number and density which allows the maximum amount of data to be generated with minimal effort. A wide range of other properties could also be measured, including: flash point, surface tension, specific heat capacity and metals concentration.

- Engine Applicability

Following the study of air flow rate and volatilisation it was determined that a condenser as used in ASTM D4636 was the best method to ensure degradation was as near to service levels as possible. The flow rate was increased to 150 ml min⁻¹ from the 83 ml min⁻¹ used in ASTM D4636: this ensures that the reaction is not oxygen limited and also brings the TAN to viscosity ratio more in line with the engine samples as discussed in § 4.3.3.

The test metals used are stainless steel, titanium, inconel, aluminium and copper. The first four of these metals were chosen as they represent some of the most common metals used with the oil system. Specific aerospace alloys were not specified as this would add additional complexity and would be unlikely to make a significant difference in test result. Copper was chosen, although rarely used in its pure form in the oil system (it is used in brass or bronze alloys), as it represents one of the more severe catalysts in the degradation process and therefore is useful for lubricant quality control.

4.6. Modified Method Data

Testing was conducted using this modified method at 175, 185, 195, 204, 218 °C; these temperatures were chosen firstly as they encompass the range of temperatures which a lubricant might reach in service. Additionally as 175, 204 and 218 °C are the ASTM D4636 temperatures currently required by SAE AS5780 (2013), testing at these temperatures allows

ease of comparison between methods. Unlike this ASTM D4636 data, the modified method meant that multiple samples could be taken during the test, therefore data at a range of durations was produced. Two lubricants were tested, a HPC and a SPC lubricant with the TAN, viscosity and density of each sample determined.

Figure 4.24 and Figure 4.25 show how Total Acid Number changes with time at each temperature. Differences between the SPC and HPC lubricants are most pronounced at lower temperatures, where the superior antioxidant performance results in a slow formation of acidic degradation species. An approximately linear correlation to degradation duration can be seen for TAN increase.

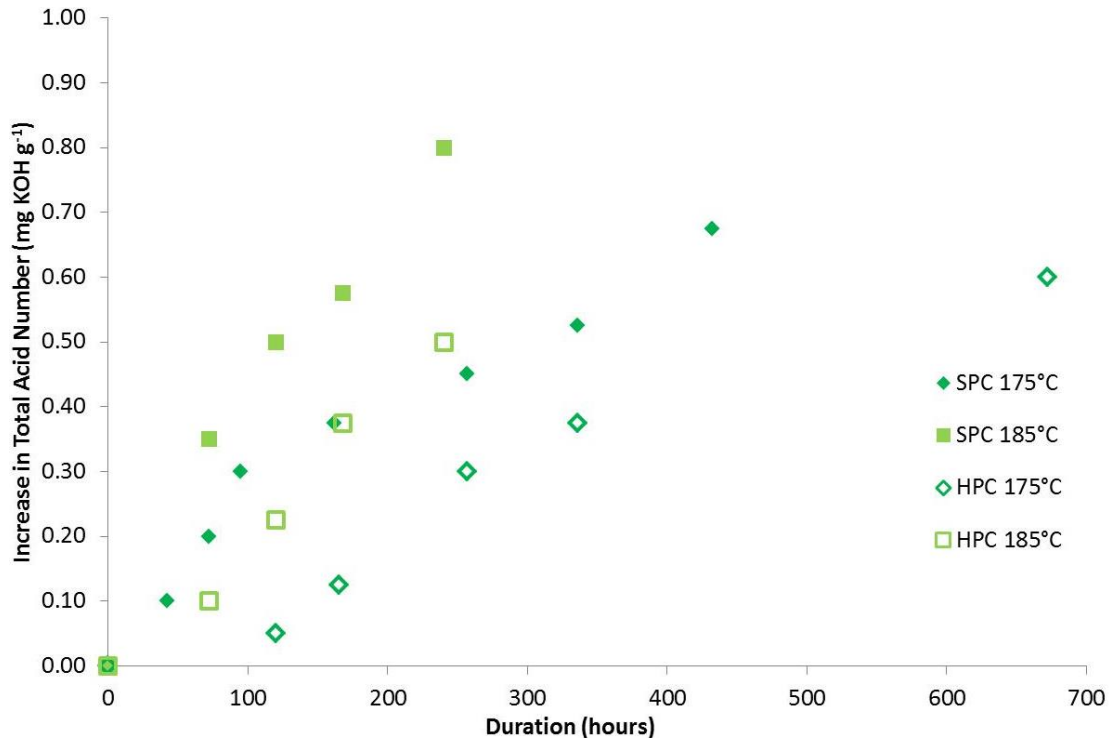


Figure 4.24 Increase in lubricant Total Acid Number as a function of time using the modified method (175 and 185 °C)

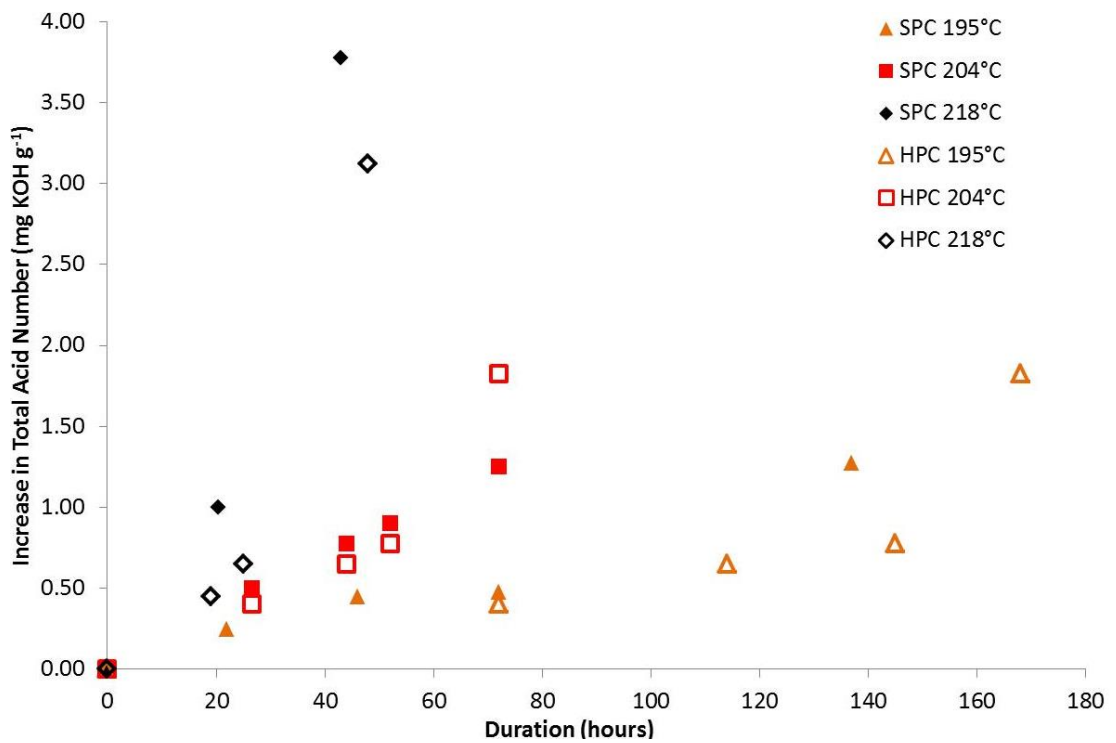


Figure 4.25 Increase in lubricant Total Acid Number as a function of time using the modified method (195, 204 and 218 °C)

Figure 4.26 and Figure 4.27 together show the increase in viscosity of the lubricant at these five temperatures. The difference between SPC and HPC lubricant is more pronounced for the viscosity data than it was for TAN, indeed the HPC lubricant gave a lower increase in viscosity at 185 °C than the SPC lubricant did at 175 °C (Figure 4.26).

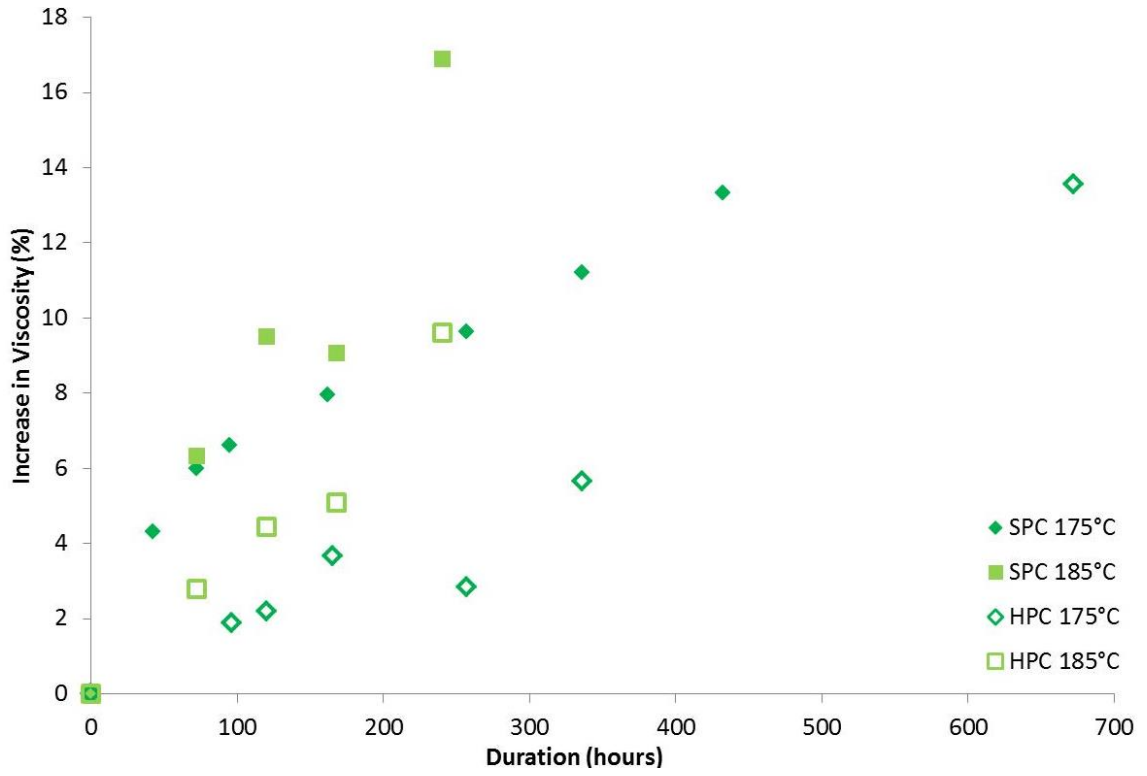


Figure 4.26 Increase in lubricant viscosity as a function of time using the modified method (175 and 185 °C)

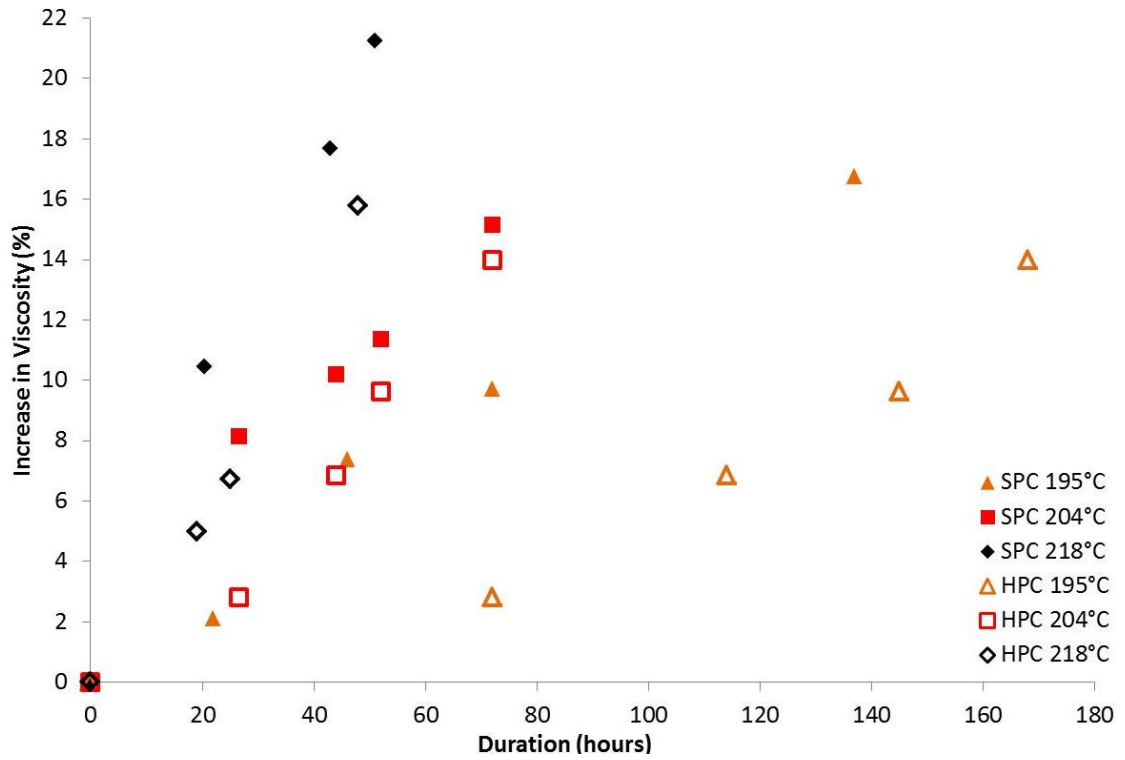


Figure 4.27 Increase in lubricant viscosity as a function of time using the modified method (195, 204 and 218 °C)

Figure 4.28 and Figure 4.29 show the increase in lubricant density and whilst similar trends are followed for viscosity, the data can be seen to be more linear. This is perhaps because density, unlike viscosity is not significantly influenced the increased hydrogen bonding which occurs as a result of oil degradation.

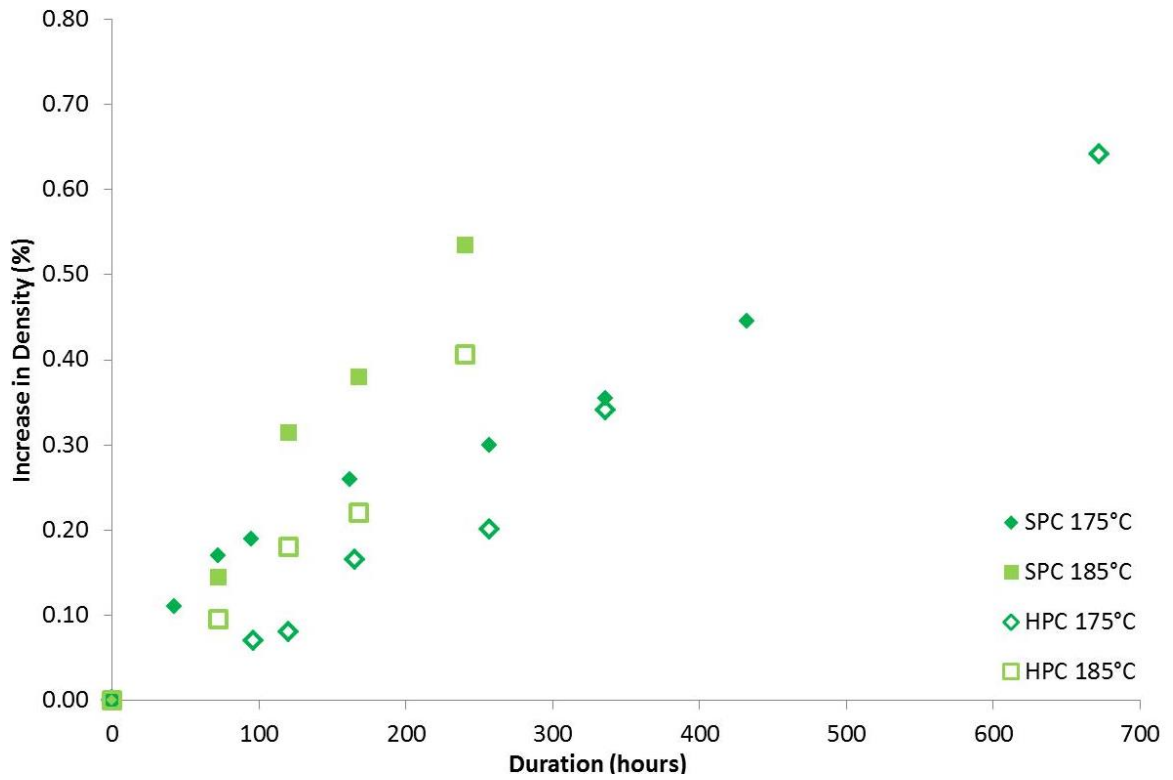


Figure 4.28 Increase in lubricant density as a function of time using the modified method (175 and 185 °C)

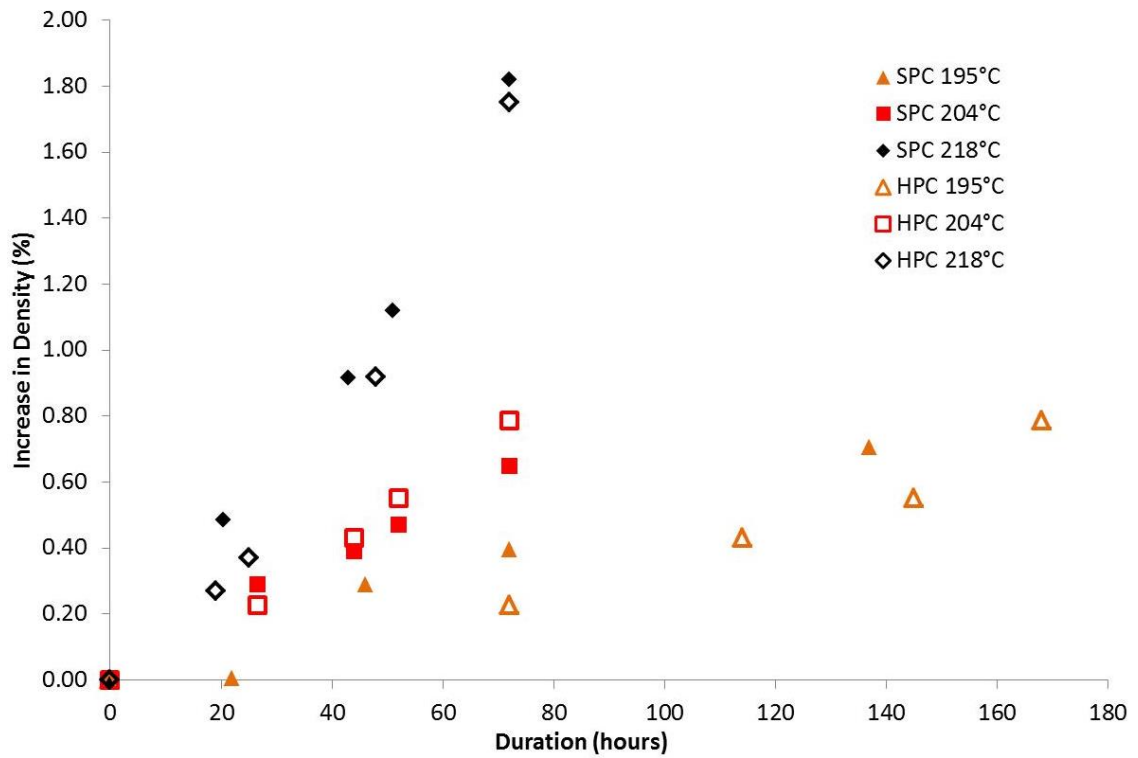


Figure 4.29 Increase in lubricant density as a function of time using the modified method (195, 204 and 218 °C)

Figure 4.30 shows a comparison of ASTM D4636 data to that generated by the modified method. The data shown is the change in TAN and increase in viscosity following a 72 hour duration test as defined by ASTM D4636. The error bars indicate standard error. It can be seen that the increase in air flow rate has, as expected, led to a decrease in oil acidity for the modified method, this is due to an increase in volatiles passing through the water condenser. Lubricant viscosity, however, is reasonably consistent between the two methods showing that the level of degradation has not been greatly affected by the changes made to the method. The small decrease in viscosity for the modified method could be explained by the removal of some of the volatile species (which would be present in ASTM D4636) causing further reaction to result in an increased oil viscosity.

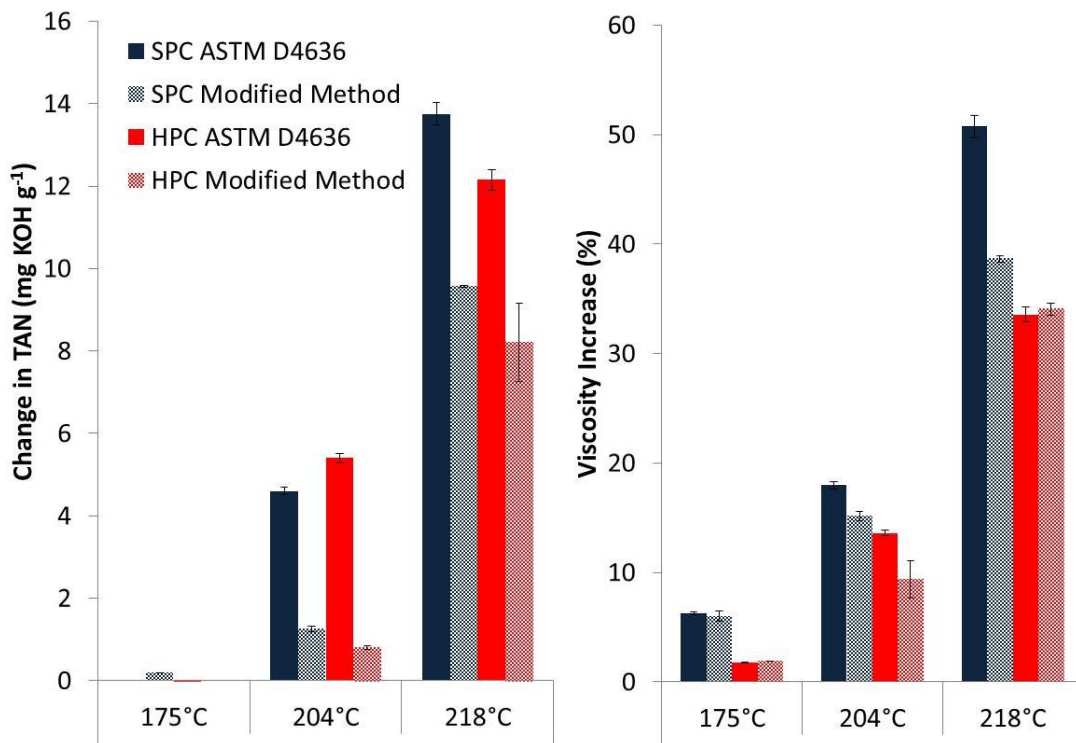


Figure 4.30 Comparison of ASTM D4636 to the modified method (72 hour duration)

In § 4.3.3 the ratio of viscosity to Total Acid Number was used as a method for comparison of service oil samples to laboratory oil samples (Figure 4.10). This showed that whilst ASTM

D4636 matched the viscosity / TAN relationship of service oils most closely, marginally higher TAN values were seen for a given viscosity. Because of this an increased air flow rate (150 mL min⁻¹) was chosen for the modified method, this is shown in Figure 4.31 to have reduced the TAN of the oil samples through increased volatilisation to bring the samples closer to service oil samples.

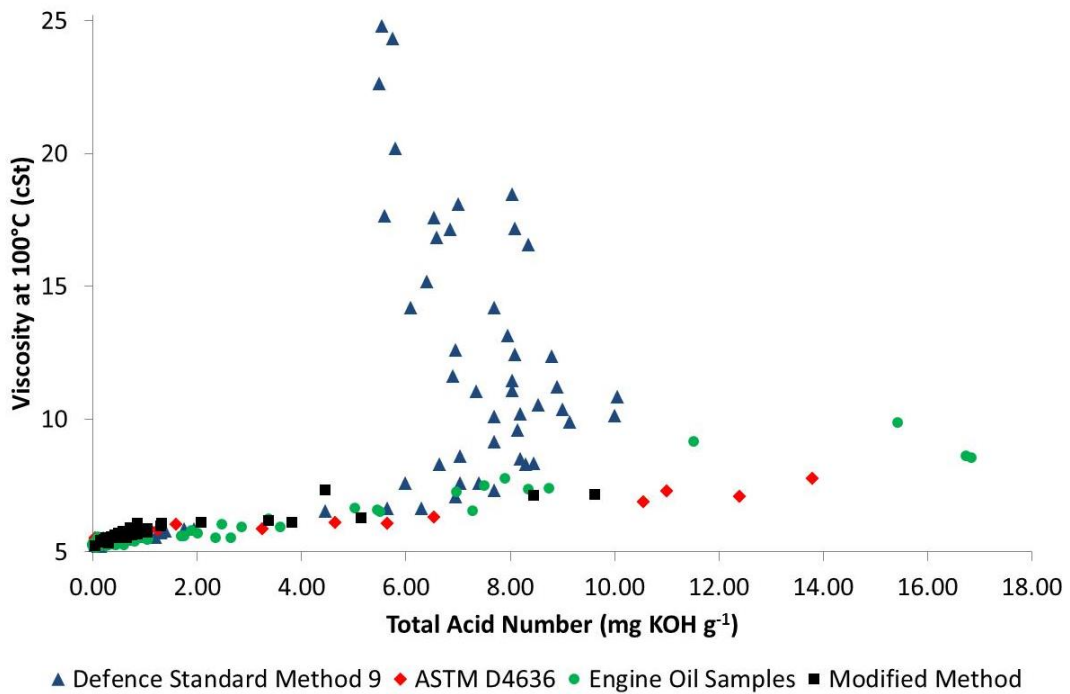


Figure 4.31 Comparison of oil Viscosity and Total Acid Number including modified method data

4.7. Closing Remarks

A need to evaluate the suitability of the current thermal oxidative stability laboratory methods to assess modern gas turbine lubricants, in a manner representative of their service use, was established. A critical review combined with comparative testing, highlighted a number of differences and compromises between the current methodology and the condition to which lubricants are exposed to in the gas turbine.

Testing was conducted to better understand the influence these parameters have on the degradation and chemistry of lubricants. This testing identified the control of species volatilised from the test vessel as a key parameter which along with a number of other parameters, must be controlled in order to maintain precision and to match the conditions to that seen in the gas turbine. The extent to which volatilisation occurs was found to be heavily dependent on the flow rate of air.

Utilising knowledge gained from both the review of existing methods and the parameter sensitivity analysis, a new methodology was devised. This method, to reduce the cost and difficulty of industry adoption, was based around the already widely used ASTM D4636 method. The method allowed the generation of a large dataset with minimal effort, when compared to other methods, due to incorporation of in test oil sampling.

Analysis of the data generated, showed this data is suitable to provide the rate of reaction information needed to produce an oil life model. Validation showed a good match between oil degraded by this method and through use in gas turbines.

The work in this chapter furthered the understanding of how thermal oxidative degradation reactions result in physical and chemical changes to the bulk fluid. In the next chapter, lubricant deposition is explored via further progression of these reactions to give the localised formation of insoluble carbon deposits.

CHAPTER 5: DEPOSITION

5.1. Introduction and Business Case

In the previous Chapter, chemical and physical changes to lubricant properties at elevated temperature were explored. The changes studied were those which occur as a result of prolonged exposure to temperature and result in a relatively homogenous, bulk fluid. In this chapter, lubricant deposition, which can be considered to be a more extreme form of thermal degradation that occurs to only a small proportion of the lubricant in a discrete area, will be investigated. Deposition is known to occur at hot wall surfaces, where lubricant molecules can be exposed to temperatures in excess of 300 °C resulting in degradation and polymerisation.

The deposits can be very hard and well adhered, as such, if allowed to accumulate they can restrict or cause blockage thereby starving components of oil. If oil flow to the mainline bearings is significantly reduced the rotating elements of the bearing will quickly overheat, possibly to the extent that the melting point of the bearing is exceeded, giving the potential to cause significant damage. Additionally, any residual oil in the vicinity of the bearing may be subjected to temperatures above the auto ignition temperature of the oil. As sealing air flows into the chamber, fire will occur causing significant damage to the surrounding components. With the result of deposit accumulation being potentially so severe, it is critical for gas turbine manufacturers to understand where, under what conditions and how quickly deposits will form.

Oil derived deposits can form in gas turbines over many thousands of hours and under a range of operating conditions, it is therefore not practical to evaluate all candidate lubricant brands via engine tests, which are extremely expensive due to their labour intensive nature, cost of

equipment, facilities and fuel. As such, laboratory rig scale lubricant simulators are required to screen candidate lubricant brands and to identify particular high risk engine locations and operating conditions.

Whilst the gas turbine lubricant industry has a number of available methods, these methods are primarily designed to act as screening tools by which the relative rates of deposit formation for different oil brands can be determined. They therefore replicate general hot wall environments and are not designed to specifically replicate gas turbine conditions. The Rolls-Royce strategy, however, is to reproduce conditions which occur within their engines as closely as possible, allowing a direct correlation to engine conditions.

Oil system simulators of this type allow Rolls-Royce to accurately evaluate candidate lubricants and select the most suitable lubricant for a particular location. This reduces the risk of potentially hazardous and costly service events. Laboratory simulators can also give an indication of deposit formation rate under particular conditions in service; this allows Rolls-Royce to schedule maintenance when needed. Whilst under-maintenance has an obvious risk, maintenance itself requires disassembly of critical oil systems components, resulting in a level of risk, therefore over-maintenance is equally undesirable. Accurate scheduling of maintenance also reduces cost and disruption to airline operations.

As part of a previous Engineering Doctorate project (Askins, 2010), laboratory simulators were designed to mimic two specific oil systems locations; the bearing chamber vent and feed pipes. Askins' thesis included the design and manufacture of these two simulators as well as the initial testing. In this thesis, further development work was conducted which is intended to make the simulator more representative of oil system conditions. Additionally testing of both

different lubricants and different engine conditions was conducted. All results presented in this thesis were obtained as part of this EngD project

This chapter is structured as follows: § 5.2 gives an overview of the different deposition methods currently available in the industry. Areas where these methods differ from the conditions within the engine are highlighted along with areas for improvement. § 5.3 includes results of work conducted into two phase deposition using the Vent Pipe Simulator (VPS). A discussion of the flow and temperature conditions within the simulator is shown. Results from the VPS on the influence of oil brand and test duration on deposition formation are presented along with oil and deposit analysis data.

§ 5.4 describes single phase, cyclic testing using the Feed Pipe Simulator (FPS). Results demonstrating the ability of the FPS to differentiate oil brands and the effect of different shutdown conditions are shown. The improvement modifications undertaken on the FPS, along with a supporting rationale are given in this section. Finally, results on the chemistry and quality of the bulk oil during testing are given.

§ 5.5 includes closing remarks for this Chapter and provides a link to work in the following chapter.

5.2. Current Laboratory Deposition Methods

The industry has a number of methods by which lubricant deposition is assessed. The methods discussed in this section are all publically available and laboratory scale, they also form part of SAE AS5780 (2013). It is known that a number of (proprietary) methods are also used by organisations within the industry, although as the details of these methods are not available and often proprietary, they are not discussed. In addition to laboratory tests, larger scale rig

and engine methods are available but this Chapter concentrates on the laboratory scale methods which are the focus of this thesis.

5.2.1. Hot Liquid Process Simulator (HLPS)

The HLPS (SAE ARP5996, 2013) is a laboratory scale method for the assessment of the propensity of a lubricant to form solid deposits under single phase conditions. This method is widely used throughout industry and forms part of SAE AS5780 (2013). A schematic of this method is shown in Figure 5.1. The closed loop HLPS system consists of an oil reservoir (which is heated using an electric jacket heater), a gear pump and a test piece. The test pieces are single use, hollow rods made from 316 grade stainless steel, with the lubricant being passed over the external surface of the heated rod. Heat is achieved by electrical resistance heating at either end of the test piece giving rise to a temperature gradient across the test specimen. The temperature of the test piece is both controlled and monitored throughout the test using a thermocouple located within the inner bore of the hollow test piece. The system is pressurised using a 200 psi compressed air source at the oil reservoir, no vent is provided on the system. The mass of deposit formed on the test piece is determined gravimetrically after the test is completed (the standard durations are 20 and 40 hours).

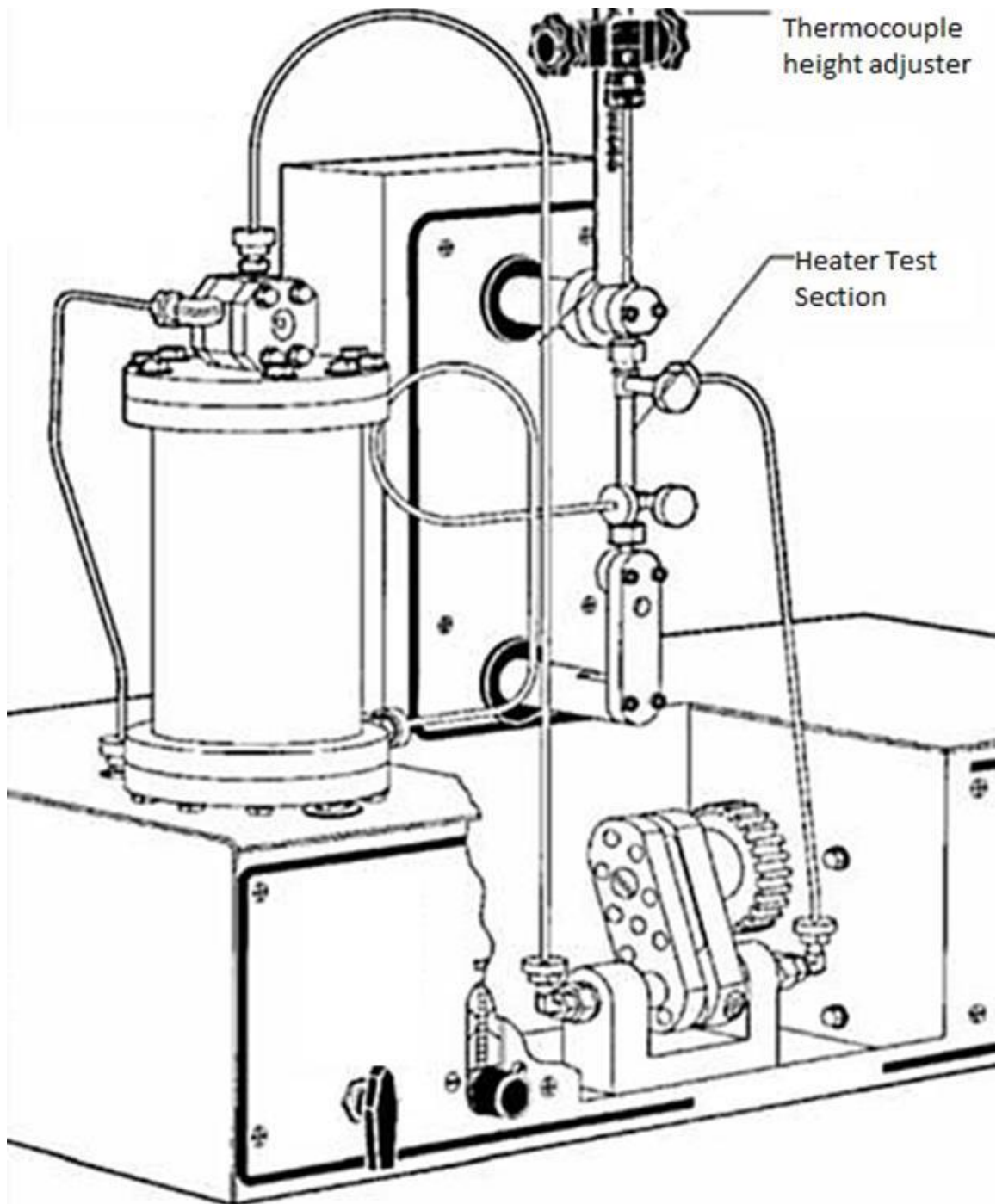


Figure 5.1 Hot Liquid Process Simulator (HLPS), taken from: SAE ARP5996 (2013)

The timescale of the method is accelerated, when compared to a gas turbine, in order to achieve deposits within the 20/40 hours. This acceleration is primarily achieved through the use of a low oil flow rate, thereby reducing surface shear stress and increasing the residence

time of the lubricant within the heated test section. Additionally, higher wall temperatures than those commonly encountered throughout the majority of a gas turbine flight cycle, are used. Additionally the system is entirely unvented, therefore any products formed as the oil degrades are unable to leave the system. This leads to oil with Total Acid Number (TAN) in excess of what would normally be seen in service oil systems.

Due to the largely increased oil and wall temperatures and the lack of an air introduction and venting system, this method is not representative of gas turbine oil systems. However, it has been proven to be effective in predicting the deposit forming propensity of lubricant brands relative to one other, approximately similar to their in-service performance. The current method only allows the assessment of lubricant deposition under steady state (engine running type) conditions.

5.2.2. ERDCO Bearing Rig

The ERDCO Bearing Rig. Federal Test Method Standard No 791C Method 3410 (US Defense Logistics Agency, 2007), forms part of SAE AS5780 (2013) and is a method by which oil deposits formed around a test bearing can be assessed. The rig incorporates a rotating, heated bearing assembly which is lubricated by means of the supply of the test lubricant. Following the test duration (a range of 'test severities' are specified in the method), the amount of deposit formed on and around the bearing is determined by a visual assessment method.

The bearing chamber arrangement is not representative of a gas turbine mainline bearing, in terms of flow rate, air sealing, speed and temperature. In addition, deposition in service operating engines is not commonly found in significant quantities inside the bearing chamber and therefore does not give significant issues. This method does not cover the most common area for deposits; within the pipes that service the bearing chamber.

5.2.3. Vapor Phase Coking Test

The only publicly available two phase method is the Vapor Phase Coking Test (SAE ARP5921, Draft) initially designed by the US Navy to replicate bearing chamber conditions. The test apparatus, shown in Figure 5.2, is configured such that the test lubricant is held in a glass flask which is externally heated. Air is then blown through the heated lubricant and out through a furnace and coker tube. As oil vapour will be carried from the oil over the tube walls heated by the furnace, deposition can occur at the walls. The propensity of the test oil to form deposits is determined from the mass of deposit formed on the coker tube.

Gas turbine vent pipes contain an oil mist generated in the bearing chamber by the shearing of the liquid oil, the mist formed under most engine conditions will comprise of fully formulated liquid phase oil droplets. Under running conditions engine vent pipes will contain a minimal proportion of oil vapour: gaseous phase oil formed by evaporation of some or all of the constituents of the oil formulation. As this method forms an oil vapour solely as a result of evaporation, it is not considered to be truly representative of a bearing chamber vent pipe under the majority of engine conditions.

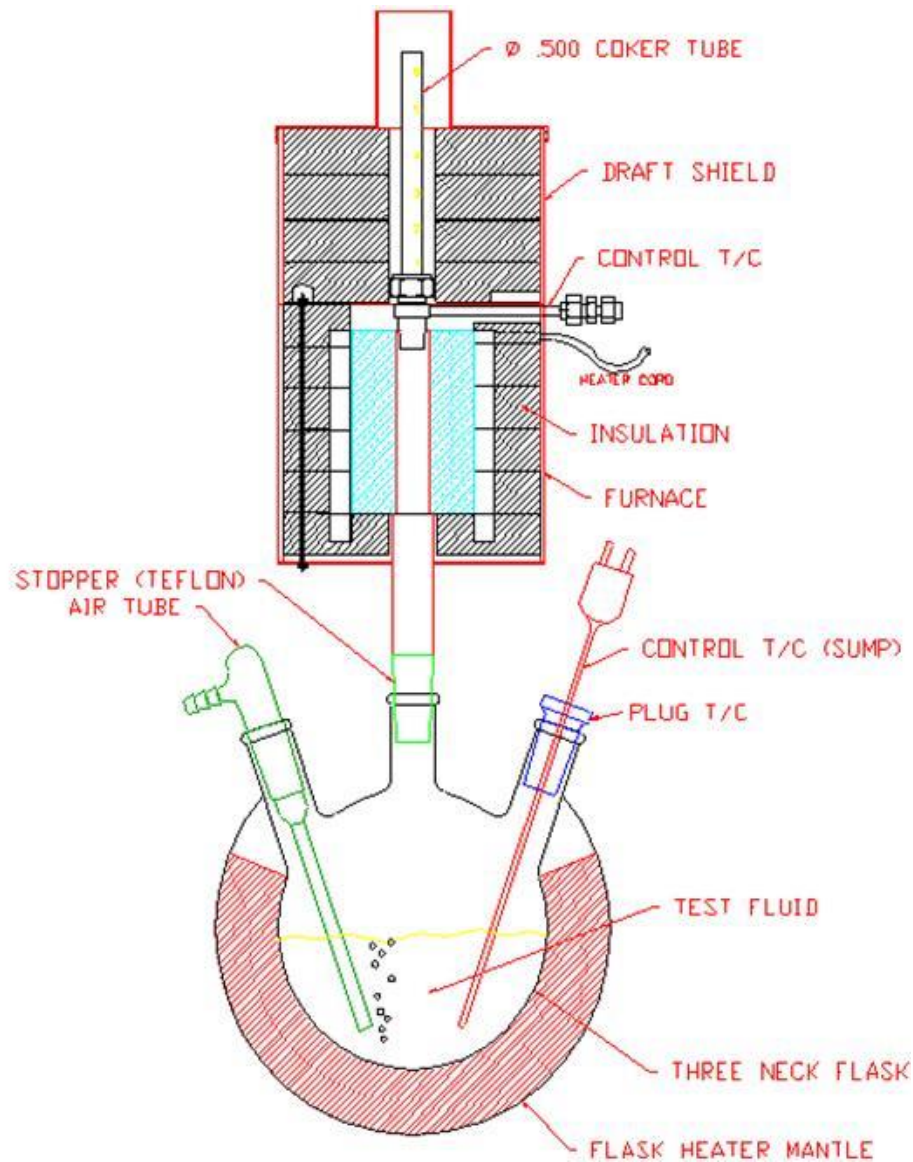


Figure 5.2 Vapor Phase Coking Test, SAE ARP5921 (2014)

5.2.4. Summary of Laboratory Deposition Tests

The current, available laboratory techniques do not accurately replicate the conditions seen in the gas turbine bearing chamber pipes (the feed, scavenge and vent). The HLPS provides an assessment of the single phase deposition conditions found in the feed pipe but with no facility to replicate the transient flow conditions or temperatures of the feed pipe. The Vapor

Phase Coker is a method for assessing deposition from pure vapour and therefore is not suitable for the assessment of the air/oil mist which is found in the bearing chamber vent pipe.

5.3. Vent Pipe Simulator (VPS)

The Vent Pipe Simulator (VPS) was originally designed and constructed as part of a previous EngD project (Askins, 2010). This section includes details of further development of the method and data generated using it, all conducted as part of this EngD project.

A schematic of the Vent Pipe Simulator is shown in Figure 5.3. In order to generate a fine (<20 μm) air oil mist similar to that found in a gas turbine vent pipe, an air/oil injector is used. Oil is supplied to the injector using a gear pump (at low pressure) where it is combined with pressurised air (up to 80 psig). Both fluids pass through a small orifice into a mist chamber, the expansion which occurs following passage through the orifice results in atomisation of the oil and the formation of an air oil mist. This air/oil mist is then passed through a $\frac{1}{2}$ inch (12.7 mm) external diameter, 300 mm long test section. The test section is heated externally using a brass block heater such that the required test section wall temperature can be achieved. As the air/oil mist contacts the hot walls of the test section, deposition occurs. The amount of deposit formed can then be assessed gravimetrically following the test. Upon leaving the test section, the remaining oil mist is coalesced and collected and the air vented.

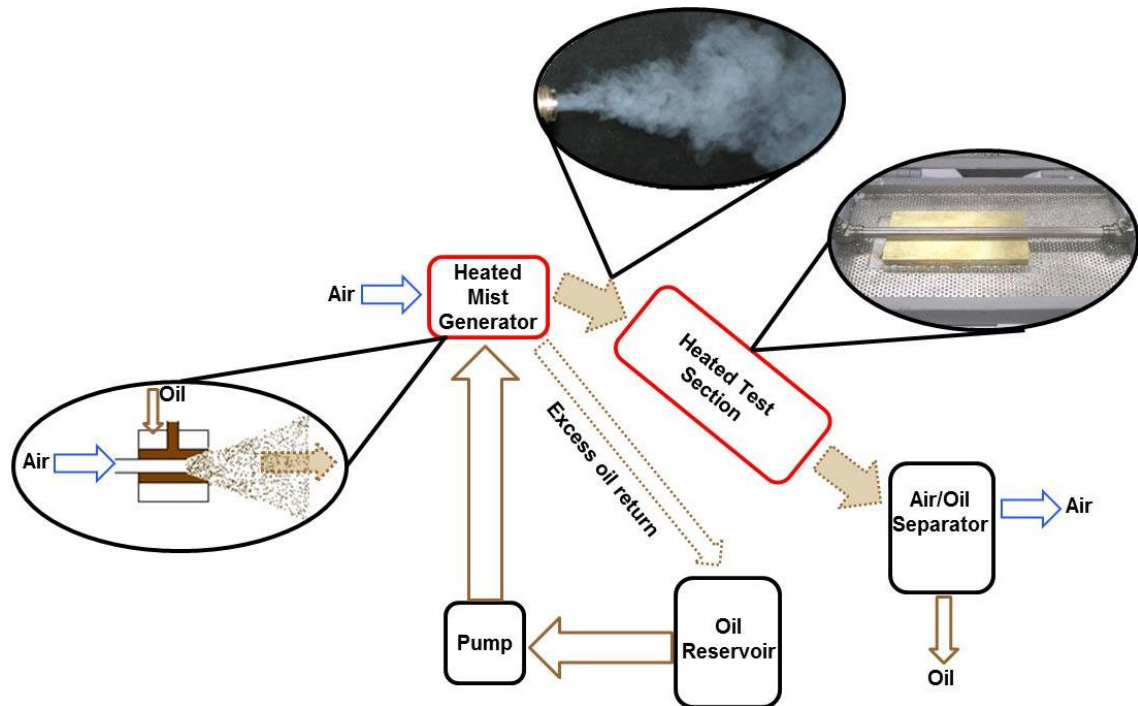


Figure 5.3 Vent Pipe Simulator Schematic

5.3.1. Flow conditions

In the gas turbine vent pipe, air flow velocities are in the order of $30\text{-}100\text{ m s}^{-1}$ therefore for the average pipe sizes used, the Reynolds number will be $10,000\text{-}50,000$, well within the turbulent flow regime. As air and oil mass flow rates are similar, annular dispersed flow is achieved in the gas turbine vent pipe (Taitel and Dukler, 1976). For reasons of practicality and to accelerate deposit formation, the air flow velocity used in the Vent Pipe Simulator is much lower, approximately 0.8 m s^{-1} (Reynolds Number of 300, Laminar). The mass flow rate ratio of air to oil is approximately 0.95, therefore the VPS is significantly more air rich than the gas turbine vent pipe. This would ordinarily give stratified flow conditions (Taitel and Dukler, 1976) in the VPS however, due to the addition of the air/oil injector, an oil mist will also be present. This gives flow conditions as shown in Figure 5.4 a, with the predicted stratified flow of oil along the base of the test section arising from oil which has coalesced at surfaces and an air oil

mist above. This pseudo-annular flow regime was confirmed simplistically with the use of a transparent test section as shown in Figure 5.4 b. The image shows the flow of oil along the base with a surrounding white mist of oil, the droplets formed on the surface were found to accumulate over time as a result of oil coalescence.

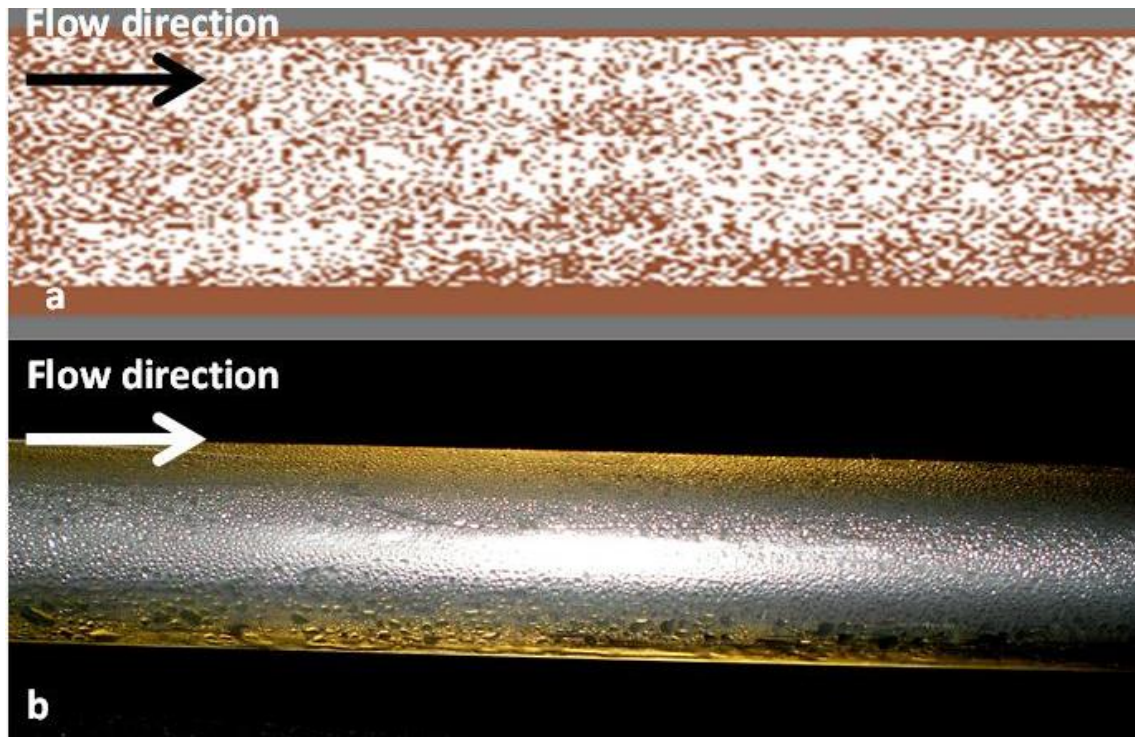


Figure 5.4 (a) Vent Pipe Simulator predicted flow conditions. (b) image of Vent Pipe Simulator flow through a transparent tube, by experiment

5.3.2. Temperature Study

During development testing of the Vent Pipe Simulator, it was noted that the temperature at which the air/oil mist exited from the test section was not constant throughout the duration of the test. The exit gas temperature was found to increase as the test progressed and deposit began to accumulate on the pipe interior, shown in Figure 5.5. For a series of tests of increasing duration and therefore increasing deposit mass formation, the temperature at the deposit outlet was found to increase noticeably when test duration was above 18 hours (a

maximum deposit thickness of approximately 1.5 mm). Figure 5.5 includes data from a repeated 100 hour test. This repeat data demonstrates that whilst there is variation in outlet temperature during a test, the general trend of increasing gas temperature is repeatable.

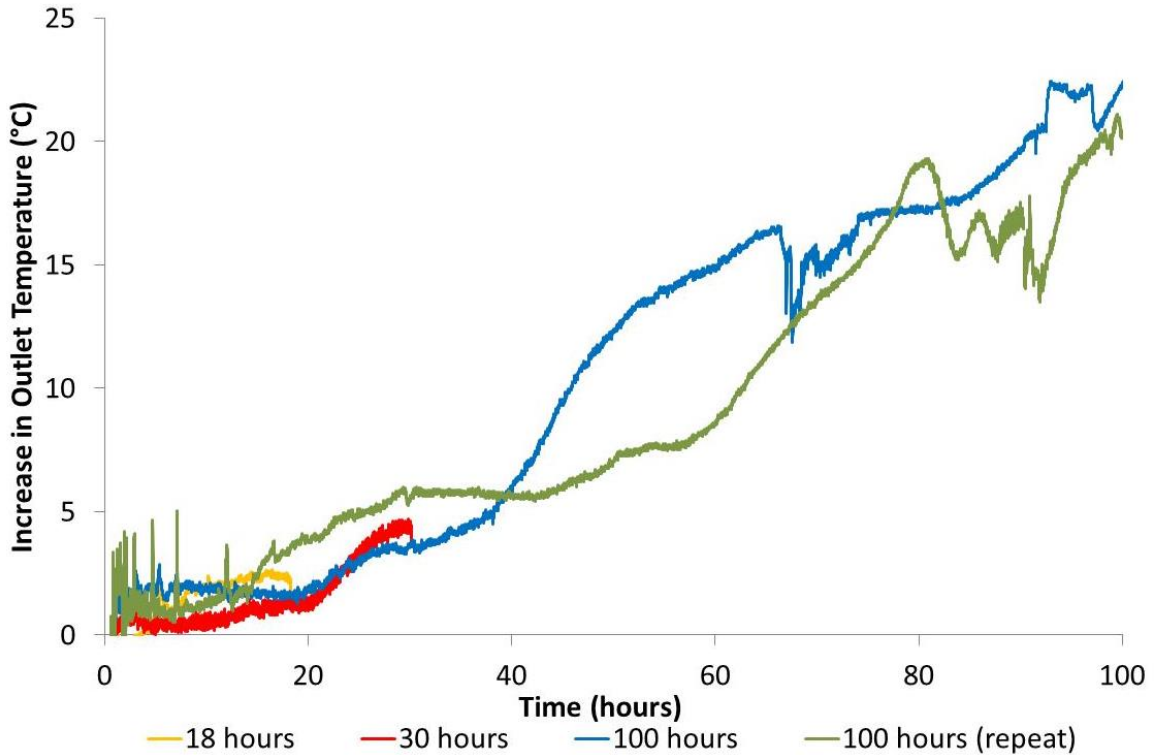


Figure 5.5 Increase in gas outlet temperature as a function of time

As discussed in the previous section, a Reynolds number of 300 in the Vent Pipe Simulator gives laminar flow. It is likely that the formation of large solid deposits would cause disruption to the flow regime.

If a flow disturbance is introduced, it takes a finite time for the eddies created to dissipate prior to the reestablishment of laminar flow. Figure 5.6 shows how the height of the deposit influences the calculated length of flow disturbance. If the height of the deposit exceeds 3 mm then the flow instability will have sufficient duration to propagate beyond the length of the

heated pipe section (16 cm). The period of instability would lead to greater heat transfer giving an increased temperature at the pipe outlet.

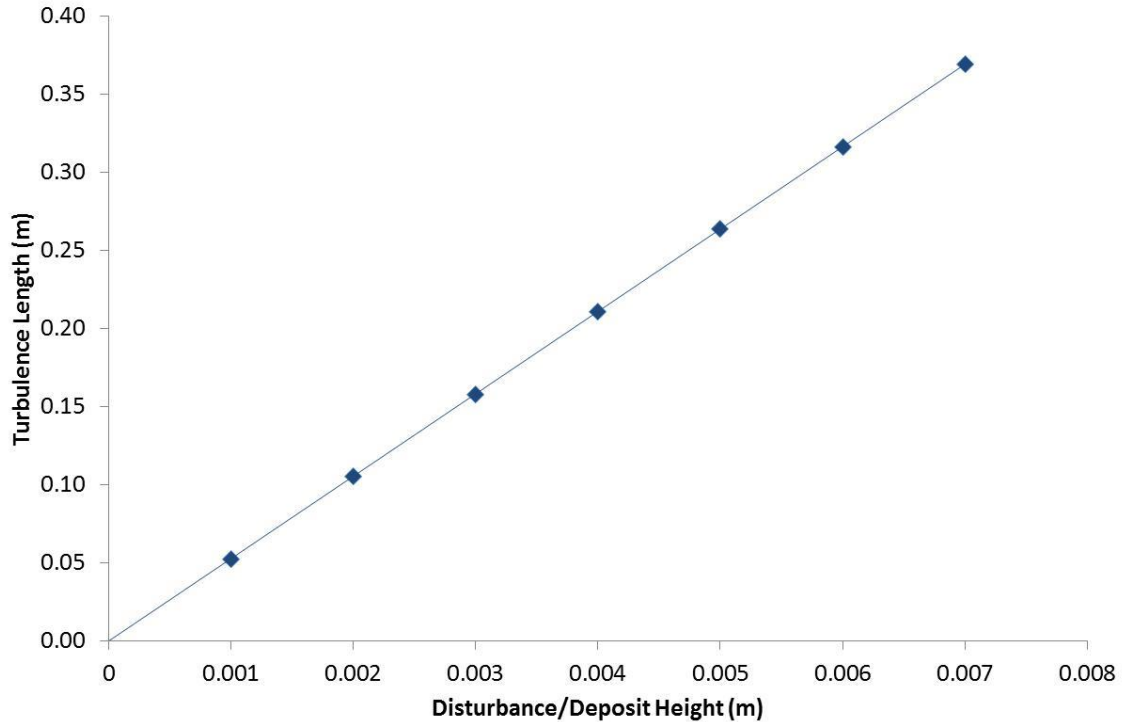


Figure 5.6 Length of turbulent flow following a range of flow disturbance heights. Calculated by $0.05 \text{ Re} \cdot \text{Pr} \cdot \text{Deposit Height}$

In order to test this hypothesis experimentally, an artificial flow disturbance was introduced to a fresh test section (free from deposit) such that the change in outlet temperature could be recorded. The artificial disturbance used was a 5 x 5 x 5 mm cube of a polymeric material; this size was chosen as it represents a similar height of deposit to that formed after 75-100 hours of testing at the conditions used in Figure 5.5. Three tests were conducted with the artificial deposit placed at the inlet, centre and end of the heated section.

Figure 5.7 shows the outlet temperature at the end of four different duration vent pipe simulator tests (with a maximum deposit thickness as marked below) and the exit temperature for the artificial deposit tests. It can be seen that when the artificial deposit is

placed at both the inlet and in the centre of the heated section disturbing the flow through the heated pipe, an exit temperature similar to the 75-100 hour deposit mass is produced. When the flow restriction is moved after the heated section no change in exit temperature was detected.

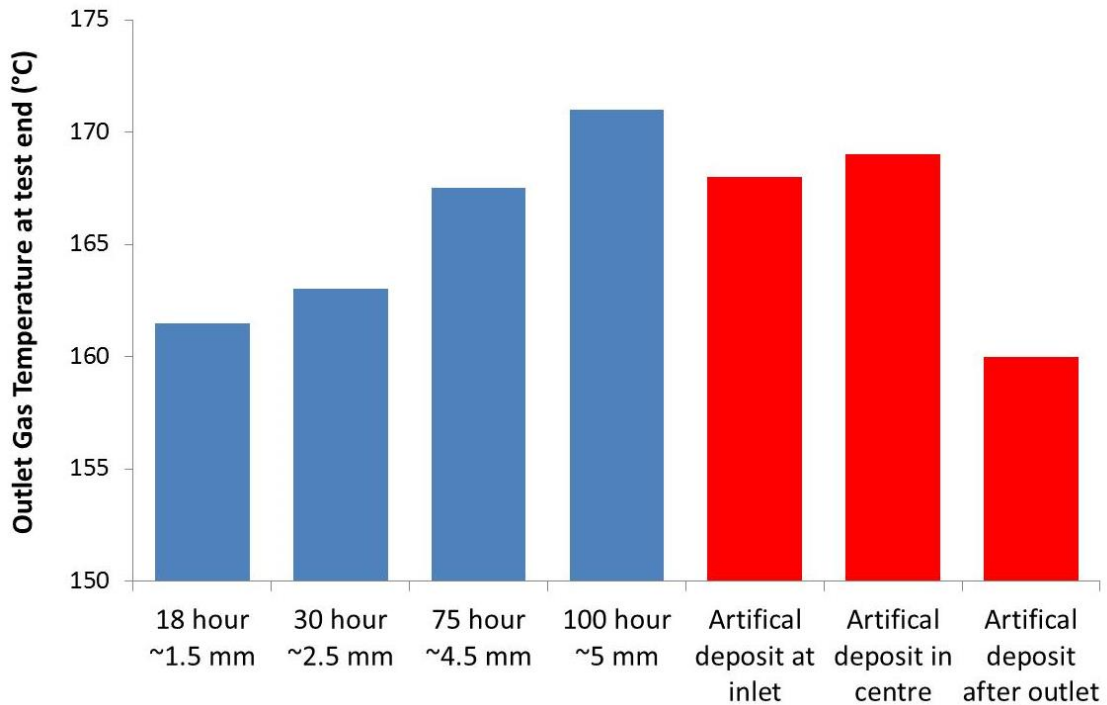


Figure 5.7 Outlet gas temperature at the end of test for a range of test durations and artificial deposits

The results indicate that the introduction of a flow disturbance as oil deposit forms on the pipe interior leads to an increase in heat transfer, an artefact of the low Reynolds number used in this test. In contrast engine vent pipes would have flows of Reynolds number 10,000-50,000. Therefore, as under the engine conditions the flow would already be turbulent, a flow disturbance is unlikely to significantly influence heat transfer. This represents a significant difference between laboratory and engine testing occurring as a result of the need to reduce flow rate to accelerate deposition formation.

5.3.3. Oil Brand Differentiation

The primary purpose of the VPS was to allow the relative deposit formation propensity of candidate oil brands to be determined. Figure 5.8 shows the mass of deposit formed by a range of lubricants after the same 18 hour test duration. The error bars shown indicate standard error. As each of the lubricants are commercial blends, the brand names are not shown, instead they are grouped by lubricant type; Standard Performance Capability (SPC), Extreme Pressure (EP), Corrosion Inhibiting (CI) and High Performance Capability (HPC).

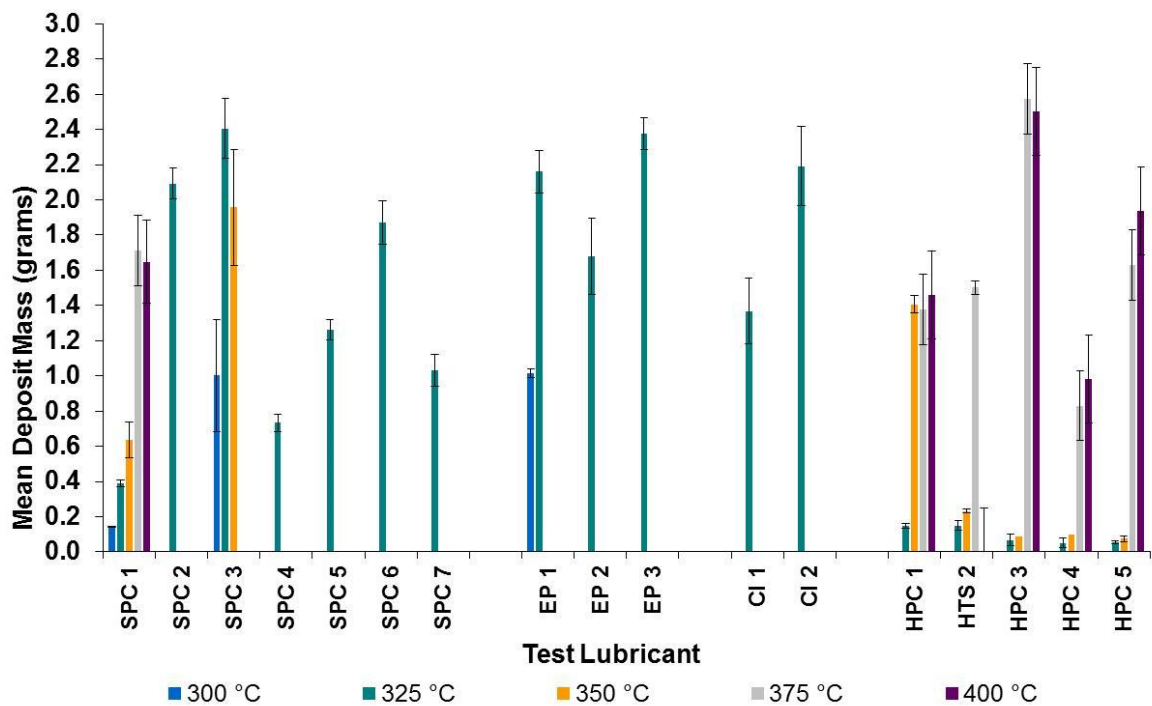


Figure 5.8 Vent Pipe Simulator data, at five temperatures after an 18 hour test - all oils

The SPC lubricants were all tested at 325 °C, this showed a range of deposit masses varying from 0.4 g to 2.4 g. SPC 1, which only produced 0.4 g of deposit at this temperature, is known through Rolls-Royce service experience to produce lower levels of deposit than other lubricant brands. SPC 1 was tested at additional temperatures of 300, 350, 375 and 400 °C, represented as a line graph in Figure 5.9. The error bars shown represent the standard error. There is a

good linear correlation between wall temperature and deposit formation between 300 and 350 °C, above this, at 375 °C and 400 °C, the deposit mass is much greater. At these higher temperatures it is possible that the mechanism of deposition has changed, potentially even progressing to hydrocarbon cracking. It should be noted that for this method, a mass of greater than 1.5 g represents a test section which is significantly filled with oil deposit. Due to this, flow conditions are greatly affected and it is more difficult to quantifying the amount of deposit (due to oil entrainment), following the test. Therefore, above 1.5 g, precision is lower and as such the results for both 375 and 400 °C could be considered to be above the maximum possible range of deposit formation for this test.

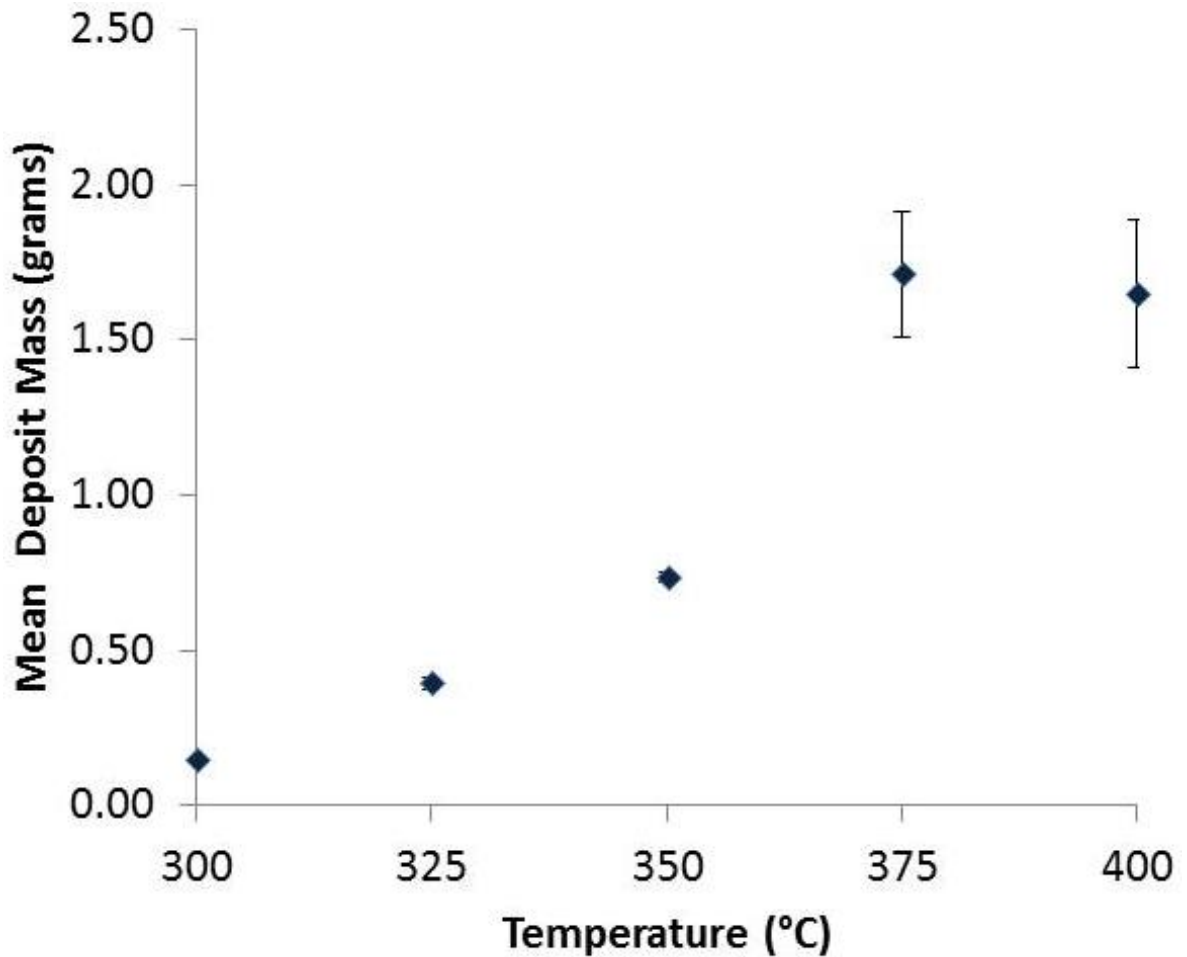


Figure 5.9 SPC 1 lubricant deposit mass as a function of temperature (18 hour test)

EP lubricants are formulated with the intention of providing improved tribological performance under high load (or extreme pressure) conditions. The additives used to achieve the EP performance are intrinsically less thermally stable and have the effect of reducing the thermal stability of the oil, they are therefore known to form more thermal deposits than other similar lubricants. CI lubricants are formulated for marine applications to provide additional protection for metallic components against corrosion and these formulations, similar to EP lubricants, also have a reduced deposition resistance as a result. When tested using the Vent Pipe Simulator, EP and CI oils were found to form greater deposits than the majority of SPC lubricants, indeed they all resulted in almost entirely blocked pipes. The

testing of these lubricants was intended to show that the VPS has the capability to distinguish these known low performing (in terms of deposition formation) lubricant types from other lubricant classes. This can be seen to be true. However, since they are intended for applications where deposition issues are not the primary concern, they were not investigated further.

High Performance Capability (HPC) lubricants are so called due their increased thermal stability when compared to SPC lubricants, this means that they typically exhibit better resistance to deposition formation. This can be seen to be the case in Figure 5.8, with the HPC lubricants producing significantly less deposit at 325 °C than any of the other lubricant types. Figure 5.10, showing only the HPC lubricants, allows comparison of the HPC lubricants at a range of temperatures. Deposit masses were found to remain low (below 0.2 g) for all lubricants, until a specific temperature at which the amount of deposit formed was found to increase sharply. This temperature was termed the 'break-point' temperature. It can be seen that HPC 1 had a lower break-point than the other HPC lubricants, therefore it was postulated that determining a more accurate break-point temperature may allow differentiation of the HPC oils.

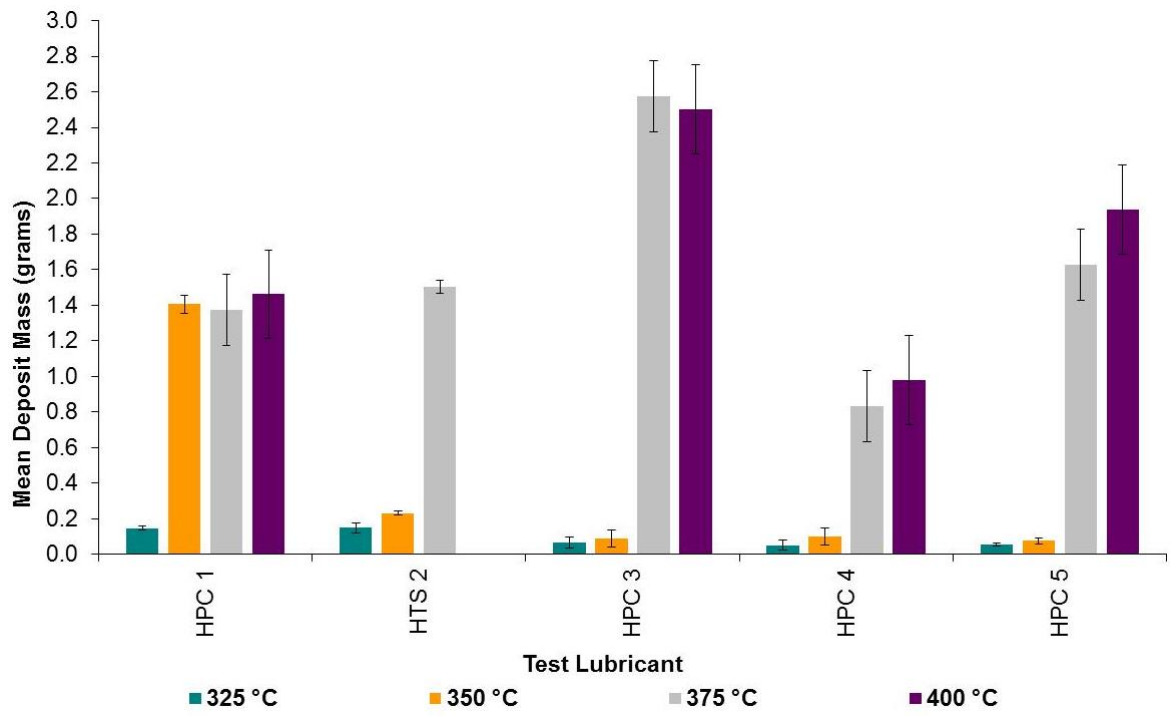


Figure 5.10 Vent Pipe Simulator data at four temperatures (18 hour test) - HPC oils

Figure 5.11 shows the deposit mass formed presented as a line graph. The error bars shown indicate the standard error. If the break-point is determined as a 25 % blockage in pipe diameter (approximately equal to 0.6 g of deposit), then it is possible to differentiate the lubricants in terms of the temperature at which this point is reached. It can be seen that a lower performing SPC lubricant (SPC 3) has a break-point of less than 300 °C, whereas the best performing SPC oil (in this test), SPC 1, has a break-point of 350 °C, marginally greater than HPC 1. This method, also allows a difference to be seen between the other HPC oil with HPC 3, 4 and 5 being the better performing lubricants. It is also interesting to note the effect that temperature has on deposition formation is different between the lubricant brands; the 'break' is much more abrupt for some lubricant brands. This is likely to be due to the differing antioxidant packages employed by each lubricant.

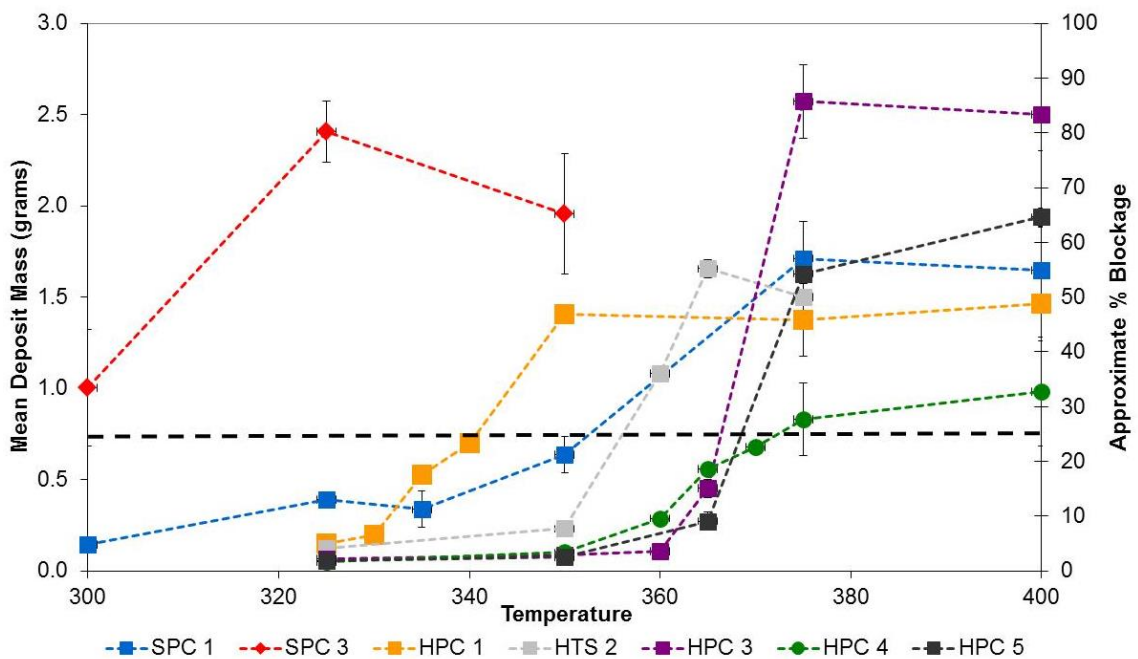


Figure 5.11 Vent Pipe Simulator data expressed as a line graph (break-point)

5.3.4. Deposition Accumulation Study

In order to understand how deposit is formed over time, a series of tests were conducted at a range of durations. Following each test, the mass of deposit was obtained gravimetrically before the pipe was split along its entire length. This allowed the measurement of the maximum deposit thickness using a pair of callipers and visual assessment of the deposit. Figure 5.12 shows the mass and thickness of deposit formed by an SPC lubricant over time. Repeat tests were conducted at some durations, these are also displayed in Figure 5.12 to give an appreciation of the level of experimental error. As with previous VPS results, experimental error was found to be greater when larger deposit mass was generated.

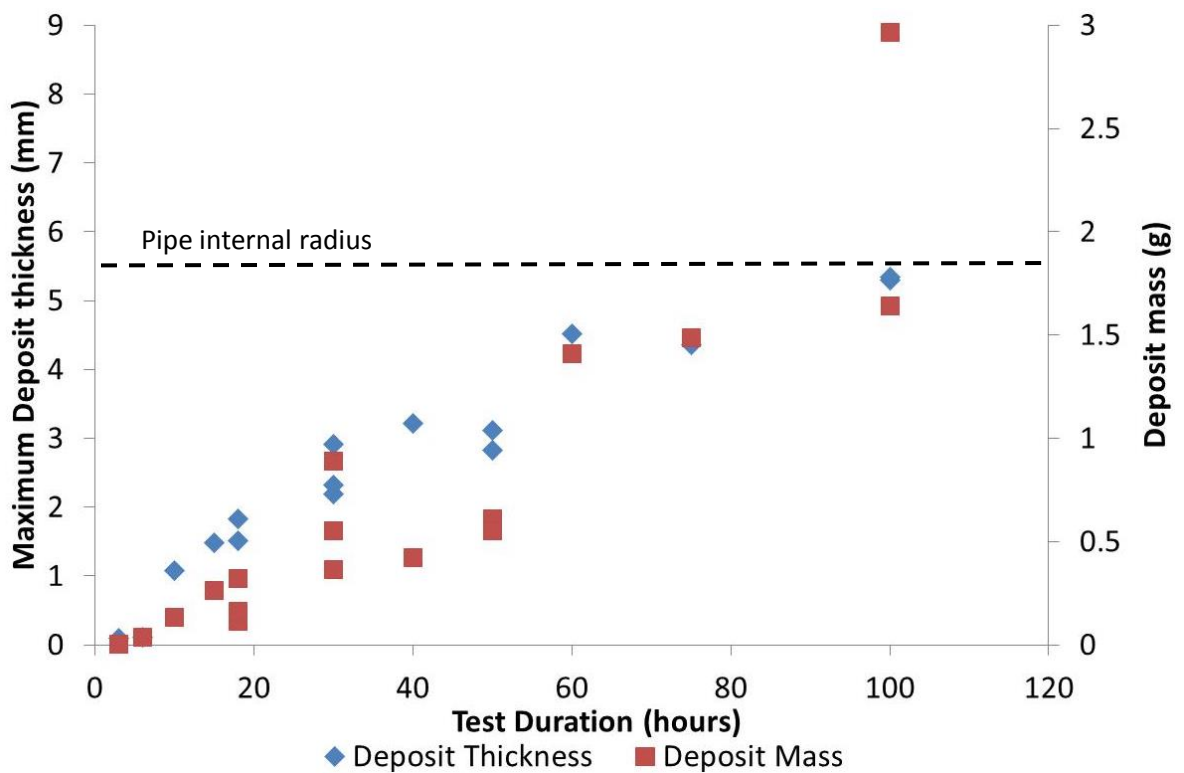


Figure 5.12 Deposit formed as a function of time (SPC 1 oil, 300 °C wall temperature)

The accumulation of deposit mass up can be seen to be linear under these test conditions. The point at which the maximum deposit was formed was found to be in the final third of the

heated section of test piece. In this region, wall temperature is at its maximum (Figure 5.13) and oil at the wall will have had been exposed to the peak temperature for the maximum duration as it transitions through the heated section. Maximum deposit thickness was found to be linear, until the point at which the thickness approaches a 100 % blocked pipe (pipe the internal radius is 5.5 mm). At this point the maximum thickness cannot increase, however the deposit does still increase in the first two thirds of the heated region, in addition to the test section areas immediately adjacent to the heated region where deposit was thinner (Figure 5.13). The mass of the test section continues to increase even when the maximum thickness is reached in the hottest region, as this is where the deposit forms and therefore the relationship for mass does not plateau as occurs with deposit thickness.

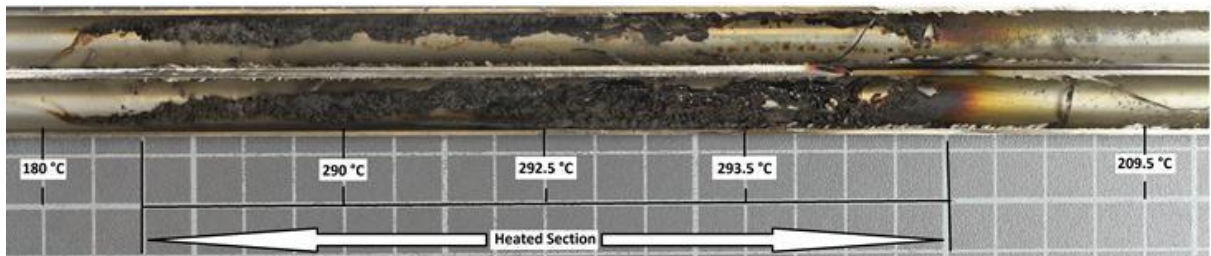


Figure 5.13 Image showed the heated region, measured wall temperatures and the areas of deposit formation (75 hour test, 300 °C outer wall temperature)

It was found that the precision of deposit mass for repeat tests decreased with increasing duration. This is likely to be due to the increased difficulty in efficiently removing the remaining liquid oil entrained within the solid deposit as the volume of deposit increases. The extent to which liquid oil remains within the solid deposit will influence the mass of deposit recorded and hence result in a spread of data. This is an intrinsic issue in quantification of deposition. By also using the thickness of deposit as a secondary measure trends can still be reliably obtained.

Figure 5.14 shows the deposit that has accumulated at four durations: 3, 18, 60 and 100 hours. These images also correspond to the equivalent points displayed graphically in Figure 5.12. It can be seen that after 3 hours the deposit has formed as a brown lacquer strongly adhering to the pipe surface. At 18 hours, the deposit has progressed to rough, textured trails of deposit, these trails flow down the pipe in the direction of the flow. As deposition progresses further, these trails of deposit widen and grow and the deposit also begins to become marginally softer at the surface. This softening is due to the entrainment of liquid oil within the deposit which has not yet progressed to the point at which a solid is formed.

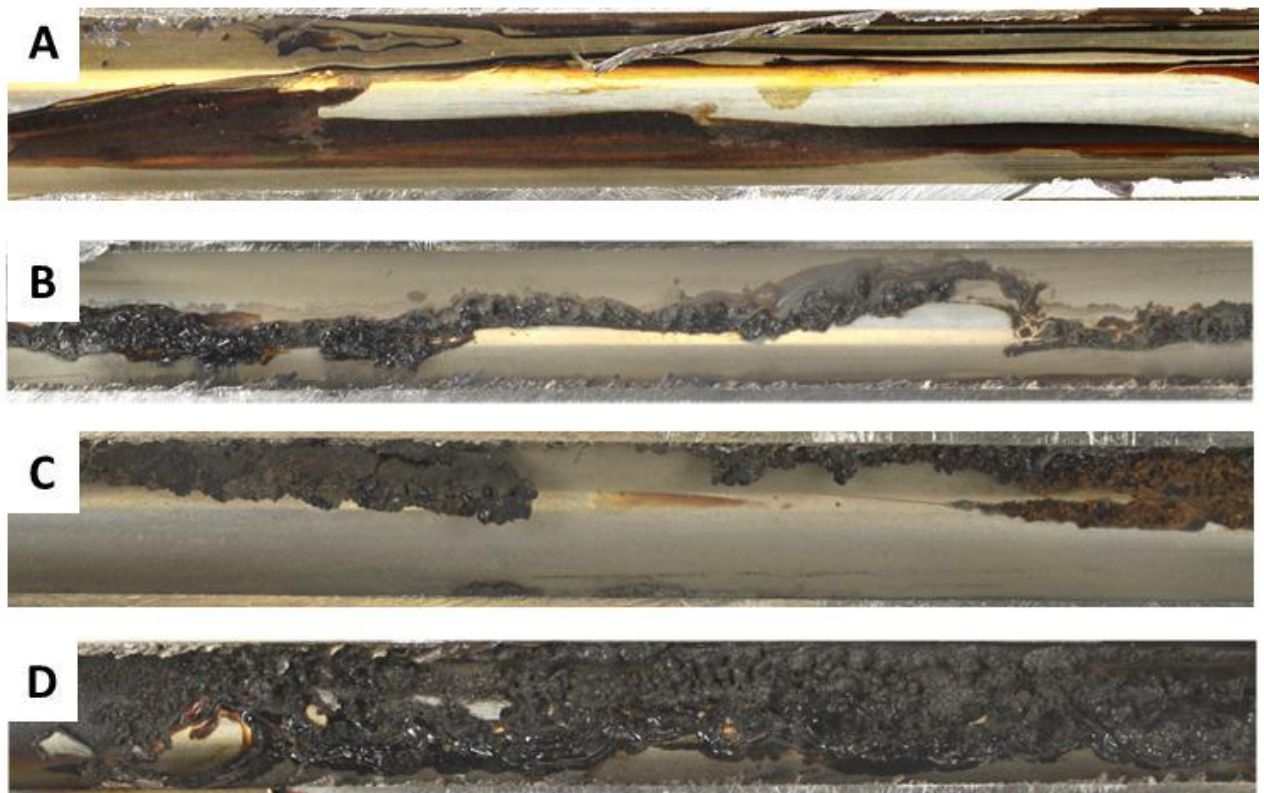


Figure 5.14 Images showing deposit building up at a range of durations, (a) 3 hours, (b) 18 hours, (c), 60 hours, (d) 100 hours

Figure 5.15 shows an example of deposits which have formed in a gas turbine vent pipe. This image represents advanced deposition which has accumulated around a narrowing of the pipe called a vent restrictor. Comparison of Vent Pipe Simulator deposits to service deposits is

difficult as such events are rare and sample availability is low. Visually there are pronounced similarities between laboratory and service samples. The deposits are black, dense, well adhered and hard. Deposits formed via other methods, without the presence of an oil mist, do not display this texturing. This gives some indication that the deposits formed have some similarity to those which could form in service. High magnification images, by scanning electron microscopy, of the VPS deposits are shown in Figure 5.16 indicate that the deposit appears to have a number of layers.



Figure 5.15 An example of gas turbine vent pipe deposits

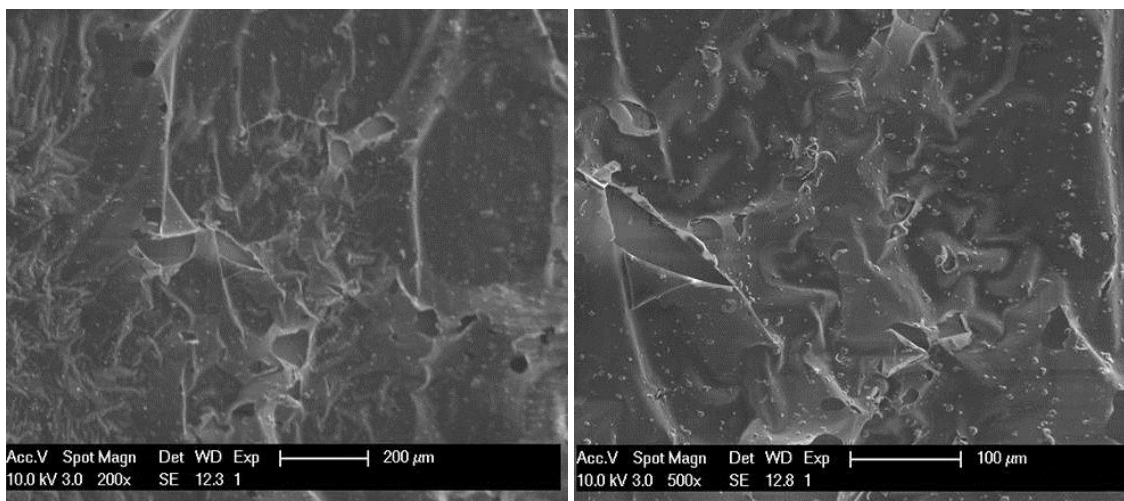


Figure 5.16 Scanning Electron Microscope images of VPS deposit

5.3.5. Oil Chemistry

Under vent pipe test conditions only a proportion of the total oil/oil mist which passes through the test section will result in solid carbon at the pipe wall. The remaining oil will pass out of the test section as either a liquid (that which has coalesced during passage through the test section), oil mist or as oil vapour. It is likely that the oil will be chemically altered as a result of exposure to temperature and air when compared to the fresh lubricant which was introduced into the test section. The extent of degradation of the oil/oil mist at the test piece exit, gives information as to how the oil degrades prior to the formation of oil deposits, therefore the following analysis was conducted.

A sample of the liquid oil and the oil mist were both collected and their Total Acid Numbers analysed, these were found to be 3.50 and 1.75 mg KOH g⁻¹ respectively. As discussed in § 2.5.1 and shown in Chapter 4, when oil degrades in the presence of oxygen the majority of oxidation products are mildly acidic, therefore an increase in acidity can be used as a measure of the degradation of the oil. The Total Acid Number of the liquid oil and oil mist would indicate that significant degradation has occurred. The liquid oil, which has coalesced in the

test section is more degraded than the oil which remained as a mist, this is likely to be due to the residence time of the oil in the heated section. The velocity of air through the test section is approximately 0.8 m s^{-1} therefore residence time of oil mist within the heated section is likely to be less than 1 second. The coalesced (liquid) oil however, will move much more slowly down the declined metal pipe. The precise residence time will depend on a number of factors including the amount of deposit already accumulated at the pipe wall.

Gas Chromatography was used to further understand the composition of the two samples, these chromatographs are shown in Figure 5.17. Both of these oil samples are missing the peak at 9.46 minutes which corresponds to PANA, an antioxidant. This peak is observable in the fresh lubricant formulation. As the antioxidant is consumed or converted in the process of inhibiting thermal oxidation, this indicates that both oils have been thermally stressed. The oil mist sample is otherwise similar in composition to the original oil, the ratios of the peak heights have remained constant with the fresh oil, indicating that the sample taken was from an oil mist and not an evaporated fraction of the oil. This is representative of a gas turbine vent pipe which will contain mostly oil mist with a minimal proportion of oil vapour, at most engine conditions.

The liquid oil sample has a depleted concentration of some of compounds which are present in the original oil formulation. This indicates that the oil has been significantly thermally stressed, resulting in chemical changes to the lubricant constituents. This finding is consistent with the greatly increased Total Acid Number. The fact that the liquid (coalesced) oil sample is more degraded than the oil mist indicates oil degradation at the surface may be the most significant mechanism in the formation of the deposits. However, degradation in the mist is likely to accelerate the process.

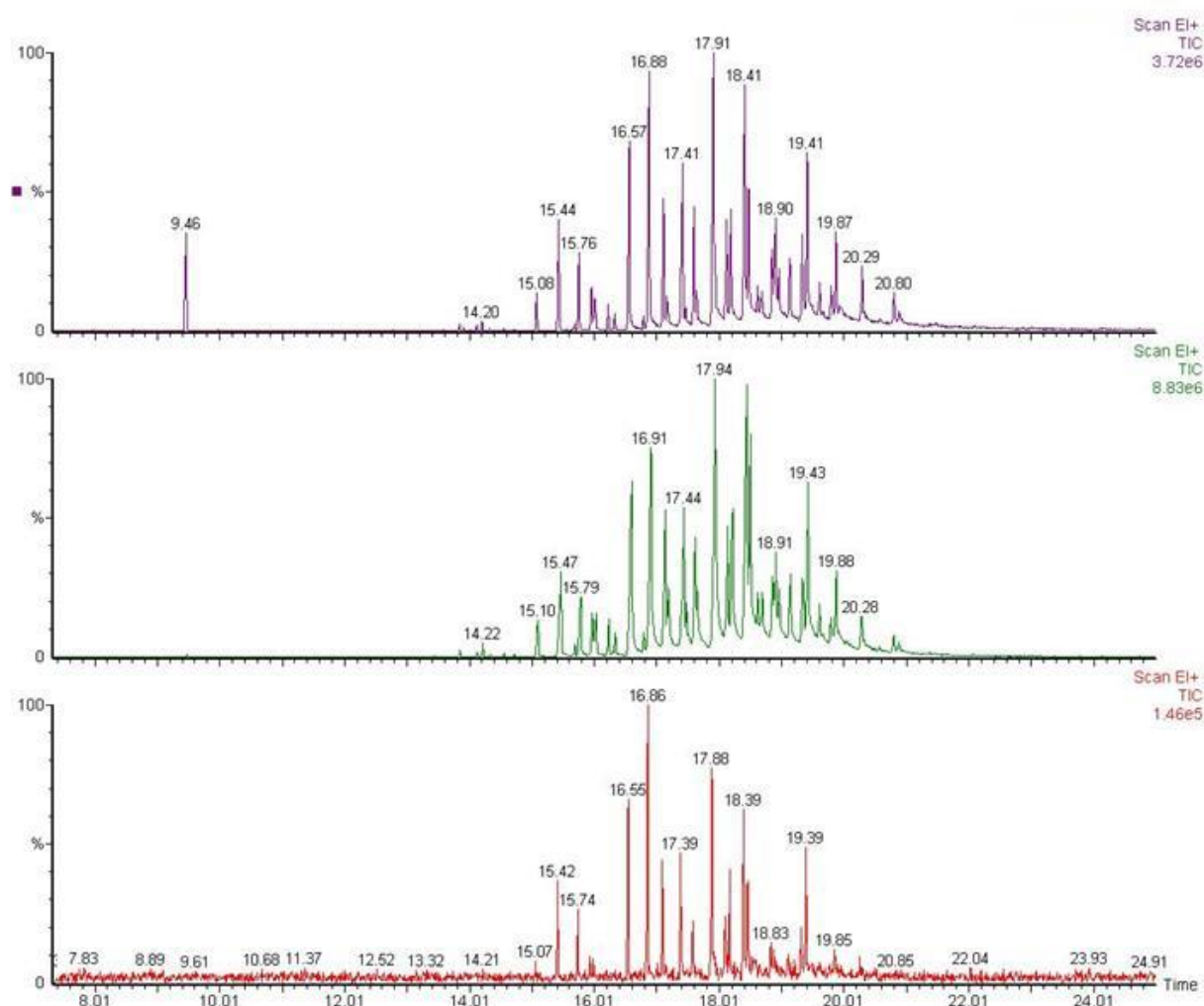


Figure 5.17 Gas Chromatograms of fresh oil (top), oil mist (middle) and liquid oil samples (bottom)

Gel Permeation Chromatography was also conducted on these samples to ascertain their molecular weight distribution (Figure 5.18). The liquid oil sample showed a greater proportion of high molecular weight species, including molecular weights larger than those present in the original formulation. Therefore, species must have formed as a result of oligomerisation reactions and could act as precursors to deposit formation. This shows the sample is significantly degraded, consistent with the high TAN value and GC analysis.

The mist sample shows a small depletion of the highest molecular weight species present in the original formulation. The sample does not appear to be significantly degraded, therefore

the increased TAN value ($1.7 \text{ mg KOH g}^{-1}$) is more likely to be due to the high volatility of acidic degradation products thereby allowing them to be carried in the air/oil mist as vapour and raising the TAN of the sample collected. This could indicate that the highest molecular species have preferentially coalesced at the pipe wall over the lower molecular weight species. Nakanishi *et al.* (1997) reported that higher molecular weight species react faster in thermal oxidative degradation, it is therefore likely that an accumulation of the species at the pipe wall as a result of coalescence, could lead to more rapid deposition.

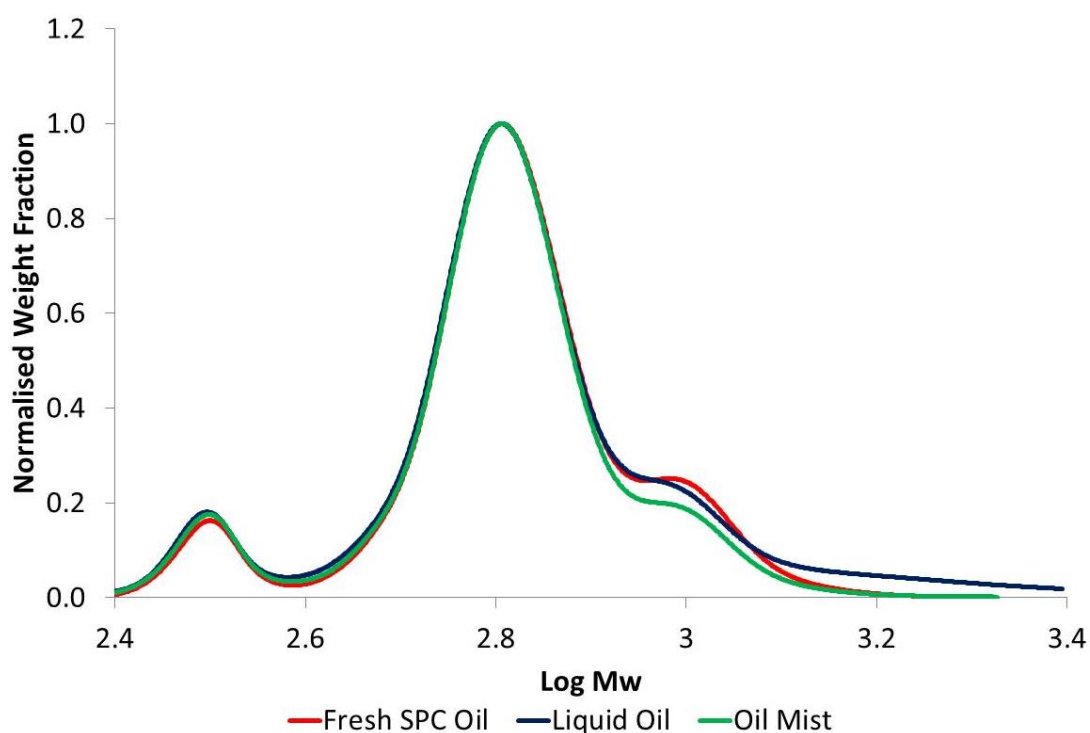


Figure 5.18 Gel permeation chromatograph of Vent Pipe Simulator samples

5.4. Feed Pipe Simulator

As with the Vent Pipe Simulator, the Feed Pipe Simulator (FPS) (Figure 5.19) was originally designed and built as part of a previous EngD project (Askins, 2010). This section details the testing conducted as parts of this EngD and the improvements made to the further develop the method.

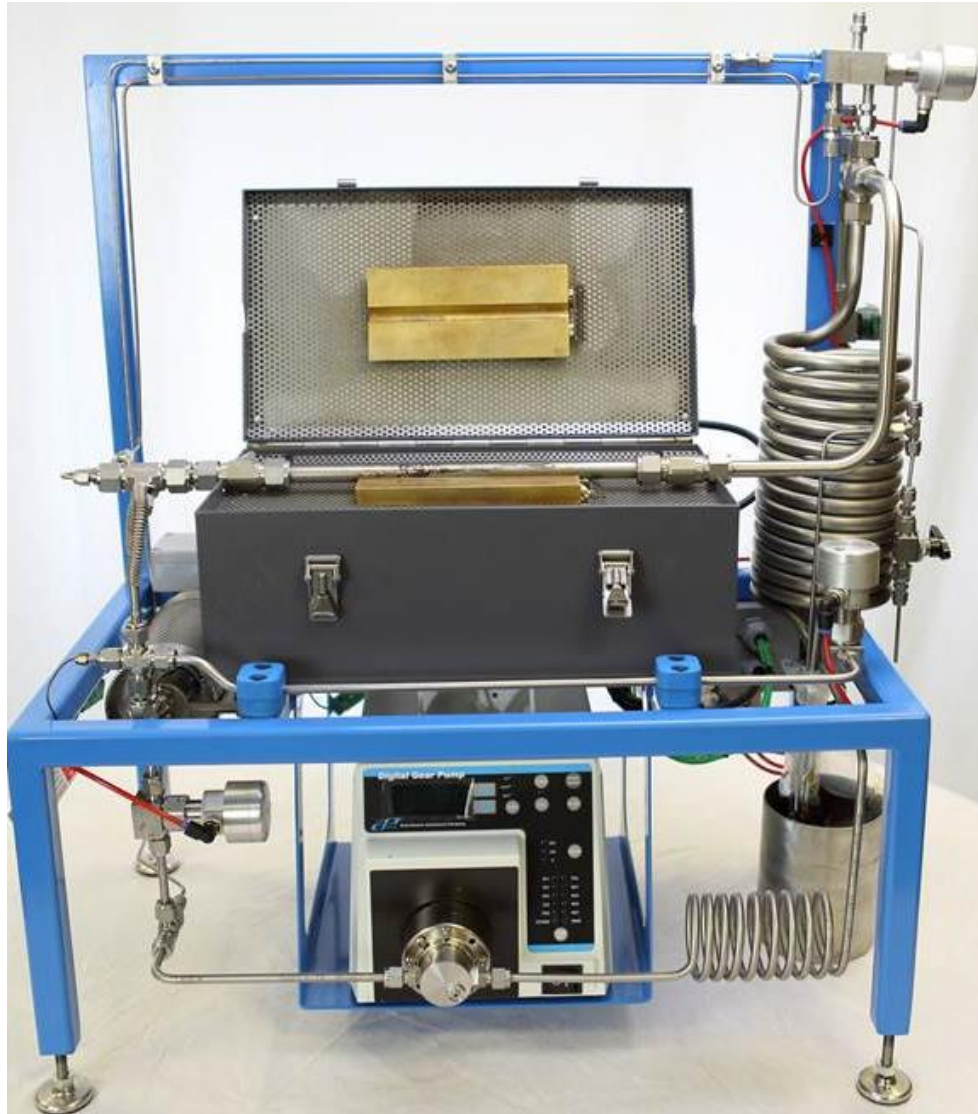


Figure 5.19 The Feed Pipe Simulator

The FPS is designed to simulate the conditions found within a bearing chamber oil feed pipe throughout entire engine cycles. Whilst the engine is running, the feed pipe carries the cool oil to the bearing chamber, it is single phase flow and will therefore retain a small amount of dissolved air. At shutdown, oil flow will cease. Pipe walls initially remain at the operating temperature and then, as a result of the loss of the cooling effect of the oil, the temperature actually increases. It is therefore believed that deposition can occur following the shutdown of an engine. Engines can be designed such that, following shutdown, the oil will drain from the

pipes back to the oil tank, or so that the oil is retained and the pipes fully filled with oil. A recent Rolls-Royce patent has been issued to achieve a filled pipe at shutdown. (Smith, 2008)

A schematic of the FPS is shown in Figure 5.20, showing the oil flow path. To replicate flowing conditions, a gear pump is used to flow oil from the oil tank, through a preheater to produce the required oil temperature at the test piece inlet. The test piece, as for the VPS, is a ½ inch (12.7 mm) external diameter tube, inside which any solid deposits will form. The wall temperature of the test piece is controlled using a brass clamshell type heater. Inlet and outlet oil temperature is measured using additional thermocouples. After leaving the test section the oil flows, via a cooling coil, back to oil tank as part of a recirculating system.

To replicate shutdown conditions the valves 1 and 2 are used. To simulate a drained shutdown, valve 2 is open and valve 1 is closed, allowing oil to drain back to the oil tank. This leaves an oil wetted pipe in the heated region therefore allowing deposits to form. To mimic the flooded shutdown, both valves are closed thereby holding a stagnant volume of oil in the heated test piece.

The FPS allows assessment of the deposit formed on the inside of the test piece in addition to the quality of the oil which is used within the oil system.

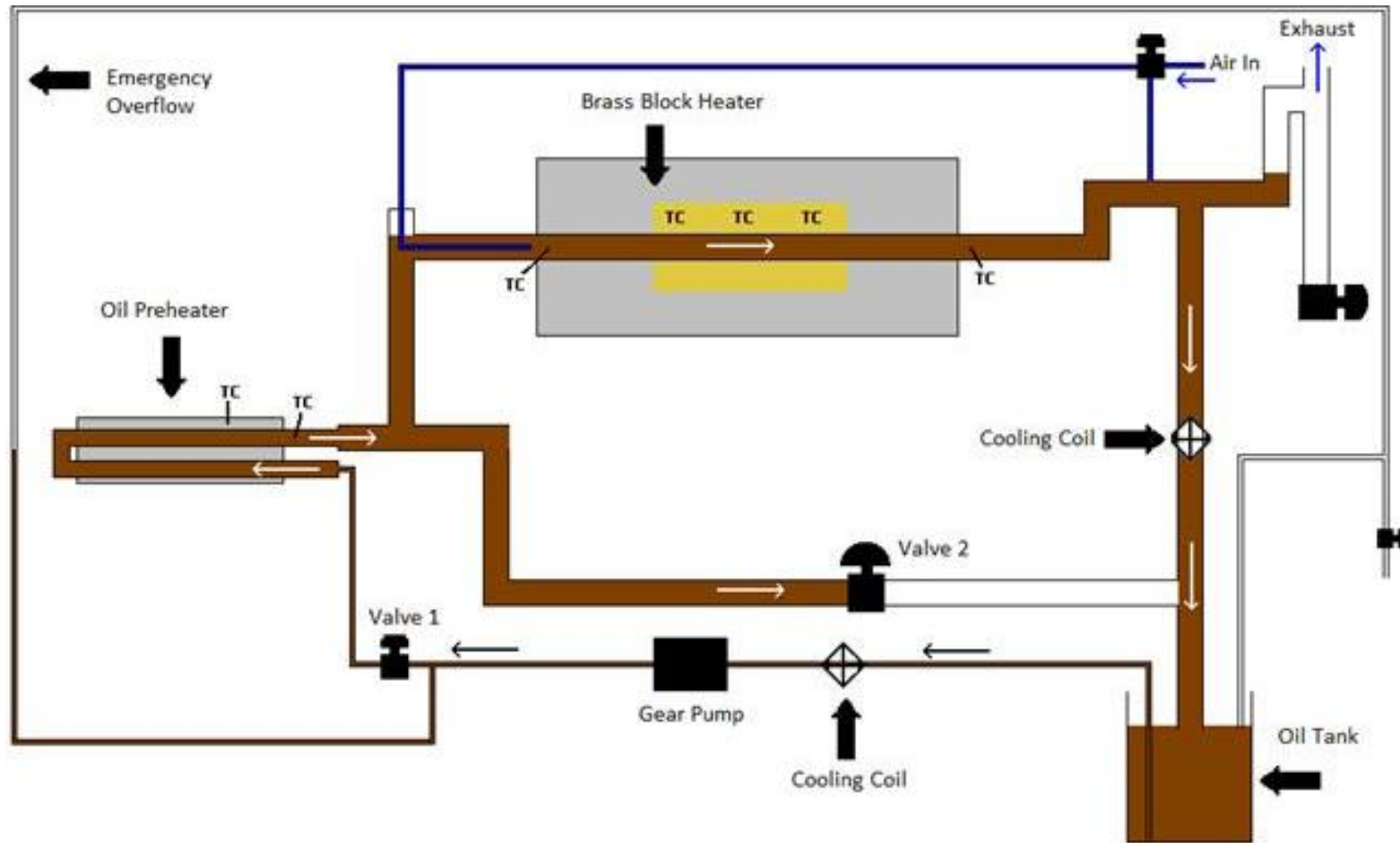


Figure 5.20 Feed Pipe Simulator schematic

5.4.1. Development Work

Initial work focussed on assessing the ability of the FPS to differentiate between oil brands which are known, through service experience, to have differing resistance of deposition formation. A high wall temperature (375 °C) was selected in order to accelerate testing and a duration of 18 hours was chosen to allow the maximum testing to be achieved by conducting overnight testing with test examination and setup during the working day. After each 18 hour cycle, the test specimen was removed, washed with petroleum spirit solvent to remove excess oil, dried and weighed. This allowed the graph shown in Figure 5.21 to be plotted. SPC 1 produced significantly less deposit than SPC 2; this is consistent with service experience as SPC 2 is known to be less resistant to deposition than SPC 1 in gas turbine operation. The HPC oils (High Performance Capability), as would be expected, gave less deposit than the SPC (Standard Performance Capability) oils. There was minimal difference seen between the two HPC oils, HPC 1 and 2. Due to the duration required to generate this test data, only one repeat test was achieved (for SPC 1) however it can be seen that the repeat tests show very good agreement. This testing showed that the FPS has the ability to rank oil brands similar to service experience and experience from other test methods.

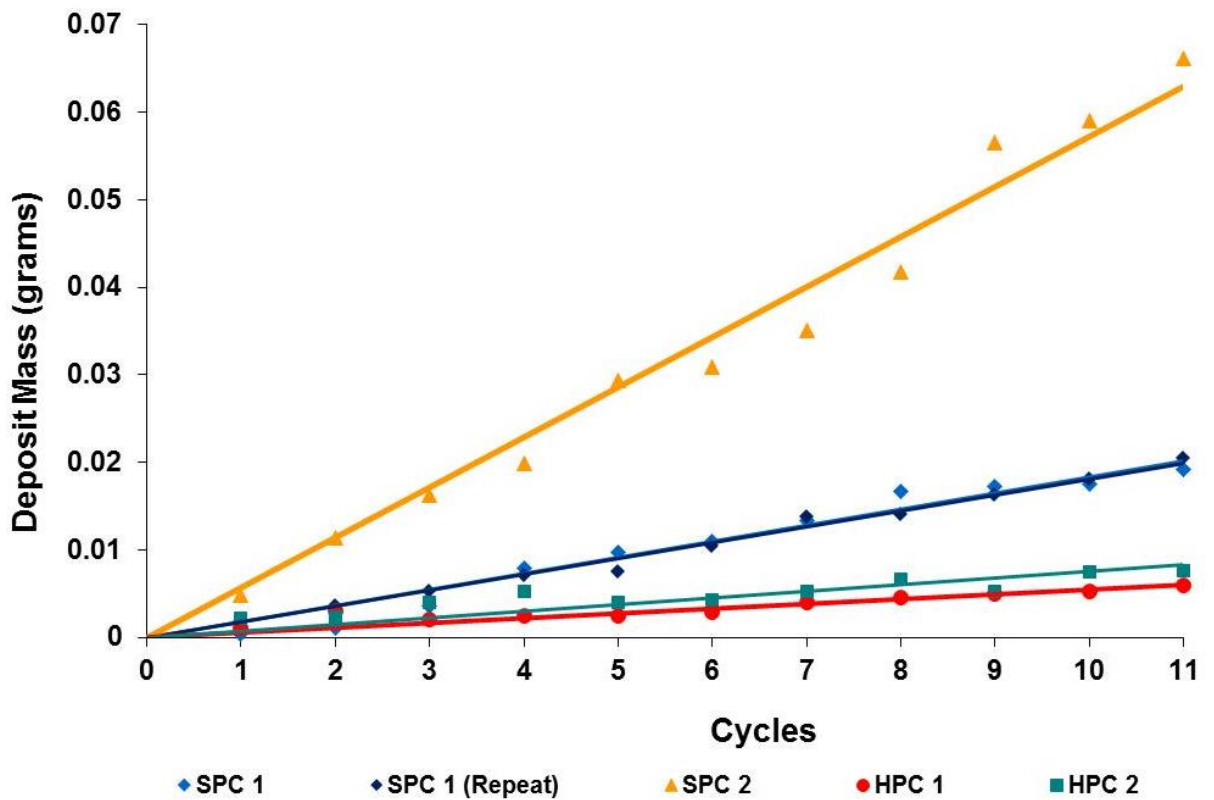


Figure 5.21 Oil brand comparison under constant oil flowing conditions, (375 °C wall temperature, 18 hour cycle)

In order to determine how shutdown conditions influence the rate at which deposit accumulates, the testing conducted with SPC 1 was repeated to include a shutdown portion in each cycle. A one hour shutdown element was performed where, whilst the simulator cooled, the oil was either drained from the test specimen or was left with a stagnant volume within it (flooded). This data is presented in Figure 5.22, including a plot of the continuous flowing shutdown conditions previously shown in Figure 5.21 as a reference. The error bars show the range of data around the mean from two tests at each condition. Error was found to increase when greater deposit mass was formed.

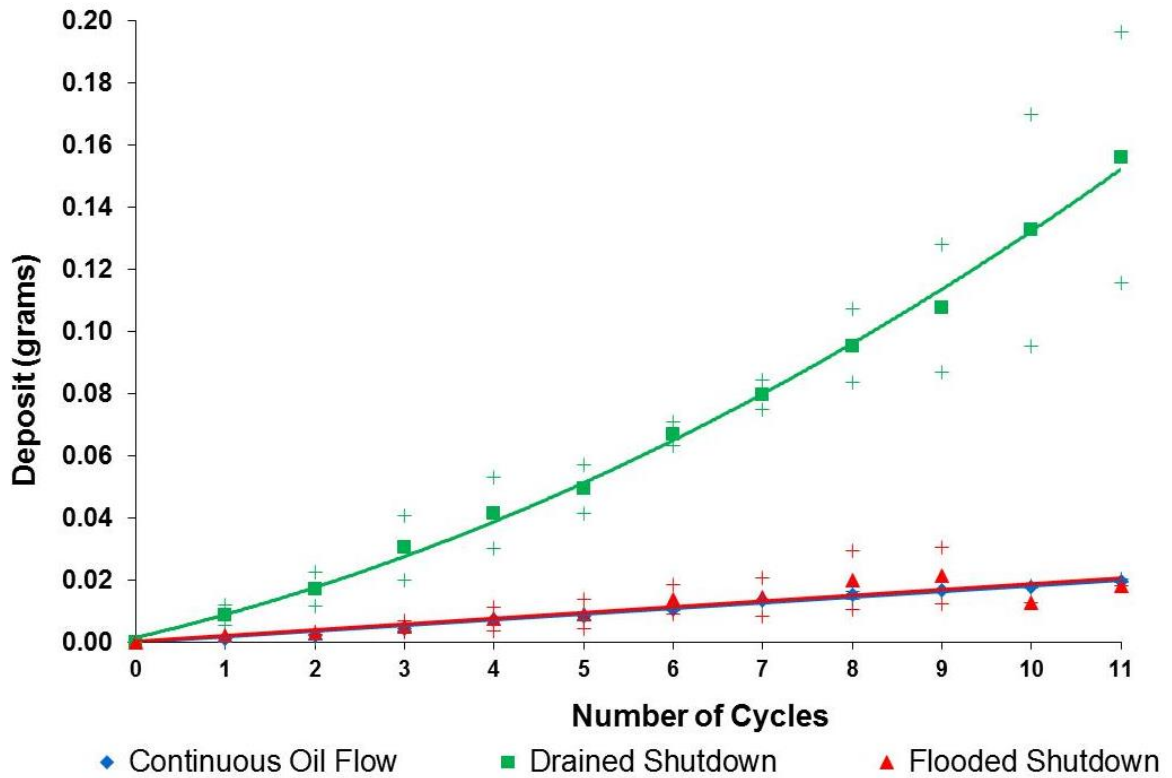


Figure 5.22 Graph showing the influence of shutdown conditions on deposition mass (375 °C wall temperature, 18 hour cycle)

Draining the pipe of oil can be seen to lead to a considerable increase in deposit formation. This is believed to be due to the presence of a thin oil film and air within the pipe; the large oil surface area combined with oxygen availability will result in degradation of the oil to form deposits. When the test section is left flooded following shutdown, the amount of deposit formed is similar to when oil is flowing through the pipe. This indicates that when a large volume of oil is present and air is excluded from the test section, degradation of the oil and subsequent deposition is of a similar low level with the flooded shutdown simulation compared to when in operation. Figure 5.23 shows images of each test section at the end of an 11 cycle test. Figure 5.23(a) shows the test specimen from where oil flow was continued at shutdown, this shows that a thin brown or black layer forms at the wall surfaces. Under drained conditions (Figure 5.23(b)) the deposit is both thicker and more friable. This can be

seen from the cracking of the deposit as a result of thermal expansion or relaxation. The flooded pipe shutdown conditions shown in Figure 5.23(c) give deposits with much greater similarity to the continuously flowing shutdown condition as the deposits also form from bulk oil and not from a thin surface layer.



Figure 5.23 Feed Pipe Simulator deposit images under a range of shutdown conditions (a) continuous oil flowing (b) drained shutdown (c) flooded shutdown

One significant issue noted was the removal, washing and weighing process. Washing of the test section, whilst necessary to quantify deposit masses in the absence of liquid oil, will also remove precursor deposits or poorly adhered deposits. Therefore, in order to remove this variable, further testing was conducted without the replacement of the test specimen following the washing and weighing process. Instead each test point was generated using a fresh test specimen which was exposed to a prescribed number of test cycles. The test cycles were also shortened to concentrate on the specific area of interest, the shutdown element. The conditions used for the shortened cycle is shown in Figure 5.24, oil was flowed for one hour (simulating engine running) and ceased for one hour (simulating shutdown) in every

cycle. The wall temperature was kept constant throughout the test to remove any potential inconsistencies between tests in heating and cooling rates.

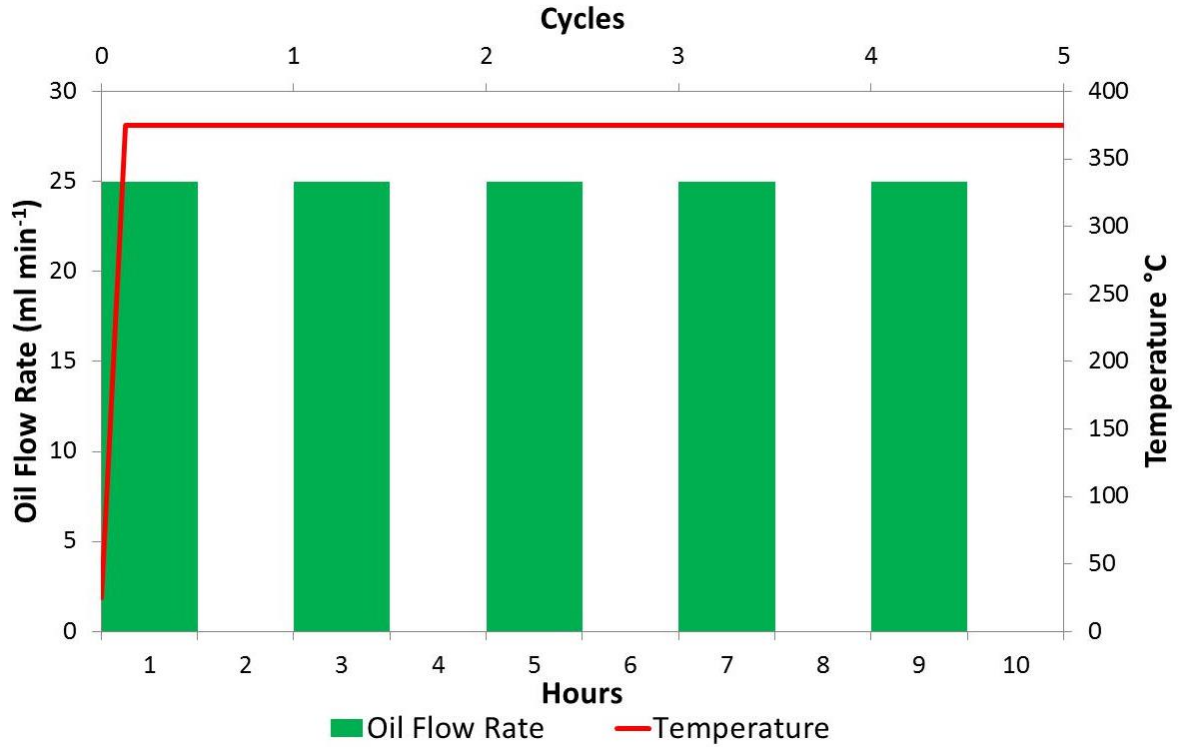


Figure 5.24 Shortened test cycle conditions

Figure 5.25 shows data for one SPC and one HPC oil using the shortened cycle. Again, it can be seen that SPC and HPC lubricants can be differentiated using this method. Although direct comparison to previous testing is difficult due to differences in the test procedures, deposit mass appeared to be dependent primarily on the number of shutdown cycles and not significantly influenced by the running duration. Indeed, a similar mass of deposit was achieved with the shortened cycles without the need to run lengthy flowing cycles in between. This indicates that the number of cycles (or flights) a gas turbine operates may be a more significant factor for deposit accumulation in the feed pipe, than the number of hours (or the duration of the flights) it operates.

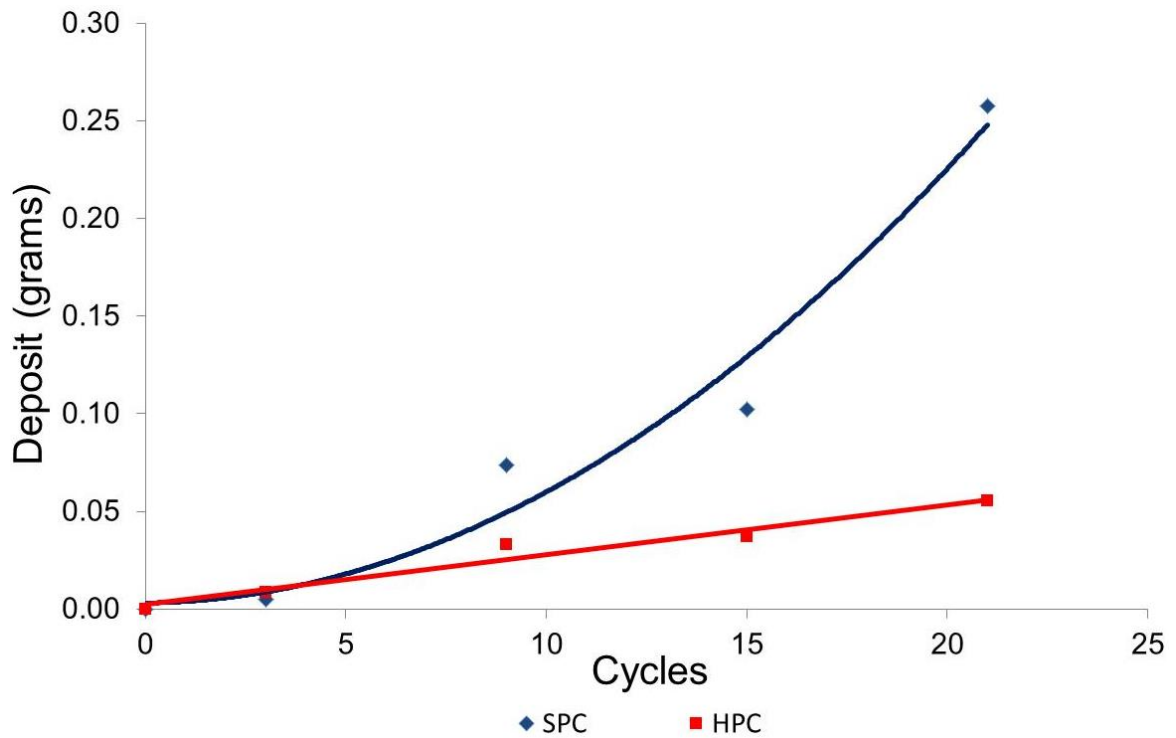


Figure 5.25 Shortened cycles, brand differentiation using drained shutdown conditions (375 °C wall temperature)

5.4.2. Feed Pipe Simulator Improvements

Having conducted the development testing described in § 5.4.1, it was recognised that in order to better replicate engine flight cycles, modifications to the rig were required to allow greater automation. Previously, as the FPS valves which allow shutdown conditions to be replicated and the oil flow rate control were both manually operated, the cycle complexity and maximum operation duration of the FPS were limited. As part of this EngD, in consultation with Scitek Consultants Ltd, hardware and software modifications were designed and implemented to allow full FPS simulator automation.



Figure 5.26 Feed Pipe Simulator control unit

A control unit (Figure 5.26) was built to allow:

- Temperature programming of both the main test specimen heater and the oil pre-heater.
- Automated control of oil flow rate.
- Automated control of the air input (used to re-aerate the oil and to encourage the evaporation of oil volatiles).
- Automated control of valves 1 and 2 to allow drained and flooded shutdown cycles to be replicated.
- Data recording of 7 thermocouples positioned at numerous locations around the system.

This unit allows for more complicated flight cycles to be performed. The transient flow rates and temperatures seen in gas turbine as a result of different power conditions can therefore be replicated. Table 5.1 shows a possible cycle which could be performed using the modified FPS. The shown conditions are for a very short flight with the temperatures and flow rate based around those predicted for a gas turbine. It should be remembered that the oil temperatures will be less than the displayed wall (metal) temperature and the flow rate of oil is considerably lower than in the engine. Decreased flow rates allow acceleration of the test due to the increased residence time of the oil in the heated zone and reduced surface shear stress.

Table 5.1 Example Feed Pipe Simulator test cycles

Simulated Flight Condition	Test Point	Time (minutes)	Specimen wall temperature (°C)	Oil Flow Rate (mL min⁻¹)
Take-off and Climb	1	30	400	30
Cruise	2	15	350	34
Descent	3	30	350	26
Shutdown	4	60	375	0 (drained)

The modifications described in this section were utilised in the testing which forms part of the following chapter, thereby allowing the evaluation of surface technologies under more engine representative flight cycle conditions.

5.4.3. Oil Chemistry

In service, lubricant deposits can form even when the quality of the bulk oil supply is good, this is because it is only the proportion of the oil resident at the wall surface for the required

duration undergoes the extreme degradation which results in deposition. The oil in the bulk, is not resident at the wall region for a significant duration and will remain of good quality. However, if the bulk oil quality is poor then deposition will be likely to increase. Due to oil system management, as described in Chapter 4, this would not ordinarily occur. Therefore, if the FPS is to be representative of service conditions, maintaining engine representative oil quality is an important factor.

Figure 5.27 shows overlaid Gel Permeation Chromatograms of samples taken from the bulk oil tank of the Feed Pipe Simulator after 14, 40 and 60 cycles. As sample duration and therefore the level of degradation of the sample increases, we can see an increase in the proportion of high molecular weight compounds present (log 3.0-3.4). This is due the polymerisation of oil components via the thermal oxidative mechanisms discussed in detail in § 2.5 and § 4.4.

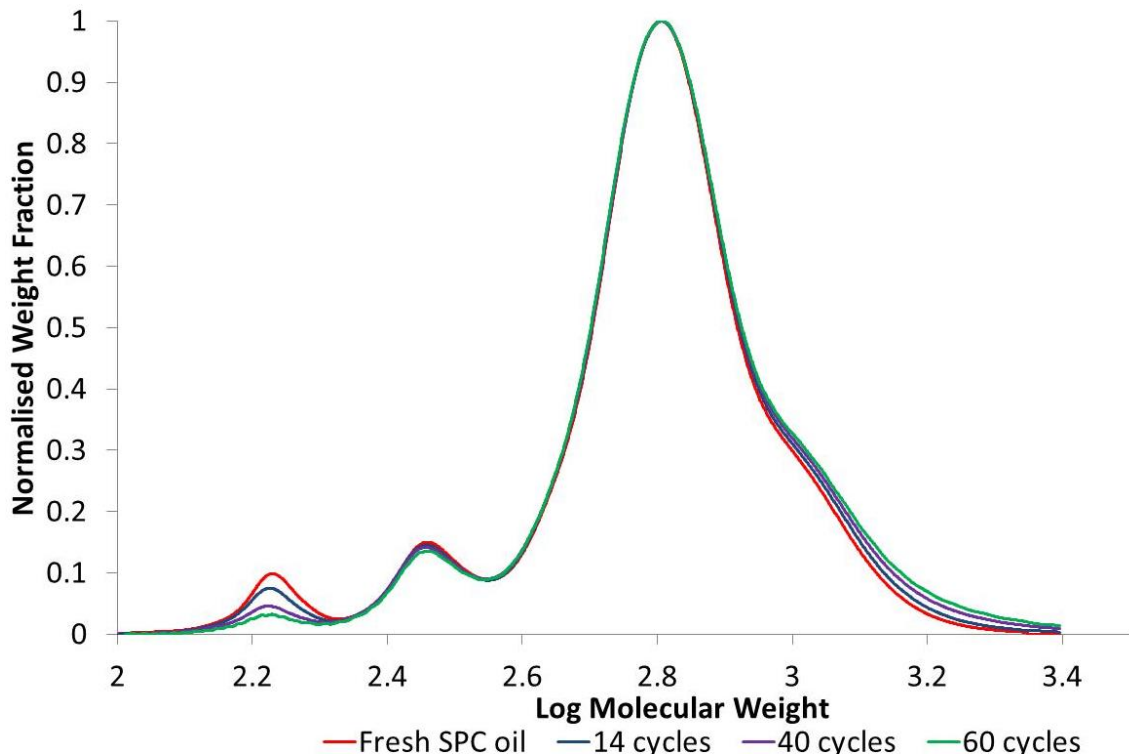


Figure 5.27 Gel permeation chromatogram of FPS oil samples at a range of durations

The peak at approximately 2.25 Log Mw, which can be attributed to PANA, an antioxidant used in this oil, can be seen to decrease as the oil becomes more degraded. Figure 5.28 shows the percentage of the original PANA content, calculated from the peak area of the GPC, co-plotted against the Total Acid Number of the sample. The consumption of PANA antioxidant can be seen to follow that of a first order reaction, this is consistent with the findings of Sniegowski (1982), however, further comparison to Sniegowski's (1982) data is not possible as it was determined on an engine with oil replenishment during the test. From the data generated using the Feed Pipe Simulator (Figure 5.28), the half-life ($t_{1/2}$) was calculated to be 44 FPS cycles.

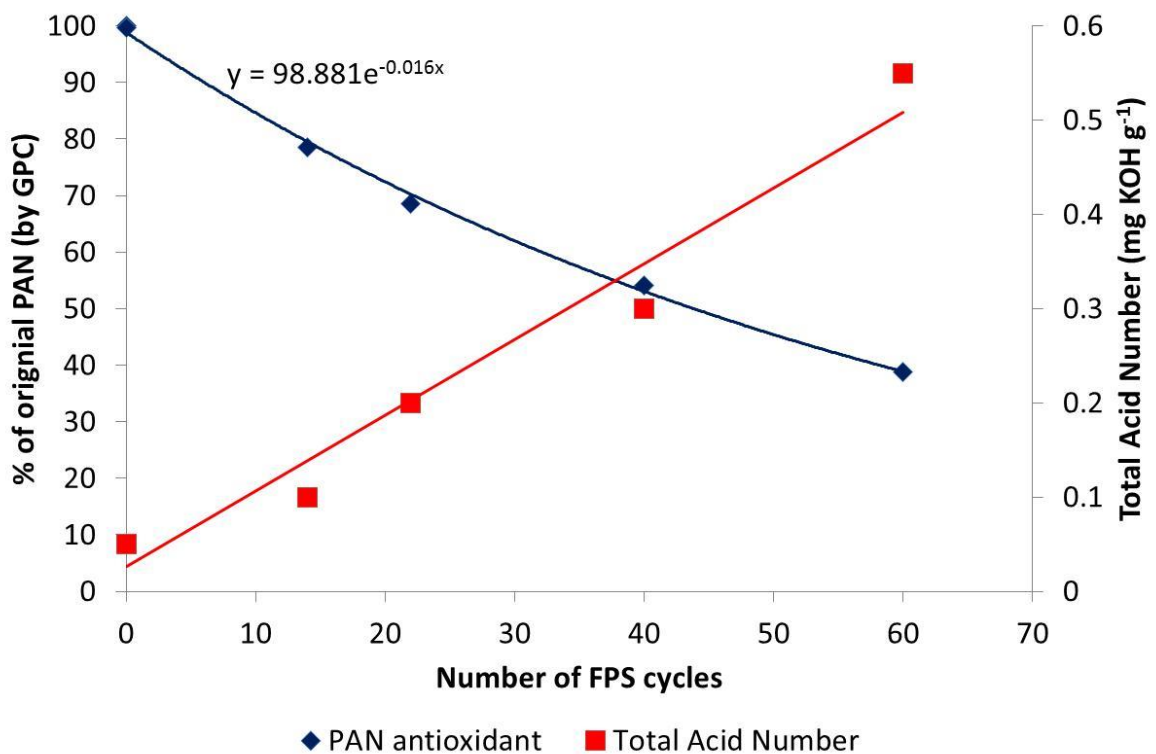


Figure 5.28 Relationship between antioxidant consumption and Total Acid Number

As seen previously, Total Acid Number is a useful expression of the extent to which thermal oxidative degradation reactions have progressed. It was seen that as the amount of PANA

antioxidant decreases, the Total Acid Number increases linearly showing that the oil is beginning to degrade. After 60 cycles, PANA content has fallen below 40 % of the original quantity and TAN has reached $0.55 \text{ mg KOH g}^{-1}$. From oil sampling exercises it is known that Rolls-Royce engines will commonly operate at TAN levels up to approximately 1 mg KOH g^{-1} . Therefore the quality of the oil used in this Feed Pipe Simulator test remains similar to that of service oil (Edge and Squires, 1969). If the test were to be run for longer an oil change would be required to prevent excess oil degradation influencing the deposition rate.

5.5. Closing Remarks

The degradation of lubricants at hot wall locations can cause solid fouling deposits to form around the oil system. As these deposits have the potential to restrict or even completely block oil flow leading to potential engine failure, they must not be allowed to accumulate. A good knowledge of how deposits form under different conditions with the range of available lubricants is therefore vital. This allows the selection of the most suitable lubricant for a specific application and where required, can also inform maintenance needs.

In this chapter, the review of the industry techniques currently available showed a need for methodology which allows more engine representative simulation of specific oil system locations and conditions.

Testing using the Vent Pipe Simulator gave the relative performance of a range of lubricants in terms of their ability to resist lubricant deposition. A study of lubricant accumulation showed how deposits may begin to accumulate in the gas turbine oil system. Analysis of oil chemistry and of deposits was also conducted. This work showed that this laboratory method, the Vent Pipe Simulator, is a useful tool in determining the likelihood of in-service vent pipe deposits occurring.

Under single phase conditions, cyclic testing was conducted using the Feed Pipe Simulator. This testing proved the method has the ability to differentiate between oil brands of known deposition propensity under simple cyclic conditions. An assessment of the influence of cyclic conditions showed that the conditions following engine shutdown contribute much more to deposit formation than engine running conditions. It also showed that the design of engines to allow oil pipes to drain of oil on shutdown is likely to give greater deposit formation than if the pipes remained oil filled. FPS development testing informed hardware and software modifications which will allow the simulation of more complicated, flight-like cycles.

The purpose of this chapter was to further develop the laboratory tools available to assess deposition formation under bearing chamber vent and feed pipe conditions. The following chapter on surface technology will focus on the efforts made to evaluate the ability of surface modified pipe hardware to resist deposit formation. Therefore the tools developed in this chapter will provide a vital means of assessing the suitability of these technologies.

CHAPTER 6: SURFACE TECHNOLOGY

6.1. Introduction and Business Case

The risk of solid lubricant deposits restricting or blocking the flow of lubricant to critical components is a key driver for the work carried out as part of this EngD project. As these deposits have the potential to lead to fire or overheating followed by damage to the engine and possible engine failure, manufacturers aim to reduce this risk to a minimum.

In the previous chapter, efforts were focussed on developing engine representative laboratory methods to allow the deposition propensity of a lubricant to be established, such that the most suitable lubricant can be selected. This work therefore assumed generalised oil system conditions including that of oil system hardware, to allow applicability across all gas turbines.

Unfortunately, even the most thermally stable lubricant currently available will form deposit if exposed to extreme conditions or even more mild conditions for a long duration. Therefore, maintenance inspection and/or action can be required to prohibit deposits from reaching a level at which they affect performance. Maintenance is undesirable as it is expensive, operationally disruptive and where disassembly and reassembly of critical components are required, carries an inherent risk. Therefore it is desirable to minimise the frequency at which maintenance is required.

Assuming that lubricant performance is optimised and service conditions are fixed, altering the part which the surface plays in deposition is the most plausible method by which to reduce deposition. The surface will participate in deposition in two primary ways; through catalysing the breakdown of the oil or by promoting the adhesion of the deposit. Modification of the metal surfaces is therefore a potential method to reduce deposition of lubricants.

The primary design concerns for the oil system pipe hardware are strength and temperature resistance to ensure they remain able to contain and transport the oil. The majority of bearing chamber pipes are currently manufactured from stainless steels. They typically contain ~70 % iron, ~20% Chromium and ~10% Nickel along with a number of other trace elements. The work of Zeman (1984) highlighted these elements as some of the most catalytically active metals in the formation of lubricant deposits. More recent work by Askins (2010), showed that using heat treatment to increase the surface oxide layer on stainless steel could reduce the amount of deposits formed under single phase conditions. Askins (2010) also showed that surface finish can influence the rate of deposit formation with rougher surfaces giving greater deposition. These results were consistent with findings of the E34 Propulsion Lubricants Committee, into the effect of HLPS test specimen surface finish variation (Cross, 2002). It is therefore evident that modification to oil pipe surfaces can reduce deposit formation. However, any change to the current pipe hardware must meet the following constraints:

- The pipe must meet a similar mechanical and thermal strength to the existing steel alloys;
- Surface modifications or coatings must be able to be applied to pipe interiors and to complex geometries;
- Coatings must be well adhered such that they themselves do not produce blockages or contamination issues.

The purpose of the experimental work conducted in this chapter was to evaluate the ability of a range of alloys, coatings and surface modification techniques, which could replace or be applied to stainless steel, in order to reduce oil deposit formation. The lubricant deposition

techniques developed in Chapter 5 were utilised as assessment methods for determining the feasibility of these candidate modifications to reduce deposition.

This Chapter is structured as follows. § 6.2 details the laboratory based methods used in this Chapter and explains the rationale for their selection. § 6.3, entitled Surface Metallurgy, includes the results of single and two phase flow testing using test specimens with a range of metallurgies. § 6.4 presents results of testing to understand the influence of surface modification on deposition. These surface modifications are treatment technologies which can be applied to the existing stainless steel alloy. § 6.5 contains the closing remarks for this chapter.

6.2. Deposition Testing Methodology

As discussed and demonstrated in the previous chapter, the mechanism and rate of deposit formation is very dependent upon the conditions to which the oil is exposed. The intention of the work in this Chapter is to find deposit reducing methods which could be applied to all three of the bearing chamber oil pipes: feed, scavenge and vent. It is therefore necessary to evaluate candidate surface technologies through a range of conditions but critically under single and two-phase conditions.

To assess lubricants under the single phase conditions found within the bearing chamber feed pipe, two methods were selected. Initial work was conducted using the Hot Liquid Process Simulator (HLPS) (SAE ARP5996, 2013) (§ 3.1.2). The HLPS was selected for this initial testing for a number of reasons. It is an industry standard lubricant deposition method, this means that the method is widely available and the results it produces are well understood. An additional benefit is that the test is configured such that the oil interaction and subsequent deposit formation is with the external surface of the test specimen. This means that candidate

surface technologies can be more easily applied to the deposition surface without the complication of applying to pipe interiors.

However, as discussed in § 5.2.1, the HLPS is not truly representative of an oil system feed pipe and does not have the facility to replicate the shutdown element of a cycle. As a result of this, the HLPS was used as a screening method before the most promising technologies were tested using the FPS, developed in § 5.4. This method allowed the surface technologies to be evaluated using more engine representative hardware and by using more realistic flight cycle conditions.

To evaluate surface technologies under two-phase conditions, it was chosen to concentrate on the more severe conditions of the vent pipe over those of the scavenge pipe. Vent pipe conditions are known to be more aggressive towards the oil due to a more heavily air biased air/oil ratio than the scavenge pipe, thus temperatures are hotter and more air is available for reaction. To replicate the vent pipe conditions, the Vent Pipe Simulator developed in § 5.3 was used, as this is believed to be the most engine representative method.

6.3. Surface Metallurgy

6.3.1. Single Phase

In order to investigate the influence of surface metallurgy on deposition formation rate, a range of HLPS test specimens were used. To produce these test specimens the standard machined stainless steel test specimens were coated using the required element. The specimens were coated at Cranfield University, Department of Materials Science & Metallurgy, using Physical Vapour Deposition (PVD). PVD was selected due to ease of application and the availability of coating metallurgies.

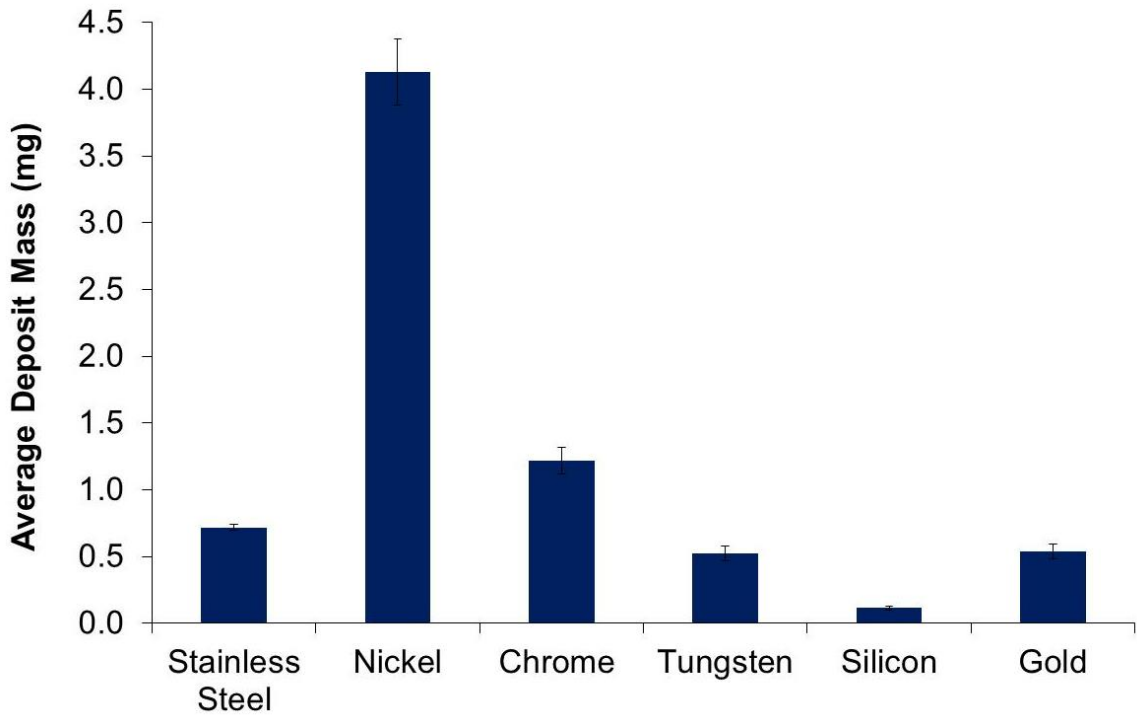


Figure 6.1 Deposit mass formed with a range of test specimen metallurgies using the HLP5 (375°C, 20 hours)

Figure 6.1 shows deposit mass formed following a 20 hour test with a peak wall temperature of 375 °C for the following metallurgies or coatings: stainless steel, nickel, chrome, tungsten, silicon and gold. The error bars shown indicate standard error. It was seen that the tungsten and gold showed small deposit reduction when compared to standard stainless steel surfaces. Silicon gave a large reduction in deposit mass of around 85 % at this temperature, this is believed to be due the inert layer which the silicon forms at the surface.

In the work conducted by Zeman (1984), chromium and nickel were found to give significantly less deposit formation than iron. It was therefore expected that a greater proportional presence of these elements would decrease deposition when compared to stainless steel. Yet in this testing both the nickel and chromium test specimens gave very high results with 490 % and 75 % increases respectively when compared to stainless steel. As this is not consistent

with the literature, analysis of the test piece surface was carried out using Scanning Electron Microscopy.

Figure 6.2 shows the surface morphology of the nickel and chrome surfaces compared with that of standard machined stainless steel. It can clearly be seen that these two PVD coated surfaces exhibit a much more textured surface, with discrete volumes of the metal coating greater than 20 μm in length. A porous surface such as this is likely to affect deposit formation in two ways, the greater surface area gives a larger surface for deposition and therefore more reactive sites. The porous nature of the surface is also likely to result in more oil being held in the boundary region and for a longer duration due to more conjugated flow path, thereby resulting in a higher average residence time of the oil in the hottest region. It is likely that the irregular surface is the primary cause of the unexpectedly high result with nickel and chromium and not an indication of their catalytic activity. Indeed, the fact that the nickel surface has smaller deposit features and therefore a larger surface area would explain the greater deposit mass than chromium. The increased surface morphology is believed to be a facet of the physical vapour deposition process which occurs if the temperature of the target surface is too low, this could be avoided by using an increased temperature which should give a smoother surface morphology. However, this did serve to highlight the importance the coating process has in the formation of the oil deposits. As PVD requires a line of sight for coating, it is not suitable for coating pipe interiors, therefore refinement of the coating process was not pursued for nickel and chromium.

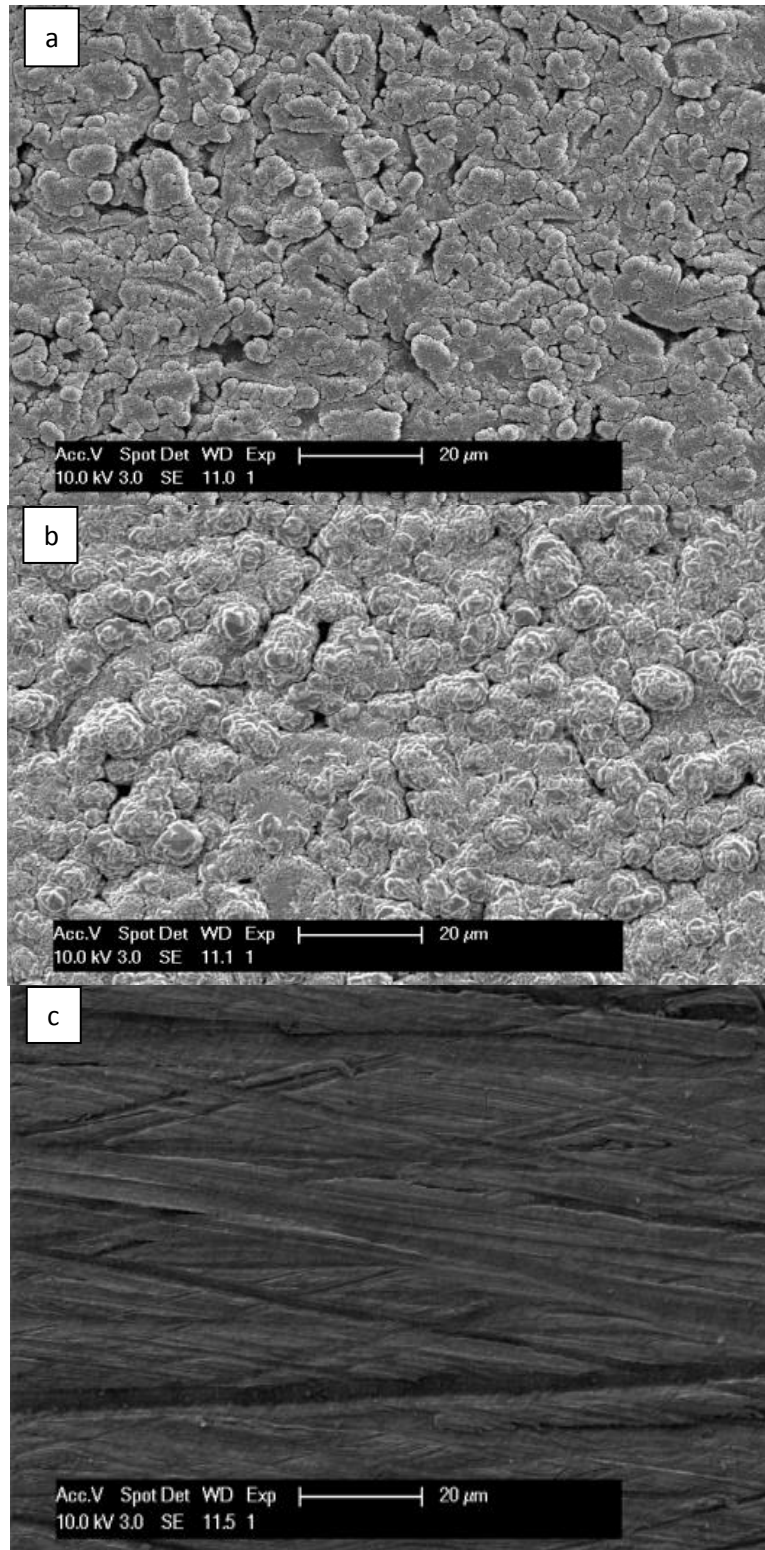


Figure 6.2 SEM Images of test piece surfaces. (a) Nickel (b) Chromium (c) Stainless Steel

As oil deposition is known to be heavily influenced by the conditions used, two of the best performing coatings from Figure 6.1 (silicon and gold) were selected for further testing. Figure 6.3 shows the two coatings (along with stainless steel for reference) at 300, 325, 350, 375 °C. Two results are shown for each test condition and coating, these repeated tests demonstrate that when deposit mass is low (<1 mg), experimental error is small. The relationship for stainless steel is linear with respect to temperature. For the other two coatings, this relationship is more complex. In the case of silicon, the deposits formed at 300, 350, 375 °C were similar in mass, while the mass deposited at 325 °C was much greater. A similar trend was exhibited for the gold test pieces but the deposit amount greatly increased at 350 °C. As these tests were repeated with similar deposit mass results, they are believed to represent true results and not test anomalies. The fact that the greatest deposit was formed at a temperature lower than the peak temperature could be due to a change in deposit adhesion with temperature. However, if the general trends are considered and high results discounted, gold provides limited benefit over stainless steel, while silicon could provide a reduction in deposition up to 85%.

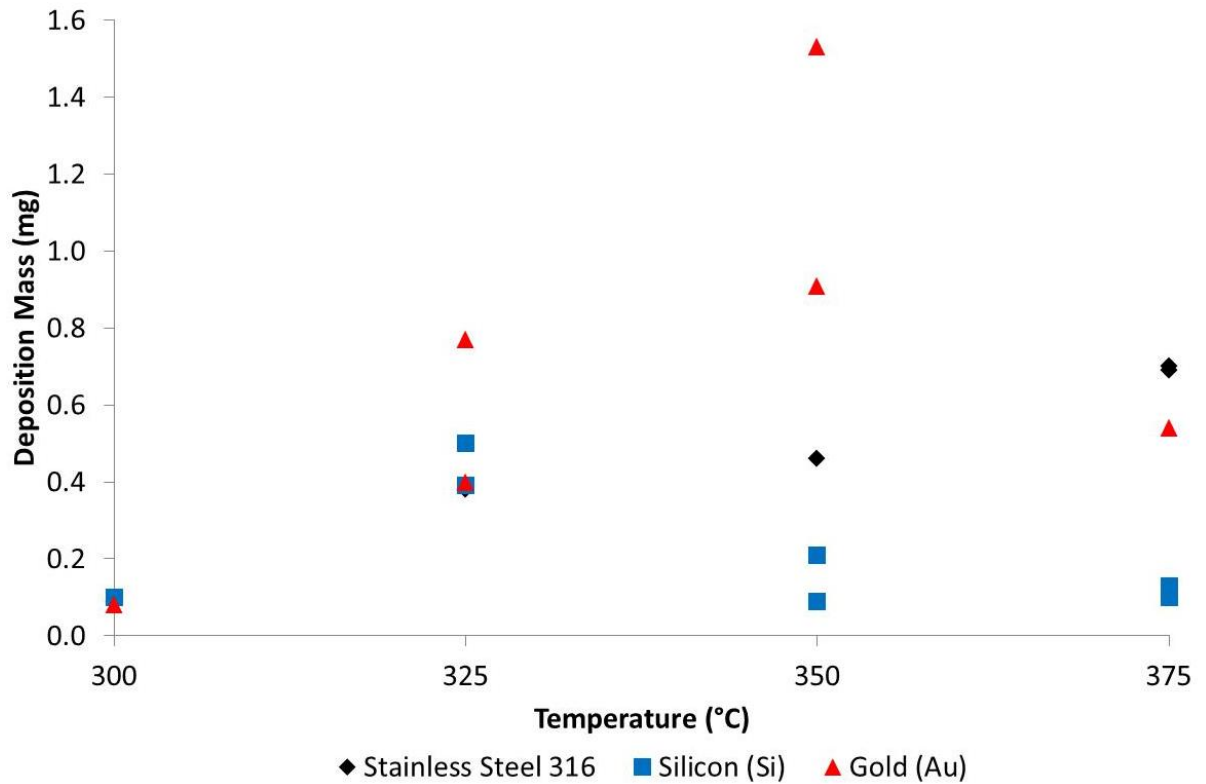


Figure 6.3 Deposit mass formed with gold and silicon test specimens at a range of temperatures using the HLPS

6.3.2. Two Phase Flow

As stated previously, deposition formation under two phase conditions differs significantly from single phase, therefore two phase testing was also required. The Vent Pipe Simulator was used for this purpose, therefore pipes of differing surface metallurgy were required. As pipes do not allow 'line of sight' coating techniques to be used, PVD was not considered a suitable option. Additionally, previous single phase testing highlighted that oil deposition can be influenced heavily by coating morphology, therefore the preferred option was to use test specimens drawn from the candidate metal or alloy. This methodology has the benefit of avoiding coating or preparation issues but limits the range of available metallurgies. Inconel 600 and titanium were selected for this testing. Inconel 600 is a nickel-chromium based alloy (Nickel 73 %, Chromium 16.5 % and Iron 9.5 %), commonly used for high temperature

applications. Testing by Askins (2010) showed that under single phase conditions, using the HLPS, Inconel showed reduced deposit formation. The work by Zeman (1984), showed that titanium was one of least catalytically active metals in oil degradation, therefore this was also selected.

Figure 6.4 shows the effect surface metallurgy for titanium and Inconel compared with stainless steel over a range of temperatures. The error bars shown indicate standard error. Stainless steel exhibits a gradual increase in deposit mass with temperature with a large increase in deposit from 350 °C to 375 °C. Titanium also exhibits an increase in deposit, however this occurs at the lower temperature of 350 °C, the deposit mass is also greater than stainless steel at 300 °C and 325 °C. Inconel exhibits similar results to stainless steel with the exception of 325 °C where it produces approximately 50 % more deposit.

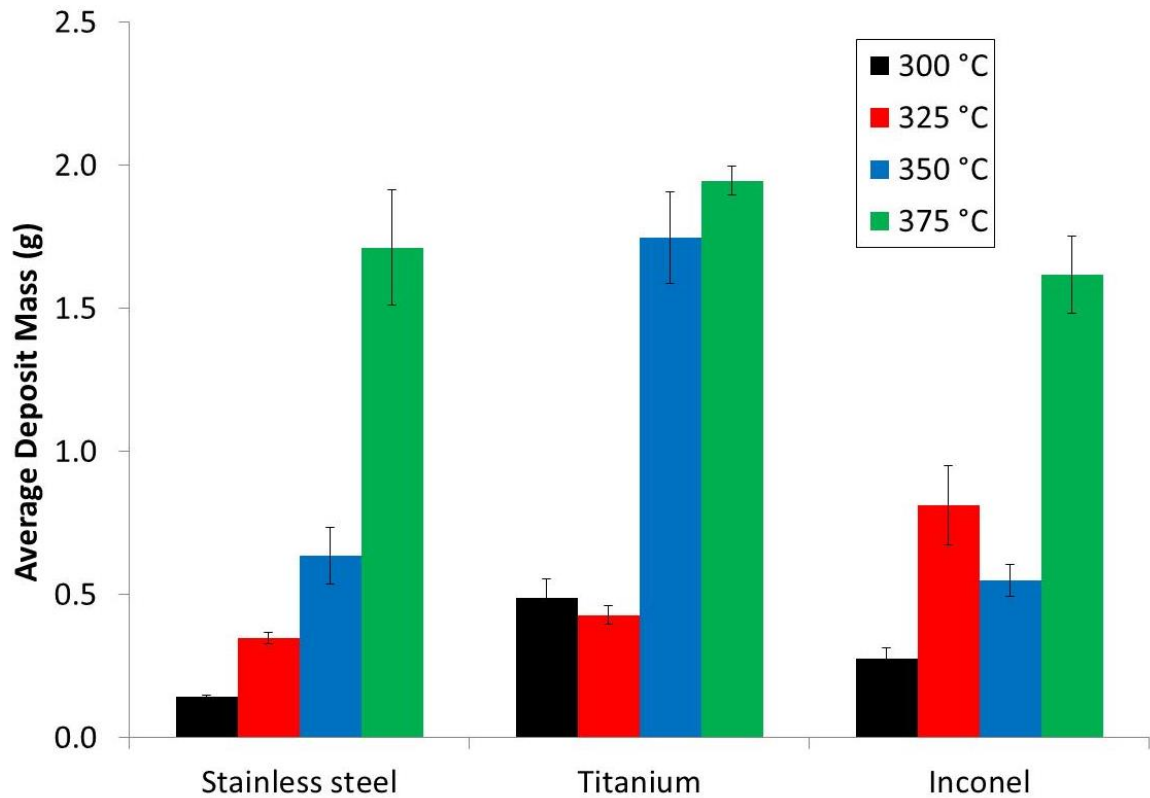


Figure 6.4 Vent Pipe Simulator results for stainless steel, titanium and Inconel following an 18 hour test duration

The significant reduction in deposit with Inconel under single phase conditions reported by Askins (2010) was not seen here under the more extreme two phase conditions. It was postulated that the benefit of a less catalytically active metal surface would be lost when a deposit layer has accumulated. Therefore, a study of deposit accumulation at the lowest temperature, the least accelerated condition, was conducted.

Figure 6.5 shows the accumulation of deposit mass over time for the two metallurgies. The error bars shown indicate the standard error. Whilst the trend for Inconel is lower than that for stainless steel, the difference between the two metallurgies is small. This indicates that the benefit of reducing metal activity is less pronounced for the vent pipe (two phase) conditions than it is for single phase conditions.

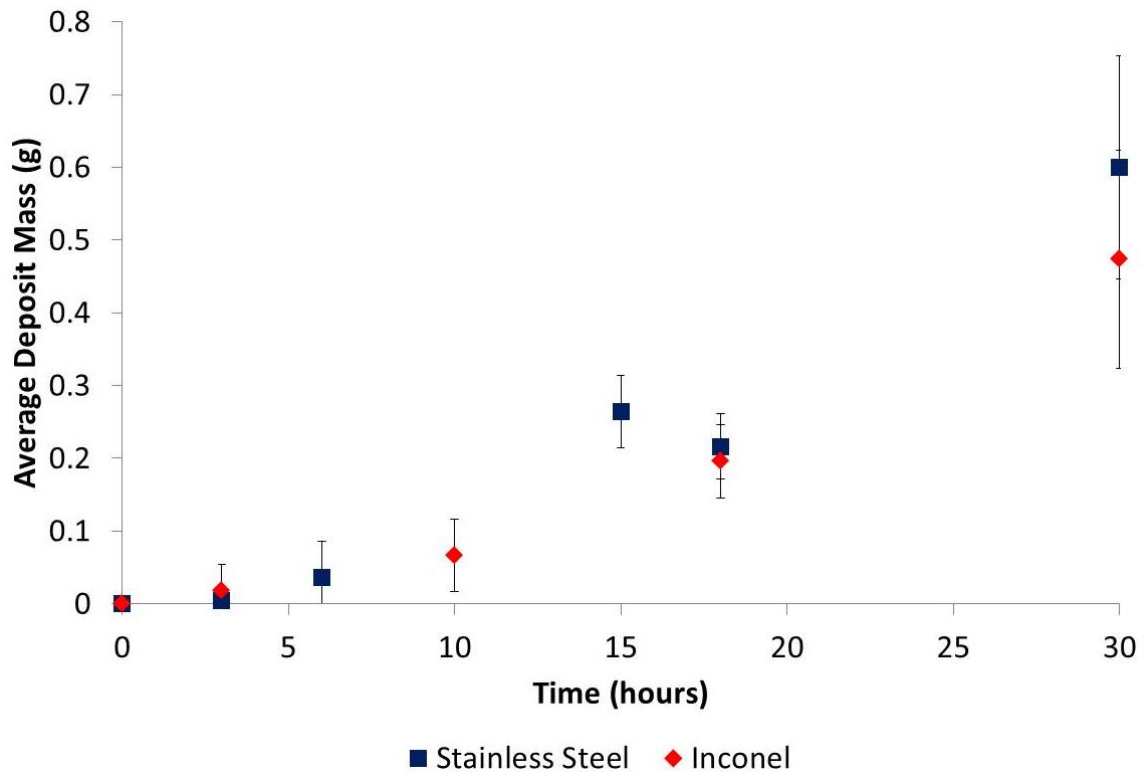


Figure 6.5 Deposit mass accumulation as a function of time at 300 °C for stainless steel and Inconel test specimens (VPS)

6.4. Surface Modification

Surface coating of gas turbine oil pipes has a number of potential issues, some of which were highlighted in the previous testing. Coatings can be difficult to apply to complex geometries, such as pipe interiors, evenly and reproducibly. If adhesion of the coating is not maintained then the coating itself could cause oil flow restriction. Therefore, the more preferable option to a gas turbine designer is to modify the existing surface of the pipe to provide a surface which produces less oil deposition. In this section, two proposed surface modifications were evaluated for their potential to reduce oil deposition. These modifications are electropolishing and acid pickling as described in § 3.1.3.

Electropolishing is an electrochemical process where the specimen surface finish is improved by electrochemical removal of material from the surface. The specimen which is to be polished

is used as the anode and submerged in an electrolyte. When a DC current is applied, material is removed from the surface and carried through the electrolyte to the cathode. This process relies on the fact that the surface asperities which protrude from the material surface are preferentially dissolved over that in the recesses of the material; this is achieved by the dissolution reaction being limited by mass transport. Mechanical surface finish improvement was shown by Askins (2010) to provide a reduction in deposit formation, however, mechanical polishing of pipe interiors is difficult and therefore electropolishing is a far more practical alternative.

Acid pickling involves the immersion of a stainless steel pipe in acid solution (in this case hydrofluoric acid) which serves to remove surface contaminants, rust or scale from the surface of the material. This then allows the surface of the stainless steel to generate its own passive oxide layer when exposed to oxygen. This passive oxide layer is postulated to reduce the activity of the surface in deposit formation.

6.4.1. Modified Surface Characterisation

HLPS Specimens

The 'as supplied' (standard) surface finish of HLPS test specimens was measured using confocal light microscopy (§ 3.1.5), to be approximately 0.35 μm Ra with the surface finish of those which were electropolished being approximately 0.2 μm Ra. Therefore, only a small improvement in surface finish was obtained.

Feed Pipe and Vent Pipe Simulator Specimens

Surface finish measurement was conducted by confocal light microscopy (§ 3.1.5) on three representative regions of the acid pickled, electropolished and standard test specimens. In

each region the surface finish was determined both longitudinally (in the direction of gas flow) and transversely (perpendicular to the flow direction). In the longitudinal direction average Ra was similar for all surfaces (Table 6.1). However, in the transverse direction, where the standard (before treatment) surface is rougher, greater improvement in Ra and Rq were seen when acid pickling and electropolishing was used. Surface finish measurements are summarised in Table 6.1 and shown in full Appendix 2.

Table 6.1 Summary of surface finish measurements

	Transverse			Longitudinal		
	Pickled Average	EP Average	Standard Average	Pickled Average	EP Average	Standard Average
Ra (μm)	0.937	1.173	1.244	0.191	0.283	0.229
Rq (μm)	1.171	1.398	1.474	0.245	0.375	0.288

Despite minimal differences in the surface finish measurements, visual inspection of the tube surface revealed it to have a more polished, reflective surface as a result of the process. Therefore, tube surfaces were studied using Scanning Electron Microscopy (SEM) to achieve high magnification imaging. Figure 6.6 shows the tube surfaces, it can be seen that both the acid pickling and electropolishing methods have succeeded in removing the numerous $<1 \mu\text{m}$ surface features. These small features, whilst not giving a measurable difference in surface finish, are postulated to contribute to the formation and adhesion of lubricant deposits.

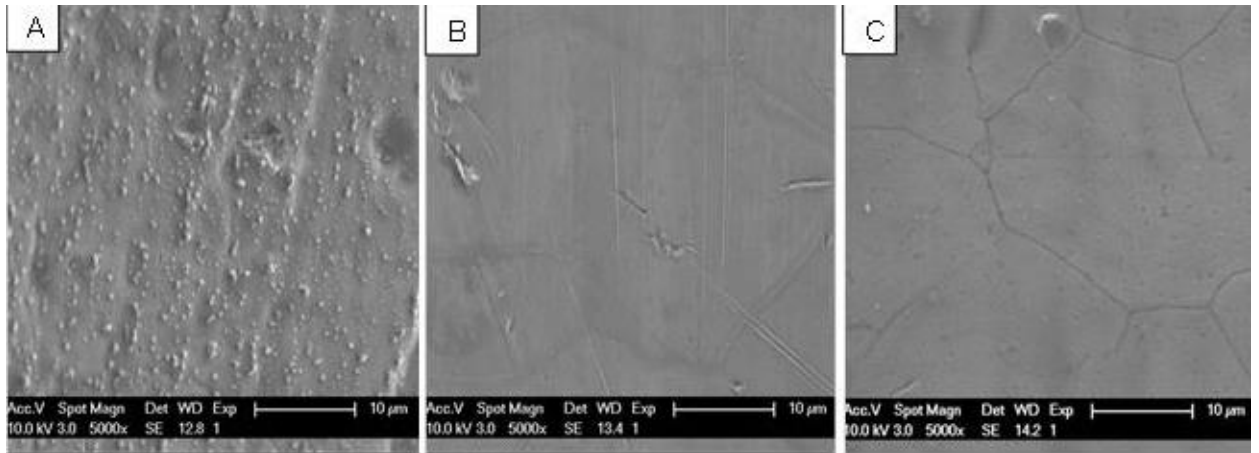


Figure 6.6 SEM images. a) Standard untreated tube b) Electropolished c) Acid Pickled

6.4.2. Single Phase

HLPS

Figure 6.7 shows how three different lubricants compare with respect to deposit formation for both electropolished and standard tube metallurgies. Based on service experience and laboratory testing, SPC 2 is known to form more deposits than SPC 1. The HPC oil, as a more thermally stable high performance oil is known to produce less deposition than either of the SPC oils. Therefore in this testing, the oil performed as expected and in accordance with experience.

The amount of deposit formed when electropolished surface test pieces were used was reduced when compared to untreated test pieces for all three oils. This indicates that the surface effect occurs, irrespective of specific lubricant chemistry, for these lubricants. The average deposit reduction, however, was approximately 79 %, 37 % and 18 % for the HPC, SPC 1 and SPC 2 respectively. This reduction in benefit was believed to be due to the absolute mass of deposit formed. Surface modifications including electropolishing can only provide a benefit when a deposit is initially formed at the surface, if deposit is already present at the surface,

and therefore deposit is being formed onto deposit (cohesion), there will be reduced benefit. The conditions used in these tests are much more severe than in the engine, as a deliberate attempt to accelerate the test, yet in conventional engine service where deposit build up will be slower this could produce a much more significant benefit. It was postulated, that if more representative testing is carried by reducing the temperature of the test, then the difference between treated and untreated surfaces, may be more pronounced.

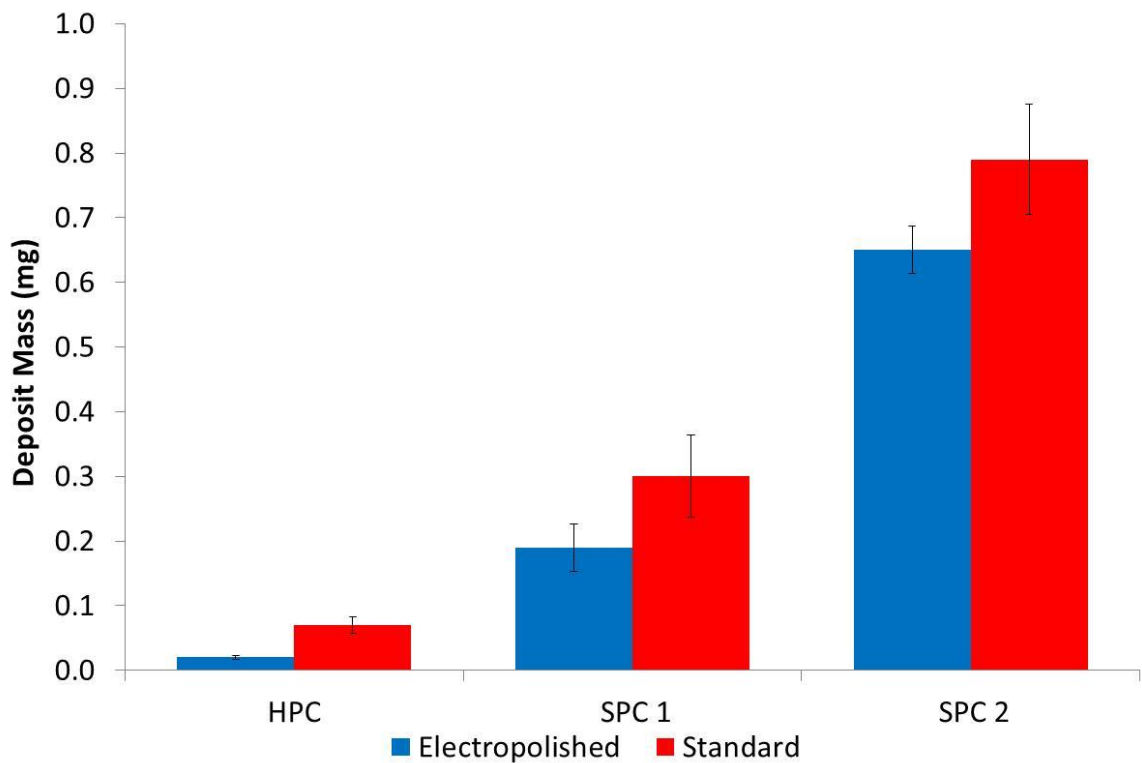


Figure 6.7 Graph showing the deposit mass produced by three lubricants with electropolished and standard tubes at 375°C test temperature

The error bars shown in Figure 6.7 indicate the standard error of test results around the mean; this is approximately consistent with the 26 % repeatability quoted in SAE ARP6255 (2013). Whilst the reproducibility of the method is specified in SAE ARP6255, as 65 %, as a single piece of equipment was used for this testing, the error is believed to be within the 26 % value. It is known that in HLP testing, as deposit mass increases then so does test variance. This is due to

an increased difficulty in washing residual oil from the deposits and in weighing the oil deposits accurately and in a repeatable way. As they become larger they will hold more liquid oil and become more likely to break away from the test piece. Due to this, deposit mass is used in conjunction with visual observation (Figure 6.8) to ensure the mass value is consistent with the amount which can be seen. Therefore whilst at high deposit mass, the error bars are large, the body of test data does indicate a significant difference between electropolished and untreated tubes.



Figure 6.8 HLPS Tubes after a testing using SPC 2 at 350°C, Electropolished (Top) and Standard (Bottom)

As deposition can vary significantly with temperature and as test precision decreases with increased deposit mass, the two SPC oils were also tested at a lower temperature. Figure 6.9 shows the data generated at 325, 350 and 375 °C for the two SPC lubricants. The error bars indicate standard error.

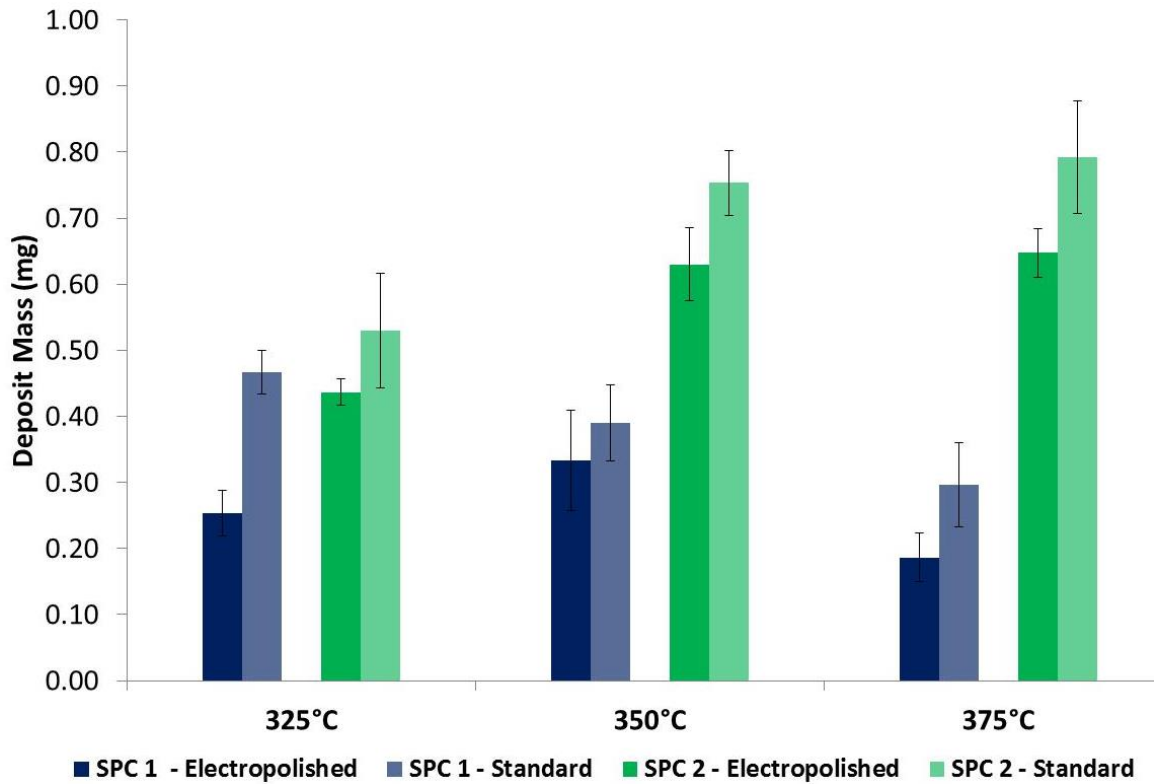


Figure 6.9 Graph showing the deposit mass produced at three temperatures for the SPC oils

Whilst Figure 6.9 shows the expected difference between electropolished and untreated specimens, the results expected with respect to temperature were not produced. SPC 1, the lubricant which is known to form the least amount of deposit of the two, gave approximately similar masses of deposit at all temperatures. This is believed to be an artefact of the test whereby the increased test temperature and deposit gives a greater likelihood of deposit being removed through cracking, either driven by the increased thermal difference or the greater size of deposit increasing the chance of being sheared away. This was confirmed by visual assessment as shown in Figure 6.10 and by filtration of the post-test lubricant. The lower amount of deposition at higher temperature could also have been influenced by activation of additives within the formulation; such that at higher temperature, additive activity reduces deposit mass. As expected there was a large difference between the electropolished and untreated tubes at the lowest temperature, potentially indicating a

benefit at less severe conditions. SPC 2 produced similar deposit masses at 350 and 375 °C with a slight reduction at 325 °C, however, the difference between electropolished and standard did not become more pronounced.



Figure 6.10 Image showing deposit on SPC 1 electropolished test specimens at 375 °C (Top), 350 °C (Middle), and 325 °C (Bottom)

Additional elemental analysis using energy-dispersive X-ray spectroscopy of the test specimen surfaces was conducted before and after testing. The results of this analysis are presented in Figure 6.11. It can be seen that there is minimal difference in elemental composition between the untreated stainless steel and the electropolished stainless steel. This indicates the process has had no effect on the surface composition with changes only occurring in the surface finish. Therefore, the reduction in deposit seen in this section can be attributed purely to a reduction in oil residence time at the wall due to reduced surface area or to a reduction in adhesive strength of oil precursors.

The most significant change to the metal surface following the test and formation of deposits was the increase in phosphorus. This increase can be explained by the adsorption of the anti-

wear additive, tricresyl phosphate (TCP), used in the oil formulation, onto the metal surface.

Although phosphorus only represents 1 % of the surface composition.

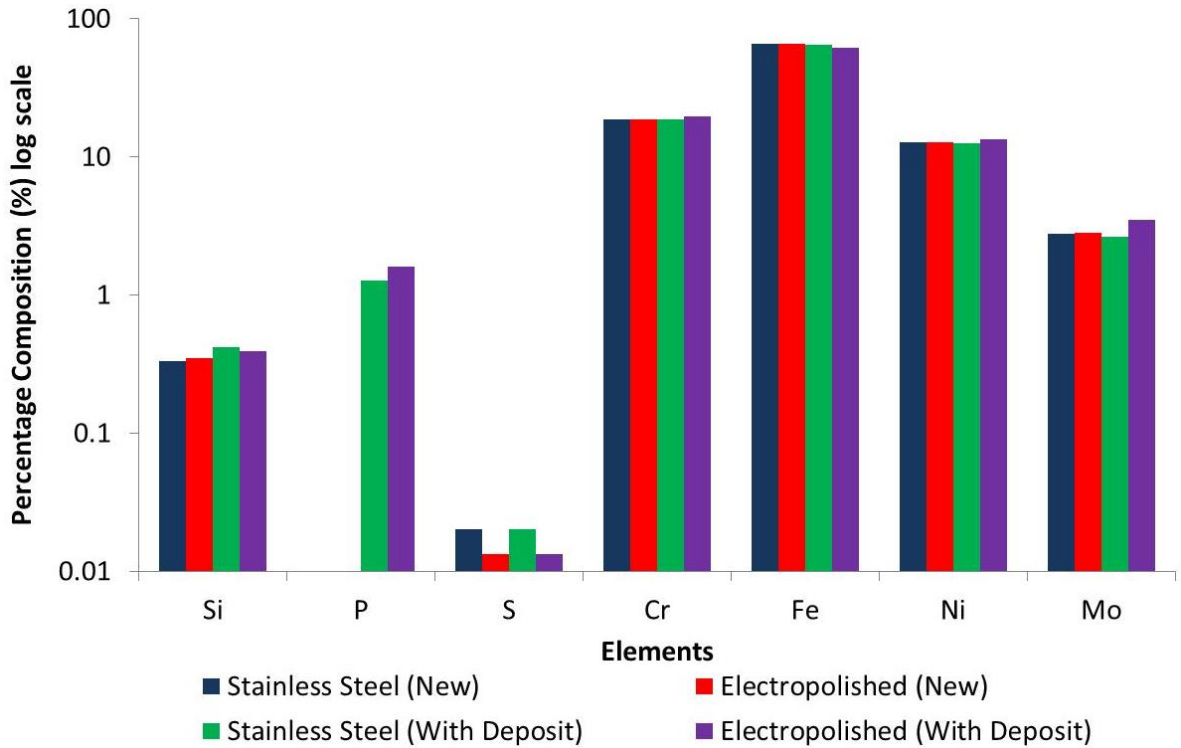


Figure 6.11 Percentage elemental composition of stainless steel and electropolished test specimens before and after test

Feed Pipe Simulator (FPS)

For the testing conducted in this section, a test cycle was devised to simulate a very short aircraft flight cycle (75 minutes). A short flight cycle means that the engine undergoes a greater number of hot shutdowns per flying hour. As hot shutdown conditions were found through previous testing (§ 5.4.1) to represent the greatest risk in terms of feed pipe deposit formation, this short test cycle, represents the most arduous service environment.

Table 6.2 Feed Pipe Simulator test cycle conditions

Simulated Flight Condition	Test Point	Time (minutes)	Specimen wall temperature (°C)	Oil Flow Rate (mL min ⁻¹)
Take-off and Climb	1	30	400	30
Cruise	2	15	350	34
Descent	3	30	350	26
Shutdown	4	60	375	0 (drained)

Testing was conducted using the test cycle shown in Table 6.2 for 60 test cycles with the SPC 1 lubricant. Following the test, the mass of deposit formed was determined gravimetrically, which is shown in Figure 6.12. The error bars indicate standard error. It can be seen that the mean deposit masses for electropolished and pickled tubes are reduced by ~45 % and ~60 % respectively, when compared to standard surface finish tubing. This reduction in deposition was confirmed visually. Therefore, both surface treatments represent a significant reduction in deposition formation over the untreated surface.

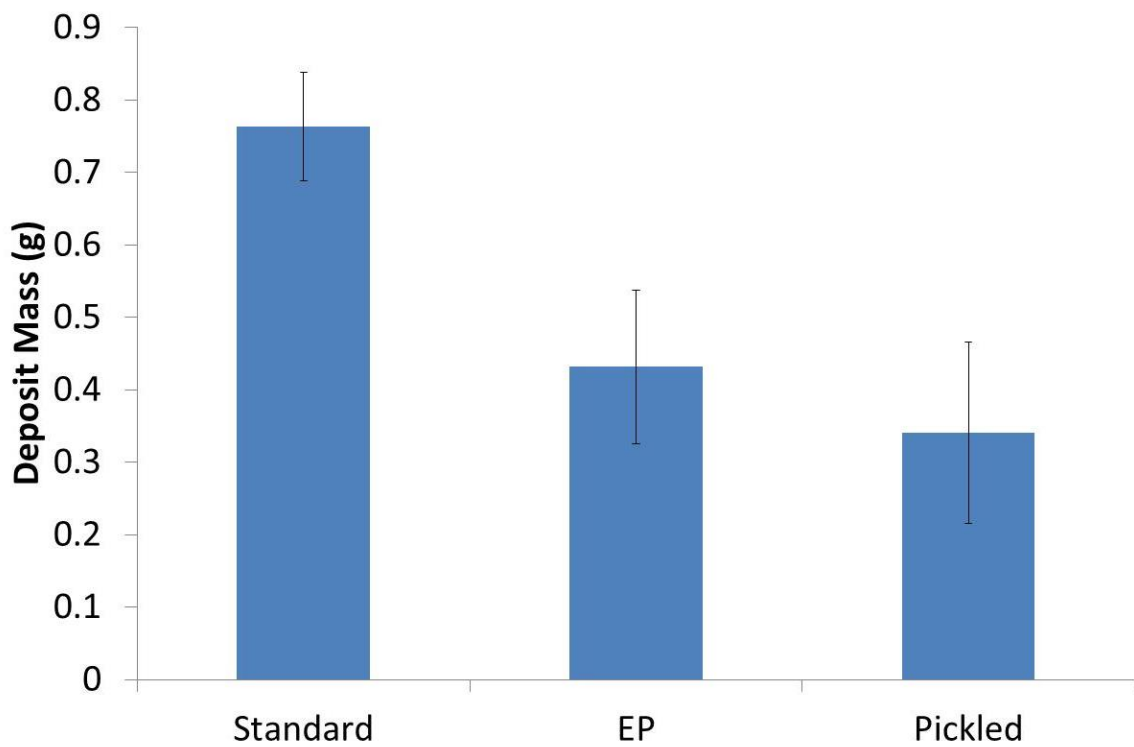


Figure 6.12 FPS Data, deposit mass formed with SPC lubricant with a standard, electropolished and acid pickled test specimens

6.4.3. Two Phase Flow

Figure 6.13 shows a number of tests run at a range of durations, under the same conditions using electropolished, untreated and acid pickled specimens. The error bars shown indicate standard error. For tests run for low duration, where the deposit is much less, both the electropolished and acid pickled tubes can be seen to produce a reduction in deposit mass. However, when the test is run for longer, deposits form over existing deposits and any benefits of surface treatment is negated, as was seen in the HLPS testing.

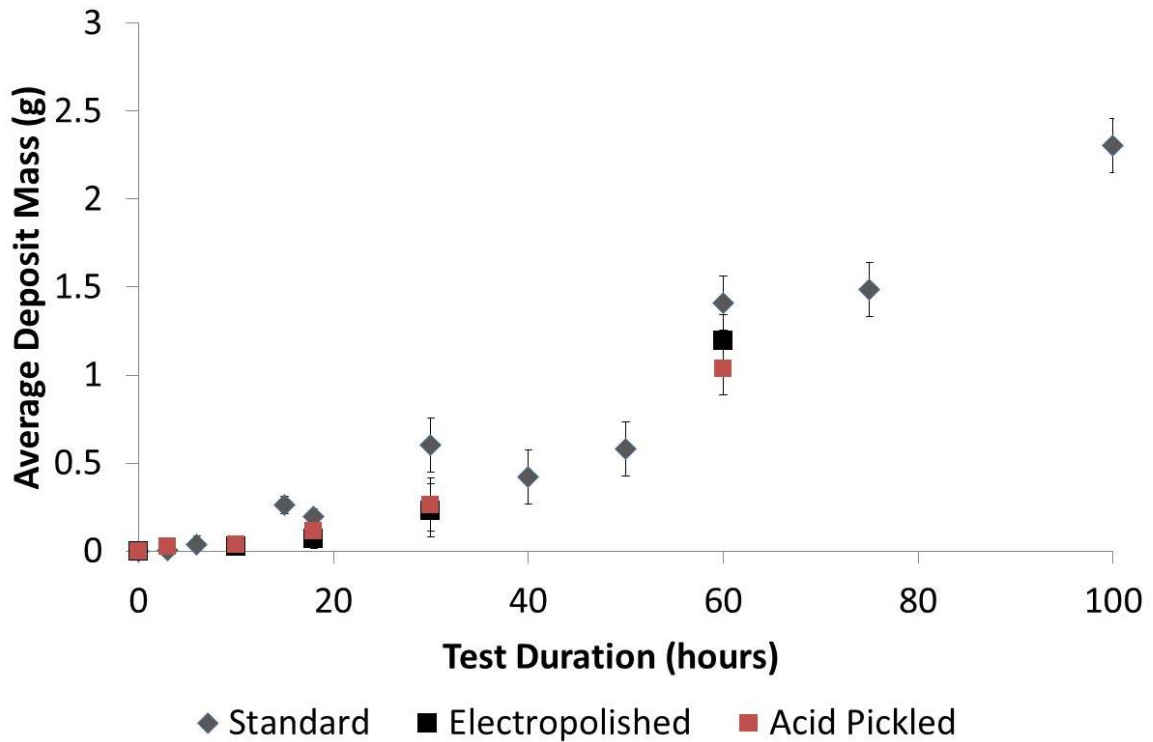


Figure 6.13 VPS results at a range of durations for standard, electropolished and acid pickled test pieces. SPC 1 lubricant with a wall temperature of 300°C

Figure 6.14 shows an enlargement of the region of 0 to 30 hours and shows a significant reduction in deposit mass for the modified specimens, with electropolished performing marginally better than acid pickled. It is not a straightforward process in converting from rig hours to engine hours in the terms of the amount of deposition which will accumulate. However, service inspection has shown that deposit thicknesses in vent pipes can remain low for many thousands of hours before deposition begins to become an issue, therefore, increasing the duration before oil deposit begins to accumulate significantly could be very beneficial in inhibiting deposit build up process.

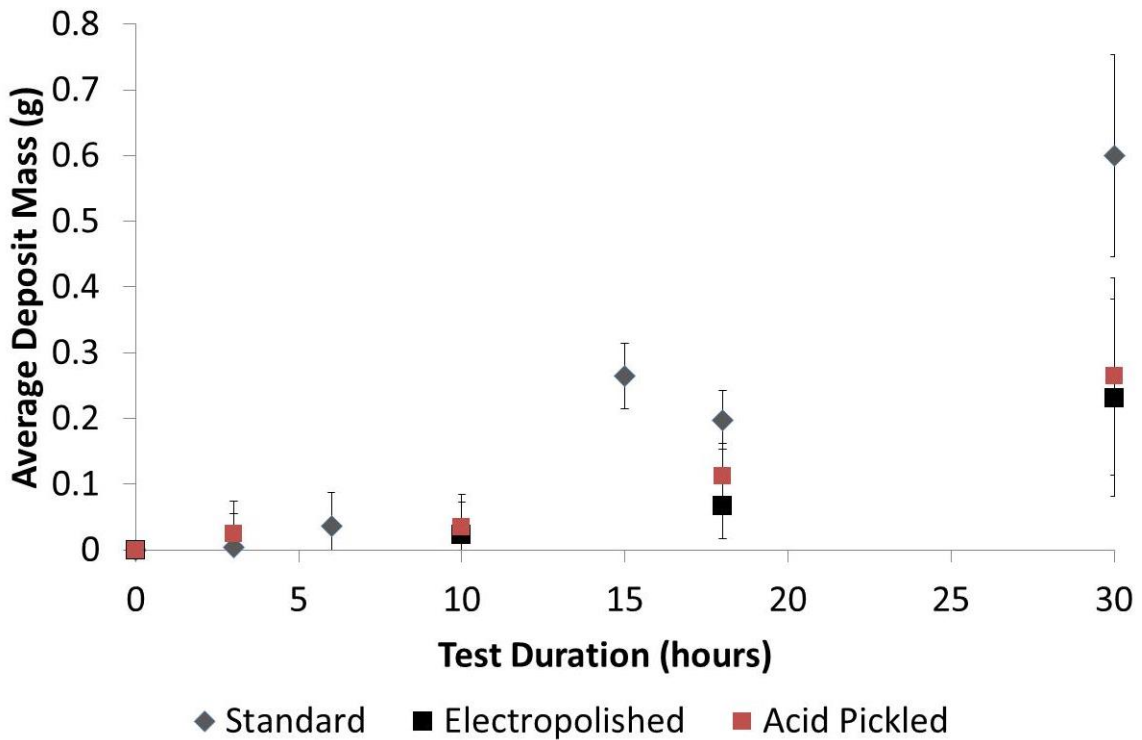


Figure 6.14 An enlargement of Figure 6.13, showing the low duration VPS results for testing at a range of durations for standard, electropolished and acid pickled test pieces. SPC 1 lubricant with a wall temperature of 300°C

6.5. Closing Remarks

Previous work in the literature and in a previous EngD project highlighted the potential to reduce deposit formation by modification to oil pipe hardware. Both pipe metallurgy and surface finish were considered to be factors in the amount of deposit formation.

The importance of flow conditions on oil deposition was established in Chapter 5 and therefore a need to evaluate surface modifications over a range of conditions was identified. Single phase testing using the industry standard, HLPS technique, was initially used due to the ease of specimen coating and the prior experience already available with the method. Additionally, testing using the Feed Pipe Simulator allowed the incorporation of shutdown elements into the cycle. Two phase testing, with more severe air/oil mist conditions was conducted using the Vent Pipe Simulator. This range of testing was planned to allow surface

technologies to be evaluated across a range of the most likely conditions which would cause deposition in the three bearing chamber oil pipes.

Initially, testing was focused on the influence of different metallurgies on deposition rate. Nickel and chromium coatings were found to give much higher deposit levels than was reported in the literature, this is believed to be due to an irregular morphology produced by PVD. Gold and tungsten coatings gave a small deposit reduction when compared to stainless steel. However, the silicon coating was found to give a much greater reduction in deposition (~85 %). Under two phase, vent pipe conditions, titanium and Inconel were found to produce limited benefit, when compared to stainless steel, at reducing deposit.

Changing the metallurgy of pipe hardware by coating, represents additional manufacturing difficulty, cost and the potential for coating delamination. Therefore, the more preferable solution would be to perform modifications to the existing stainless steel surface to reduce deposition. Surface modifications were therefore also considered.

Electropolishing and acid pickling processes were found to improve the surface morphology by removal of surface features < 10 µm in size. Testing using the HLPS showed that electropolishing gave a reduction in deposit formation; the extent of the improvement was dependant on the oil brand and temperature. Testing using the Feed Pipe Simulator showed a greater potential reduction (~50 %) from both electropolishing and acid pickling. Under two phase conditions the benefit of electropolishing was most pronounced at low duration before a significant oil deposit had formed.

From the work conducted in this chapter, it is believed that a reduction in deposition formation rate could be achieved by a modification to pipe surfaces by electropolishing or acid pickling. Due to their pronounced simplicity over coating methods, these modifications appear

to be the most favourable option. It is, however, recognised that if a further reduction in deposit is required then a more inert coating, such as the silicon coating trialled here, could give greater benefits.

CHAPTER 7: TRIBOLOGY

7.1. Introduction and Business Case

The majority of the work conducted as part of this thesis was focused on understanding the influence of elevated temperature upon fluid degradation. The higher temperatures of modern gas turbines are primarily as a result of the need for increased gas compression ratios which will also result in greater mechanical loads. At higher operating temperatures, the viscosity of the lubricant will be decreased; this combined with increased mechanical loading, causes a reduction in oil film thickness.

A reduction in the thickness of the oil films, which provide critical separation of metal surfaces, will result in an increase in metal to metal asperity contact thereby reducing component life. In the most extreme cases, where full metal to metal contact occurs, this could lead to catastrophic component failure. The components most susceptible to failure by tribological wear mechanisms are the highest loaded and fastest rotating components, such as bearings and gears. Progressive bearing and gear failures can often be detected in advance by a vibration measurement technology. However, these components are expensive and often difficult to replace, meaning that the service disruption as a result of these failures can be extensive and therefore a maximum component life is demanded.

In recent years, development efforts of lubricant formulation chemistry have focused on improving thermal stability properties while tribological performance has been allowed to remain approximately constant in the transition from standard to high performance lubricants. As the role which the lubricant plays in the tribological contact is critical to component wear and life, this represents a significant research gap.

Tricresyl phosphate (TCP) is the anti-wear additive used in the vast majority of gas turbine lubricants and therefore represents the most likely influence on lubricant tribological performance. TCP, due to its relative volatility and surface active nature, is known to deplete in concentration through engine operation, potentially reducing oil performance. In addition to TCP, it is possible other additives, such as antioxidants and metal deactivators, as well as the polyol ester base stock itself, will influence wear performance. However, minimal research has been published on the individual and synergistic effects of additives on aviation polyol ester lubricant tribological performance.

In this chapter, scoping experiments are carried out to assess the capability of a range of oil formulations to inhibit abrasive wear. § 7.2 includes an explanation of the experimental approach used and the rationale for the use of the Aviation Lubricant Tribology Evaluator (ALTE). § 7.3 contains test results of four commercially available lubricants, under a range of loadings and temperatures. § 7.4 includes a study of the influence of the TCP concentration used in these commercially available lubricants on their wear inhibiting ability. § 7.5 contains a study of the effect of different additives on abrasive wear. These additives were a simple monomeric type antioxidant, a polymeric antioxidant and a metal deactivator. Closing remarks for the chapter are given in § 7.6.

7.2. Aviation Lubricant Tribology Evaluator (ALTE)

The tribology testing in this chapter was conducted using a piece of equipment termed the Aviation Lubricant Tribology Evaluator (ALTE). The ALTE is used to assess the ability of a lubricant to reduce abrasive wear under sliding conditions. Sliding interaction occurs between a fixed ball bearing (applied with a known load) and a rotating, lubricated metal ring. Lubricant performance can then, most simply, be assessed by the measurement of the size of the wear

scar generated on the ball bearing. The industry standard method for the ALTE is SAE ARP6255 (2013). The deviations made from this method, required for the work in this thesis, are described in § 3.1.4.

Whilst many other tribological assessment tools are available, the ALTE was deemed to be appropriate for this testing, for a number of reasons. The ALTE is low cost with repeatable test specimens readily available, the test duration is short and the oil volume required, low. These factors were critical to allow the assessment of the large number of oil samples required for this thesis. Additionally, the use of pure sliding contact conditions allows the relative performance of oil formulations to be evaluated under the more extreme conditions likely to be seen in gas turbine operation.

7.3. Oil Brand Evaluation

Initial testing was focused on current, commercially available lubricant formulations. These formulations are all SAE AS5780 (2013) qualified polyol ester lubricants, however, they all have different proprietary formulations. The concentration of the tricresyl phosphate (TCP) anti-wear additive, used in each formulation, was determined by Inductively Coupled Plasma Optical Emission Spectrometry (ICP-OES). Figure 7.1 shows the size of wear scar generated for each formulation at 100 °C under a range of loads. The error bars shown indicate standard error. The legend shows in brackets the percentage (by weight) of TCP present in the lubricant formulation.

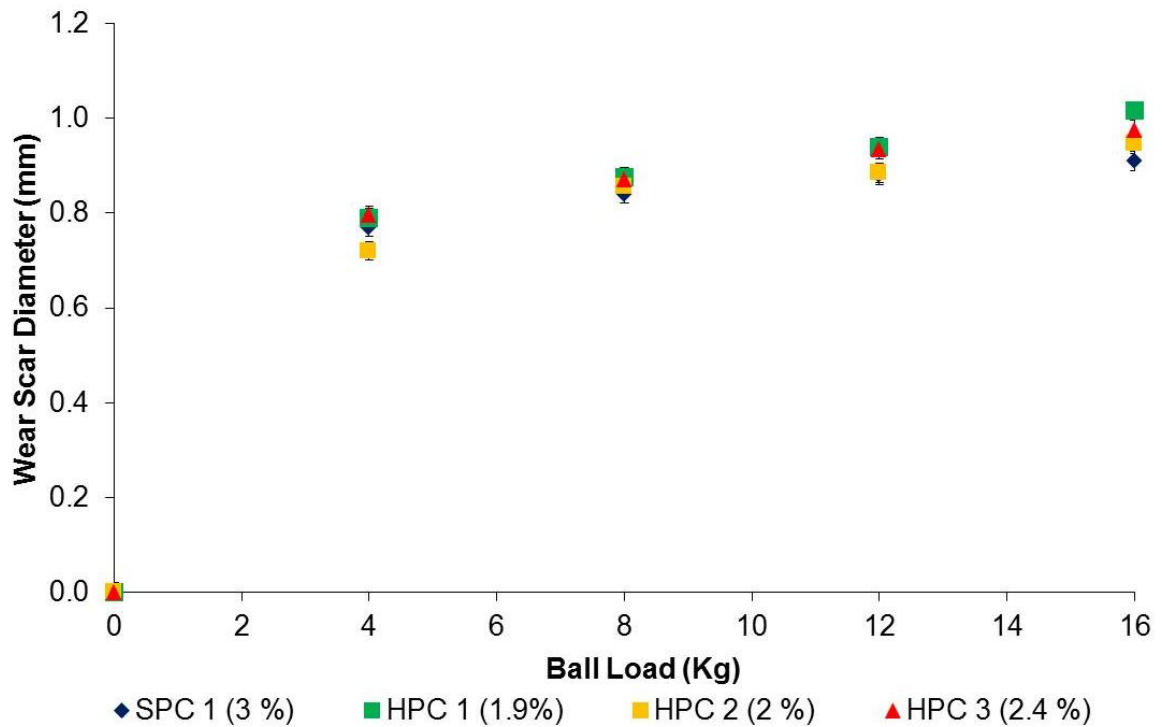


Figure 7.1 Oil brand evaluation at 100 °C. The TCP concentration of each oil is shown in brackets

Figure 7.1 shows an approximately linear relationship between the amount of wear exhibited and the load placed on the ball bearing test specimen, for loads between 4 and 16 kg. This linear trend does not intercept the origin. However, the origin is a true value (wear does not occur without load). Indeed, if load is sufficiently low that the lubricant film retains component separation, wear will not occur. As such it is likely that the mechanism of wear differs below 4 kg where film thickness is greater, resulting in the deviation from the linear trend.

Increasing load at the ball will result in a thinner oil film and a larger frictional force between the ball bearing and the rotating ring resulting in increased wear. Similar performance can be seen between lubricant brands and whilst there are small differences in wear scar diameter, these are not significant when the precision of the method is considered. This indicates minimal effect of lubricant chemistry in this test.

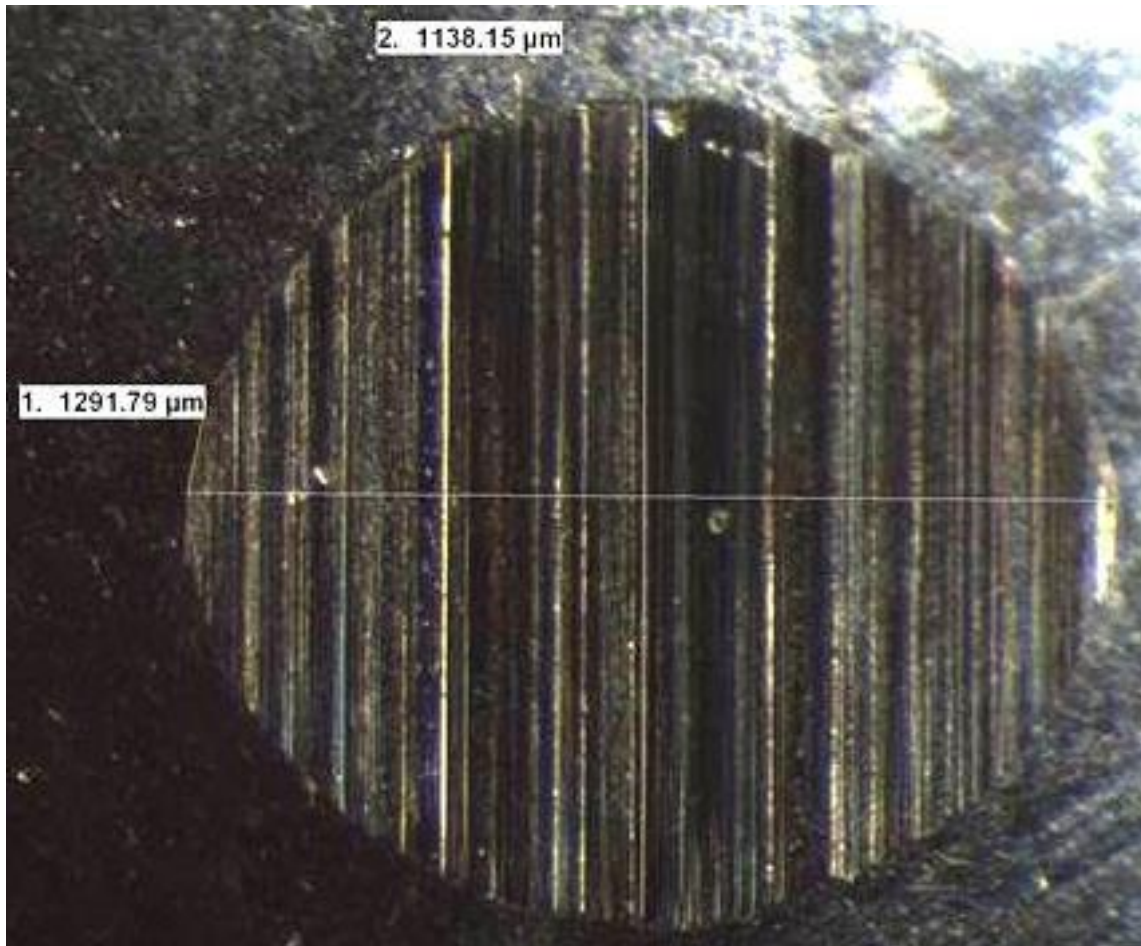


Figure 7.2 Image showing the wear scar generated on the ball bearing at the contact

Figure 7.2 shows an example of the wear scar generated at the ball bearing surface. The wear scar is of an elliptical shape as would be expected between cylindrical and spherical contacting surfaces. Grooves can be seen in the elliptical wear region, these grooves have been formed in the direction of sliding and represent typical abrasive wear. Abrasive wear grooves occur when thin lubricating films result in contact between surface asperities, it is under this regime where protective additives (such as TCP) are relied upon to reduce wear.

Following this testing with an oil temperature of 100 °C, the experiments were repeated with an oil temperature of 150 °C. These two temperatures were selected as they represent the range of bulk oil temperatures likely to be found in bearing and gearbox locations. It should, of

course, be remembered that flash temperature in the localised contact areas will be far in excess of the bulk oil temperature.

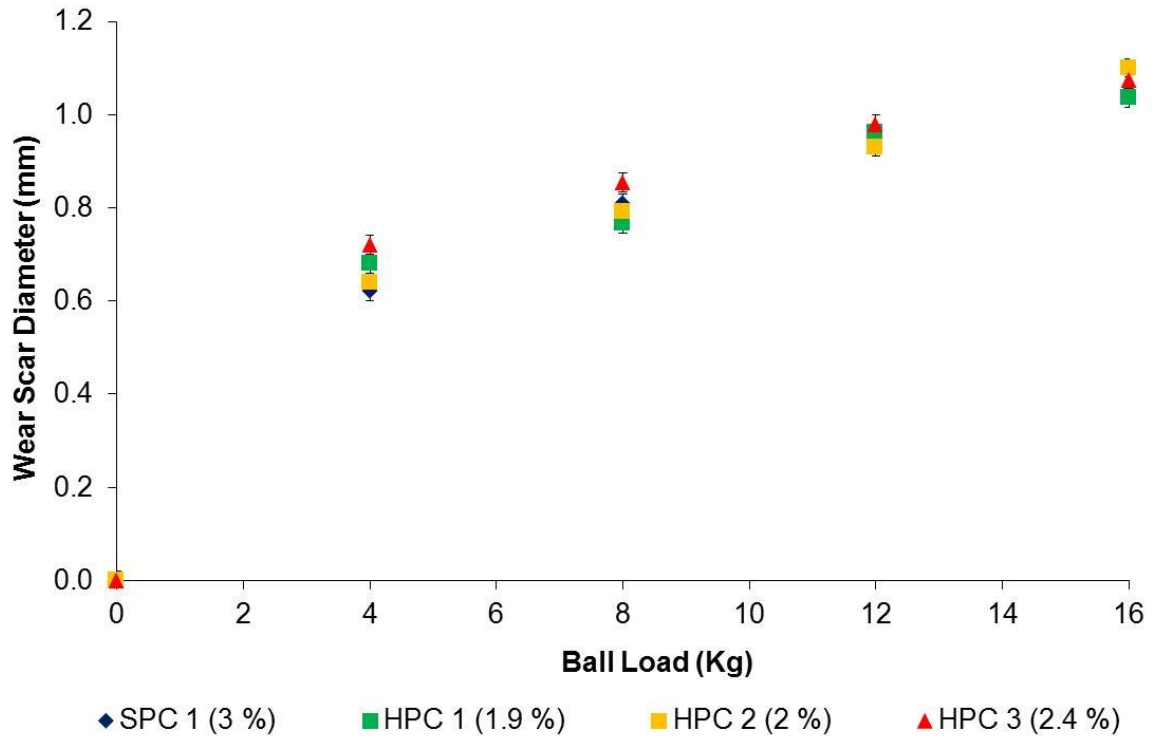


Figure 7.3 Oil brand evaluation at 150 °C. The TCP concentration of each oil is shown in brackets

Figure 7.3 shows a plot of wear scar diameter against load at 150 °C. The error bars shown indicate standard error. As with the lower temperature testing, wear increases linearly with increasing load (above 4 kg load). However it can be seen that the gradient of the line is steeper than at a lower temperature. This increased sensitivity to increasing load is likely to be due to the reduced viscosity of the lubricant at 150 °C, which will lead to much poorer oil film formation and increased wear.

As with the previous testing at 100 °C there are small differences in wear between lubricant formulations. However, at 150 °C these differences are sufficiently large that they are likely to indicate an effect of lubricant chemistry.

Figure 7.4 shows a comparative plot of the SPC 1 and HPC 1 lubricants at 100 °C and 150 °C, these two oils representing the highest and lowest amounts of TCP, respectively. The error bars shown indicate standard error. It can be seen that at low load (4 kg) a higher temperature actually generates a lower amount of wear. It is possible that this is due to the higher temperature required to activate the TCP additive (Faut and Wheeler, 1983). Therefore, as the 150 °C test conditions provide the required activation temperature, the increased wear protection afforded by the TCP outweighs the reduction in oil film as a result in temperature. However, as discussed previously, at high load, the difference in temperature gives a minimal effect on wear.

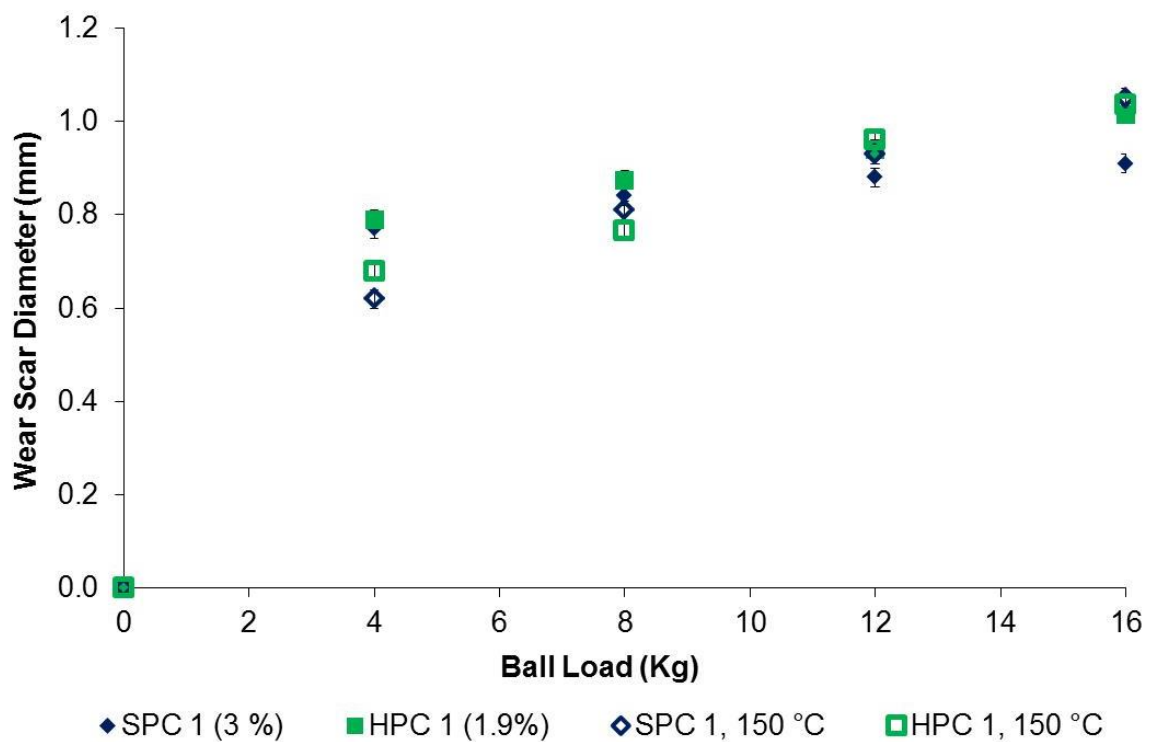


Figure 7.4 Oil brand evaluation, comparison of 100 °C and 150 °C

7.4. Tricresyl Phosphate Concentration

During service operation the TCP concentration of lubricant formulations is known to reduce. This is due to its relative volatility and consumption through surface adsorption and

subsequent wear losses. It is therefore possible that the tribological performance of the lubricant could change throughout its life.

In order to understand the influence which TCP concentration has on anti-wear performance, a series of tests were conducted with three of the oil formulations tested previously, but with a range of TCP concentrations. This data is shown in Figure 7.5 and was obtained using a 4 kg load at 150 °C. The error bars shown indicate standard error. In Figure 7.5 concentration of phosphorus (measured by ICP-OES) is shown, this is directly proportional to concentration of TCP. It can be seen that the SPC 1 oil shows a trend towards reducing wear when the concentration of TCP increases. For the SPC 1 oil these differences are believed to be large enough to attribute them to a result of TCP concentration, however, it is clear that the effect is small. In the case of the HPC 2 oil, although there is a general trend, the differences are less pronounced indicating that TCP has little or no effect. The third and lowest performing oil, HPC 3 showed no change in wear performance with increasing TCP concentration. This indicates in these formulations, under these conditions TCP is not providing significant anti-wear protection.

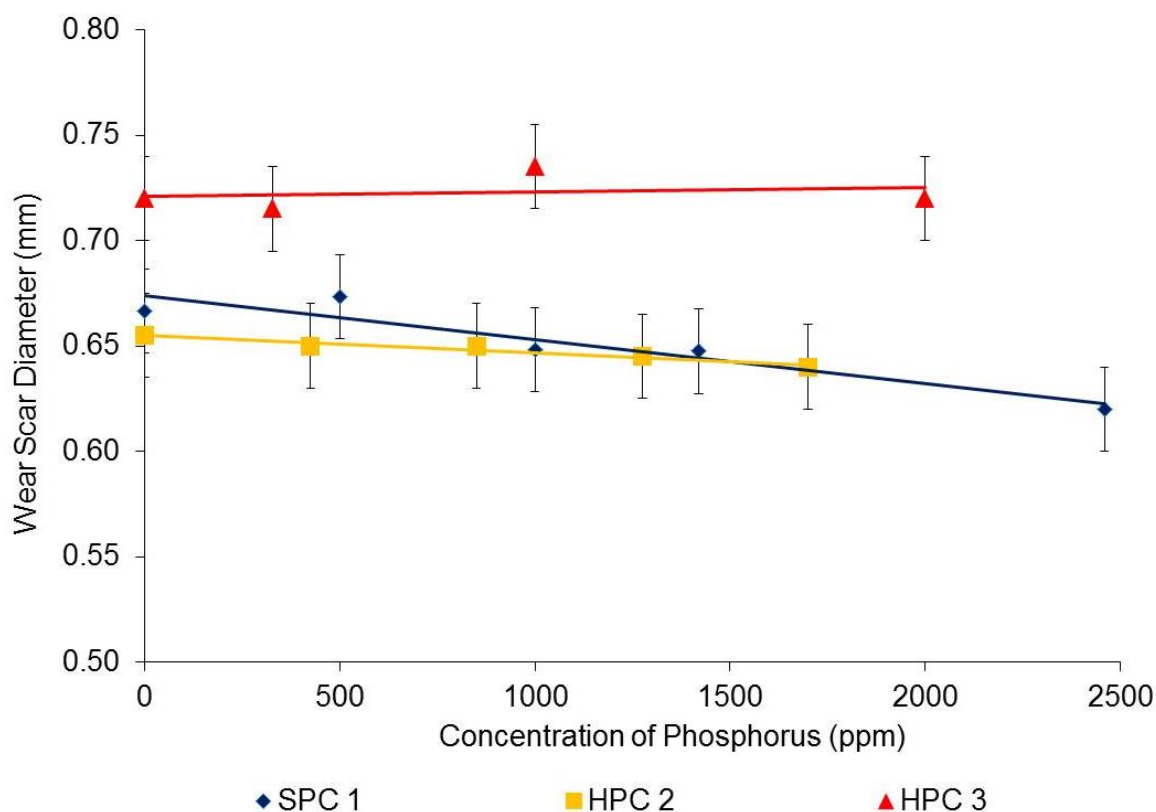


Figure 7.5 Graph showing the influence of tricresyl phosphate concentration (proportional to concentration of phosphorus) on wear scar diameter at 150 °C with a 4 kg load

7.5. Additive Contribution Testing

As previously stated, the most recent developments in aviation gas turbine lubricants are improvements to antioxidant performance with a view to improving lubricant thermal stability. These thermally improved (HPC) lubricants are assessed as a fully formulated product for their tribological performance, however, no public data of individual additive contributions are available. Therefore, in this chapter an initial assessment is made, using the ALTE, of the relative contribution of antioxidants and other additives to wear performance of the lubricant.

For this testing, a single load was used (28 kg) along with an oil bath temperature of 150 °C. These extreme conditions were chosen with the aim of giving maximum differential between oil formulations.

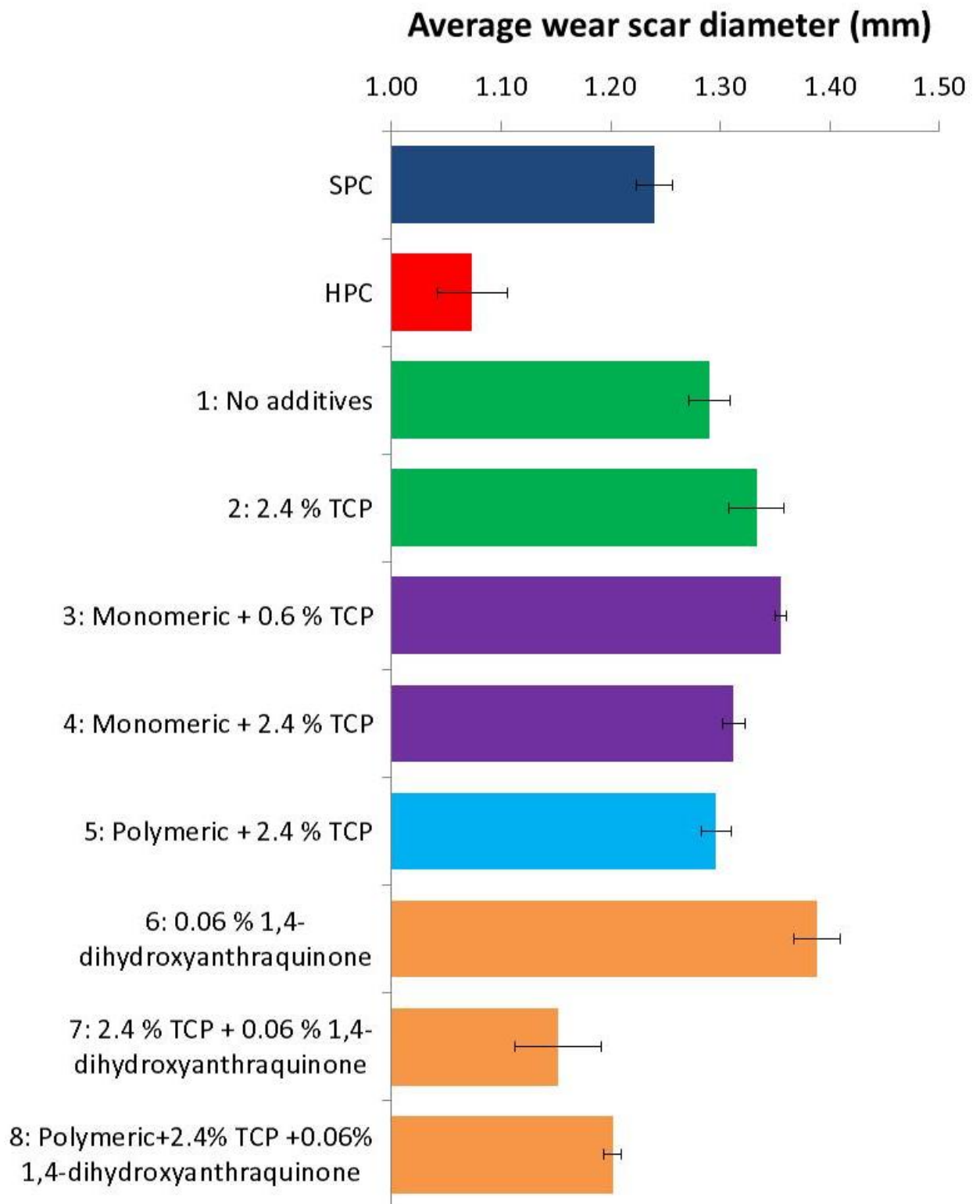


Figure 7.6 Abrasive wear results showing the contribution of different additives

Figure 7.6 shows the wear data produced from this testing. The error bars shown indicate standard error. The figure shows two fully formulated commercial oils, an SPC and an HPC lubricant. It can be seen that at these more extreme conditions, the HPC oil performs better than the SPC lubricant. The blend described as being no additives, is a polyol ester base stock. This base stock constitutes ~95 % of the two formulated oils. However, as this 'no additive' blend produces more wear than the two fully formulated products it is clear that the additive package does influence the wear performance, as previously suggested.

Given that previous testing indicated TCP has an influence on wear performance, a base stock and TCP blend was tested. 2.4 % TCP concentration was chosen for this test as this represents an approximately average value for SAE AS5780 (2013) specified lubricants. Unexpectedly, the addition of TCP resulted in minimal difference in wear. In fact, wear was actually increased marginally. The previous testing on the influence of TCP concentration (Figure 7.5) was conducted using oils containing the other additives present in a lubricant formulation (antioxidants and metal deactivators) and therefore ineffectiveness of TCP in the absence of these additives could indicate a synergistic effect between additives.

To explore this further, first the effect of antioxidant presence was investigated. The antioxidants used were both of aryl-amine chemistry. The first 'monomeric' antioxidant, a blend of simple monomeric amines such as N-phenyl-1-naphthylamine (PANA) similar to those used in standard performance lubricants (SPC). The second 'polymeric' antioxidant contained polymerised aryl-amines. Polymerised aryl-amines have been found to provide better antioxidant protection than their monomeric equivalent and therefore, are often used for high performance capability lubricants (HPC).

Figure 7.6 shows that the monomeric additive with 2.4 % TCP blend gives a similar performance to the pure base stock and the base stock with 2.4 % TCP. Similarly, whilst reducing the concentration of TCP to 0.6 % appeared to increase wear, the differences between the four blends are not significant. The polymeric additive (with 2.4 % TCP) gave a very similar result to both the sample containing a monomeric antioxidant, and the sample without any antioxidant. Therefore, this suggests that the presence of antioxidant additives have a minimal influence on wear performance in this test.

This leaves only one significant additive type which could give rise to the performance improvement of the formulated oils over the additive blends tested thus far, metal deactivators. These additives are included in lubricant formulations to provide a barrier to the oil at the metal surface. This barrier is intended to provide protection from metal corrosion and to inhibit catalytic promotion of oil degradation. However, as these additives are adsorbed to the metal surface, it is probable that they could influence metallic wear. As shown in Figure 7.6 the addition of 0.06 %, 1,4-dihydroxyanthraquinone to the base stock gave no significant change in anti-wear performance. However, it was found that when both 1,4-dihydroxyanthraquinone (0.06 %) and TCP (2.4 %) were used, wear was significantly reduced (~11 % reduction). This would indicate a synergistic effect between 1,4-dihydroxyanthraquinone and TCP as a result of both compounds being present at the contact surface. It was found that when a polymeric antioxidant was added to the blend containing 1,4-dihydroxyanthraquinone and TCP, performance was not influenced, thereby ruling out an influence from antioxidants.

7.6. Closing Remarks

A gap in research knowledge, in terms of the specific influence of polyol ester lubricant additives on lubricant tribological performance, was established. The Aviation Lubricant Tribology Evaluator was selected to evaluate a range of commercial blends and bespoke blends containing a range of common oil additives.

Initial testing, with four commercially available lubricant blends, showed only small differences between each lubricant formulation. The influence of TCP concentration in the lubricant blend was tested further using commercial blends which were altered only in their TCP concentration. This showed that for one oil, the amount of TCP additive was inversely proportional to wear, however, for the other two oils, TCP concentration had little or no detectable effect.

Testing under high load conditions showed that antioxidants have minimal effect on the amount of wear seen. The most pronounced influence on abrasive wear reduction was found to be when the metal deactivator additive 1,4-dihydroxyanthraquinone was used in the presence of TCP, possibly indicating a synergistic effect between the two surface active additives.

This chapter presents only initial scoping experiments with the intention of indicating significant trends, from which areas for further work might be informed. The research in this chapter has shown that the role which the lubricant and its additives play in tribological interactions is complicated and dependant not only on formulation, but also heavily on the contact conditions.

CHAPTER 8: CONCLUSIONS AND FURTHER WORK

8.1. Conclusions

Following a review of current industry thermal oxidative test methods and supplementary practical testing, it was concluded that there was significant scope for method improvement. An opportunity was identified to remove duplicated effort within the industry oil specification (SAE AS5780), to produce one method which fulfils, as far as possible, the needs of all interested parties. It was also concluded that efforts were required to identify how representative of gas turbines such a revised laboratory method was to ensure the mechanism and rate of lubricant degradation could be confidently compared and modelled to oil degradation in the gas turbine.

As part of the effort to produce a more gas turbine representative laboratory oil oxidation method, a study into the most significant parameters in the mechanism and rate of oil degradation, was conducted. Air flow and volatilisation were identified as two key parameters which significantly influence the physical and chemical properties of the lubricant. It was therefore concluded that the air input and subsequent volatilisation losses from the system should be controlled in order to produce chemical and physical changes to the lubricant similar to those seen in the gas turbine.

A modified method was devised and the degraded oil it produced was shown to have similar chemical and physical properties to gas turbine degraded oils. In addition, improvements in parameter control and the ability to produce larger amounts of data, in less time were achieved. It is concluded that the more engine representative nature of this test, offers an

improvement on the current industry methodologies, with the potential to provide high quality data without the need for multiple methods to be used.

In the area of lubricant deposition, testing using the Vent Pipe Simulator (VPS) showed that deposit accumulation results in a flow disturbance, this gives a subsequent increase in heat transfer as deposit accumulates. This was concluded to be an artefact of the low flow rates used; a key difference between the laboratory scale test and engine conditions. Testing showed that VPS was able to distinguish performance differences between a range of lubricant brands and to show their accumulation over time. Analysis of oil mist and coalesced oil from the VPS showed that the heavily degraded coalesced fraction is most likely the primary contributor to deposit formation.

It was shown using the Feed Pipe Simulator, that engine shutdown conditions present a greater risk of deposit formation than standard engine running conditions. It was also demonstrated that pipes which are flooded with oil at shutdown, instead of being drained, are less susceptible to deposit formation.

In the assessment of surface technologies and their ability to reduce lubricant deposition, it was found that whilst some materials, such as silicon, have the potential to significantly reduce the amount of deposit which forms at pipe walls, the morphology of the coating is critical. Additionally, coating on the interior of pipes and on complex geometries makes the application of coating technologies difficult. Therefore, it is concluded that for coating of pipe interiors to be viable, a suitable coating technique would need to be established.

Modification to stainless steel using electropolishing and acid pickling techniques were shown under a range of conditions to reduce deposit formation. As these techniques can be easily applied to existing hardware metallurgies, with minimal difficulty of application, it is concluded

that these technologies are currently a more viable method to reduce lubricant deposition formation than coatings.

In the area of lubricant tribology, testing showed minimal differences in anti-wear performance between the four oils evaluated. It was concluded that the amount of TCP present in a formulation had a small effect on wear performance for one oil, however, this was not seen for the other two oils. It was also concluded that antioxidants have minimal effect on abrasive wear yet there appeared to be a synergistic effect when TCP and 1,4-dihydroxyanthraquinone were both used, leading to increased performance.

8.2. Impact on the Business

Development of improved thermal oxidative stability and deposition methodologies which more closely replicate gas turbine conditions will allow Rolls-Royce to more accurately evaluate the lubricants which are to be used.

The thermal oxidative stability method developed in this thesis, has provided accurate oil data which will, in the future, be used in Rolls-Royce oil life prediction. Planned incorporation of this method into the industry oil specification will allow future oil formulations to be evaluated under more engine representative conditions to ensure future lubricant products meet system requirements.

Data produced in this engineering doctorate project, using the defined deposition methodologies, has been utilised to support approval of new oil brands for Rolls-Royce products. This allowed a reduction of the risk associated with new product approval. It is planned that this methodology will be used for future oil and oil system component evaluations where required.

Recommendations for oil pipe surface modifications have been made to Rolls-Royce, these recommendations have been incorporated in the design rules for future oil system pipe designs. This will allow their incorporation to be considered for future hardware.

The scoping work conducted into the tribology of lubricants highlighted a gap in research knowledge and a need for further method development. This work, is therefore, likely to inform the direction of future research in this area.

8.3. Further Work

In order to further develop the thermal oxidative stability method proposed in this thesis, testing with more lubricant brands is required. This will allow further comparison to data from established methodology and to gas turbine degraded oil data. Additionally, this will allow a robust precision statement to be defined for the method repeatability and reproducibility. Following this, it is proposed that the method would be published as an industry standard method to allow the potential incorporation into the oil specification SAE AS5780 (2013).

The knowledge obtained on the key oil oxidation parameters allows the generation of aged oil samples comparable to those commonly in operation in gas turbines. Further work could involve the transfer of this knowledge from laboratory to simulator or rig scale methodology. This could be implemented simply through the use of pre-aged lubricant from the laboratory method in the larger scale rig, or by the use of the parameter control described here, to generate engine representative oil in situ.

It was shown that a key difference between the conditions used in the VPS and those seen in a gas turbine oil pipe, is that the laboratory simulation does not achieve turbulent flow. As a high residence time is required for the laboratory test which is most easily achieved using low

flow rates, a turbulator could be used prior to the test section, to induce flow instabilities without the need for high flow rates.

Further work could involve the combination of the VPS and FPS simulators such that the oil which is atomised in the vent pipe element, is pre-aged oil produced by the feed pipe element. This would allow more engine representative conditions to be achieved.

Evaluation of other potential surface modification techniques, such as carburising and nitriding of surfaces to identify the effect which they have on deposit formation could be undertaken. Other more novel coatings, such as 'oleophobic' coatings with the potential to resist oil coalescence and therefore subsequent deposition, could be explored. An assessment of the interaction of surface technologies with specific oil additives (particularly anti-wear additives), should be conducted.

The tribological work conducted in thesis was intended as a scoping exercise and therefore there are numerous areas for further work. Testing using different tribological regimes to replicate other wear conditions is critical, as most additives or formulations will perform best at specific conditions with potentially poor results at other conditions. The many more additive and base stock combinations could be explored as well as novel lubricants and additives. However, for gas turbine manufacturers the topic of tribological changes due to service degradation is perhaps of greater interest. In this area, degradation of both the base stock and depletion of additives are of interest for the potential to influence metallic wear.

CHAPTER 9: REFERENCES

Ali, A., Lockwood, F., Klaus, E.E., Duda, J.L., Tewksbury, E.J. (1978), The Chemical Degradation of Ester Lubricants. **ALSE Transactions**, 22 (3): 267-276

Askins, J.S. (2010) **The Performance and Supply of Fluids in a Modern Gas Turbine**, University of Birmingham. EngD Thesis, University of Birmingham

ASTM International. (2009) **Standard Test Method for Corrosiveness and Oxidation Stability of Hydraulic Oils, Aircraft Turbine Engine Lubricants, and Other Highly Refined Oils**. ASTM D4636-09

ASTM International. (2011) **Standard Test Method for Density, Relative Density, and API Gravity of Liquid by Digital Density Meter**. ASTM D4052-11

ASTM International. (2013) **Standard Test Method for Multielement Determination of Used and Unused Lubricating Oils and Base Oils by Inductively Coupled Plasma Atomic Emission Spectrometry (ICP-AES)**. ASTM D5185-13

ASTM International. (2011) **Standard Specification for Seamless Copper Tube**. ASTM B75-11

ASTM International. (2011) **Standard Specification for Seamless Nickel and Nickel Alloy Condenser and Heat-Exchanger Tubes**. ASTM B163-11e

ASTM International. (2012) **Standard Specification for Aluminum and Aluminum-Alloy Drawn Seamless Tubes**. ASTM B210-12

ASTM International. (2012) **Standard Test Method for Kinematic Viscosity of Transparent and Opaque Liquids (and the Calculation of Dynamic Viscosity)**. ASTM D445-12

ASTM International. (2013) **Standard Specification for Seamless and Welded Austenitic Stainless Steel Tubing for General Service.** ASTM A269-13

ASTM International. (2013) **Standard Specification for Seamless and Welded Titanium and Titanium Alloy Tubes for Condensers and Heat Exchangers.** ASTM A338-13a

Bakunin, V.N. and Parenago, O.P. (1992) A mechanism of thermo-oxidative degradation of polyol ester lubricants. **Journal of Synthetic Lubrication**, 9 (2): 127-143

Bartl, P., Völkl, C. and Kaiser, M. (2008) Chemical characterization of polyol ester aviation lubricant residues. **Journal of Synthetic Lubrication**, 25: 1-16

Bieber, H.E., Klaus, E.E. and Tewksbury, E.J. (1968) A study of tricresyl phosphate as an additive for boundary lubricant. **ASLE Transactions**, 11 (2) 155-161

Braid, M., Law, D. A., (1971) **Lubricant Compositions.** US Patent, US 3,573,206

Brook, J.H.T., Matthews, J.B. and Taylor, R.P. (1953) The role of oxidation in the deterioration in use of I.C engine crankcase oils. **Journal of the Institute of Petroleum**, 39: 454-462

Chakraverty, N.K., (1963) The influence of Pb, Fe, Sn and Cu on the oxidation of lubricating oils. Metal catalyzed oxidation of oils. **Journal of the Institute of Petroleum** 49 (479): 353-358

Chung, Y.W., (1992) Effects of surface composition, environment and morphology on friction and wear: an overview. **Surface and Coatings Technology** 54/55: 423-427

Cross, A. (2002) Review of HLPS Method SAE ARP5996 by SAE Committee Task Team (Oral Presentation). **E34 Propulsion Lubricant Committee.**

D’Orazio, J., Karpovich, P.A. and Nowack, C.J. (1976) A study of the factors affecting deposition characteristics of synthetic lubricants for gas turbines. **Naval Air Propulsion Test Center Report** (Public Release), NAPTC-PE-71

Dexter, M. (1992) **Antioxidants in Encyclopedia of Chemical Technology**. 4th ed., In Kroschwitz, J. L. (ed.), John Wiley & Sons New York. pp. 424-447

Diaby, M., Sablier, M., Le Negrate, A., El Fassi, M., Bocquet, J. (2009) Understanding carbonaceous deposit formation resulting from engine oil degradation. **Carbon** 47: 355-366

Diamond, H., Kennedy, H.C. and Larsen, R.G. (1952) Oxidation characteristics of lubricating oils at high temperatures. **Industry and Engineering Chemistry**, 44: 1834-1843

Edge, R.G. and Squires, A.T.B.P. (1969) Lubricant Evaluation and Systems Design for Aircraft Gas Turbine Engines. **SAE Technical Paper**, 690424

Ervin, J.S. and Williams, T.F. (1996) Dissolved oxygen concentration and jet fuel deposition. **Industrial & Engineering Chemistry Product Research and Development**, 35 (3): 899–904

Faut, O. D. and Wheeler, D. R. (1983) On the mechanism of lubrication by tricresylphosphate (TCP) – the coefficient of friction as a function of temperature for TCP on M-50 steel. **ASLE Transactions**, 26 (3): 344-350

Fowler, J., Shepherd, T. and Pagnell, J. (1996) **Strategic review of synthetic gas turbine engine lubricating oil specification requirements**. MOD FS(Air)4 PDS Contract

Frapin, P., Issalatif, G., Mansoux, J-L. (2010) **Anti-oxidation and/or anti-corrosion agent, lubricating composition containing said agent and method for preparing the same**. US 2010/030511 A1

Fuchs, H. and Zeman, A. (1993) Polymer formation during thermal oxidative ageing of aviation turbine oils. **Journal of Synthetic Lubrication**, 10 (1): 1-22

Glocker, D.A. and Shah, S.I. (1995) **Handbook of Thin Film Process Technology**. Institute of Physics, Bristol

Godfrey, D. (1965) The lubrication mechanism of tricresyl phosphate on Steel. **ASLE Transactions**, 8 (1): 1-11

Hamrock, B.J., Schmid, S.R. and Jacobson, B.O. (2004) **Fundamentals of Fluid Film Lubrication**. 2nd ed. Marcel Dekker Inc.

Han, D.H. and Masuko, M., (1998) Elucidation of the antiwear performance of several organic phosphates used with different polyol ester base oils from the aspect of interaction between additive and base oil. **Tribology Transactions**, 41 (4): 600-604

Hart, K. (2008) **Gas Turbine Oil Systems Analysis – Advanced Course**. University of Hertfordshire

Hazlett, R.N. (1991) **Thermal oxidation stability of aviation turbine fuels**. ASTM, Monograph 1

Hunter, M., Klaus, E.E. and Duba, J.L. (1993) A kinetic study of antioxidation mechanisms. **Lubrication Engineering**, 49 (6): 492-498

Hutchings, I. M. (1992) **Tribology**. Edward Arnold Publishing, ISBN 0-340-56184-X

Jantzen, E. (1996) The origins of synthetic lubricants: The work of Hermann Zorn in Germany, Part 1, basic studies of lubricants and the polymerisation of olefins. **Journal of Synthetic Lubrication**, 12 (4): 283-301

Jantzen, E. (1996) The origins of synthetic lubricants: The work of Hermann Zorn in Germany part 2 esters and additives for synthetic lubricants. **Journal of Synthetic Lubrication**, 13, (2): 113–128

Jensen, R.K., Korcek, S. and Mahoney, L.R. et al. (1981) Liquid phase autoxidation of organic compounds at elevated temperatures Part 2 – Kinetics and mechanism of the formation of cleavage products in n-hexadecane autooxidation. **Journal of the American Chemical Society**, 103 (7): 1742-1749

Karis, T.E., Miller, J.L. and Hunziker, H.E. et al. (1999) Oxidation chemistry of a pentaerythritol tetraester oil. **Tribology Transactions**, 42 (3): 431-442

Klaus, E.E. and Tewksbury, E.J. (1973) Microcorrosion Studies with Functional Fluids. **Lubrication Engineering**, 29 (5): 205-211

Koh, C.S., Butt, J.B., (1995) Experimental and modelling study of kinetics and selectivity in the oxidation of a poly(α -olefin) lubricant. **Industrial & Engineering Chemistry Product Research and Development**, 34: 524-535

Kohler, M., Heeb, N.V., (2001) Characterization of ageing products of ester-based synthetic lubricants by liquid chromatography with electrospray ionization mass spectrometry and by electrospray ionization (tandem) mass spectrometry. **Journal of Chromatography A**, 926: 161-165

Kunina, E.A., Echin, A.I. and Kuznetsov, V.G. (1991) Spectrophotometric method for evaluation of the oxidative thermal stability of synthetic oils. **Chemistry and Technology of Fuels and Oils**, 27 (3): 168-170

Lee, S. (2008) Oxidative Task Team Report (Oral Presentation). **E34 Propulsion Lubricant Committee** Maier, K. (1986) Aircraft engine oils and their behaviour at high temperatures. **Journal of Synthetic Lubrication**, 3 (3): 163-180

Maier, K. (1989) Aircraft Engine Deposits. **European Lubricant Deposition Group**

Mattox, D.M. (2004) **The Foundations of Vacuum Coating Technology**. William Andrew Publishing.

Mattox, D.M. (2010) **Handbook of Physical Vapor Deposition (PVD) Processing**. 2nd ed. William Andrew Publishing.

Mortier, R.M., Fox, M.F. and Orszulik, S.T. (2010) **Chemistry and Technology of Lubricants**. Springer, ISBN 978-1402086618

Moses, C.A. (2002) Reynold's number effects on deposition. **Paper Presented at CRC Aviation Group Meeting**, NASA Grant NAG3-2270, Glenn Research Center

Mousavi, P., Wang, D., and Grant, C.S. et al. (2006) Effects of antioxidants on the thermal degradation of polyol ester lubricant using GPC. **Industrial & Engineering Chemistry Product Research and Development**, 45: 15-22

Naidu, S. K, Klaus, E. E. and Duda, J. L. (1984) Evaluation of liquid phase oxidation products of ester and mineral oil lubricants. **Industrial & Engineering Chemistry Product Research and Development**, 23: 613-619

Naidu, S., Klaus, E. and Duda, J. (1986) Kinetic model for high-temperature oxidation of lubricants. **Industrial & Engineering Chemistry Product Research and Development**, 25 (4): 596-603

Nakanishi, H., Onodera, K. and Inoue, K. et al. (1997) Oxidation stability of synthetic lubricants. **Lubrication Engineering**, 53 (5): 29-37

Panchal C.B., and Watkinson, A.P. (1994) Development of an analytical model for organic-fluid fouling, **US Department of Energy**

Rajadurai, J.S. (2003) **Thermodynamics and Thermal Engineering**. New Age International

Rolls-Royce plc. (2005) **The Jet Engine**. ISBN: 0 902121 2 35

Rudnick, L.R. (2013) **Synthetics, Mineral Oils, and Bio-based lubricants**. 2nd ed. Chemistry and Technology, CRC Press

SAE International. (2006) **Test Method for the Determination of Total Acidity in Polyol Ester and Diester Gas Turbine Lubricants by Automatic Potentiometric Titration**. Aerospace Recommended Practice, ARP5088, Rev A

SAE International. (2010) **WAM High Speed Load Capacity Test Method**. Aerospace Recommended Practice, ARP6156 (Draft)

SAE International. (2013) **Aviation Lubricant Tribology Evaluator (ALTE) Method to determine the lubricating quality of gas turbine lubricants**. Aerospace Recommended Practice, ARP6255

SAE International. (2013) **Evaluation of coking propensity of aviation lubricants using the single phase flow technique**. Aerospace Recommended Practice, ARP5996, Rev. B

SAE International. (2013) **Specification for Aero and Aero-derived Gas Turbine Engine Lubricants**. Aerospace Standard, AS5780, Rev. B

SAE International. (2014) **Gas Turbine Lubricant Specifications: Current Technical Review and Future Direction**. Aerospace Information Report, AIR6056

SAE International. (2014) **Vapor Phase Coking**. Aerospace Recommended Practice, ARP5921

Siouris, S., Shepherd, T., Wilson, C., et al. (2013) Development of an apparatus for the degradation of aviation gas turbine lubricants. **Tribology Transactions**, 56 (2): 215-223

Smith, P.A. (2008) **Lubrication arrangement for bearings**. European Patent, EP 1 731 719 B1

Sniegowski, P.J. (1977) Selectivity of the oxidative attack on a model ester lubricant. **ASLE Transactions**, 20 (4): 282-286

Sniegowski, P.J. (1982) **A kinetic study of lubricant antioxidant depletion in aircraft gas turbine engines**. Naval Research Laboratory

Spadaccini, L.J. and Huang, H. (2003) On-line fuel deoxygenation for coke suppression. **Journal of Engineering for Gas Turbines and Power**, 125 (3): 686-692

Spencer, M., Shepherd, T., Greenwood, R. and Simmons, M. (2013) An Assessment of the Influence of Gas Turbine Lubricant Thermal Oxidation Test Method Parameters Towards the Development of a New Engine Representative Laboratory Test Method. **SAE International Journal of Aerospace**, 6(2): 819-827, doi:10.4271/2013-01-9004.

Taylor, W.F. (1974) Deposit formation from deoxygenated hydrocarbons. I. General Features. **Industrial & Engineering Chemistry Product Research and Development**, 13 (2): 133–138

Taitel, Y. and Dukler, A.E. (1976) A model for prediction flow regime transitions in horizontal and near horizontal gas-liquid flow. **American Institute of Chemical Engineers Journal**, 22 (1): 47-55

Turbomeca, **Turbomeca Thermal Ageing Test** No published method.

UK Ministry of Defence. (1982) **Lubricating oil, aircraft turbine engine, synthetic type. NATO Code No O-149, Joint Service Designation: OX-38.** MODUK DERD 2487, Issue 5

UK Ministry of Defence. (2001) **Lubricating oil, gas turbine engine, synthetic grade. 7.5 cSt. NATO Code: O-149, Joint Service Designation: OX-38.** Defence Standard 91-98

UK Ministry of Defence. (2003) **Method 9: resistance to oxidation and thermal decomposition.** Standards for Defence, DEF STAN 05-50 (Part 61)/2, Method 9.

US Defense Logistics Agency. (2007) **Corrosiveness and oxidation stability of light oils (Metal Squares).** Federal Standard, FED-STD-791, Rev. D, Method 5308

US Defense Logistics Agency. (2007) **High temperature deposit and oil degradation characteristics of aviation turbine oils.** Federal Standard, FED-STD-791, Rev. D, Method 3410

US Defense Logistics Agency. (2007) **Load carrying capacity of lubricating oils. (Ryder Gear Machine).** Federal Standard, FED-STD-791, Rev. D, Method 6508

US Defense Logistics Agency. (2007) **Thermal stability and corrosivity of aircraft turbine engine lubricants.** Federal Standard, FED-STD-791, Rev. D, Method 3411

US Department of Defense. (1997) **Performance specification, lubricating oil, aircraft turbine engine, synthetic base.** NATO Code Number O-156 MIL-PRF-23699, Rev. F

US Department of Defense. (1997) **Performance specification, lubricating oil, aircraft turbine engine, synthetic base.** MIL-PRF-7808L

Wang, D., Mousavi, P., Hauser, P.J., Oxenham, W. and Grant, C.S., (2004) Novel testing system for evaluating the thermal stability of polyol ester lubricant. **Industrial & Engineering Chemistry Product Research and Development**, 43: 6638-6646

Watkinson A.P., and Wilson, D.I. (1997) Chemical reaction fouling: A review. **Experimental and Fluid Science**, 14: 361-374

Whittle, F. (1930) **Improvements relating to the propulsion of aircraft and other vehicles.**
United Kingdom Patent GB347206

Wirtz, R.H. and Zeman, A. (1987) Spontaneous ignition temperatures of aviation turbine oils. **Thermochemica Acta**, 112: 297-305

Wu, Y., Li, W. and Zhang, M. et al. (2013) Oxidative degradation of synthetic ester and its influence on tribological behaviour. **Tribology International**, 64: 16–23

Young, A., Venditti, S., Berrueco, C., Yang, M., Waters, A., Davies, H., Hill, S., Millan, M., Crittenden, B. (2011) Characterisation of crude oils and their fouling deposits using a batch stirred cell system. **Heat Transfer Engineering**, 32(3-4): 216-227

Zeman, A., Becker, V., Peper K., (1993) Deposit formation in aero engines – investigation by pressure differential scanning calorimetry (PDSC), **Thermochemica Acta**, 219: 305-313

Zeman, A., Koch, K., and Bartl, P. (1985) Thermal oxidative ageing of neopentylpolyol ester oils: Evaluation of thermal-oxidative stability by quantitative determination of volatile ageing products. **Journal of Synthetic Lubrication**, 2 (1): 1-21

Zeman, A., Römer, R. and von Roenne, V. (1986) Fate of amine antioxidants during thermal oxidative ageing of neopentylpolyol ester oils: Part 1. **Journal of Synthetic Lubrication**, 3 (4): 309-326

Zeman, A., Stuwe, R. and Koch, K. (1984) The DSC cell – A versatile tool to study thermal-oxidative degradation of lubricants and related problems. **Thermochimica Acta**, 80: 1-9

Zeman, A., von Roenne, V. and Trebert, Y. (1987) Fate of amine antioxidants during thermal oxidative ageing of neopentylpolyol ester oils. **Journal of Synthetic Lubrication**, 4 (3): 179-201

Vent / Feed Pipe Simulator Test Specimen Surface Finish Measurements

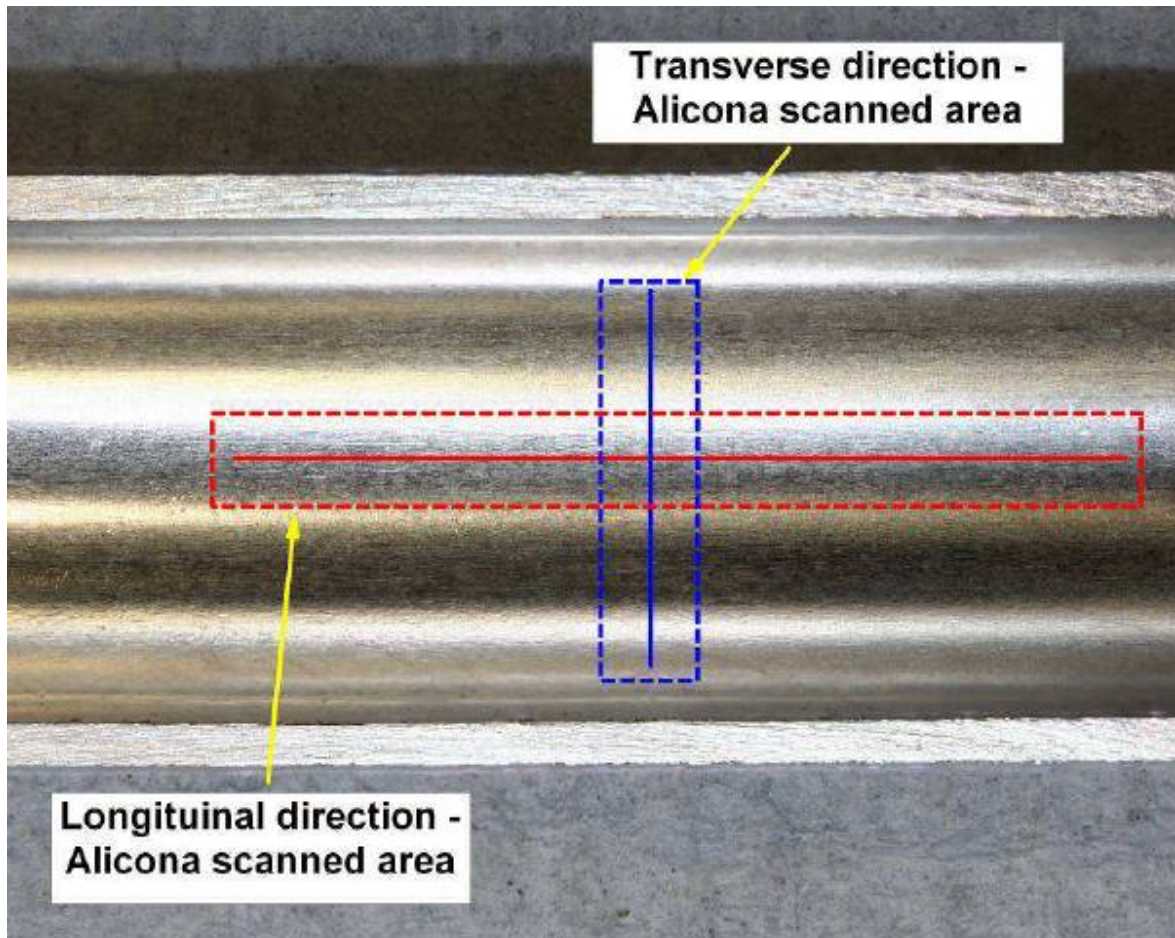


Figure 9.1 Surface finish measured areas

The following measurements were determined using an Alicona Infinite Focus Microscope:

			Transverse								
			Pickled 1	Pickled 2	Pickled 3	EP 1	EP 2	EP 3	Standard 1	Standard 2	Standard 3
Ra	Average roughness of profile	μm	0.927	0.865	1.018	1.391	0.921	1.207	0.937	1.363	1.434
Rq	Root-Mean-Square roughness of profile	μm	1.248	1.077	1.187	1.670	1.116	1.407	1.113	1.606	1.703
Rt	Maximum peak to valley height of roughness profile	μm	5.373	5.248	4.798	7.425	5.564	5.336	4.492	6.637	6.774
Rz	Mean peak to valley height of roughness profile	μm	5.134	5.090	4.666	6.898	5.526	5.104	4.393	5.838	6.274
Rmax	Maximum peak to valley height of roughness profile within a sampling length	μm	5.296	5.240	4.798	7.425	5.531	5.279	4.462	6.637	6.774
Rp	Maximum peak height of roughness profile	μm	3.829	3.507	2.911	5.299	4.110	3.198	2.711	4.343	4.806
Rv	Maximum valley height of roughness profile	μm	1.544	1.741	1.886	2.126	1.454	2.137	1.780	2.294	1.968
Rc	Mean height of profile irregularities of roughness profile	μm	4.482	4.352	4.295	6.378	4.202	4.569	3.394	5.472	5.978
Rsm	Mean spacing of profile irregularities of roughness profile	μm	465.3	431.8	421.5	600.8	172.7	435.6	281.5	507.6	588.9
Rsk	Skewness of roughness profile		1.334	0.985	0.494	1.015	0.998	0.397	0.452	0.627	0.924
Rku	Kurtosis of roughness profile		4.195	3.443	2.228	2.879	3.711	1.979	2.283	2.213	2.560
Rdp	Root-Mean-Square slope of roughness profile		0.058	0.059	0.059	0.059	0.171	0.065	0.075	0.078	0.054
Rt/Rz	Extreme Scratch/Peak value of roughness profile		1.046	1.031	1.028	1.077	1.007	1.045	1.022	1.137	1.080
I	Profile Length	mm	5.134	5.225	5.106	5.423	5.230	5.078	5.407	5.084	5.314

			Longitudinal								
			Pickled 1	Pickled 2	Pickled 3	EP 1	EP 2	EP 3	Standard 1	Standard 2	Standard 3
Ra	Average roughness of profile	μm	0.220	0.205	0.226	0.250	0.283	0.347	0.224	0.258	0.205
Rq	Root-Mean-Square roughness of profile	μm	0.289	0.257	0.282	0.331	0.344	0.480	0.283	0.322	0.260
Rt	Maximum peak to valley height of roughness profile	μm	2.535	1.915	1.870	2.850	1.947	6.723	1.839	2.037	2.082
Rz	Mean peak to valley height of roughness profile	μm	1.773	1.488	1.468	2.042	1.585	4.089	1.551	1.595	1.407
Rmax	Maximum peak to valley height of roughness profile within a sampling length	μm	2.157	1.915	1.662	2.533	1.947	6.723	1.839	1.864	1.898
Rp	Maximum peak height of roughness profile	μm	1.497	0.805	0.905	1.669	1.081	5.355	0.992	1.084	1.162
Rv	Maximum valley height of roughness profile	μm	1.039	1.110	0.965	1.181	0.866	1.368	0.847	0.954	0.920
Rc	Mean height of profile irregularities of roughness profile	μm	0.973	0.779	0.867	1.358	1.080	3.098	0.858	0.932	0.826
Rsm	Mean spacing of profile irregularities of roughness profile	μm	107.9	82.4	67.7	198.1	122.8	440.2	89.0	82.1	109.1
Rsk	Skewness of roughness profile		0.267	-0.143	-0.037	0.186	0.271	2.092	0.084	0.022	-0.042
Rku	Kurtosis of roughness profile		4.857	3.225	2.852	4.513	2.594	14.80	3.099	2.963	3.849
Rdp	Root-Mean-Square slope of roughness profile		0.048	0.042	0.055	0.043	0.045	0.095	0.043	0.051	0.039
Rt/Rz	Extreme Scratch/Peak value of roughness profile		1.430	1.287	1.274	1.395	1.229	1.644	1.186	1.278	1.480
l	Profile Length	mm	5.031	7.576	5.077	5.040	5.453	9.661	5.076	5.186	5.006